Università degli Studi di Cagliari

Dipartimento di Fisica

PhD Degree in Physics
XXXI cycle

Black Holes, Holography and the Dark Universe

Scientific Disciplinary Sector: Fis/02

PhD Candidate:	**Matteo Tuveri**
Coordinator of the PhD Program:	**Prof. Paolo Ruggerone**
Supervisor:	**Prof. Mariano Cadoni**

Final exam. Academic year 2017/2018
Thesis defence: January-February 2019 Session

Abstract

We investigate various aspects of gravity with the aim to shed light on the deep relation between the infrared and ultraviolet regimes of gravitational interaction. We focus on black holes, holography, the emergent properties of spacetime and gravity itself and its relation to the behaviour of gravity at galactic scales. In the first part of the thesis, we study geometrical, thermodynamical and holographic properties of two dimensional and higher dimensional black holes in Anti-de Sitter spacetime in the context of the AdS/CFT correspondence. We discuss two different applications of the AdS/CFT correspondence: the shear viscosity to entropy density ratio for five dimensional charged Reinssner-Nordström and Gauss-Bonnet black branes and black holes and quantum holographic properties of two dimensional dilaton gravity. For black branes we find an universal thermodynamical behaviour and a monotonic flow from the UV to the IR of the shear viscosity to entropy density ratio as a function of the temperature. In the black hole case we find an interesting connection between phase transitions in the bulk and a hysteretical behaviour of the shear viscosity to entropy density ratio in the dual quantum field theory. For two dimensional dilaton gravity we show that the pattern of conformal symmetry breaking is crucial to understand the microscopic properties of two dimensional dilaton black holes. In the second part of the thesis we describe the emergent laws of gravity in a corpuscolar picture and derive the implications of our emergent gravity scenario at galactic scales. We first describe spacetime as a Bose-Einstein condensate of gravitons, then we demonstrate that, without assuming the existence of exotic matter, the phenomenology commonly attributed to dark matter at galactic scales (the flattening of rotational curves) can be described as a reaction of the cosmological condensate to the presence of localized baryonic matter. We show how this corpuscolar picture of gravity allows for an effective description in terms of general relativity sourced by an anisotropic fluid. Finally, using a more conservative approach, we derive an exact, analytic, static, spherically symmetric, four-dimensional solution of minimally coupled Einstein-scalar gravity, sourced by a scalar field which could be considered as a possible dark matter candidate.

Contents

Preface

The work presented in this thesis has been carried out at the Physics Department of the University of Cagliari in the triennium 2015-2018.

The thesis is devided in two parts. The first part, "Black Holes and Holography", is the result of the collaboration with Mariano Cadoni, Antonia Micol Frassino, Edgardo Franzin and Matteo Ciulu. For what concerns my research, it is based on the following papers:

- M. Cadoni, A. M. Frassino and M. T., "*On the universality of thermodynamics and η/s ratio for the charged Lovelock black branes*", **JHEP 1605 (2016) 101**, arXiv:1602.05593.
- Mariano Cadoni, Edgardo Franzin and M. T., "*Van der Waals-like Behaviour of Charged Black Holes and Hysteresis in the Dual QFTs*", **Phys.Lett. B768 (2017) 393-396**, arXiv:1702.08341.
- Mariano Cadoni, Edgardo Franzin and M. T. "*Hysteresis in η/s for QFTs dual to spherical black holes*", **Eur.Phys.J. C77 (2017) no.12, 900**, arXiv:1703.05162.
- Mariano Cadoni, Matteo Ciulu and M. T., "*Symmetries, Holography and Quantum Phase Transition in Two-dimensional Dilaton AdS Gravity*", **Phys.Rev. D97 (2018) no.10, 103527**, arXiv:1711.02459.

The second part of the thesis, called "The Dark Universe", is the result of the collaboration with Mariano Cadoni, Roberto Casadio, Andrea Giusti, Wolfgang Mück and Edgardo Franzin. For what concerns my research, it is based on the following papers:

- M. Cadoni, R. Casadio, A. Giusti and M. T., "*Emergence of a Dark Force in Corpuscular Gravity*", **Phys.Rev. D97 (2018) no.4, 044047**, arXiv:1801.10374.
- M. Cadoni, R. Casadio, A. Giusti, W. Mück and M. T. "*Effective Fluid Description of the Dark Universe*", **Phys.Lett. B776 (2018) 242-248**, arXiv:1707.09945.
- E. Franzin, M. Cadoni and M. T. "*Sine-Gordon solitonic scalar stars and black holes*", **Phys.Rev. D97 (2018) no.12, 124018**, arXiv:1805.08976.

Introduction

General relativity is a classical theory of gravity [1–4]. Its success ranges over many scales, from the millimeter scale, to the Solar system (precession of planetary orbits, bending of light, gravitational redshift) and the cosmological ones [5]. Not least, the very recent discoveries of gravitational waves due to the coalescence of two binary black holes [6, 7] and neutron stars [8] has marked an important step towards the confirmation of Einstein's predictions about the dynamics of black holes and stars in the universe, leading to the new multi-messenger era of astronomy [9]. Nevertheless, a century after its discovery, Einstein's theory still remains a challenging topic in physics. Despite its great success a lack of theoretical explanation of all the gravitational phenomena at galactic and very large scales, as well as at Planck scales is evident. Moreover, the theory seems to be incompatible with quantum mechanics.

For what concerns gravity at large scales, a tension between theoretical predictions of general relativity and the observations appears. Indeed, the latter can be explained in the framework of general relativity, only assuming the presence of exotic form of matter (dark matter and dark energy) whose true nature still remains a mistery. As far as we know, in order to explain galactic dynamics and the expansion of the universe, the ΛCDM model [10] is the most reliable and conservative approach, but particles out of the standard model [11, 12] to include dark matter and the existence of a dark fluid permeating spacetime, i.e. the dark energy, are needed. Another possibility is to extend general relativity trying to include higher dimensions and new curvature effects [13] or new (gravitating) fields as, for example, scalar fields [14, 15]. However, none of these approaches seem to cover all the phenomenology cited above. On the contrary, the ultraviolet (UV) regime of gravity is even more mysterious and black holes seem to be the most promising laboratory to test general relativity in this case. Indeed the semi-classical (quantum) properties of black holes are well known since the seventies of the last century, when Bekenstein [16, 17] and Hawking [18, 19] discovered that black holes carry a certain quantity of entropy proportional to their area [1]

$$S_{BH} = \frac{A_{hor}}{4\ell_p^2}, \tag{0.0.1}$$

where ℓ_p is the Plack length. The equation above shows the quantum properties of black holes and suggests that, at the Planck scale, spacetime behaves as a pure quantum object. Unfortunately, from a pure theoretical point of view a complete and satisfactory quantum theory of gravity is still missing. There are many attempts trying to quantize gravity, from the Wheeler-DeWitt equation [20], to string theory [21] and loop quantum gravity [22] or group field theory [23], however none of these approaches

[1] We shall use units with $c = 1$ but display explicitly the Planck constant $\hbar = \ell_p\, m_p$ and Newton constant $G_N = \ell_p/m_p$.

is still able to describe the quantum aspects of spacetime, yet. Moreover, their are not able to reproduce all the aspects of classical and quantum gravitational physics as, for example in the case of black holes, the information loss paradox [24, 25] and the microscopic origin of black holes entropy [26, 27]. The real difficult for all the theories cited above is the possibility to match their predictions with direct or even indirect real experiments. In particular, quantum gravity effects are expected to be relevant at the Planck scale $l_P = 10^{-35}m$ or in terms of the Planck energy, $E_P = 10^{19}GeV$. Thus, compared to the typical energies we currently reach in our laboratories (even in the case of astrophysical observations involving very extreme gravitational phenomena), we are very far from being able to directly or indirectly test these phenomena [28].

The Bekenstein-Hawking formula above, not only shows that black holes are intrinsically quantum objects, but also that their thermodynamical properties are in some sense unexpected: contrarily to what we know from statistical mechanics of conventional field theories, black holes entropy scales as an area, not as a volume. This suggests, that, from a quantum point of view, the gravitational interaction seems to have *holographic* properties. Holography, at least in theoretical high energy physics, means that the properties of any $(D+2)-$dimensional region (of spacetime) can be described by degrees of freedom living in its $(D+1)-$boundary [29, 30]. The deep relationship between holography and gravity is a widely studied subject in theoretical physics. In particular, holography finds a natural realization in the case of the so-called Anti-de Sitter/Conformal field theory (AdS/CFT) correspondence. It is a conjecture which states that string theory or a gravity theory in AdS spacetime in $(D+2)-$dimensions is equivalent to a conformal quantum field theory in $(D+1)-$dimensions. It was firstly formulated by Maldacena [31] at the end of nineties of the last century. It has been extended to several contexts and it has gained a lot of interest in all the comunity, especially for its results in describing black hole physics, in quantum gravity [32–35] and in condensed matter physics [36–65]. The AdS/CFT correspondence can be also thought as a weak/strong duality, i.e. weakly interacting gravity theories correspond to strong coupled quantum field theories and viceversa. This helps to circumvent the difficulties in studying the strong coupling limit in gauge theory by focusing on the weak field regime of gravitational interaction.

For many years, physicists have tried to face up with problems related to the IR and UV regimes of gravity separetely. In fact, due to the different phenomenology and physical description (e.g. dark matter, dark energy and a metric theory of gravity based on a smooth classical spacetime in the IR, black hole physics, the information paradox, quantum gravity presumibly based on some quantum spacetime geometry in the UV) it seems, at least at first sight, that the gravitational physics at large and small scales are completely decoupled one from each other. However, there are many indications showing that this is not completely true. These indications have been triggered by recent advances in the understanding of gravity and they come from two different corners of gravitational physics: the first is black hole physics, the second the behaviour of gravity at galactic and cosmological scales.

Due to their peculiar features, black holes are a good example of the deep interplay between IR and UV regimes of gravity. Let us consider for instance black holes thermodynamics and hydrodynamics. All these aspects can be described both from a classical and quantum point of view, involving infrared and ultraviolet features of the system, respectively. This is particularly evident in the case of AdS/CFT corre-

spondence where properties of classical black holes at IR scale can be translated in properties of the dual quantum fields at UV scale and viceversa. Since black holes are thermal objects we can treat the dual quantum field theory as a CFT at finite temperature. The presence of this (thermal) scale opens the possibility to study black holes in particular regimes as, for example, the hydrodynamical one. Depending on the actual content of the gravity theory, i.e. matter fields and couplings, the bulk gravity theory may allow in the asymptotic and near-horizon regimes for different solutions characterized by their symmetries, which correspond to UV and IR fixed points in the dual QFT. It is therefore crucial to understand how the transport coefficients in the dual QFTs are affected by the flow from the UV to the IR. A quantity, which plays a distinguished role in the hydrodynamic regime of thermal QFTs with gravitational duals is the shear viscosity to entropy density ratio η/s. It has been shown that η/s attains an *universal* value $1/4\pi$ for all gauge theories with Einstein gravity duals [66–73]. This fact motivated the formulation of a fundamental bound $\eta/s \geqslant 1/4\pi$, known as Kovton, Son and Starinets bound [74, 75], which also found support from energy-time uncertainty principle arguments in the weakly coupled regime [75] and known experimental data for quark-gluon plasma [75, 76]. However, it was soon realized that in higher curvature gravity theories [77], the presence of particular fields that break the translational invariance of the background [78–81], or curved backgrounds [82] may generically violate the bound. In general, η/s is a function of the temperature and although the breaking of translation symmetry prevents a purely hydrodynamic interpretation of η, there are strongly indication that bounds on η/s are completely determined by IR physics and insensitive to the UV regime of the theory. This is an interesting point because even if the microscopic interpretation of η assumes the existence of the UV regime of the theory, its value depends only on its IR behaviour. Another important point in the holographic context is the possibility of using the information about transport coefficients in the dual QFTs to understand the behaviour of black holes as thermodynamical system, e.g. their phase transitions. Although this is not the usual approach pursued by the AdS/CFT community, it seems a very promising one.

Another example of non trivial flow from the ultraviolet to the infrared regime of gravity is given by two dimensional dilaton gravity [83, 84]. These models are very usefull to study quantum gravity in a very simplified context. Also in the 2D case, the symmetries of the bulk geometries in the asymptotic and near-horizon regimes and the thermodinamical behaviour during the flow from the UV to the IR play a crucial role for understanding many features of gravity such as the microscopic interpretation of black hole entropy.

Moving to a cosmological context, let us now consider the case of dark energy: from a macroscopic point of view, the present accelerated expansion of the universe is driven by an unknown perfect fluid that permeates spacetime which is called dark energy. However, from a quantum point of view dark energy can be seen as the vacuum energy of spacetime whose nature is purely quantum. In this case, the infrared and ultraviolet scale are deeply related being two side of the same coin.

The infrared and ultraviolet description of gravity seems to be deeply linked in the instrinsic structure of spacetime itself. In fact, one of the major ideas triggering recent theoretical progress about the gravitational interaction is that of *emergent gravity*: the classical spacetime structure and gravity emerge together from an underlying micro-

scopic quantum theory [85–87]. In particular, the power of this emergent paradigm is that it must depend loosely on the details of the underlying microscopic theory and it is essentially determined by its fundamental quantum nature.

The notion of emergent gravity is quite general and it has been used in several different contexts [85, 86, 88–94]. Two main realisations of this idea, which have recently attracted a lot of attention, involve the entanglement entropy and the idea of corpuscolar gravity. The first one uses the *entanglement* of microscopic quantum states as the origin of space-time geometry. This route historically starts from the discovery of the Bekenstein-Hawking (BH) entropy area law for black holes [17], goes through the development of the AdS/CFT correspondence [31] and the Ryu-Takayanagi formula, where it clearly appears that the BH formula is related to the quantum entanglement of the vacuum [32]. Subsequently, it was also realized that quantum entanglement could explain the connectivity of classical space-time [95], and that the linearized Einstein's equations can be derived from quantum information principles [96]. The second main realization of the idea that gravity is emergent uses the notions of *quantum compositeness* and *classicalization* [90, 91]. Gravitational systems, such as black holes and cosmological spaces, can be described as a composite quantum system of a large number N_G of soft gravitons. It has been shown that these gravitational systems exhibit properties of a Bose-Einstein condensate (BEC) at the quantum critical point. Moreover, the usual classical space-time structure emerges in the limit $N_G \to \infty$ of this picture [90, 91]. This corpuscular realization of the paradigm of emergent gravity has been also successfully used to describe Hawking radiation [97, 98] and inflation [91, 99, 100].

As already pointed out, an intrinsic feature of gravitational interaction that manifests also in both the above realizations of emergent gravity is that of *holography*. The intrinsic holographic nature of the quantum entanglement approach is evident in the Ryu-Takayanagi derivation of the entanglement entropy and, more in general, in the quantum information picture of black holes and cosmological horizons [32, 87]. The same holographic nature is at the heart of the corpuscular approach, which is based on the fact that the number N_G of soft gravitons in a BEC at the critical point scales, in terms of the size r of the system, as,

$$N_G \sim \frac{r^2}{\ell_p^2}. \tag{0.0.2}$$

The holographic character of this description is also very important for understanding the quantum information counted by the BH entropy (see the complementary, firewall and ER=EPR discussion [101, 102]) and for the description of black holes as BEC of gravitons at the critical point [90, 91].

A striking feature of this approach is that the emergent gravity scenario provides a connection between the microscopic ultraviolet (UV) scale ℓ_p and the infrared (IR) cosmological scale $L = H^{-1}$ of gravity (here H is the Hubble parameter and L the Hubble scale). Indeed, in the quantum entanglement setup, the entropy associated to the de Sitter (dS) spacetime can be explained, similarly to the BH entropy, as a long range entanglement connecting bulk excitations with the dS horizon [87]. In the corpuscular setup, both black holes and our observable universe are "maximally classical" systems, i.e. BEC at the critical point satisfying the relation (0.0.2) with $r = R_H$ (the Schwarzschild radius) and $r = L$, respectively.

In general, the theoretical aparatus of emergent gravity is very usefull to study gravity at cosmological and black hole scales, separetely. However, the success of emergent gravity in describing the holographic regimes of gravity shown in Eq. (0.0.2), gives a strong motivation to use it also at intermediate scales, i.e. at galactic scales. This corresponds exactly to the scales where dark matter phenomena appears and where classical predictions of Einstein's gravity fail. It is evident that from a quantum point of view, the behaviour of the gravitational interaction at these scales cannot be simply described by the maximally packing condition (0.0.2). On the other hand, explaining the phenomenology of gravity at galactic scales has been one of the main motivations for introducing dark matter [103–105] and the ΛCDM model [106–109]. One is therefore led to expect that the application of the emergent gravity scenario at galactic scales may hold the key for understanding the dark matter mystery.

In a fully emergent gravity scenario, in which matter and spacetime are intimately related, the existence of a form of matter different from the baryonic one is conceptually weird. Moreover, despite the extensive agreement with large scale structure and cosmic microwave background observations, the ΛCDM model is not completely satisfactory, not only from a conceptual point of view, but also because there is some tension at the level of the phenomenology of galaxies and galaxy clusters. Concerning the Milky way galaxy, for example, three problems arise: the *missing satellite problem* [110, 111] (N−body simulations predict too many dwarf galaxies within the Milky Way virial radius), the *cusp-core problem* [112] (too much dark matter in the innermost regions of galaxies w.r.t. observations) and the *too-big-to-fail problem* [113, 114] (the dynamical properties of the most massive satellites in the Milky way are not correctly predicted by simulations). In particular, these problems become more and more evident when one tries to study galaxy rotation curves. Typically, the rotational velocity in galaxies approaches a non-zero asymptotic value with increasing distance from a galaxy's centre. This asymptotic value satisfies an empirical relationship with the galaxy's total luminosity known as the Tully-Fisher relation [115]. Rephrased as a relation between the asymptotic velocity v and the total baryonic mass m_B, it takes the form $m_B \sim v^4$ (baryonic Tully-Fisher relation) [116, 117]. With adjusted units, it is equivalent to

$$v^2 \approx \sqrt{a_0\, G_N\, m_B}, \tag{0.0.3}$$

where a_0 denotes an empirically determined factor with dimensions of an acceleration. The surprising fact is that the value of a_0 appears to be $a_0 \approx H/(2\pi) \approx H/6$, where H is the current value of the Hubble constant. This coincidence begs for a deeper physical explanation and points to a deep connection between the dark matter and dark energy (DE) phenomena.

To explain the Tully-Fisher relation within a ΛCDM model, one must assume that the dark matter halos of all galaxies contain just the right amount of dark matter, which is obviously not a physically motivated assumption. For this reason, the Tully-Fisher relation has been used to argue in support of modified theories of gravity, where the standard description of the gravitational interaction given by Einstein's general relativity is modified at large scales. As mentioned before, the departure from general relativity in such alternative approaches may involve modifications of the Einstein-Hilbert action, like in $f(R)$ theories [13, 118], string inspired brane-world scenarios [119], or a change of the paradigm that describes gravity by means of a metric and covariant theory. To this last class of approaches belongs Milgrom's Modified

Newtonian dynamics (MOND) [120, 121]. In the MOND framework, in which the acceleration a_0 is promoted to a fundamental constant, the gravitational acceleration is modified with respect to its Newtonian form. At distances outside a galaxy's inner core, it reads

$$a_{\mathrm{MOND}}(r) = \sqrt{a_0\, a_{\mathrm{B}}(r)}\ , \tag{0.0.4}$$

where $a_{\mathrm{B}}(r) = G_{\mathrm{N}} m_{\mathrm{B}}(r)/r^2$ is the Newtonian radial acceleration that would be caused by the baryonic mass $m_{\mathrm{B}}(r)$ inside the radius r. Phenomenologically, the simple formula (0.0.4) turns out to explain the rotation curves of galaxies surprisingly well [117, 122], although it cannot explain the mass deficit in galaxy clusters [123]. More recently, Verlinde [87] has given a controversial [124, 125] derivation of the MOND formula (0.0.4). In his work, it was shown that, when applied at galactic scales, the laws of emergent gravity contain an additional dark gravitational force, which may explain the phenomenology commonly attributed to dark matter and reproduce the MOND acceleration (0.0.4). Following Verlinde [87], the long range entanglement connecting bulk excitations with the dS horizon (i.e. the positive dark energy) generates a (thermal) volume contribution to the entanglement entropy and a subsequent competition between area and volume laws. This can be seen as an elastic response of the dark energy medium to the presence of baryonic matter which, in turn, implies an additional dark gravitational force correctly reproducing the MOND acceleration [87].

However one common problem of these approaches is the difficulty of performing a "metric-covariant uplifting" of the theory [125, 126]. In fact, such theories are usually formulated in the weak-field regime, whereas we know that gravity must allow for the metric-covariant description given by general relativity, at least at solar system scales. Fluid space-time models may provide a simple way to perform such an uplifting. For example, it is well known that de Sitter space is equivalent to the space-time of an isotropic fluid with constant energy density and equation of state $p = -\varepsilon$. Phenomenologically, galaxy rotation curves and gravitational lensing have been described using two-fluids [127, 128] and anisotropic fluid models [129–131]. It is also possible to extend such models to contain DE [132], although the physical nature of these fluid models has yet to be established.

This thesis represents a step towards the understanding of holographic and emergent properties of gravity underlined above. Our main goal is to study and clarify the deep relation between the infrared and ultraviolet regime of gravity. The holographic properties of the gravitational interaction will play a central role in the investigation of all these aspects. In particular, we will focus on black holes in the context of AdS/CFT correspondence and on the emergent properties of gravity at galactic scales in a corpuscolar picture, facing up with the dark matter problem.

The work has been organized in two different parts. In the first part we will explore various black holes and black branes solutions and their geometrical and thermodynamical properties in AdS spacetime. We will focus on the holographic principle and, in particular, on the AdS/CFT correspondence and its applications in black holes physics. We will compute the shear viscosity to entropy ratio for five dimensional charged Reinssner-Nordström and Gauss-Bonnet black branes and black holes. In particular we will investigate the behaviour of transport coefficients in the hydrodynamical limit of the dual QFTs when one goes from the IR to the UV regime of

the theory. Finally, we will study the quantum properties of two dimensional dilaton gravity, the role of symmetries and of temperature in quantum phase transitions.

In Chapter 1 we will study black holes and black branes in four and higher dimensions in presence of an electrocmagnetic field. We will focus on Lovelock gravity, a higher curvature gravity theory with second order field equations for the metric and on five-dimensional Gauss Bonnet gravity. We will also investigate gravity in two dimensions by means of scalar fields, i.e. dilaton gravity. Moreover, we will discuss the thermodynamics of these solutions with the aim to set the general framework to study their quantum properties through the AdS/CFT correspondence.

In Chapter 2 we review the AdS/CFT correspondence and, in particular, we focus on hydrodynamics. We will discuss about the definition of a hydrodynamical limit for quantum fields with gravity duals both in Minkowski and curved spacetime by means of the shear viscosity. We will define the shear viscosity in both spacetimes by means of Kubo formula by giving particular attention to the case of curved spacetime. In the final part of the Chapter we investigate the holographic principle and its applications in two dimensional dilaton gravity. We will focus on the definition of the microscopic features of the model and their possible consequences for quantum gravity at Planck scales.

In Chapter 3 we will discuss about AdS/CFT applications in two different cases. Firstly we will compute the shear viscosity to entropy ratio for five dimensional charged Reinssner-Nordström and Gauss-Bonnet black branes and black holes. In particular we will focus on the behaviour of transport coefficients in the hydrodynamical limit of the dual QFTs when one goes from the IR to the UV regime of the theory. Particular attention will be given to the interplay between thermodynamics and hydrodynamics in the case of spherical black holes. Finally we will discuss in detail about quantum properties of two dimensional dilaton gravity.

The second part of the thesis is devoted to the investigation of the emergent gravity scenario in the context of corpuscolar gravity and its applications at galactic scales. In particular, we will consider the gravitational galactic dynamics and we will present a theoretical explanation of its phenomenology in the corpuscol picture of emergent gravity without adding exotic matter. Finally we will study a possible dark matter candidate in the case of Einstein's gravity coupled to a real scalar field.

In Chapter 4 we will review both the emergent gravity paradigm presented in [87] and the corpuscolar description of gravity of Dvali *et al* [90, 91, 97, 133–137].

In Chapter 5 we shall begin with a critical discussion of various regimes of gravity in the corpuscular scenario. We will start by arguing that, describing dark energy as a critical BEC of soft gravitons (the DEC) implies not only the presence of a non-extensive regime of gravity satisfying Eq. (0.0.2), but also of an extensive regime in which $N_G \sim r^3/(L\,\ell_p^2)$. The local gravitational interaction with baryonic matter can then be naturally described in terms of gravitons pulled out from the DEC. We will first consider baryonic matter in the diluted approximation, when the local reaction of the condensate to the presence of baryonic matter can be (ideally) neglected. We will then proceed by describing what happens when we go beyond the diluted approximation and baryonic matter begins to clump. We will show that, in this regime, the reaction of the DEC to the presence of baryonic matter is also associated to gravitons pulled out from the DEC. They generate an additional gravitational dark force on baryonic probe sources, which correctly reproduces the MOND acceleration. In Chapter 6 we

will show how this description allows for an effective description in terms of general relativity sourced by an anisotropic fluid.

Finally, in Chapter 7 we will derive an exact, analytic, static, spherically symmetric, four-dimensional solution of minimally coupled Einstein-scalar gravity, sourced by a scalar field which could be a possible dark matter candidate.

Part I

Black Holes and Holography

Chapter 1

Black holes in Anti-de Sitter Spacetime

The interest in studying black holes extends from general relativity and astrophysics to quantum physics. On one side, the fact that black holes are characterized only by their asymptotic charges (mass, charge, angular momentum) and the fact that they behave as a thermodynamical ensamble makes these objects an interesting laboratory to test the limits of general relativity. On the other side, the very famous formula about black hole entropy upsets what we generically expects from thermodynamics. Moreover, it suggests the existence of a deep interplay between quantum physics and black hole thermodynamics. For example, this has led to the formulation of the so-called holographic principle and to AdS/CFT correspondence.

For these reasons, the first part of this thesis is devoted to the investigation of general features of black holes in Anti-de Sitter spacetime both from a geometric and a quantum perspective.

In the first Chapter, we study charged black branes (i.e. black holes with planar topology) and black holes in higher dimensions and, in the final part, two dimensions dilaton gravity by giving a detailed description of their geometrical and thermodynamical properties. The Chapter is mainly based on:

- M. Cadoni, A. M. Frassino and M. T., "*On the universality of thermodynamics and η/s ratio for the charged Lovelock black branes*", **JHEP 1605 (2016) 101**, arXiv:1602.05593.

- Mariano Cadoni, Edgardo Franzin and M. T., "*Van der Waals-like Behaviour of Charged Black Holes and Hysteresis in the Dual QFTs*", **Phys.Lett. B768 (2017) 393-396**, arXiv:1702.08341.

- Mariano Cadoni, Edgardo Franzin and M. T. "*Hysteresis in η/s for QFTs dual to spherical black holes*", **Eur.Phys.J. C77 (2017) no.12, 900**, arXiv:1703.05162.

- Mariano Cadoni, Matteo Ciulu and M. T., "*Symmetries, Holography and Quantum Phase Transition in Two-dimensional Dilaton AdS Gravity*", **Phys.Rev. D97 (2018) no.10, 103527**, arXiv:1711.02459.

Note: we set the speed of light as $c = 1$.

1.1 Black holes: general features

Black holes are the final state of the gravitational collapse of sufficiently massive stars ($M > 3M_\odot$). From a pure gravitational point of view they are regions of spacetime where gravity is so strong that even light cannot escape from there. At the beginning, black holes were thought to be non-physical, viz. just a mathematical solution of Einstein's equations of motion, but nowadays we have a lot of (indirect) astrophysical evidences of their existence [138].

Moreover, from a pure theoretical point of view, their existence and fate give rise to two of the most deep puzzles of contemporary fundamental physics: the information problem in the black hole evaporation process [139] and the microscopic interpretation of Bekenstein-Hawking black hole entropy [16–19].

For these reasons they are studied in many branches of physics as, for example, astrophysics [140], gravitational waves [6] or quantum gravity [141].

In general relativity (GR) and in four dimensions, the simplest black hole can be described by the Schwarzschild metric [142],

$$ds^2 = -\left(1-\frac{2GM}{r}\right)dt^2 + \frac{dr^2}{1-\frac{2GM}{r}} + r^2\left(d\theta^2+\sin^2\theta d\phi^2\right), \tag{1.1.1}$$

where M is the mass of the black hole. The surface $r = 2GM$ defines the so-called event horizon. Eq. (1.1.1) represents a spherical black hole and, for $r > 2GM$, the geometry of any object with the same mass M. A similar solution is represented by black holes with planar topology, i.e. black branes, where the 2−plane, $d\Sigma^2 = dx^2+dy^2$ replaces the 2−sphere in Eq. (1.1.1). Notice that the existence of planar black brane solution is not generic, but requires peculiar form of the sources. As we will seen later, black branes are an important class of solutions with many applications from gravity to quantum gravity, in particular for holography. A more involved solution of Einstein's equations is the Kerr metric [143] which, in Boyer-Lindquist coordinates, can be written as

$$\begin{aligned} ds^2 =& -\left(1-\frac{2GMr}{\Sigma}\right)dt^2 - \frac{4GMra}{\Sigma}dtd\phi + \frac{\Sigma}{\Delta}dr^2 + \Sigma d\theta^2 \\ &+ \left(\frac{2GMra^2\sin^2\theta}{\Sigma} + r^2 + a^2\right)\sin^2\theta d\phi^2, \end{aligned} \tag{1.1.2}$$

where $a = J/M$ is the total angular momentum per unit mass, $\Delta = r^2 - 2GMr + a^2$ and $\Sigma = r^2 + a^2\cos^2\theta$. This metric describes the spacetime outside a spinning black hole. A generalization of these two metrics to the charged case has been given in the past [144–146] even though one expects that astrophysical black holes are rotating uncharged objects. Moreover, it seems that during the collapse, once matter reaches the Schwarzschild radius all its details disappear leaving an object characterized only by its mass, its angular momentum and its charge. This important feature of black holes has led to the formulation of the so-called no-hair theorems [147, 148].

Another important and still fascinating feature of black holes is that the laws of black hole mechanics are very similar to the laws of thermodynamics. In particular, Bekenstein [16, 17] and Hawking [18, 19] discovered in the seventies of the last century that black holes are thermal objects with a characteristic temperature and entropy,

$$T_{BH} = \frac{\hbar\kappa}{2\pi k_B} \qquad S_{BH} = \frac{A_{hor}}{4\hbar G}, \tag{1.1.3}$$

where κ is the surface gravity, k_B the Boltzmann constant and A_{hor} the area of the horizon. These quantities appear to be inherently quantum gravitational, in the sense that they depend on both Planck's constant $\hbar$ and Newton's constant G. Classical black holes should be perfect absorbers that is they should not posses any temperature nor entropy. The result expressed in Eq. (1.1.3) suggests that when one goes to semi-classical gravity, the quantum corrections cannot be ignored. In ordinary thermodynamic systems, thermal properties reflect the statistical mechanics of underlying microstates. In particular, entropy is a mesure of the number of microstates of the system. However, black hole entropy is atypical: for an ordinary non-gravitational system, entropy is extensive, scaling as volume. In the case of black holes, on the contrary, it is "holographic" since it scales as an area. If the Bekenstein-Hawking entropy really counts black hole microstates, this holographic scaling suggests that a black hole has far fewer degrees of freedom than we might (classically) expect [149]. This aspect together with another puzzling topic in black hole physics, i.e. the "information loss paradox" [24, 25], are currently very active field of research. However, in this thesis we will not deal with these issues.

There are many solutions of Einstein's equations regarding black hole physics in literature. These solutions are obtained considering different sources for the gravitational field, different spacetime topologies and different spacetime asymptotics. However, in the last decades, a lot of interest has been devoted to a particular class of black holes, e.g. black holes in anti-de Sitter (AdS) spacetime and in higher dimensions [150]. In particular, this has been motivated by string theory, which requires gravity in higher dimensions and the discovery in the late nineties of the AdS/CFT correspondence. Under particular assumptions (see the next Chapter for discussions), the AdS/CFT correspondence gives a mathematical correspondence between a gravity theory in AdS spacetime in $(D+2)-$ dimensions and a dual quantum field theory in $(D+1)-$dimensions (see Ref. [151] and Chapter 2 for details). Anti-de Sitter spacetime is a maximally symmetric solution of Einstein's equation of motion with a negative cosmological constant, Λ. This means that it is a solution of Einstein's equations following from the minimization of the Hilbert-Einstein action,

$$S[g] = \frac{1}{16\pi G_{D+2}} \int d^{D+2}x\sqrt{-g}\left(R + \frac{D(D+1)}{L^2}\right), \tag{1.1.4}$$

where G_{D+2} is the $(D+2)-$Newton constant, R is the Ricci scalar and L is the (anti-)de Sitter radius, related to the cosmological constant by $\Lambda = D(D+1)/L^2$. The AdS spacetime is described by the following metric

$$ds^2 = -\left(1+\frac{r^2}{L^2}\right)dt^2 + \frac{dr^2}{1+\frac{r^2}{L^2}} + r^2 d\Omega_D^2, \tag{1.1.5}$$

where $d\Omega_D$ is the $D-$dimensional sphere (plane). We will discuss in detail the importance of this metric in the AdS/CFT correspondence perspective in the next Chapter.

Up to now, general relativity continues to be an extremely successful and well-accepted theory for gravitational phenomena. However several issues and shortcomings appeared in the theory in the last decades (e.g. the origin of dark matter and dark energy, strong gravity and so on) leading to the conclusion that Einstein's general relativity is not the final theory of gravitational interaction. This has produced several proposal for extended theories of gravity [13]. These are basically higher curvature

theories, i.e. theories where the Hilbert-Einstein action is generalized by introducing functions of the various curvature invariants. Among the various extended theories of gravity one can formulate, Lovelock gravity [152] has been a fruitful and widely explored subject [153–156]. The peculiarity of the theory is to be a higher curvature gravity theory with second-order field equations for the metric as four dimensional Einstein's gravity. This nice feature not only allows to avoid some of the shortcomings of generic higher-derivative theories (such as ghosts in the linearized excitation spectrum and ill-posed Cauchy problem) but also enables us to derive exact black hole (and black brane) solutions of the theory. As a consequence, the thermodynamics of Lovelock black holes is well known and has several interesting, nontrivial features. One of these features is that the thermal entropy [157, 158] and the holographic entanglement entropy [159] of a black hole depend on the higher-curvature gravitational couplings. It is also well understood that there are in these theories new types of phase transitions that also depend on the value of the gravitational couplings [160–163]. Among the Lovelock gravity theories, one of the most investigated cases, that will also be the main subject of this Chapter, is the five-dimensional (5D) Gauss-Bonnet (GB) theory. Specifically, GB gravity is the 2nd-order Lovelock gravity, i.e. it includes only quadratic curvature corrections in the Einstein-Hilbert action. The main reason to study 5D GB in the AdS/CFT framework is that the dual QFT lives in four spacetime dimensions. As we will see in the next two Chapters, Lovelock and GB gravity are interesting also from the holographic point of view.

From a quite different perspective, gravity in less than four dimensions has gained a lot of interest in the last decades [164–166]. Even if gravity becomes topological for $D < 4$, when particular fields such as scalar fields are coupled to it, non trivial solutions appears. This important feature opens the possibility to investigate difficult issues of quantum gravity, the AdS/CFT correspondence and black hole physics in a simplified mathematical context. Moreover lower dimensional gravity seems to be deeply related with quantum properties of spacetime at Planck scales [167, 168]. Also in the 2D case, gravitational solutions with AdS asymptotic behaviour play a prominent role. This is due to several reasons. First, the AdS/CFT correspondence in 2D and 3D has rather peculiar features, whose understanding would shed light on the whole subject [169, 170]. Secondly, black sole solutions (in particular charged ones) behaves in the extremal, near horizon limit, as two-dimensional AdS black holes.

In the next sections, we discuss and analyze features of AdS black branes and black holes holes both in higher dimensions and in two dimensions.

1.2 Black brane solutions of Lovelock gravity

Let us consider black branes (BB) that are solutions of Lovelock higher curvature gravity in $(D+2)-$dimensional spacetime coupled to the electric field. The theory is described by the following action

$$S_{tot} = \frac{1}{16\pi G_{D+2}} \int dx^{D+2}\sqrt{-g} \sum_{k=0}^{k_{max}} \alpha_k \mathcal{L}_k - \frac{1}{4}\int d^{D+2}\sqrt{-g} F_{ab}F^{ab} \tag{1.2.6}$$

where G_N is the $(D+2)$-dimensional Newton's constant, α_k are the rescaled Lovelock coupling constants and $\mathcal{L}_k$ denotes the Lovelock Lagrangian,

$$\mathcal{L}_k = 2^{-k}\delta^{a_1b_1\ldots a_kb_k}_{c_1d_1\ldots c_kd_k} R^{c_1d_1}_{a_1b_1}\cdots R^{c_kd_k}_{a_kb_k}, \tag{1.2.7}$$

being $R^{c_1 d_1}_{a_1 b_1} \cdots R^{c_k d_k}_{a_k b_k}$ the Riemann tensors. The tensor F_{ab} denotes the usual electromagnetic tensor. For the purposes of this thesis we will only consider electrically charged black branes (no magnetic components in F_{ab} will be taken into account). Using the rescaled Lovelock coupling constants,

$$L^{-2} = \alpha_0 = \frac{\hat{\alpha}_{(0)}}{D\,(D+1)}\,, \quad \alpha_1 = \hat{\alpha}_{(1)}\,, \quad \alpha_k = \hat{\alpha}_{(k)} \prod_{n=3}^{2k} (D+2-n) \quad \text{for } k \geqslant 2\,, \tag{1.2.8}$$

the field equations read

$$\sum_{k=0}^{k_{max}} \hat{\alpha}_{(k)} \mathcal{G}^{(k)}_{ab} = 8\pi G_N \left(F_{ac} F_b{}^c - \frac{1}{4} g_{ab} F_{cd} F^{cd} \right). \tag{1.2.9}$$

Each of the Einstein-like tensors $\mathcal{G}^{(k)\,a}{}_b$ defined by

$$\mathcal{G}^{(k)\,a}{}_b = -\frac{1}{2^{(k+1)}} \delta^{a\,c_1 d_1 \ldots c_k d_k}_{b\,e_1 f_1 \ldots e_k f_k} R_{c_1 d_1}{}^{e_1 f_1} \cdots R_{c_k d_k}{}^{e_k f_k}\,, \tag{1.2.10}$$

independently satisfies a conservation law $\nabla_a \mathcal{G}^{(k)\,a}{}_b = 0$. The higher-curvature terms contribute to the equations of motion only for $D > 2k-2$. For $D = 2k-2$ the higher-curvature corrections are topological, and they vanish identically in lower dimensions. Setting $\hat{\alpha}_{(k)} = 0$ for $k \geqslant 2$, one can recover the standard form of general relativity.

To describe the static, electrically charged, radially symmetric AdS Lovelock BB, we use the following line element and electromagnetic (EM) field

$$ds^2 = -f(r)\, N^2 dt^2 + f(r)^{-1} dr^2 + \frac{r^2}{L^2} d\Sigma_D^2\,, \qquad F = \frac{Q}{r^D}\, dt \wedge dr\,, \tag{1.2.11}$$

where $d\Sigma_D^2$ denotes the $D-$dimensional space with zero curvature and planar topology, whereas L is related to the cosmological constant $\hat{\alpha}_{(0)}$ by $L^{-2} = \hat{\alpha}_{(0)}/D(D+1)$.

Notice that the metric in Eq. (1.2.11) differs from that in the usual Schwarzschild gauge by a (constant) rescaling $t \to Nt$ of the time coordinate t. As we will see later, this rescaling is necessary in order to have a unit speed of light in the dual CFT.

In the notation (1.2.8), the field equations (1.2.9) reduce to the requirement that $f(r)$ solves the following polynomial equation of degree $k_{max} = \left[\frac{D+1}{2}\right]$ (see e.g., [153–156, 171–173])

$$\mathcal{P}(f) = \sum_{k=0}^{k_{max}} \alpha_k \left(\frac{\kappa - f}{r^2} \right)^k = \frac{\omega_d M_{ADM}}{N r^{D+1}} - \frac{8\pi G_N Q^2}{D(D-1)} \frac{1}{r^{2D}}\,. \tag{1.2.12}$$

Here M_{ADM} is the ADM mass of the black brane and ω_d is

$$\omega_{D+2} = \frac{16\pi G_N}{D} \frac{L^D}{V^D} \tag{1.2.13}$$

where V^D is the volume of the D-dimensional space with curvature $\kappa = 0$. The electric charge Q of the brane is

$$Q = \frac{L^D}{2V_D} \int *F\,. \tag{1.2.14}$$

Universality of black brane thermodynamics in Lovelock gravity

In order to find the thermodynamic quantities characterizing the Lovelock black brane, let us firstly introduce the effective mass M and temperature T related to the usual ADM mass M_{ADM} and Hawking temperature T_H by the relations

$$M = \frac{M_{ADM}}{N}, \quad T = \frac{T_H}{N}. \tag{1.2.15}$$

Let r_+ denotes the radius of the event horizon, determined as the largest root of $f(r) = 0$. The black brane mass M, the temperature T, the entropy S, and the gauge potential Φ are given by [153, 174–176]

$$M = \frac{1}{\omega_d L^2} r_+^{D+1} + \frac{V_D}{2(D-1)L^D} \frac{Q^2}{r_+^{D+1}}, \tag{1.2.16}$$

$$\begin{aligned} T &= \frac{1}{2\pi N} \frac{1}{\sqrt{g_{rr}}} \frac{d\sqrt{-g_{tt}}}{dr}\Big|_{r=r_+} \\ &= \frac{1}{4\pi r_+} \left[(D+1) \left(\frac{r_+}{L}\right)^2 - \frac{8\pi G_N Q^2}{D r_+^{2(D-1)}} \right], \end{aligned} \tag{1.2.17}$$

$$S = \frac{V^D}{4G_N} \left(\frac{r_+}{L}\right)^D, \quad \Phi = \frac{V_D}{(D-1)L^D} \frac{Q}{r_+^{D-1}}. \tag{1.2.18}$$

The rescaling of the physical parameters (1.2.15) of the Lovelock BB having the dimensions of energy is essentially due to the presence of the constant N^2 in the metric. The two time coordinates t and Nt correspond to using two different units to measure the energy. However, when we deal with Einstein-Hilbert branes the rescaling of the time coordinate is not necessary and we will simply set $M = M_{ADM}$ and $T = T_H$. Notice that the area-law for the entropy S always hold for the generic Lovelock black brane.

A striking feature of these thermodynamic expressions is that *they do not depend on the Lovelock coupling constants* α_k *for* $k \geqslant 2$ but only on α_0 and α_1, i.e., they depend only on the cosmological constant and on Newton constant. This means that the thermodynamic behavior of the BB in Lovelock theory is universal, in the sense that *it does not depend on the higher order curvature terms* but only on the Einstein-Hilbert term, the cosmological constant and the matter fields content (in our case the EM field). This implies, in turn, that as thermodynamic system the charged BBs of Lovelock gravity are indistinguishable from the Reissner-Nordström BBs of Einstein-Hilbert gravity. Notice that this feature is not shared by the black hole solutions of the theory, i.e., solutions with spherical or hyperbolic horizons. In fact, in the Lovelock thermodynamic expressions (see Refs. [153, 175]) the dependence on the Lovelock coupling constants $\alpha_{k\geqslant 2}$ is introduced by the dependence on the curvature κ of the $D-$dimensional spatial sections (see next sections for discussion). This dependence drops out when $\kappa = 0$.

We remark, however, that the universal thermodynamic behavior of charged Lovelock black branes is strictly true only when we choose $N = 1$ in the metric (1.2.11). As we will see later, the parameter N has to be fixed in terms of the Lovelock coupling constants $\alpha_{k\geqslant 2}$. Hence, the ADM mass and the Hawking temperature of the Lovelock BB will depend on $\alpha_{k\geqslant 2}$. The universality of the Lovelock BB thermodynamics is recovered simply by rescaling the units we use to measure the energy, i.e., by using in Eqs. (1.2.16) and (1.2.17) the effective parameters M and T instead of M_{ADM} and T_H.

In the following, we provide a detailed calculation for the case $k_{max} = 2$, i.e. GB gravity in five spacetime dimensions, which is also the most interesting case from the AdS/CFT point of view. However, we expect that most of our considerations can be easily generalized to every charged BB solution of Lovelock gravity in generic dimensions.

1.3 5D Reissner-Nordström black brane solution

Let us preliminary review some known facts about the RN BB solutions of Einstein-Maxwell gravity. This will be necessary in order to stress differences and similarities with the BB solutions of the GB theory. Setting $\alpha_k = 0$ for $k \geqslant 2$ and $D = 5$ in Eq (1.2.10), we have standard GR equations sourced by an electromagnetic field. For this choice of the parameters, Eq. (1.2.12) is a linear equation in f that gives the following solution:

$$f = \alpha_0 r^2 - \frac{\omega_5 M}{r^2} + \frac{4\pi}{3}\frac{G_N Q^2}{r^4}, \tag{1.3.19}$$

where ω_5 is given by Eq. (1.2.13) and G_N is the five dimensional Newton's constant. Performing the asymptotic limit $r \to \infty$, the function (1.3.19) reduces to $f = r^2/L^2$, i.e. AdS_5 with AdS length $L^2 = \alpha_0^{-1}$.

Setting $r^2 = Y$ in Eq. (1.3.19), the RN BB horizons are determined by the cubic equation

$$Y^3 - \omega_5 M L^2 Y + \frac{4\pi}{3} G_N L^2 Q^2 = 0. \tag{1.3.20}$$

This equation has two positive roots for

$$M^3 \geqslant 12\pi^2 \frac{G_N^2 Q^4}{\omega_5^3 L^2}, \tag{1.3.21}$$

which gives the extremal (BPS [177, 178]) bound for the RN black brane in 5D. In general, we will have an inner and outer horizon, when the bound is saturated the two horizons merge at r_0 and the RN BB becomes extremal. In the extremal case, Eq. (1.3.20) has a double root at $Y_0 = \sqrt{\omega_5 M L^2/3}$ and $f(r)$ can be factorized in the following way

$$f(r) = \frac{1}{L^2 r^4}\left(r^2 + r_0^2\right)(r - r_0)^2 (r + r_0)^2, \quad r_0 = \left(\frac{\omega_5 M L^2}{3}\right)^{1/4}. \tag{1.3.22}$$

The extremal near-horizon geometry can be determined expanding the metric near r_0 and keeping only the leading term in the metric

$$f(r) = \frac{12}{L^2}(r - r_0)^2. \tag{1.3.23}$$

A simple translation of the radial coordinate $r \to r + r_0$ gives the $AdS_2 \times R_3$ extremal near-horizon geometry with AdS_2 lenght l

$$ds^2 = -\left(\frac{r}{l}\right)^2 dt^2 + \left(\frac{l}{r}\right)^2 dr^2 + \left(\frac{r_0}{L}\right)^2 d\Sigma_3^2, \qquad l^2 = \frac{L^2}{12}. \tag{1.3.24}$$

The extremal solution given in Eq. (1.3.22) is a soliton interpolating between the asymptotic AdS_5 geometry in the UV and the $AdS_2 \times R_3$ geometry (1.3.24) in the IR.

1.4 Gauss-Bonnet black brane solution

To derive the Gauss-Bonnet black brane solution, we use the form (1.2.11) with coupling constant (1.2.8). For $k = 2$ and generic curvature κ, Eq. (1.2.12) reduces to a quadratic equation

$$\alpha_2 \frac{(\kappa - f)^2}{r^4} + \frac{(\kappa - f)}{r^2} + \alpha_0 - \frac{\omega_d M}{r^{d-1}} + \frac{8\pi G_N Q^2}{(d-2)(d-3)r^{2d-4}} = 0\,, \tag{1.4.25}$$

from which one obtains two possible solutions, $f_\pm$. In the following, we will refer to the solution f_- as the '*Einstein branch*' because it approaches the Einstein case when the Gauss–Bonnet coupling α_2 goes to zero and to f_+ as the '*Gauss–Bonnet branch*' [161]. The quadratic Eq. (1.4.25) gives the following necessary condition requirement for the existence of $f_\pm$ for large r:

$$1 - 4\alpha_0\alpha_2 \geqslant 0\,. \tag{1.4.26}$$

When this inequality is violated, the space becomes compact because of the strong nonlinear curvature [161]. Therefore, there is no asymptotic 'AdS region' and consequently no proper black hole with standard asymptotics.

5D GB black brane

In this subsection, we discuss the special case of 5D GB BB ($\kappa = 0$). Moreover, from now on we set $\alpha_1 = 1$ in order to recover the usual Newtonian limit. It is easy to check that for $D = 5$ and $\kappa = 0$, then Eq. (1.4.25) reduces to the following equation

$$\alpha_2 \frac{f^2}{r^4} - \frac{f}{r^2} + \alpha_0 - \frac{\omega_5 M}{r^4} + \frac{4\pi Q^2}{3r^6} = 0 \tag{1.4.27}$$

and the two branches are respectively

$$f_\pm = \frac{r^2}{2\alpha_2}\left[1 \pm \sqrt{1 - 4\alpha_0\alpha_2}\sqrt{1 + \frac{4M\alpha_2\omega_5}{(1-4\alpha_0\alpha_2)}\frac{1}{r^4} - \frac{16\pi G_N}{3}\frac{Q^2\alpha_2}{1-4\alpha_0\alpha_2}\frac{1}{r^6}}\right]. \tag{1.4.28}$$

In case of positive GB coupling $\alpha_2 > 0$ that satisfy the condition (1.4.26), the two branches describe two asymptotically AdS_5 spacetimes, however, from Eq. (1.4.28) one can see that f_+ has no zeroes, hence the f_+-branch does not describe a BB but a solution with no event horizon. Thus, only the f_--branch describes a BB solution.
Let us now study the asymptotic geometry of the GB BB. At leading order for $r \to \infty$ the metric coefficient $g_{tt} = N^2 f(r)$ in Eq. (1.2.11) becomes

$$g_{tt} \to N^2 \frac{r^2}{2\alpha_2}\left(1 \pm \sqrt{1 - 4\alpha_0\alpha_2}\right)\,. \tag{1.4.29}$$

In order to have the boundary of the asymptotic AdS_{D+2} conformal to $(D+1)$-Minkowski space with speed of light equal to 1, $ds^2 \approx \alpha_0 r^2(-dt^2 + d\Sigma_3^2)$, the constant N^2 has to be chosen as

$$N^2 = \frac{1}{2}\left(1 \mp \sqrt{1 - 4\alpha_0\alpha_2}\right), \tag{1.4.30}$$

where we have the $+$ sign for the f_- branch, the BB solution, while the $-$ sign has to be used when we consider the f_+ branch.

For $\alpha_2 < 0$, only the f_- branch is asymptotically AdS. Conversely, the f_+ branch describes a spacetime which is asymptotically de Sitter (dS) and can be therefore relevant as a cosmological solution.

Singularities

To determine the position of the singularities of the spacetime we calculate the scalar curvature for both the $f_\pm$ branches:

$$\begin{aligned} R^{(\pm)} = &\mp \frac{\beta r^2(20r^{10}+30\sigma r^6-31\rho r^4+6\sigma^2 r^2-9\rho\sigma)}{2\alpha_2 r^3(r^6+\sigma r^2-\rho)^{3/2}} \\ &\pm \frac{20r^3(r^6+r^2\sigma-\rho)^{3/2}+2\beta\rho^2}{2\alpha_2 r^3(r^6+\sigma r^2-\rho)^{3/2}}, \end{aligned} \tag{1.4.31}$$

where the $\pm$ sign refers respectively to the $f_\pm$ branches. To simplify expressions we used (here and after) the following notation

$$\begin{aligned} \beta =&\sqrt{1-4\alpha_0\alpha_2}, \quad \sigma = \frac{4\alpha_2\omega_5 M}{\beta^2}, \\ \rho =&\frac{16\pi G_N\alpha_2 Q^2}{3\beta^2}, \quad e = \frac{1}{\beta^2}-1 = \frac{4\alpha_0\alpha_2}{\beta^2},\ Y = r^2. \end{aligned} \tag{1.4.32}$$

There are curvature singularities at $r = 0$ and at the zeroes of the argument of the square root in Eq. (1.4.31) (branch-point singularities). The position of the physical singularities of the spacetime is therefore determined by the pattern of zeroes of the function $g(Y)$, with

$$g(Y) = Y^3 + \sigma Y - \rho. \tag{1.4.33}$$

The singularity will be located at the biggest positive zero Y_1 of $g(Y)$ or at $r = 0$ when $g(Y)$ has no zeroes for positive Y. The singularity at $Y = Y_1$ is a branch point singularity. The pattern of zeroes of $g(Y)$ is determined by the signs of the coefficients ρ, σ and the discriminant $\Delta = \left(\frac{\rho}{2}\right)^2 + \left(\frac{\sigma}{3}\right)^3$.

- For $\sigma > 0$, the function $g(Y)$ is a monotonic increasing function of Y with a single zero which, depending on the sign of ρ, will be positive $Y = Y_1$ ($\rho > 0$) or negative ($\rho < 0$). The physical spacetime singularity will be therefore located at $r = \sqrt{Y_1}$ for $\rho, \sigma > 0$ and at $r = 0$ for $\rho < 0$, $\sigma > 0$.

- For $\sigma < 0$, the function $g(Y)$ is an oscillating function with a maximum at negative Y and a minimum at positive Y, it may therefore have one, two or three zeros. For $\sigma < 0$, $\rho > 0$, $g(Y)$ has at least a positive zero. For $\sigma < 0$, $\rho < 0$ we have a positive zero for $\Delta \leqslant 0$ and no positive zeros for $\Delta > 0$. For $\Delta = 0$ we have a double zero of $g(Y)$ so that Y_1 is not anymore a branch point singularity. In this latter case the singularity is at $r = 0$.

Summarizing, the physical singularity is always located at $r = \sqrt{Y_1}$ unless $\sigma > 0, \rho < 0$ or $\sigma < 0, \rho < 0, \Delta \geqslant 0$ in which case the singularity is at $r = 0$.

f_--branch

In this subsection, we study in detail the horizons of the f_--branch, solution of Eq. (1.4.28), describing the GB black brane. In general the BB will have an inner ($r = r_-$) and outer ($r = r_+$) event horizon. The BB becomes extremal when $r_+ = r_-$. Using the notation (1.4.32), (1.4.33), one finds that the necessary condition for the

existence of the BB is the positivity of the argument in the square root in Eq. (1.4.28), i.e., $g(Y) \geqslant 0$. The position of the event horizon(s) is determined by the *positive* roots of the cubic equation

$$h(Y) = eY^3 - \sigma Y + \rho = 0. \tag{1.4.34}$$

We will first consider the case $\alpha_2 > 0$, which corresponds to $\sigma, \rho, e > 0$ (since also $\alpha_0 > 0$). The condition for the existence of real roots of the function $h(Y)$ can be easily found: the function $h(Y)$ has a maximum (minimum) for, respectively

$$Y = Y_{M,m} = \pm\sqrt{\frac{\sigma}{3e}} = \pm\sqrt{\frac{\omega_5 M L^2}{3}} \tag{1.4.35}$$

also, $h(Y = 0) = \rho > 0$, hence the cubic equation (1.4.34) always has a negative root. The existence of other roots is determined by the sign of $h(Y_m)$. We will have two (one) positive roots hence a BB with two (one) event horizons for $h(Y_m) \leqslant 0$, i.e., for

$$\rho \leqslant \frac{2}{3}\sigma\sqrt{\frac{\sigma}{3e}}. \tag{1.4.36}$$

Using Eq. (1.4.32), the previous inequality can be written in terms of the charge Q and the effective mass M and gives *the same* Bogomol'nyi-Prasad-Sommerfield (BPS) bound (1.3.21) found in the RN case. However, the BPS bound is modified when we instead express it in terms of the ADM mass:

$$M_{ADM}^3 \geqslant 12N^3\pi^2\frac{G_N^2 Q^4}{\omega_5^3 L^2}. \tag{1.4.37}$$

When the bound is saturated, the inner and outer horizon merge at $r_- = r_+$, the BB becomes extremal, and the solution describes a soliton. The striking feature of the BPS bound (1.4.36) is that the *BPS bound of* 5D *Gauss-Bonnet BB does not depend on the Lovelock coupling constant, and it is exactly the same one gets for GR ($\alpha_2 = 0$), i.e., for the* 5D *Reissner-Nordström BB.* When M does not satisfy the inequality (1.4.36), the spacetime describes a naked singularity. For $\alpha_2 > 0$, the condition $M > 0$ implies $\sigma, \rho > 0$ and the function $g(Y)$ is a monotonic increasing function which cuts the Y-axis at the point Y_1, and, in view of the previous discussion, it also gives the position of the singularity. Since, the position of the event horizon Y_h is determined by the equation

$$\beta\sqrt{g(Y_h)} = Y\sqrt{Y_h}\,, \tag{1.4.38}$$

from which follow that $g(Y_h) > 0$ hence $Y_h > Y_1$, this checks that in the region where the bound (1.4.36) holds the condition $g(Y) > 0$ is always satisfied and that the physical singularity is always shielded by two (one in the extremal case) event horizons.

The behavior of the metric function f_- for $\alpha_2, M > 0$ and selected values of the other parameters is shown in Fig. 1.1. The solid red, green and brown lines describe respectively a naked singularity, extremal and two-horizon BB geometry. The solid blue line represents a zero-charge, BB solution with single horizon. The case $\alpha_2 < 0, M > 0$ gives exactly the same BPS bound. Now, we have $\sigma, \rho, e < 0$. The function $h(Y)$ in Eq. (1.4.34) always has a negative root and a minimum (maximum) for

$$Y = Y_{m,M} = \pm\sqrt{\frac{\sigma}{3e}} = \pm\sqrt{\frac{\omega_5 M L^2}{3}}\,. \tag{1.4.39}$$

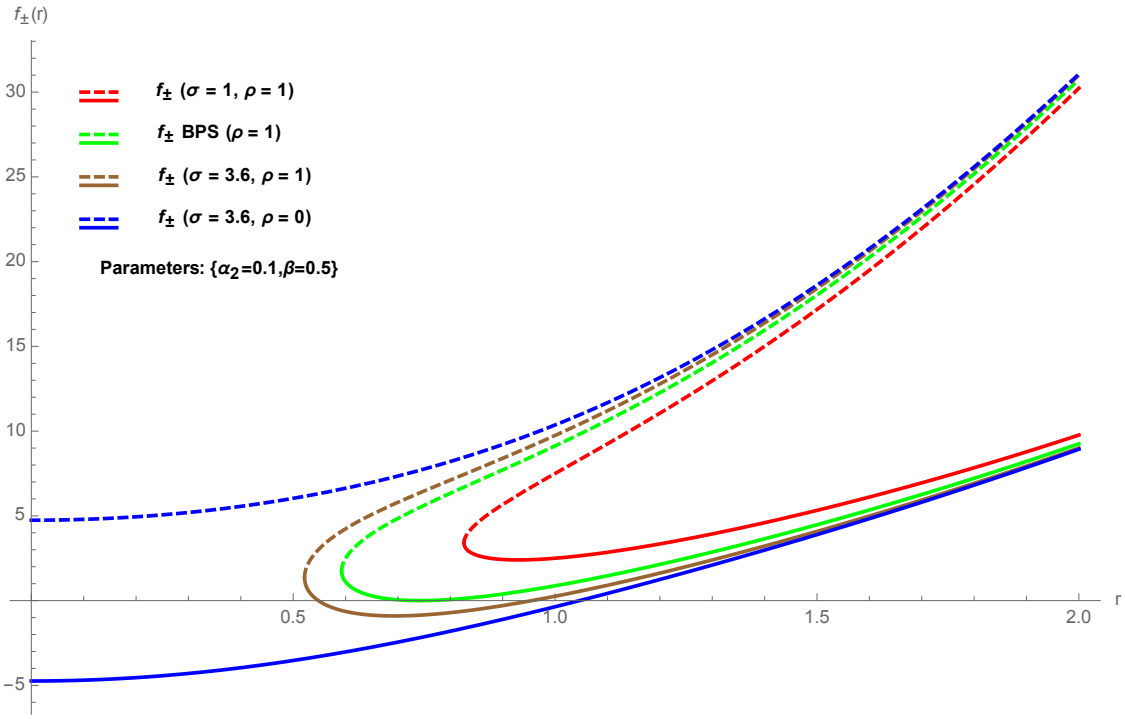

Figure 1.1: Behavior of the metric functions $f_\pm$ for $\alpha_2, M > 0$ and selected values of the other parameters. The dashed (solid) lines describe the f_+ branch (f_--branch). The red, green, brown and blue solid lines describe respectively a naked singularity, an extremal, two-horizon and vanishing charge BB geometry. The corresponding dashed lines describe spacetimes with a naked singularity.

The conditions for the existence of two positive roots become $|\rho| \leqslant \frac{2}{3}|\sigma|\sqrt{\frac{\sigma}{3e}}$ leading to the same BPS bound (1.4.36). However, there is a crucial difference from the $\alpha_2 > 0$ case. When $\alpha_2 < 0$, the condition $M > 0$ implies $\sigma, \rho < 0$. Taking into account that $|e| < 1$ owing to (1.4.26), we see that the condition $\Delta < 0$ implies the BPS bound (1.4.36). This means that the two horizons are separated by a region in which the solution does not exist. The spacetime breaks into two disconnected parts. The physical part, having an asymptotic AdS region, describes a BB with singularity shielded by a *single* event horizon. The behavior of the metric function f_- for $\alpha_2 < 0$ and selected values of the other parameters is shown in Fig. 1.2. The solid red, green and brown lines describe respectively a naked singularity, extremal and single-horizon BB geometry. The solid blue line represents a zero-charge, BB solution with horizon.

Near horizon extremal solution

When the bound (1.4.36) is saturated, the BB becomes extremal and the metric function (1.4.28) has a double zero at

$$\Upsilon_h = \Upsilon_m = \sqrt{\frac{\sigma}{3e}} = \sqrt{\frac{\omega_5 M L^2}{3}}, \tag{1.4.40}$$

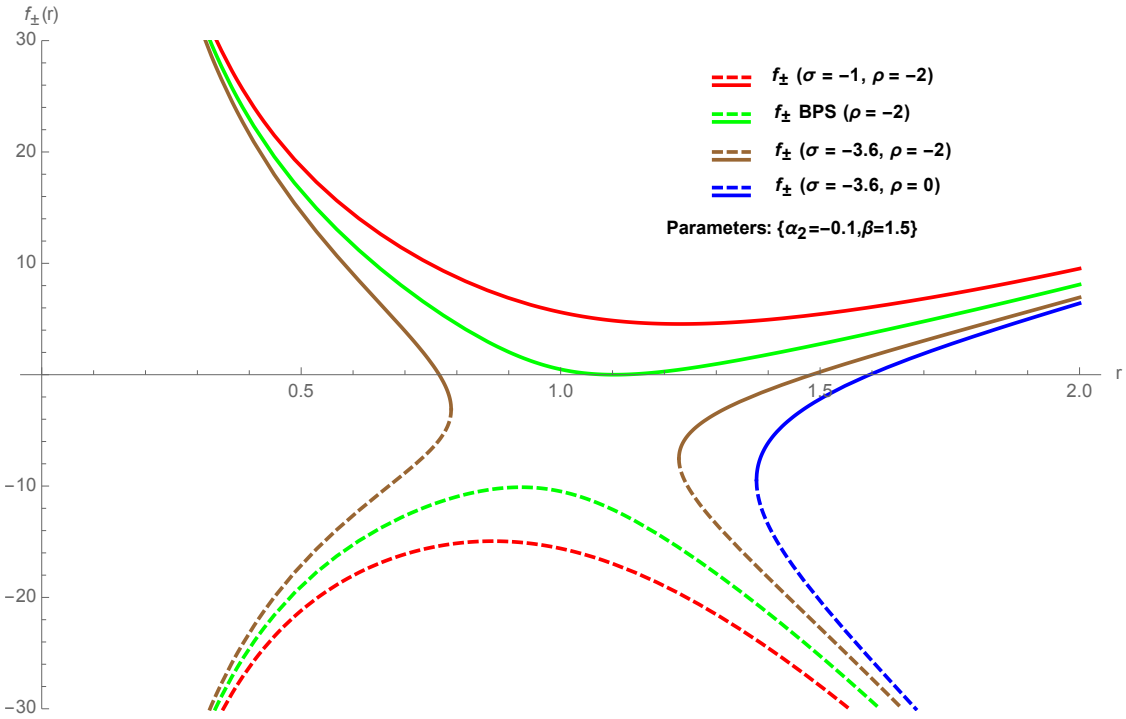

Figure 1.2: Behavior of the metric functions $f_\pm$ for $\alpha_2 < 0, M > 0$ and selected values of the parameters. The dashed (solid) lines describe the f_+ branch (f_- branch). The red, green, brown, blue solid lines describe respectively a naked singularity, an extremal, single-horizon, vanishing charge BB geometry. The corresponding dashed lines describe cosmological solutions with a singularity which approach asymptotically to the dS spacetime.

thus, the solution f_- can be factorized as

$$f_-^{(ex)}(Y) = \frac{e\beta^2}{2\alpha_2}\frac{(Y+2Y_m)(Y-Y_m)^2}{Y^2+\beta\sqrt{Y^4+\sigma Y^2-\rho Y}}. \tag{1.4.41}$$

This solution represents the extremal GB soliton.

Let us now consider the near-horizon geometry. In this regime, the solution (1.4.41) can be expanded around $r = r_0 = \left(\frac{\sigma}{3e}\right)^{1/4}$. At the leading order the Einstein branch reads

$$f_-^{(ex)}(r) = 12\alpha_0(r-r_0)^2. \tag{1.4.42}$$

Translating the radial coordinate $r \to r + r_0$ and rescaling the time coordinate as $t \to t/N$ we get the extremal, near-horizon geometry:

$$ds^2 = -\left(\frac{r}{l}\right)^2 dt^2 + \left(\frac{l}{r}\right)^2 dr^2 + \left(\frac{r_0}{L}\right)^2 d\Sigma_3^2, \qquad l^2 = \frac{1}{12\alpha_0}. \tag{1.4.43}$$

i.e., $AdS_2 \times R_3$ with the AdS_2 length l being determined uniquely by α_0. Thus, the extremal near-horizon geometry does not depend on α_2 and fully coincides with the extremal near-horizon geometry (1.3.24) one gets in the RN case.

Near horizon metric as exact solution of equations of motion

In this Section, we will show that the near-horizon solution given in Eq. (1.4.43) is an exact solution of the equations of motion (EOM). For the GB case, Eqs. (1.2.9) read

$$\begin{aligned} R_{ab} - \frac{1}{2}Rg_{ab} =& \frac{6}{L^2}g_{ab} + 8\pi G_N\left(F_{ac}F_b{}^c - \frac{1}{4}g_{ab}F_{cd}F^{cd}\right) \\ &+ \frac{\alpha_2}{2}g_{ab}\left(R_{cdef}R^{cdef} - 4R_{cd}R^{cd} + R^2\right) \\ &+ \alpha_2\left(-2RR_{ab} + 4R_{ac}R^c{}_b + 4R_{cd}R^c{}_a{}^d{}_b - 2R_{acde}R_b{}^{cde}\right) . \end{aligned} \tag{1.4.44}$$

We note that, since the Eq. (1.4.43) describes a spacetime with $AdS_2 \times R_3$ geometry, the contribution to the curvature tensors coming from the planar geometry R_3 vanishes. Thus, the EOM includes only the contribution of the AdS_2 part of the metric which is a two dimensional maximally symmetric space.

For a generic n-dimensional maximally symmetric space with $R = \Lambda$ the two terms in Eqs. (1.4.44), that are quadratic in the curvature tensors, are given respectively by

$$\alpha_2\Lambda^2\frac{(n-2)(n-3)}{2n(n-1)}, \quad -2\alpha_2\Lambda^2\frac{(n-2)(n-3)}{n^2(n-1)}. \tag{1.4.45}$$

These relations are consequence of the fact that the GB term in the action is topological for $D = 4$ and identically vanishes for $D = 2$ and $D = 3$. The previous equations imply that in the case of the $AdS_2 \times R_3$ geometry, the contributions given by the GB terms to the EOM vanish; therefore, the near horizon metric (1.4.43) is an *exact* solution of both Einstein and GB EOM. In particular, the latter reduces to the usual Einstein-Maxwell equations in 5D.

Summarizing, we have seen that the $AdS_2 \times R_3$ geometry is not only a near horizon approximation but it is an exact solution of the field equations of GB-Maxwell gravity. The presence of two exact extremal solutions (the extremal soliton interpolating through a throat region the $AdS_2 \times R_3$ geometry with the asymptotic AdS geometry and the $AdS_2 \times R_3$ geometry itself) is a typical feature of extreme black branes describing BPS states (see e.g. Refs. [179, 180]). The two solutions correspond to two different extremal limits. As we will see in Sect. 1.5, the presence of two different extremal, exact, solutions give rise to a non-trivial extremal thermodynamic behavior.

f_+ branch

This branch does not describe a BB but a spacetime with a singularity for every value of the parameters $Q \neq 0, M \neq 0$. Depending on the value of the parameter α_2 we have either a spacetime with a naked singularity (for $\alpha_2 > 0$) or a cosmological, asymptotically de Sitter (dS) solution with a singularity (for $\alpha_2 < 0$.) This follows from the above discussion of the singularities of the scalar curvature (1.4.31). In the f_+ branch the spacetime always has a singularity, which can be located at $r = 0$ or $r = \sqrt{Y_1}$ depending on the values of the parameters. This is consistent with the results of Ref. [171], according to which the f_+ branch is unstable and contains ghosts[1].

[1]In principle, one could have hoped to have a regular spacetime when the function $g(Y)$ has a double zero at positive Y. In fact in this case the branch point singularity is removed and if the spacetime in

For $M, \alpha_2 > 0$, the metric functions for the f_+ branch are the dashed lines shown in Figs. 1.1. An interesting, peculiar feature is that in this case, all the solutions of the f_- branch are continuously connected with the solution of the f_+-branch passing through the singularity. This feature has a simple analytic explanation. In the cases under consideration the singularities are the zeros of the function $g(Y)$ and when $g(Y) = 0$ then $f_+ = f_-$. This fact can have interesting holographic implications: we have two CFTs with different central charges connected through the same singularity.

For $M > 0$ and $\alpha_2 < 0$, the f_+ branch describes a cosmological solution with a singularity. The corresponding metric functions are shown (dashed lines) in Fig. 1.2. Also in this case the solutions of the f_- branch with an horizon are continuously connected with the solution of the f_+-branch passing through the singularity. We have now an asymptotically AdS solution continuously connected through a cosmological singularity to a late de Sitter geometry. On the other hand, the solutions of the f_- branch describing a naked singularity are disconnected from the cosmological solutions.

For $\alpha_2, M < 0$, the f_+ branch describes a cosmological solution with a singularity with late de Sitter behavior, whereas the f_- branch describes an asymptotically AdS spacetime with a naked singularity. However, here the two branches are disconnected. The metric functions for this case are shown in Fig. 1.3.

It should be stressed that in the $Q = 0$ case, the f_+ branch has ghosts in the spectrum [171]. We naturally expect this to extend to the charged case and is consistent with the intrinsic instability of these branch of solutions connected with the presence of naked singularities.

1.5 Charged GB black brane thermodynamics

In this Section, we will study the thermodynamics of the GB BB solutions, i.e. solutions in the f_- branch and make a comparison with the Reissner-Nordström black branes.

The effective thermodynamic potentials $M = M_{ADM}/N, S, \Phi$ and the temperature $T = T_H/N$ can be written as functions of the horizon radius r_+ and the charge Q by specializing Eqs. (1.2.16), (1.2.17), (1.2.18) to $D = 5$. We obtain the following equations

$$M = \frac{r_+^4}{\omega_5 L^2}\left(1 + \frac{4\pi}{3}\frac{G_N Q^2 L^2}{r_+^6}\right), \tag{1.5.46}$$

$$T = \frac{1}{\pi L^2}\left(r_+ - \frac{2\pi G_N Q^2 L^2}{3 r_+^5}\right),$$

$$S = \frac{V_3}{4G_N}\left(\frac{r_+}{L}\right)^3, \quad \Phi = \frac{V_3}{2L^3}\frac{Q}{r_+^2}, \tag{1.5.47}$$

that satisfy the first principle $dM = TdS + \Phi dQ$. As pointed out in Sect. 1.2, because of the universality of the thermodynamic behavior, the thermodynamic relations (1.5.46) hold for both for the charged GB and the RN BB. The only difference is that for the

the region $Y_1 \leqslant Y < \infty$ is geodesically complete we have regular, solitonic geometry. The function $g(Y)$ has a double zero at positive Y for $\sigma, \rho < 0$, $\Delta = 0$, but unfortunately the spacetime cut at $Y = Y_1$ thus it is not geodesically complete.

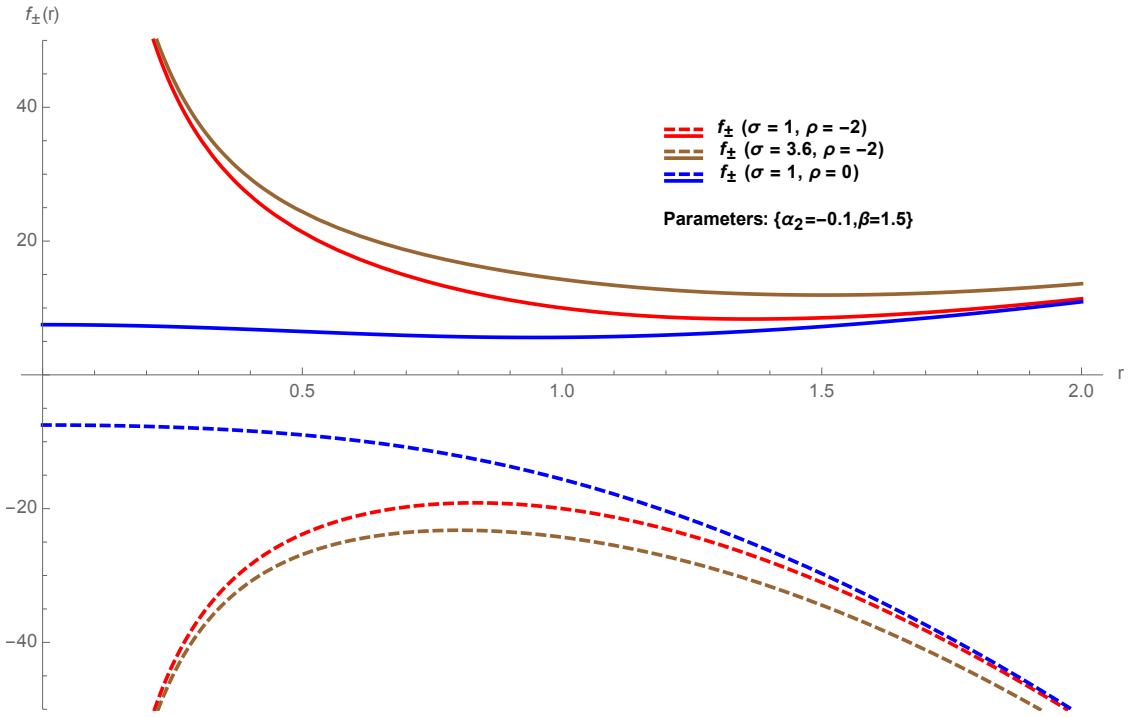

Figure 1.3: Behavior of the metric functions $f_\pm$ for $\alpha_2, M < 0$ and selected values of the other parameters. The dashed (solid) lines describe the f_+ branch (f_-branch). The solid lines describe spacetimes with naked singularities, whereas the dashed lines describe cosmological, asymptotically dS solutions with a singularity.

GB brane, with metric function (1.4.28), M and T are the effective parameters whereas in the RN case $M = M_{ADM}$ and $T = T_H$.

In order to have a clear and complete description of the GB BB thermodynamics, one should eliminate r_+ from the Eqs. (1.5.46) and write $M(T,Q)$, $S(T,Q)$. This parametrization cannot be done in analytic form because we have to solve a 6^{th} grade equation in r_+. Thus, we will derive the explicit scaling behavior of M and S as a function of the temperature in the large and small T limit. These relations will shed light on the holographic interpretation of the solutions. The functions $M(T,Q)$ and $S(T,Q)$ can be obtained in implicit form by using the second equation in (1.5.46) as an implicit definition of the function $r_+(T,Q)$, and they read

$$M(T,Q) = \frac{r_+^3}{\omega_5 L^2}\left(3r_+ - 2\pi L^2 T\right), \qquad S(T,Q) = \frac{V_3}{4G_N}\left(\frac{r_+}{L}\right)^3. \tag{1.5.48}$$

Let us now consider separately the two limits of interest: $T \to \infty$ and $T \to 0$.

Large temperature

The limit $T \to \infty$ corresponds to large radius BB, i.e., $r_+ \to \infty$. In this regime, the temperature scales linearly with r_+

$$T \simeq \frac{r_+}{\pi L^2} \tag{1.5.49}$$

and, at the leading order, we get for M and S

$$M = \frac{3V_3 L^3}{16\pi G_N}(\pi T)^4, \qquad S = \frac{V_3 L^3}{4G_N}(\pi T)^3. \tag{1.5.50}$$

This is exactly the scaling behavior one expects for a UV fixed point described by a CFT_4.

Because of the universality of the thermodynamic behavior, the relations (1.5.50) hold for both the RN and the GB BB. In the former case, Eqs. (1.5.50) hold when $M = M_{ADM}, T = T_H$, in the latter when M, T are given by the effective values in Eq. (1.2.15). Thus, for the GB BB, mass and entropy acquire a $1/N^3$ factor.

Finally, let us focus on an interesting quantity, whose meaning will be more clear in the next Chapter, i.e. the so called central charge, c. It is of particular interest in the case of AdS/CFT correspondence and quantum field theory, since the central charge of the dual CFT is determined by the AdS length. The CFTs dual to GB gravity in both branches ($f_\pm$) have central charge different from the RN case. Only in the $\alpha_2 \to 0$ limit the central charge of the f_--branch coincides with that of the CFT dual to the RN theory. However, a naive computation of the central charge in terms of the AdS length does not work in this case because of the rescaling of the time coordinate. One way to compute c is to use the scaling law of the mass and entropy as a function of the temperature. In fact, the central charge c of the associated CFT is determined by the proportionality factor and can be easily calculated. In the case of the RN BB, when $M = M_{ADM}$ and $T = T_H$ in Eq. (1.5.46), we have $c \propto L^3/G_N$. On the other hand, in the GB BB case, we have seen that the same thermodynamic relations (1.5.46) hold for M, T given by the effective values in Eq. (1.2.15) and we will get from Eqs. (1.5.50)

$$c \propto \frac{L^3}{N^3 G_N}. \tag{1.5.51}$$

Small temperature

The $T \to 0$ thermodynamic behavior corresponds to extremal BBs in which the BPS bound (1.4.37) is saturated. This is achieved at non vanishing, constant value of the BB radius

$$r_+ = \left(\frac{2\pi G_N L^2 Q^2}{3}\right)^{1/6} \equiv r_0 \tag{1.5.52}$$

that corresponds, as expected for BPS states, to the extremal brane $T = 0$ state with non vanishing mass and entropy given by

$$M_{ext} = \frac{3r_0^4}{2\omega_5 L^2}, \qquad S_{ext} = \frac{V_3}{4G_N}\left(\frac{r_0}{L}\right)^3. \tag{1.5.53}$$

We can now expand in Taylor series the temperature near r_0 to obtain

$$T \simeq \frac{3}{\pi L^2}\left[2(r_+ - r_0) - \frac{5}{r_0}(r_+ - r_0)^2\right], \tag{1.5.54}$$

and the behavior of M and S near $T = 0$ is of the form

$$M - M_{ext} = \frac{2r_0^2}{3\omega_5}(\pi L T)^2 + \mathcal{O}(T^4), \quad S - S_{ext} = \frac{\pi r_0^2 V_3}{8G_N L} T + \mathcal{O}(T^2). \tag{1.5.55}$$

Again, universality of the thermodynamic behavior implies that the relations in Eq. (1.5.55) hold both for the RN and for the GB BB. For the RN case, the relations take the same form with $M = M_{ADM}$ and $T = T_H$. For the GB case, when we express the relations (1.5.55) in terms of ADM mass and Hawking temperature we get

$$\begin{aligned} M_{ADM} &= N M_{ext} + \frac{2r_0^2}{3N\omega_5}(\pi L T_H)^2 + \mathcal{O}(T^4) \\ S &= S_{ext} + \frac{\pi r_0^2 V_3}{8N G_N L} T_H + \mathcal{O}(T^2). \end{aligned} \tag{1.5.56}$$

Excitations near extremality and near-horizon limit

An important feature of the RN BB, which in view of the previous results extends to the charged GB BB, is that the semi-classical analysis of its thermodynamic behavior breaks down near extremality [179, 180]. In fact, the energy of an Hawking radiation mode is of order T_H and the semi-classical description breaks down when this energy is comparable with the energy above extremality $M - M_{ext}$ given by Eq. (1.5.55). This results in an energy gap for excitations above extremality [179], which in the case under consideration is $E_{gap} \sim (N\omega_5)/L^2 r_0^2$. The fact that the extremal limit is singular can be also understood in geometrical terms. It has been observed that at extremality the geometry splits into two spacetimes: an extremal black hole and a disconnected AdS space [181].

The presence of this energy gap has important consequences for what concerns the spectrum of BB excitations near extremality. In particular, whereas in the extremal case the near-horizon geometry is given, as shown in Sect. 1.4, by $AdS_2 \times R_3$, finite energy excitations of $AdS_2 \times R_3$ are suppressed. Analogously to the RN case in 4D [179], one can consider near-horizon limits not restricted to zero temperature and excitation energy. These limits are obtained by letting the 5D Planck length L_P go to zero, holding fixed some of the other physical parameters of the BB (energy, charge and temperature).

1.6 Black holes solutions in five dimensions

In the previous Sections we have considered charged black brane solutions in both the Maxwell-Einstein theory and the GB theory. In this Section we will extend our considerations to black holes in the same theories, i.e. to solutions with horizons with spherical topology.

In particular, differently from the BB case, the thermodynamics and the BPS bound depend on the GB coupling constant, i.e. they are not anymore universal. As we will see later this has important consequences on the phase portrait of charged Black holes both in the Einstein and GB theory.

Geometrical features of 5D GB black holes

Let us consider the field equations of five-dimensional Einstein-Gauss-Bonnet gravity in (1.2.9) in the following form

$$G_{(1)}{}^b_a + \alpha_2 \, G_{(2)}{}^b_a = 8\pi G_5 \, T_{(M)}{}^b_a \,, \tag{1.6.57}$$

where $G_{(1)}{}^{b}_{a} \equiv R^{b}_{a} - \frac{1}{2}R\delta^{b}_{a}$ is the Einstein tensor, α_2 is the GB coupling constant, G_5 is the five-dimensional Newton constant and $T_{(M)}{}^{b}_{a}$ is the stress-energy tensor [153, 157, 163]. The tensor $G_{(2)}{}^{b}_{a}$ is the GB contribution already seen in Eq. (1.4.44),

$$G_{(2)}{}^{b}_{a} \equiv R_{ca}{}^{de}R_{de}{}^{cb} - 2R^{c}_{d}R_{ca}{}^{db} - 2R^{c}_{a}R^{b}_{c} + RR^{b}_{a} - \frac{1}{4}\delta^{b}_{a}\left(R_{cd}{}^{ef}R_{ef}{}^{cd} - 4R^{d}_{c}R^{c}_{d} + R^2\right). \tag{1.6.58}$$

For later convenience we define $\lambda \equiv \alpha_2/L^2$, being L the AdS length. In the case under study, the source term contains only a negative cosmological constant and an electromagnetic field. In particular, we consider static BH solutions to (1.6.57) i.e. solutions with spherical horizons in the form

$$ds^2 = -f(r)\,dt^2 + \frac{dr^2}{f(r)} + r^2\,d\Omega_3^2\,. \tag{1.6.59}$$

For the AdS-RN BHs of GR the metric function is

$$f_{RN}(r) = 1 + \frac{r^2}{L^2} - \frac{8G_5M}{3\pi r^2} + \frac{4\pi G_5Q^2}{3r^4}\,, \tag{1.6.60}$$

while, in the branch that allows for BH solutions, the metric function for GB gravity is

$$f_{GB}(r) = 1 + \frac{r^2}{2\ell L^2}\left[1 - \sqrt{1 - 4\ell L^2\left(\frac{1}{L^2} - \frac{8G_5M}{3\pi r^4} + \frac{4\pi G_5Q^2}{3r^6}\right)}\right]. \tag{1.6.61}$$

In Eqs. (1.6.60) and (1.6.61), M and Q are, respectively, the BH mass and charge.

Black holes in Gauss-Bonnet gravity

As in the black brane case, asymptotically AdS BH solutions of GB gravity exist only for $\lambda < 1/4$. Moreover, it is known that the unitarity bounds for the dual QFT constrain the value of λ [77, 175, 182], so that we will take λ in the following range $0 < \lambda \leqslant 9/100$.

The BH horizons are determined by the positive zeroes of the function

$$h(Y) = \frac{Y^3}{L^2} + Y^2 - \sigma Y + \rho\,, \tag{1.6.62}$$

where $Y = r^2$, $\sigma = 8G_5M/3\pi - \lambda L^2$, $\rho = 4\pi G_5Q^2/3$. The BH becomes extremal when $h'(Y) = 0$.

Asymptotically AdS BH solutions with inner (r_-) and outer (r_+) horizons exist for

$$M \geqslant \frac{3\pi}{8G_5}\left[\lambda L^2 + \frac{L^2}{3}\left(z_0^2 + 2z_0\right)\right], \tag{1.6.63}$$

where z_0 is the real, positive solution of the cubic equation $2z^3 + 3z^2 - 27\rho/L^4 = 0$. This is the BPS bound for GB BHs, which is analogue to that obtained for GB black branes (see Eq. Eq. (1.4.37)). It is important to stress that, diffrently from the BB case, the bound Eq. (1.6.63) depends on the GB coupling constant. As already remarked this is a quite generic feature of the BH solutions of GB gravity opposed to the BB solutions of the same theory, which as we will see later is also shared by the thermodynamics.

When the inequality is saturated, the inner and outer horizons merge, i.e. the BH becomes extremal and in the near-horizon regime the solution factorizes as $AdS_2 \times S^3$

$$ds^2 = -\frac{r^2}{l^2}\,dt^2 + \frac{l^2 dr^2}{r^2} + r_0^2\,d\Omega_3^2\,, \tag{1.6.64}$$

where r_0 is BH radius at extremality, determined by the solution $Y_0 = r_0^2$ of the cubic equation

$$h_{ext}(Y) = \frac{2Y^3}{L^2} + Y^2 - \rho = 0\,, \tag{1.6.65}$$

and l is the AdS_2 length

$$l^{-2} = \frac{2h''(r_0)}{r_0^2 + 2\lambda L^2} = \frac{2(6r_0^2 + 2L^2)}{L^2(r_0^2 + 2\lambda L^2)}\,. \tag{1.6.66}$$

For the moment, let us concentrate on the extremal GB black hole in Eq. (1.6.64). As already seen in the previous Sections, in the BB case we have found the remarkable property that the extremal, near-horizon solution of the charged GB black brane is exactly the same as the RN black brane. One can easily show that this is not the case for the extreme, near-horizon GB black hole. In the RN case the extremal, near-horizon, solution, which actually is an exact solution of the field equation is the $AdS_2 \times S_3$ geometry (S_3 is the three sphere), i.e. the direct product of two maximally symmetric spaces, respectively with negative curvature $R^{(2)} = -2/l^2$ and positive curvature $R^{(3)} = 12/L^2$, where l and Λ can be written in terms of the 5D cosmological constant and the $U(1)$ charge Q.

Using Eqs. (1.4.45) one can show that the individual contributions of the AdS_2 and S_3 spaces to the two terms in Eq. (1.4.44) that are quadratic in the curvature tensors vanish. Nevertheless there are still some cross-product contributions arising from the mixing of AdS_2 and S_3 terms. Splitting the 5D indices (a, b) into $\mu, \nu = 0, 1$ (running on AdS_2) and $i, j = 1, 2, 3$ (running on S_3) it easy to show that the contribution to the μ, ν components and to the i, j one of the field equations are different.

We see that the $AdS_2 \times S_3$ solution of the RN field equations cannot be also solution of the GB field equations. Obviously, this not prevents the existence of a *different* $AdS_2 \times S_3$ solution, i.e. a solution with different curvatures for AdS_2 and S_3. However, from the structure of the field equations and from Eqs. (1.4.45) one can infer that these solutions, if existing, imply a dependence of l and/or L not only from the 5D cosmological contant and from the black hole charge Q but also from the GB coupling constant α_2.

The BH thermodynamical parameters temperature T, mass M and entropy S can be expressed in terms of the horizon radius r_+ as [153]

$$T(r_+) = \frac{\frac{4r_+^4}{L^2} + 2r_+^2 - \frac{8\pi G_5 Q^2}{3r_+^2}}{4\pi r_+(r_+^2 + 2\lambda L^2)}, \tag{1.6.67}$$

$$M(r_+) = \frac{3\pi r_+^4}{8G_5}\left(\frac{1}{L^2} + \frac{1}{r_+^2} + \frac{\lambda L^2}{r_+^4} + \frac{4\pi G_5 Q^2}{3r_+^6}\right), \tag{1.6.68}$$

$$S(r_+) = \frac{\pi^2 r_+^3}{2G_5}\left(1 + \frac{6\lambda L^2}{r_+^2}\right). \tag{1.6.69}$$

The spherical geometry of the horizon introduces another scale in the system, i.e. the radius of the sphere, which couples in a non-trivial way to the higher-curvature terms in the equations of motion (1.6.57). This scale introduces dependence on the GB coupling in the mass bound (1.6.63) and in the thermodynamical expression (1.6.67) to (1.6.69). As a result, the thermodynamical and near-horizon behaviors of the GB BHs are completely different from their brane counterparts. Indeed, for charged GB black branes, such behaviors are universal, i.e. do not depend on λ, and are essentially the same of the RN black branes of GR [183]. Instead, in the case of GB black holes, their thermodynamics is different from the one of RN black holes[2] due to the presence of the coupling constant λ.

Notice that although the extremal radius r_0 is determined only by the BH charge and the cosmological constant, the AdS_2 length l and hence the extremal geometry (1.6.64) depend on the GB coupling constant. Notice also that the expression in the parenthesis in Eq. (1.6.67) is proportional to $h_{ext}(Y_+)$ meaning that the extremal geometry is obtained at zero temperature.

The thermodynamical parameters (1.6.67) to (1.6.69) near-extremality are

$$T(r_+) = \frac{2}{\pi L^2}\frac{3r_0^2+L^2}{r_0^2+2\lambda L^2}(r_+-r_0) + \mathcal{O}\left((r_+-r_0)^2\right), \tag{1.6.70}$$

$$\begin{aligned} M(T) = {} & \frac{3\pi}{8G_5}\left(\frac{3r_0^4}{L^2}+2r_0^2+\lambda L^2\right) \\ & + \frac{3\pi^3}{8G_5}\frac{L^2(r_0^2+2\lambda L^2)^2}{L^2+3r_0^2}T^2 + \mathcal{O}\left(T^3\right), \end{aligned} \tag{1.6.71}$$

$$\begin{aligned} S(T) = {} & \frac{\pi^2 r_0^3}{2G_5}\left(1+\frac{6\lambda L^2}{r_0^2}\right) \\ & + \frac{3\pi^3}{4G_5}\frac{L^2(r_0^2+2\lambda L^2)^2}{L^2+3r_0^2}T + \mathcal{O}\left(T^2\right). \end{aligned} \tag{1.6.72}$$

The first terms in expressions (1.6.71) and (1.6.72) represent, respectively, the BH mass and entropy at extremality.

Phase structure of AdS-Reissner-Nordström black holes

Although the metric function f_{GB} in Eq. (1.6.61) is singular for $\lambda = 0$, the thermodynamical behavior of the charged AdS-RN solution can be simply obtained by putting $\lambda = 0$ in Eqs. (1.6.63) and (1.6.67) to (1.6.69).

To characterize the phase structure of these BHs, one can distinguish between two cases: fixed electric potential or fixed electric charge [184, 185]. In this thesis we only discuss the canonical ensemble, i.e. we work at fixed charge. We will not consider the grand canonical ensemble, i.e. the case of fixed chemical potential. As the charge of BH decreases to a critical value $Q_c = L^2/6\sqrt{5\pi}$, the system undergoes a second-order phase transition. Below the critical charge, there are three possible branches of solutions that depend on the radius and therefore on the temperature of the system. For small temperatures, a small BH is the only locally stable solution; as the temperature increases, we have a meta-stable configuration describing intermediate BHs; for sufficiently high temperatures, large BHs are globally preferred — see Fig. 1.4.

[2]To obtain the thermodynamics of RN black holes is sufficient to put $\lambda = 0$ in Eqs. (1.6.67) to (1.6.69).

The evolution from small to large BHs through the meta-stable region corresponds to a first-order phase transition. Above the critical charge, the BH solution is always globally preferred. This behavior can be understood by analyzing the temperature as a function of the BH radius given by Eq. (1.6.67) with $\lambda = 0$. For $Q > Q_c$ it is a monotonic function, whereas it develops local extrema for $0 < Q < Q_c$ and an inflection point for $Q = Q_c$. Notice that the case $Q = 0$ is not included in the range of existence of the first order phase transition. In fact, $Q = 0$ corresponds to the AdS-Schwarzschild BH. The phase portrait of the AdS-RN BHs is very similar to a liquid/gas Van der Waals phase transition where the BH temperature plays the role of the pressure, the BH radius that of the volume and the BH charge that of the temperature [184, 185]. This portrait has been extended by Kubizňák *et al.* in Refs. [186, 187] and to topological AdS BHs in massive gravity [188].

Let us conclude with a brief comment on the zero-charge limit. For $Q = 0$, the metric (1.6.60) reduces to that of an AdS-Schwarzschild BH. However, from the thermodynamical point of view, this limit is singular. We have a discontinuity at $Q = 0$, we cannot obtain the phase diagram of an AdS-Schwarzschild BH as the $Q \to 0$ limit of the AdS-RN one. In fact, the BH temperature as a function of the radius, Eq. (1.6.67), when $Q = 0$ becomes a monotonic function and shows no Van der Waals-like behaviour as in the RN case [189].

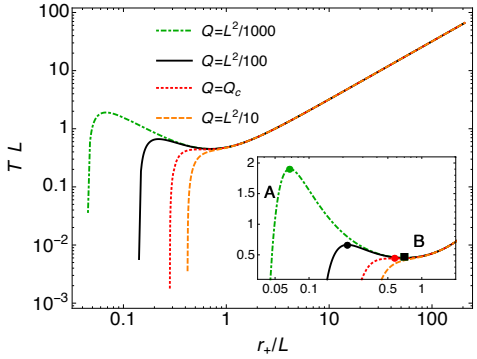

Figure 1.4: Plot of the function $T(r_+)$ for selected values of Q above, at and below the critical charge Q_c. Inset: Zoom in the region where the function has local extrema. The dots and squares mark the critical temperatures. A and B denote, respectively, the small and large black hole stable regions. Notice that the minima of the $Q = L^2/1000$ and $Q = L^2/100$ curves almost coincide.

Phase structure of neutral Gauss-Bonnet black holes

Neutral GB BH solutions and their thermodynamical parameters are obtained by putting $Q = 0$ in Eqs. (1.6.61) and (1.6.67) to (1.6.69). These BHs are characterized by the absence of a regular, zero temperature extremal limit which, in turns, means the absence of an IR fixed point for the dual QFT in the holographic description. For positive λ, the $T = 0$ extremal limit is a state with $r_+ = 0$, zero entropy and positive non-vanishing mass. Therefore, the small temperature thermodynamical behavior is always singular.

Neutral GB BHs exhibit an interesting phase structure. Differently from Einstein gravity, where small BHs are not stable and a thermal AdS state is energetically pre-

ferred [151, 190], in GB gravity there exists a stable small BH.[3] It starts with a small positive free energy, becomes unstable and evolves to a thermal AdS phase. Additionally, we also have the usual stable BH phase for large radii [192]. By inspecting the behavior of the specific heat and the free energy, one finds that the phase structure of neutral GB BHs strictly depends on the values of the GB coupling constant and the BH radius [163]. For values of the GB coupling constant below the critical one, $\lambda_c = 1/36$, there are three different branches of solutions that correspond to small, intermediate and large BHs. The specific heat is positive in the first and third branch, whereas it is negative in the second branch. This behavior is a consequence of the fact that $T(r_+)$ given by Eq. (1.6.67) with $Q = 0$ is monotonically increasing for $\lambda > \lambda_c$, whereas it develops local extrema for $\lambda < \lambda_c$ [163]. For $\lambda \geqslant \lambda_c$ the second branch disappears and BHs are always locally stable but not necessarily globally preferred. Computing the free energy one finds that the BH solution is globally stable and energetically preferred with respect to thermal AdS in the parameter region $\lambda_1(r_+) \leqslant \lambda \leqslant \lambda_2(r_+)$, where $\lambda_1(r_+)$ and $\lambda_2(r_+)$ are some functions of the horizon radius [163]. Outside this region we have a Hawking-Page phase transition, BHs become globally unstable and thermal AdS is energetically preferred. Therefore, in the parameter region where BHs are energetically preferred with respect to thermal AdS, the phase diagram of uncharged GB BHs has the same Van der Waals form described in the previous section for AdS-RN BHs and shown in Fig. 1.4, with the GB parameter λ playing the role of the BH charge Q.

Analogously to the $Q \to 0$ limit, also the limit $\lambda \to 0$ is singular from the thermodynamical point of view. In fact for $\lambda \to 0$ one cannot recover the phase diagram of an AdS-Schwarzschild BH. First, the metric (1.6.61) becomes singular. Second, similarly to what we have seen for charged BHs in GR, the temperature as a function of the horizon radius exhibits a a discontinuous behavior in the $\lambda \to 0$ limit. The limits $Q \to 0$ and $\lambda \to 0$ have a similar singular behavior also in the case of charged GB BHs.

Phase structure of charged Gauss-Bonnet black holes

The thermodynamical description of charged GB BHs is determined by the GB coupling constant λ and the charge Q. There are critical values of these parameters such that these BHs can exhibit the typical Van der Waals gas behavior in the T-S plane [193, 194].[4] Thus, charged GB BHs possesses both the Hawking-Page phase transition [190, 195] and a second-order one [194]. The former represents the transition from a stable AdS thermal state to a stable BH spacetime. Let T_c be the r_+-dependent critical value of the temperature and $r_c^2 = 6\lambda L^2$. Then, for $T > T_c$ and $r_+ > r_c$ (or $T < T_c$ and $r_+ < r_c$) AdS is preferred with respect to the BH, whereas for $T < T_c$ and $r_+ > r_c$ (or $T > T_c$ and $r_+ < r_c$), the BH is preferred with respect to AdS. It is remarkable that due to presence of λ and Q, the standard critical point becomes a critical line in the T-r_+ phase diagram [195].

Again, the phase portrait has the Van der Waals-like form described in the previous two subsections if one considers only the parameter region where the BH phase is globally preferred with respect to the thermal AdS phase and if one holds either Q or λ fixed. In the former (latter) case, at the critical value λ_c (Q_c) the system undergoes

[3] Small BHs can be gravitationally unstable for values of λ larger than those considered here [191].

[4] This is analogous to consider the cosmological constant as a pressure term in the BH equation of state [161].

a second-order phase transition. For $\lambda < \lambda_c$ ($Q < Q_c$), varying the temperature we have again a stable small BH phase and a stable large BH phase connected by a metastable phase. Moreover, the function $T(r_+)$ has always the typical behavior described in Sects. 1.6 and 1.6.

1.7 2D dilaton gravity

The previous Sections have been devoted to the investigation of charged black brane and black hole solutions of general relativity and GB theory in $D \geqslant 5$. We have seen that quite generically in the near-horizon and near extremal regime the black hole (black brane) solutions are described by an $AdS_2 \times S_3$ ($AdS_2 \times R_3$) geometry. This is not only true for higher dimensional solutions which are asymptotically AdS, thus asymptotically flat solutions. In these particular regimes the spacetime therefore allows for an effective 2D description that, in most of the cases, can be modelled by a 2D dilaton gravity theory. This will be the subject of this Section.

Two-dimensional (2D) dilaton gravity models have a long history (see Refs. [164–166] for a review). They have been first proposed for studying quantum gravity in a simplified context [167]. Later, they have been developed along several different directions as an arena to understand gravity in a simplified setting, as effective description of the radial modes (the S-wave sector) of black holes [196] and as toy models for black hole evaporation and related information puzzles [197]. 2D dilaton gravity models have been also used to explore the AdS/CFT correspondence in two dimensions [27, 169, 170, 198] and to investigate the microscopic origin of the Bekenstein-Hawking black hole entropy [27].

The most interesting fact is that from a pure gravitational perspective, 2D gravity is topological, in the sense that Einstein's gravity does not exist in a line: the Einstein's tensor vanishes identically and the Einstein-Hilbert action is purely a surface term and it does not lead to any field equation. For this reason one should invent a model in $(1+1)$ dimensions which contains a non-trivial gravitational dynamics. This can be done by introducing an additional gravitational variable, a world scalar Lagrange multiplier field μ, with which, together with the Riemann scalar, one can construct non-trivial actions, e.g.

$$\mathcal{L} = \sqrt{-g}\mu(R - \lambda) \tag{1.7.73}$$

where λ is a cosmological constant. This model is called the Jackiw-Tetelboim model (JT). However, this model was discarded very quickly since it was soon realized that similar theories arise in a limit of string theory [164]. Another particularly popular model is given by the Callan-Giddings-Harvey-Strominger Lagrange density [197],

$$\mathcal{L} = \sqrt{-g}(\mu R - \lambda). \tag{1.7.74}$$

where the scalar field μ was actually called "dilaton". A generalization of this model was recently proposed by Almheiri and Polchinksi (AP). This model has been investigated in the past in diffrent contexts and with different purposes. However, the main motivation behind this proposal was to understand the infrared (IR) behavior of higher-dimensional black holes, which flow in the IR to an $AdS_2 \times S_D$ spacetime. Among many others, this is for instance the case of charged Reissner-Nordström black

holes in general relativity. The IR behavior of these black holes is problematic for several reasons. In fact, the $T = 0$ extremal black hole is a zero temperature vacuum state with non vanishing entropy and the backreaction is so strong that there are no finite energy excitations above the vacuum [179, 199, 200].

The AP dilaton gravity model coupled to a matter field, f, is described by the action [83] (we set the dimensionless Newton constant to $G_2 = 1/8\pi$)

$$S = \int d^2x \left[\frac{1}{2}\sqrt{-g}\,(\mu R - V(\mu)) + \mathcal{L}_m\right] + \int dt \mathcal{L}_b, \tag{1.7.75}$$

where μ is a scalar field (the dilaton). The matter and boundary Lagrangian $\mathcal{L}_m$, $\mathcal{L}_b$ are given by

$$\mathcal{L}_m = -\frac{1}{8}\sqrt{-g}(\nabla f)^2, \qquad \mathcal{L}_b = \sqrt{|h|}\mu\mathcal{K}, \tag{1.7.76}$$

where h_{ij} is the induced metric on the boundary and $\mathcal{K}$ is the trace of the second fundamental form. The potential for the dilaton is

$$V(\mu) = 2\lambda^2(\alpha^2 - \mu). \tag{1.7.77}$$

Notice that the potential contains a dimensionless parameter α^2 and a parameter λ with dimensions $[L]^{-1}$.

The AP model extends the well-known Jackiw-Teitelboim (JT) model [167], characterized by a simple homogeneous potential, by including the constant term $2\lambda^2\alpha^2$.

The most important feature of the AP model is that it allows for two kinds of vacuum AdS solutions. One with constant dilaton, pure AdS_2, to which we will refer as constant dilaton vacuum (CDV). The other one is a solution with a non-constant, linearly varying, dilaton which we will call linear dilaton vacuum (LDV). When uplifted to $(D + 2)-$dimensions, these vacuum solutions produce different spacetimes. The CDV produces a spacetime of the form $AdS_2 \times R_D$, i.e. an intrinsically 2D spacetime. On the other hand, the uplifting of the LDV leads to a hyperscaling violating geometry H_{D+2} [48], which describes the warping of AdS_2 with R_D. In this case, the dilaton plays the role of the radius of R_D.

The JT model has been widely used as a 2D toy model for higher-dimensional black holes, to give a microscopic interpretation of black entropy [27] and to understand the AdS/CFT correspondence in 2D in terms of asymptotic symmetries [169, 170, 201]. Conversely, the extended AP model has been recently used as a description of extremal black holes in 2D (in particular to investigate the breakdown of semi-classical thermodynamics and the flow from LDV to CDV). Moreover it has also been used to describe the backreaction on holographic correlators [83, 199] and to investigate its relation with the conformal symmetry breaking [202].

In this Section and in the next two Chapters we present a revisitation of the AP model from a 2D bulk perspective. Particular attention will be given to the quantum features of the solution from the AdS/CFT perspective [84] in the next two Chapters.

Solutions and vacua

In Schwarzschild coordinates and in absence of matter ($f = 0$), owing to 2D Birkhoff theorem, the most general solution of the model (1.7.76) is a two-parameter family of

solutions,

$$ds^2 = -(\lambda^2 x^2 - a^2)dt^2 + (\lambda^2 x^2 - a^2)^{-1}dx^2,$$
$$\mu = \alpha^2 + \mu_0 \lambda x. \tag{1.7.78}$$

where a^2 and μ_0 are dimensionless integration constants. Being our solution asymptotically AdS, we can use the standard ADM procedure to assign a mass to it [203]. The mass defined in this way, i.e. the ADM mass, has the physical meaning of the energy of the gravitational configuration measured with respect to the reference AdS background solution [203].

The ADM mass of the solution depends on both μ_0 and a and on the parameter λ [83]

$$M_{ADM} = \frac{\mu_0 \lambda a^2}{2}. \tag{1.7.79}$$

It is important to stress that the ADM mass does not depend on the parameter α^2 appearing in the AP potential (1.7.77) for the dilaton.

An important feature of the AP model is that it allows for two different vacuum solutions, i.e. solutions with $M_{ADM} = 0$. In fact, for $\mu_0 = 0$ and $\alpha^2 \neq 0$ we have the *constant dilaton vacuum*. It describes the AdS_2 spacetime with a constant dilaton. It is already well known that at classical level this vacuum does not allow for finite energy excitations [83, 179, 199]. This is immediately evident from Eq. (1.7.79): for $\mu_0 = 0$, M_{ADM} identically vanishes, independently from the value of a. Conversely, for $\mu_0 \neq 0$ we have the *linear dilaton vacuum*, which is AdS_2 endowed with a linear dilaton. Differently from the CDV, this vacuum allows for continuous excitations with $a^2 > 0$.

It is important to stress that we have two different LDV depending on the value of the parameters (μ_0, a) and α. For $\alpha^2 = 0$ the AP model reduces to the JT model and the solution for the dilaton is linear and homogeneous. Notice that this is not an exact solution of the AP model (i.e. the model with $\alpha^2 \neq 0$) but appears only as an asymptotic solution for $x \to \infty$. On the other hand, for $\mu_0 \neq 0$ and $\alpha^2 \neq 0$, the LDV is an exact solution of the AP model and interpolates between the CDV at small x and a linear, homogeneous dilaton at large x. Whenever the distinction between these two LDV will be necessary, we will call the LDV with $\alpha^2 \neq 0$ *interpolating linear dilaton vacuum* (ILDV).

If one uses M_{ADM} as the mass of the solution the three vacuua become completely degenerate. They all have $M_{ADM} = 0$, as it is evident from Eq. (1.7.79), because the CDV is characterized by $\mu_0 = 0$, whereas the LDV and the ILDV have $a = 0$. Actually, in view of the physical meaning of the ADM mass, the three vacua are degenerate by definition. This means that they represent three different sectors of the theory, which strictly speaking cannot be compared.

The finite, $M_{ADM} > 0$, excitations of the LDV and ILDV can be interpreted as 2D black holes with horizon radius $x = a/\lambda$ and temperature and entropy given by

$$T = \frac{\lambda a}{2\pi}, \quad S = 2\pi\mu_h = 2\pi\alpha^2 + 2\pi\mu_0 a, \tag{1.7.80}$$

$$M_{ADM} = \frac{2\pi^2 \mu_0}{\lambda} T^2. \tag{1.7.81}$$

Notice that the interpretation of the $a^2 > 0$ solutions as 2D black holes is not completely straightforward. In fact, it is well known that the metric (1.7.78) can

be brought by a coordinate transformation in the maximally extended form $ds^2 = -\cosh^2\rho\, d\tau^2 + \frac{d\rho^2}{\lambda^2}$, $-\infty < \tau, \rho < +\infty$, which describes full, geodesically complete AdS_2 (see e.g. Ref. [204]). This is not anymore true if one takes into account the fact that points where the dilaton vanishes have to be considered spacetime singularities. This makes solutions with different a^2 as globally inequivalent and allows for the interpretation of the $a^2 > 0$ solution as a 2D black hole [205].

The previous argument forbids the existence of 2D black hole solutions with constant dilaton, in agreement with the absence of finite energy excitations of the CDV. On the other hand, we can formally consider zero mass thermal excitation of the CDV of the form

$$\begin{aligned} ds^2 &= -(\lambda^2 x^2 - \frac{4\pi^2 T^2}{\lambda^2})dt^2 + (\lambda^2 x^2 - \frac{4\pi^2 T^2}{\lambda^2})^{-1} dx^2, \\ \mu &= \alpha^2. \end{aligned} \tag{1.7.82}$$

This solution can be obtained from the CDV by a coordinate transformation, which generates a horizon with related temperature T. Because in the CDV there is no space-time singularity, there is no obstruction to extend (1.7.82) beyond the horizon, to cover the whole CDV spacetime. Thus, the solution (1.7.82) is geometrically equivalent to the CDV, but can be formally used to describe zero mass thermal excitation of the CDV.

The discussion of the spacetime singularities is much simpler using light-cone coordinates $x^{\pm}$. Using the $SL(2,R)$ isometric transformations, the solution (1.7.78) becomes

$$\begin{aligned} ds^2 &= -\frac{4}{\lambda^2 (x^+ - x^-)^2} dx^+ dx^-, \\ \mu &= \alpha^2 + \frac{2\frac{\mu_0}{\lambda} - M_{ADM} x^+ x^-}{x^+ - x^-}. \end{aligned} \tag{1.7.83}$$

The $\mu = 0$ singularity is located at

$$\left(x^+ + \frac{\alpha^2}{M_{ADM}}\right)\left(x^- - \frac{\alpha^2}{M_{ADM}}\right) = \frac{\frac{2\mu_0}{\lambda} M_{ADM} - \alpha^4}{M_{ADM}^2}, \tag{1.7.84}$$

whereas the time-like asymptotic boundary of AdS_2 is located at $x^+ = x^- = t = \pm\sqrt{\frac{2\mu_0}{\lambda M_{ADM}}}$. The nature of the singularity depends on the value of M_{ADM}. For $M_{ADM} > \lambda\alpha^4/(2\mu_0)$ the singularity is space-like whereas for $M_{ADM} < \lambda\alpha^4/(2\mu_0)$ it is time-like.

For planar spatial topology the ILDV gives a nice, effective, 2D description of the flow from an $AdS_2 \times R_D$ [5] geometry in the IR to a hyperscaling violating geometry [48] in $(D+2)-$dimension in the UV, of which AdS_{D+2} is a particular case. From the 2D perspective this flow is a simple consequence of both the relation $R \propto \mu^p$ between the dilaton and the radius R of R_D and of the constant/linear behavior of the dilaton at small/large x. We briefly discuss the uplifting of the AP model to a (D+2)-dimensional theory with hyperscaling violation in the Chapter 3.

From the thermodynamical point of view, the CDV gives the typical $T = 0$, extremal, state with non vanishing entropy of a large class of $(D+2)-$dimensional

[5] $AdS_2 \times S_D$ in the case of spherical spacial topology.

extremal black holes, like e.g. charged Reissner-Nordström black holes in four dimensions. Near extremality, the mass-temperature relation for the excitations, $M_{ADM} \propto T^2$ in Eq. (1.7.81), implies the breakdown of the thermodynamical semi-classical description and the appearance of a mass gap [199, 200]

$$M_{gap} = \frac{\lambda}{2\pi^2 \mu_0}. \tag{1.7.85}$$

The generation of the mass gap is the quantum counterpart of the absence of finite energy excitations of the CDV [179], which in turns is related to the strong backreaction on AdS_2. From the AdS/CFT correspondence point of view, the appearance of the mass gap (1.7.85) can be also explained in terms of the pattern of breakdown of the conformal symmetry which generates, in the IR, a mass scale of order λ [83, 199, 202].

Despite the successes of the AP model described above, two aspects are still not completely clear. The first is the characterization of the energy of the solution trough the ADM mass (1.7.79). This mass does not distinguish between the different vacua of the theory, in fact it is independent from α. Due to the different features of the two vacua, the ADM-mass degeneracy between the CDV and LDV becomes particularly ambiguous. Moreover, M_{ADM} does not keep informations about the presence of the mass gap. Last but not least, it also does not seem a suitable physical parameter to characterize the singularity. Indeed, the transition between space-like and time-like singularities occurs not when M_{ADM} changes sign, as expected, but rather at strictly positive values.

The second aspect is the characterization of the pattern of conformal symmetry breaking. This pattern has been described using correlation functions in the dual conformal field theory. However, in the spirit of the AdS/CFT correspondence one should be able to characterize completely this pattern also using only the 2D gravity theory. In what follows, we will show how the peculiarities of dilaton gravity in 2D spacetime can help us to clarify the picture presented above.

Covariant mass

The first peculiarity of 2D dilaton gravity is that the metric always admits the existence of a Killing vector whose explicit form depends on the dilaton [201, 206, 207]

$$\chi^\mu = F_0 \epsilon^{\mu\nu} \partial_\nu \mu, \tag{1.7.86}$$

where F_0 is a normalization factor. The second is the existence of a covariant, conserved mass [206, 208]

$$M = -\frac{F_0}{2}\left[\int^\mu V(s)ds + (\nabla\mu)^2\right]. \tag{1.7.87}$$

In this thesis we will use the normalization prescription of Refs. [206, 207], i.e. $F_0 = (\lambda\mu_0)^{-1}$.

The covariant mass M gives a definition of the energy of the solution, which is invariant under Weyl transformation of the metric [207]. It may differ from the standard ADM mass only by a constant (temperature independent) term. For this reason it is particularly appropriate to quantify the energy of the different vacua of the AP model.

Computing the covariant mass for the general solution (1.7.78) of our model we get,

$$M = \frac{a^2\mu_0\lambda}{2} - \frac{\alpha^4\lambda}{2\mu_0} = M_{ADM} - \frac{\alpha^4\lambda}{2\mu_0}. \tag{1.7.88}$$

There are several reasons indicating that the covariant mass M and not the ADM mass M_{ADM} has to be considered as the physical mass of the solutions. For $\alpha = 0$ we have $M = M_{ADM}$. By using M instead of M_{ADM} we remove the degeneracy between the CDV and the LDV and keep also track about the non-existence of finite energy excitations of the CDV. The ILDV has negative energy $M = -\frac{\alpha^4\lambda}{2\mu_0}$, whereas for the CDV we have $M \to -\infty$. Moreover, the r.h.s. of Eq. (1.7.84) can be written as $2\mu_0 M/M_{ADM}^2$. Thus, the spacetime singularity is space-like for $M > 0$, whereas it becomes time-like for $M < 0$.

1.8 Summary and conclusions

In this Chapter, we have discussed in detail geometrical and thermodynamical properties of charged 5D GB black branes, black holes and two dimensional dilaton gravity.

In the case of spherical black holes, we have reviewed their geometrical and thermodynamical properties in 5D RN and GB gravity with particular attention to phase transitions.

For what concerns black branes, although our discussion has been mainly confined to the GB case, we expect that most of our results can be generalized to Lovelock gravity theories in any spacetime dimensions. This is the case, for instance, of black brane thermodynamics which, when expressed in terms of effective parameters, does not depend on Lovelock coupling constants. In particular, we have shown that the combination of GB higher curvature terms added to the Einstein gravity action have three main effects:

- They introduce a new branch of brane solutions, which are however not black branes but describe naked singularities. The global structure of the RN geometry of Einstein gravity is preserved only for $\alpha_2 > 0$. For $\alpha_2 < 0$ the spacetime splits into two disconnected regions (an inner and outer region), with the external region having a single event horizon also in the non-extremal case. An interesting feature is that the solutions of the two branches may be, in some cases, continuously connected one with the other through the singularity. When this is the case, they describe transitions of the kind: $AdS_5 \to$ singularity $\to AdS_5$, AdS_5-black brane $\to$ singularity $\to AdS_5$ or AdS_5-black brane $\to$ singularity $\to dS_5$. Although, it is known that one of the two branches of the solution (f_+) is unstable [171] one expects that the first two of these transitions have a holographic interpretation as the flow between two CFTs of different central charge through a singularity.

- The thermodynamic behavior of charged GB black brane is universal, i.e. when expressed in terms of effective mass and temperature is indistinguishable from that of the RN black brane.

- Higher curvature terms modify the asymptotics (the AdS length) of the 5D AdS-RN gravity leaving unchanged the $AdS_2 \times R_3$, extremal near-horizon geometry of

the RN black brane. At thermodynamic level, when expressed in terms of M_{ADM} and T_H a dependence on the normalization factor N of the metric is introduced but not for the extremal, near-horizon geometry $AdS_2 \times R_3$. In terms of the dual CFTs, this property can be described as a deformation of the CFT which changes the UV behavior but leaves unchanged the IR. This behavior is very similar to the attractor mechanism found in supergravity theories [209–212], where the $AdS_2 \times R_D$ (or $AdS_2 \times S_D$) geometry is always the same irrespectively from the asymptotic values of the scalar fields.

Finally, we have also revisited the AP dilaton gravity model focusing mainly on its bulk features. In particular, we have seen that the model admits two different kind of vacua characterized, respectively, by a constant and linear varying dilaton. When uplifted to $(D+2)-$dimensions, these vacuum solutions produce different spacetimes. Indeed, the CDV produces a spacetime of the form $AdS_2 \times R_D$, i.e. an intrinsically 2D spacetime. On the other hand, the uplifting of the LDV leads to a hyperscaling violating geometry H_{D+2} [48], which describes the warping of AdS_2 with R_D. In this case, the dilaton plays the role of the radius of R_D. Moreover, we have shown that it is always possible to use a covariant definition of the mass by means of bulk Killing vectors. It is useful to define the energy of the solution, since it appears to be invariant under Weyl transformation of the metric [207]. It may differ from the standard ADM mass only by a constant (temperature independent) term. For this reason it is particularly appropriate to quantify the energy of the different vacua of the AP model.

Chapter 2

Holography and AdS/CFT correspondence

We review the AdS/CFT correspondence with particular attention to its application in relativistic hydrodynamics and to 2D dilaton gravity theories. In particular, we focus on the shear viscosity for QFTs dual to planar geometries. We then proceed by discussing the shear viscosity for QFTs dual to spherical black holes. Even if the usual hydrodynamical limit of a quantum field theory it is not well understood in a curved spacetime, we also propose a definition of the (analogue) shear viscosity for QFTs which live in a sphere. This is of particular interest to study black hole thermodynamics (e.g. phase-transitions - see next Chapter) from the quantum perspective of AdS/CFT.

In the final part of this Chapter we investigate the holographic principle and its applications to two dimensional gravity, focusing in particular to the microscopic interpretation of the black hole entropy, symmetries, phase transitions and their possible consequences for quantum gravity at Planck scales.

This Chapter is mainly based on:

- Mariano Cadoni, Edgardo Franzin and M. T. "*Hysteresis in η/s for QFTs dual to spherical black holes*", **Eur.Phys.J. C77 (2017) no.12, 900**, arXiv:1703.05162.
- Mariano Cadoni, Matteo Ciulu and M. T., "*Symmetries, Holography and Quantum Phase Transition in Two-dimensional Dilaton AdS Gravity*", **Phys.Rev. D97 (2018) no.10, 103527**, arXiv:1711.02459.

Note: we set the speed of light as $c = 1$.

2.1 AdS/CFT correspondence

The Anti-de Sitter/Conformal field theory correspondence [31, 213, 214] is a useful tool to study strongly coupled field theories. It is a conjecture and it states that a gravity theory in AdS spacetime in $(D+2)-$dimensions is equivalent to a conformal quantum field theory in $(D+1)-$dimensions. In its original formulation [31], the gravitational theory is an AdS spacetime and means type IIB string theory with $AdS_5 \times S_5$ boundary conditions, whereas CFT is a $\mathcal{N} = 4$ supersymmetric Yang-Mills quantum field theory (SYM).

The type IIB string theory contains a finite number of massless fields, including the graviton, the dilaton, some other fields (forms) and their fermionic superpartners, and an infinite number of massive string excitations. It can be characterized by three parameters: the string length l_s, the string coupling g_s and the radius R of the AdS space. The $\mathcal{N} = 4$ SYM theory is a gauge theory with a gauge field, four Weyl fermions, and six real scalars, all in the adjoint representation of the color group [215]. Moreover it is a conformal field theory. The parameters characterizing the group are the rank of the gauge group $\mathcal{N}$ and the Yang-Mills coupling constant, g_{YM}, which is more naturally expressed in terms of the 't Hooft coupling [216] $\lambda_{tH} = g^2_{YM}\mathcal{N}$ when the number of colors is large. We can map the parameters of a theory into the other in the following way

$$g^2_{YM} = 4\pi g_s, \qquad g^2_{YM}\mathcal{N} = \frac{R^4}{l_s^4}. \tag{2.1.1}$$

If one wants to keep string theory weakly interacting, then the gauge coupling in field theory must be small. More interestingly, we can see that a large 't Hooft coupling limit in field theory corresponds to the limit when the curvature radius of space-time is much larger than the string length l_s. In this limit, one can reliably decouple the massive string modes and reduce string theory to supergravity [215]. The practical utility of the AdS/CFT correspondence comes, in large part, from its ability to deal with the strong coupling limit in gauge theory. In fact, AdS/CFT correspondence can be also thought as a weak/strong duality, i.e. weakly interacting gravity theories correspond to strong coupled quantum field theories and viceversa. However the latter are difficult to study since all perturbative techniques fail, hence we can study it using the duality. This has been the most utilized aspect of the correspondence [216]. Let us note that the gauge theory dual to $AdS_5 \times S_5$ is at zero temperature. A non-zero temperature would introduce an energy scale in the system responsible of the conformal symmetry breaking and makes more difficult the calculations. However, the holographic dual to a thermal conformal field theory is a black hole (brane) in the bulk with a given Hawking temperature. In other words, a black hole is analogous (dual) to a hot gas of fermions and gauge bosons. This fact has carried to the possibility to study many open problems in condensed matter physics with the help of AdS/CFT correspondence [36], e.g. superconductors [37–40], holographic phase transitions [41, 42], quantum criticality [43–45], hyperscaling violation in critical systems [46–63], hydrodynamic regime of strongly coupled quantum field theories [64, 65] and entanglement entropy [32–35]. In particular, scalar fields (charged or neutral) play a crucial role in many applications of the AdS/CFT correspondence. In fact they act as order parameters in the dual QFT, triggering symmetry breaking and/or phase transtions. We will come back to this point in the 2D gravity context, when we will investigate the breaking of symmetries and the phase transition generated by a non-trivial dilaton in the bulk.

A way to implement this duality is to put in correspondence bulk fields "ϕ" in (super)gravity with operators $\mathcal{O}$ of a field theory. This can be mathematically translated into the following expression

$$Z_d[J] = e^{iS[\phi_{cl}]}. \tag{2.1.2}$$

On the left side it appears the partition function of a field theory, where the source J is considered coupled to the operator $\mathcal{O}$,

$$Z_d[J] = \int D\phi \exp\left(iS + i\int d^{d+1}x J\mathcal{O}\right). \tag{2.1.3}$$

On the right, the classical action of the classical solution ϕ_{cl} to the field equations with suitable boundary conditions [215]. Differentiating (2.1.2) with respect to J, one can find the correlation functions of $\mathcal{O}$. For example, the two-point Green's function of $\mathcal{O}$ is obtained by differentiating $S_{cl}[\phi]$ twice with respect to the boundary value of ϕ,

$$G(x-y) = -i\langle T\mathcal{O}(x)\mathcal{O}(y)\rangle = \frac{\delta^2 S[\phi_{cl}]}{\delta J(x)\delta J(y)}\Big|_{\phi(z=0)=J}. \tag{2.1.4}$$

The AdS/CFT correspondence thus maps the problem of finding quantum correlation functions in field theory to a problem in classical gravity. For this reason, starting from Einstein equations one can immediately see that the background metric g_{ab} corresponds to the stress-energy tensor T_{ab}. The classical field g_{ab} will be a solution of Einstein equations which, in general, is asymptotically a conformal metric in AdS space. The quantum fields are represented by the stress-energy tensor. As we will see in the next Section, this will play a fundamental role in the context of the hydrodynamic limit of a quantum field theory.

To make the correspondence more precise, we need bulk fields and an action for the bulk theory. The classical gravitational action in $(D+2)-$dimensions will determine the dual $(D+1)-$dimensional large $\mathcal{N}$ field theory. We start from the (simplest) case in which only a gravitational field is present in the bulk. We can then introduce other fields (e.g. electromagnetic) which will act as sources of operators in the dual QFT. Because we need an asymptotically AdS background, the simplest choice is given by the action in Eq. (1.1.4). As a solution of Einstein's equations we can consider the asymptotic behavior of Eq. (1.1.5), i.e.

$$ds^2 = \frac{r^2}{L^2}\left(-dt^2 + dr^2 + L^2 dx^i dx^i\right) \tag{2.1.5}$$

which represents the AdS spacetime in the so-called Poincare patch. The coordinates $\{t, x^i\}$ parametrize the space on which the dual field theory lives, while r is the extra radial coordinate running from $r = 0$ (the "boundary") to $r = \infty$. The full isometry of the metric is $SO(D+1,2)$, which is isomorphic to the conformal group in $(D+1)-$dimensions. This means that the symmetries of the bulk action act on the "boundary" QFT as conformal transformations [213, 214]. In particular, the scaling symmetry of the QFT acts on the spacetime as $\{t, x^i, r\} \to \{\lambda t, \lambda x^i, \lambda r\}$, which leaves the metric invariant.

The length scale L is more precisely the radius of the AdS spacetime. In order to classical gravity to be a valid description, the AdS radius should be large in Planck units, i.e.

$$c \sim \frac{L^D}{16\pi G_{D+2}} \gg 1. \tag{2.1.6}$$

This limit ensures that quantum corrections to Einstein's equations are negligible (or absent). Let us note that (2.1.6) is the area enclosing a spatial volume of AdS in Planck units. The holographic principle suggests that this quantity should be associated with the number of degrees of freedom of the dual field theory. In particular, c is proportional to the central charge of the CFT living on the boundary of the AdS spacetime [217–219]. The central charge c can be defined as the coefficient of the large

temperature expansion of the free energy (see Sect. 1.5). In most of the established examples of the AdS/CFT correspondence $c \propto \mathcal{N}$ and, for example, in $3+1$ dimensions, $c \sim \mathcal{N}^2$ where $\mathcal{N}$ is the rank of the gauge group. It is easy to understand that (2.1.6) refers to the large $\mathcal{N}$ limit discussed above and in a certain sense, the central charge counts the number of degrees of freedom per Planck unit [220].

Finally, as already mentioned in the introduction, AdS/CFT is one of the most famous (and likely the only explicit) realization of the holographic principle [221]. Indeed, the CFT lives on the boundary of the bulk AdS space and thus has one lower dimension than the full bulk spacetime. For this reason, it is holographic in the sense of the proposal of 't Hooft [29] and, later, Susskind [30]. According to 't Hooft, at Planckian scales our universe is not $3+1$ dimensional, rather it is better described by a two-dimensional lattice evolving with time. This suggested the idea that at those scales, the quantum information contained in a spacetime region is encoded in its boudary. This ideas are also enforced by recent developments in the field of emergent gravity, see for example [84, 88, 89, 168, 222].

2.2 Holographic hydrodynamics

We are interested in the transport properties, mainly the shear viscosity, of QFTs which have a holographic dual. Our interest is twofolds: on the one hand, using the AdS/CFT correspondence, we want to obtain information about transport features of strongly coupled QFTs by investigating the properties of a classical gravitational background like a black hole. On the other hand, this paradigm can be reversed and the properties of the dual QFT can be used to infer about the behaviour of bulk gravity solutions as black holes, for instance.

The natural framework to do this is relativistic hydrodynamics. In this Section we will first describe holographic hydrodynamics in flat space then, we will extend our considerations to curved spaces.

Relativistic hydrodynamics in flat spacetime

Relativistic hydrodynamics is an effective long-distance description for a classical or quantum many-body system at non-zero temperature. In particular, it can be used to describe the non-equilibrium real-time macroscopic slow evolution of the system, both in space and time, with respect to a certain microscopic scale.

In the holographic framework of the AdS/CFT correspondence, the QFT lives in the boundary of a certain gravitational bulk region. In some cases, the QFT can be described by kinetic theory and the microscopic scale is determined by the mean free path of particles l_{mfp} and the typical momentum scale of the process k. When the kinetic theory is absent or unknown, it is possible to give a thermal description and interpret the inverse temperature as the microscopic scale [223, 224]. Thus, the hydrodynamic limit of a QFT corresponds to large relaxation time, i.e. small frequencies, and large scales compared to the typical one of the system, i.e. $\tilde{\lambda} \gg 1/T \sim l_{mfp}$, where $\tilde{\lambda}$ is the wavelength of the excitations of the system.

In general, the existence of a hydrodynamic description is essentially due to the presence of conserved quantities, i.e. to the isometries of the system, whose densities can evolve (oscillate or relax to equilibrium) at arbitrarily long times provided the

fluctuations are of large spatial size. Correspondingly, the expectation values of such densities are the hydrodynamic fields.

Relativistic hydrodynamics for a fluid in any spacetime can be formulated starting from the following definition of the stress-energy tensor [223, 225–227]

$$T^{ab} = \epsilon u^a u^b + T^{ab}_{\perp}\,, \tag{2.2.7}$$

where ϵ is the energy density and the fluid velocity u^a (commonly evaluated in the frame in which the fluid is at rest) is time-like. The tensor $T^{ab}_{\perp}$ is the spatial part of the stress-energy tensor and it is made by time-independent functions of the hydrodynamic variables ϵ, u^a and their derivatives. The dependence of T_{ab} on the velocity (as well as on the temperature $T(x)$) is a consequence of local thermal equilibrium: if perturbations of the system have long wavelengths, in every point at given time the state of the system can be determined by the temperature and the local fluid velocity [215]. In the simplest case, the hydrodynamic equations (also known as constitutive equations) are obtained by requiring the stress-energy tensor to be covariantly conserved, i.e. $\nabla_a T^{ab} = 0$. Particular attention should be done to generic curved backgrounds, where it is not always possible to define globally conserved currents associated with symmetries of the system (see below for discussion). In general, the hydrodynamic modes are infinitely slower than all other modes and the latter can be integrated out. Thus, all quantities appearing in the hydrodynamic equations are averaged over these fast modes and are functions of the slow-varying hydrodynamic variables.

Following the standard procedure of effective field theories, Equation (2.2.7) can be expanded in powers of derivatives of the velocity and, at second order, the most general expansion is given by

$$T^{ab} = (\epsilon + P)\, u^a u^b + P g^{ab} + \Pi^{ab}\,, \tag{2.2.8}$$

where $P = P(\epsilon)$ is a scalar function and it can be interpreted as the thermodynamical pressure. The tensor Π^{ab} contains the derivatives of the fluid velocities, i.e. the dissipative contributions to T^{ab}. Its explicit form is given by [223, 225]

$$\begin{aligned}\Pi^{ab} =& -\eta\sigma^{ab} - \eta\tau_\Pi\left[\langle\mathcal{D}\sigma^{ab\rangle} + \frac{1}{D}\sigma^{ab}(\nabla_c u^c)\right]\\ &+\chi\left[R^{\langle ab\rangle} - (D-1)u_c R^{c\langle ab\rangle d}u_d\right] + \dots\end{aligned} \tag{2.2.9}$$

where for a rank-2 tensor, $\langle A^{ab\rangle} = A^{\langle ab\rangle} \equiv \frac{1}{2}\Delta^{ca}\Delta^{db}\,(A_{ab} + A_{ba}) - \frac{1}{D}\Delta^{ab}\Delta^{cd}A_{cd}$. Δ^{ab} is a symmetric and transverse tensor given by $\Delta^{ab} = g^{ab} + u^a u^b$. In the local rest frame, it is the projector tensor on the spatial subspace. The dots represent the non-linear terms in the fluid velocity and η, τ_Π, χ are transport coefficients. The symbol $\mathcal{D}$ represents the derivative with respect to the velocity direction, i.e. $\mathcal{D} = u_a\nabla^a$. The tensor σ^{ab} is a symmetric, transverse $u_a\sigma^{ab} = 0$ and traceless $g_{ab}\sigma^{ab} = 0$ tensor constructed with the first derivative in the fluid velocity given by $\sigma^{ab} = 2\langle\nabla^a u^{b\rangle}$. The parameter $\eta = \eta(\epsilon)$ is the shear viscosity and τ_Π is the relaxation time.

We conclude with some remarks about the conservation of the stress-energy tensor. For translation-invariant backgrounds, the conservation of the stress-energy tensor leads to the conservation of global currents

$$\nabla_a J^a = 0. \tag{2.2.10}$$

As a consequence, the constitutive equation contains two terms:

$$J^a = \rho u^a - C\Delta^{ab}\nabla_b \alpha, \tag{2.2.11}$$

where ρ is the charge density in the fluid rest frame and C is some constant. The first term corresponds to convection, the second one to diffusion. In the fluid rest frame, we can define the so-called Fick's law of diffusion, $\mathbf{j} = -C\nabla\rho$ being C the diffusion constant [215]. More generally, from the projection of $\nabla_a T^{ab}$ along the fluid velocity u_b, one can relate second-order hydrodynamics with the second law of thermodynamics [223]. At linear order by using Eqs. (2.2.8) and (2.2.9) one finds that the entropy is conserved, i.e. $\nabla_a(su^a) = 0$, where s is the entropy density. Thus to have entropy production, one needs to go to the next order in derivative expansion. In particular, at second order one finds that

$$\partial_t s = \frac{\eta}{2T}\,\sigma_{ij}\sigma^{ij}. \tag{2.2.12}$$

Equation (2.2.12) represents the rate of entropy production in a fluid due to a slowly varying strain and it can be also used to define the shear viscosity [78] (see later for discussion).

Kubo's formula and the shear viscosity

Hydrodynamics is a useful tool to study the dynamics of a system at large lengths and time scales. In particular, holographic hydrodynamics can help us to extract information about the low-momentum behavior of Green's function on the quantum field theory side.

The two-point correlation functions can be extracted as follow. We start from the action in Eq. (2.1.3) where the source $J_a(\mathbf{x})$ and the (bosonic) operators $\mathcal{O}_a(x)$ are coupled, i.e.

$$S = S_0 + \int_x J_a(x)\mathcal{O}_a(x). \tag{2.2.13}$$

The source will introduce a perturbation of the system and the average values of $\mathcal{O}_a$ will be different from the equilibrium ones, which we assume to be zero. If the perturbations are small, we can consider linear perturbation theory and mesure the perturbations as

$$\langle \mathcal{O}_a(x)\rangle = -\int_y G^R_{ab}(x-y)J_b(y), \tag{2.2.14}$$

where G^R_{ab} is the retarded Green's function defined as

$$G^R_{ab}(x-y) = -i\theta(x^0-y^0)\langle[\mathcal{O}_a(x),\mathcal{O}_b(y)]\rangle. \tag{2.2.15}$$

In case of gravity, to determine the correlation functions of T^{ab} we need to couple a source to the stress-energy tensor. This is not difficult to find, since the source of T^{ab} is the metric g_{ab}. Once included, we can use hydrodynamics theory to find the correlators at low momenta.

Thus we consider small metric perturbations around the boundary background metric, i.e. $g_{ab} \to g_{ab} + h_{ab}$, where g_{ab} is the boundary metric. In general we can consider three different types of perturbations: shear, sound and transverse (scalar) modes. The behavior of these modes will be encoded in three different correlators

$G_{1,2,3}(\omega, k)$. When the system preserve all the symmetries, especially the translational invariance (also when translation invariance is broken by external matter fields) at $k = 0$ these three functions are equal, owing to rotational symmetry [77]. By contrast, when translational invariance is broken, as for example in the spherical case we will consider later, the momentum k cannot be taken to zero by construction and the correlators will be different. Thus, in general, any definition of the two point functions based on linear response to small disturbances will be channel-dependent. In this thesis we will focus on the transverse perturbations. The computations for the sound and shear channel are left for future investigations.

For the moment, let us consider a QFT parametrized by the stress-energy tensor in (2.2.8) living on the boundary of AdS_{D+2} whose spatial sections have planar topology (see (1.1.5) and make the limit $r \to \infty$). The particular case of spherical topology where the translational symmetry is not preserved will be discussed later. Without loss of generality, we can choose transverse and traceless perturbations with $h_{ab} = 0$ if $(a, b) \neq (i, j)$, $h_{ij} = h_{ij}(t, \mathbf{x})$ in Eq. (2.2.8). Thus, by considering the fluid at rest, i.e. $u^a = (1, \mathbf{0})$, we obtain

$$T_{ij} = -P h_{ij} - \eta \partial_t h_{ij} + \eta \tau_\Pi \partial_t^2 h_{ij} - \frac{\chi}{2}\left[(D-2)\partial_t^2 h_{ij} + L^2 \nabla_{\mathbf{x}} h_{ij}\right], \tag{2.2.16}$$

where $i = x$, $j = y$, T^{ij} are the spatial components of the stress-energy tensor. By comparison with the expectation from the linear response theory, we can extract the value of the retarded Green's function at zero spatial momentum in the low-frequency limit. By choosing a harmonic time dependence for the perturbation, $h_{ij}(t, \mathbf{x}) = e^{-i\omega t} h_{ij}(\mathbf{x})$, we obtain

$$G^R_{ij,ij}(\omega, \mathbf{0}) = \int dt d\mathbf{x} e^{i\omega t} \theta(t) \langle [T_{ij}(t, \mathbf{x}), T_{ij}(0, \mathbf{0})] \rangle = -i\eta\omega + O(\omega^2) \tag{2.2.17}$$

modulo contact terms and ω and k are the frequency and wave vector of the perturbation, respectively. This expression define the Kubo's formula relating thermal correlators to kinetic coefficients such as dissipative ones, in this case the shear viscosity. For a relativistic QFT in flat spacetime, the Kubo formula gives a general definition of the shear viscosity in terms of the retarded Green function for the stress-energy tensor [75, 78, 228]

$$\eta = -\lim_{\omega \to 0} \frac{1}{\omega} \operatorname{Im} G^R_{T^{ij} T^{ij}}(\omega, k \to 0)\,. \tag{2.2.18}$$

When translational invariance is preserved and a hydrodynamic limit exists, Eq. (2.2.18) becomes the Kubo's formula for the transverse momentum. In this case, η defined by Eq. (2.2.18) coincides with the usual hydrodynamical definition in terms of conserved quantities obtained from the Einstein relation $C = \eta / sT$, where C is the diffusion constant appearing in the Fick law [78].

Relativistic hydrodynamics in curved spacetime

As mentioned before, we should take particular attention to the case in which the system does not preserve the translational symmetry. In fact, the usual hydrodynamic description of a system using the conserved charges falls. However, we can circumvent these difficulties by means of the definition of the stress-energy tensor and the

hydrodynamic equations written in terms of expansion in derivatives of hydrodynamic fields (as the fluid velocity) [223]. In holographic hydrodynamics this approach is useful to formulate the hydrodynamic description of a fluid in a spherical background holographically dual to AdS spherical BHs [82].

In fact, on the sphere, due to its intrinsic geometry, the translational invariance is broken. As a consequence, the momentum is not conserved and it is not possible to define an associated conserved current. At first sight, this should prevent us from studying transport coefficients as the shear viscosity η which is, by definition, a measure of the momentum diffusivity due to a strain in a fluid. Hence, in principle, without translational symmetry it is not possible to define a conserved current, from which one can derive the Fick's law of diffusion [215]. Nevertheless, as we will see below, we can circumvent these difficulties and give a rigorous definition of η for the hydrodynamic limit of a QFT in a spatial background without translational isometries.

The analogue shear viscosity

Let us consider a QFT living on the boundary of AdS_{D+2} whose spatial sections have spherical topology. Although bulk BHs allow for dual QFTs living on a sphere [192, 213, 214, 229], we are not interested in the explicit form of the holographically dual QFT. However, we can study its hydrodynamic limit in the sense described above. The boundary metric is conformal to $\mathbb{R} \times S^D$

$$ds^2 = \frac{r^2}{L^2}\left(-dt^2 + L^2\, d\Omega_D^2\right), \tag{2.2.19}$$

where $d\Omega_D^2 = g_{ij}\, dx^i dx^j$ is the metric of a D-sphere. In this case, due to the spherical shape of the boundary, the metric perturbations used to describe the non-equilibrium real-time macroscopic slow evolution of the system are characterized by two parameters, the relaxation time or the frequency ω and L/ℓ which "measures" angular distances on the sphere. The integer number ℓ parametrizes the eigenvalue of the Lichnerowicz operator on the sphere (see Eq. (2.2.21) below) and is analogous to the momentum scale k for a flat topology. In the spacetime (2.2.19), we define the hydrodynamic limit of the holographic QFT as the limit in which the metric perturbations have slow relaxation time and are much larger than the typical scale of the system, i.e. $\omega \to 0$ and $L/\ell \gg 1/T$. Since we are dealing with a D-sphere, the number ℓ cannot be arbitrarily small, i.e. there is a minimum value ℓ_0 [230–232] which corresponds to a maximum spatial scale, and to a maximum size for the global modes propagating on the sphere. On the contrary, in flat space, there is no constraint on the values of k, so one can set $k \to 0$ which, in turns, corresponds to fluctuations of very large (in principle infinite) wavelength.

In order to extend the Kubo formula (2.2.18) to spherical backgrounds, we first consider the stress-energy tensor (2.2.8). Then we consider small metric perturbations around the boundary background metric (2.2.19), i.e. $g_{ab} \to g_{ab} + h_{ab}$. As in the planar case, choosing transverse and traceless perturbations and considering the fluid at rest, the stress-energy tensor (2.2.8) takes the following form

$$T^{ij} = -P h_{ij} - \eta \partial_t h_{ij} + \eta \tau_\Pi \partial_t^2 h_{ij} - \frac{\chi}{2}\left[(D-2)\partial_t^2 h_{ij} + L^2 \triangle_L h_{ij}\right], \tag{2.2.20}$$

where $\triangle_L = \nabla_k \nabla^k$ is the Lichnerowicz operator and it corresponds to a generalization of the Laplacian for the D-sphere, with $D \geqslant 3$. Equation (2.2.20) is analogous to the

one obtained in Ref. [223] for planar topology. As requested by linear response theory, we compute the retarded Green function for the tensor channel: by choosing a harmonic time dependence for the perturbation, $h_{ij}(t,\mathbf{x}) = e^{-i\omega t}\, h_{ij}(\mathbf{x})$ and by expanding in hyper-spherical harmonics [233–235], we can extract the retarded Green function from Eq. (2.2.20),

$$G^{R}_{T^{ij}T^{ij}}(\omega,\ell) = -P - i\omega\eta - \omega^2\eta\tau_\Pi - \frac{\chi}{2}\left[(D-2)\omega^2 + L^2\gamma\right], \tag{2.2.21}$$

where $\gamma = \ell(\ell+D-1)-2$ are the eigenvalues of the Lichnerowicz operator and $\ell = 1,2,3,\ldots$ is an integer associated with the hyper-spherical harmonic expansion. The eigenvalues γ are positive and form a discrete set [230–232, 235]. Given the retarded Green function above we can extract the dissipative coefficients η and τ_Π. In particular, we are led to define the analogue of shear viscosity in the hydrodynamic limit for a QFT in a spatial spherical background in the transverse channel as,

$$\tilde{\eta} \equiv -\lim_{\omega\to 0}\frac{1}{\omega}\,\mathrm{Im}\, G^{R}_{T^{ij}T^{ij}}(\omega,\ell\to\ell_0)\,, \tag{2.2.22}$$

where ℓ_0 is the minimum value of ℓ. Notice that the shear viscosity $\tilde{\eta}$ in Eq. (2.2.22) is defined as the $\ell\to\ell_0$ limit of the retarded Green function in analogy with Eq. (2.2.18), see [82]. In planar hydrodynamics, the $k\to 0$ limit describes long wavelength modes and probes large scales on the plane. In the spherical case, the $\ell\to\ell_0$ modes probe large angles on the sphere.

It is also important to stress that, with respect to the planar case, the expression in square brackets in Eq. (2.2.20) has an additional contribution to the stress-energy tensor ruled by the transport coefficient κ. However this contribution drops out in the Kubo formula (2.2.22), when we take the imaginary part of the Green function.

Let us note that, since the translational invariance is broken, the definition of the (analogue) shear viscosity in terms of the Kubo formula (2.2.22) is channel dependent. In fact, as already noted, the momentum k cannot be taken to zero by construction and correlators corresponding to different kind of perturbations (shear, sound or scalar) will be different. Thus, in general, any definition of the two point functions based on linear response to small disturbances will be channel-dependent. We stress the fact that for translation-invariant backgrounds, the conservation of the stress-energy tensor leads to the conservation of global currents and to the Fick law [215]. In our case with the background metric (2.2.19) we can only consider local conservation since the translational invariance is broken and the Fick law is not satisfied but, even if it is channel dependent, Eq. (2.2.12) still holds.

2.3 Shear viscosity to density entropy ratio

An important result of the gauge/gravity results is the calculation of the ratio between the shear viscosity and the density entropy of holographic plasmas. It assumes a very easy value for all the theories with Einstein gravity duals,

$$\frac{\eta}{s} = \frac{\hbar}{4\pi k_B}. \tag{2.3.23}$$

The interesting fact is that it appears to be *universal* in the sense that it does not depend on the fine details of the underlying microscopic theory. This result has led to

conjecture the existence of a fundamental lower bound

$$\frac{\eta}{s} \geqslant \frac{\hbar}{4\pi k_B} \tag{2.3.24}$$

called the Kovtun-Son-Starinets (KSS) bound [75] which is also supported both by energy-time uncertainty principle arguments and by quark-gluon plasma experimental data [74–76]. First found for the hydrodynamic regime of the QFT dual to black branes and black holes of the Einstein-Hilbert theory [66, 74, 75], the KSS bound[1] has been extended to a variety of cases. These include Einstein-Hilbert gravity with all possible matter terms in the action, hence, among others the QFT dual to Reissner-Nordström 5D gravity [74, 75] and the important case of the quark-gluon plasma (see e.g. [236]). It has been also conjectured that the KSS bound holds for any fluid in nature. For a detailed discussion on the shear viscosity to entropy ratio see Refs. [66, 74, 75, 77, 182, 236–240].

By now, it is well-known that the KSS bound can be violated by two main different kinds of effects: higher-curvature terms in the Einstein-Hilbert action [77, 175, 183, 236, 237, 239, 241–246] and breaking of the translational or rotational symmetry of the black brane background [78–81, 183, 247–251]. In the case of higher curvature theories, the KSS bound depends on the coupling constant for the higher curvature terms [77, 237]. For example, in 5D Gauss-Bonnet gravity, the shear viscosity to entropy ratio is [77, 237]

$$\frac{\eta}{s} = \frac{1}{4\pi}\left(1 - 4\lambda\right). \tag{2.3.25}$$

The KSS bound still holds if $\lambda \leqslant 0$ but is violated for $0 < \lambda \leqslant 1/4$ (the upper bound follows from Eq. (1.4.26)). The dependence of the bound from the coupling constant λ makes the bound not anymore universal as in the Einstein-Hilbert theory. In terms of the dual gauge theory, the curvature corrections to the Einstein-Hilbert action correspond to finite $\mathcal{N}$ and λ_{tH} effects. It has been argued that the universality of the KSS bound strictly holds in the limit $\mathcal{N} \to \infty$ whereas, in general, finite $\mathcal{N}$ effects will give lower bounds for η/s [70].

A crucial issue is that the relation (2.3.25) seems to allow for arbitrary violations of the KSS bound. However, consistency of the QFT dual to bulk GB gravity as a relativistic field theory constrains the allowed values of λ. For instance, in [77, 237, 252, 253] it was found that causality and positivity of the energy for the dual QFT describing the Gauss-Bonnet plasma require $-7/36 < \lambda < 9/100$ implying $4\pi\eta/s > 16/25$, a bound lower then the KSS bound. On the other hand, the hydrodynamic description of the dual GB plasma is valid in the IR regime, i.e. for $\omega, k << T$, whereas causality is determined by the propagation of modes in the $\omega, k > T$, UV regime. Thus, the existence of lower bounds for η/s implies a higher non-trivial relationship between the transport properties in the IR and causality requirements in the UV regime of the QFT dual to GB gravity. A direct link between the properties of the theory in the two regimes is possible if the same phase of the theory extend over the entire range of energy scales. In other words, there must not be any phase transitions in the system. For this reason the temperature, playing the role of both microscopic and macroscopic scale of the system, assumes an important role in controlling the behavior of the theory from the infrared to the ultraviolet regime [236].

[1] From now on, we will set $\hbar$ and k_B equal to one

On the other hand, the violation of the KSS bound due to the breaking of translational symmetry has a more fundamental nature. In this case, the shear viscosity does not have the usual hydrodynamic meaning but might be interpreted as the rate of entropy production due to a strain [78–81, 225, 249]. In this framework, the behavior of η/s as a function of the temperature T is non-trivial [254, 255] and carries information about the infrared (IR) and ultraviolet (UV) behaviour of the QFT, the existence of global diffusive modes of the system and the nature of the effect responsible for the breaking of translational invariance. For instance, when this breaking is generated by the presence of a non-homogeneous scalar field in the bulk, the behavior of η/s at small T is determined by the flow of the QFT in the IR. If the translational invariance is restored in the IR then η/s goes to a constant as $T \to 0$, signalizing the presence of an IR collective diffusive mode. Conversely, if the translational invariance is not restored, η/s scales as $T^{2\nu}$ for $T \to 0$ and the IR geometry in $(D+2)-$dimensions is typically $AdS_2 \times \mathbb{R}_D$ [78, 256, 257]. The charged GB BB represents a nice example of this behavior, particularly in view of the universality of the IR $AdS_2 \times R_3$ fixed point [183]. In the next Chapter we will also discuss the general validity of this behavior for spherical BH backgrounds. In this case, the translational symmetry is intrinsically broken and cannot be restored in the IR, but holds only in the UV, where the spherical horizon can be approximated by a plane. Although for these backgrounds the breaking of translational invariance prevents an hydrodynamical interpretation of the viscosity, this behavior of η/s is clearly related to the emergence of extremely interesting physics in the far IR.

2.4 Holography in two dimensions

Holography and AdS/CFT in two dimensions is an interesting and puzzling subject [258]. Analogously to the higher dimensional cases, gravitational structures (e.g. black holes) can be still investigated using conformal field theory techniques. One interesting feature of AdS_2 spacetime is that it appears as near-horizon geometry of a variety of higher dimensional black holes not only in string theory but also in the general relativity context (the Reissner-Nordstrom solution) even if, from the gravity side, it appears as a complete topological solution [169, 179, 198, 259–262]. Full AdS spacetime in $D = 2$ has cylindrical topology, so that its boundary is not connected, making difficult the identification of the boundary CFT that should be dual to the gravity theory. Moreover, it is not completely clear if the CFT is 1D or 2D. Owing to this difficulties it is almost impossible to discuss the correspondence in general. However the AdS_2/CFT_1 duality can be used to test general ideas about the correspondence in particular and the holographic principle in general. Of particular conceptual relevance is the fact that it should provide a correspondence between a field theory (2D gravity) and conformal mechanics.

Hints from several different models of quantum gravity suggest that at Planckian scales, spacetime becomes effectively two-dimensional [168, 263]. In this section we will see how this "spontaneous dimensional reduction" can be realized in the case of dilaton gravity. In order to do so, we will use the bulk perspective presented in Chapter 1 by comparing energetically two kind of vacua, the CDV and LDV vacuum. We will show that whereas at non-vanishing temperature the LDV is always energetically preferred, at $T = 0$ the situation is reversed and the CDV is favourite. This signals a

$T = 0$ quantum phase transition which, from an higher-dimensional perspective, can be thought as a spontaneous dimensional reduction from a $D+2$ to $D = 2$ dimensions spacetime, whose possible role in quantum gravity has been emphasized in Ref. [168].

Quantum phase transition and spontaneous dimensional reduction

The AP model allows for two different class of solutions, namely the 2D black hole (1.7.78) and the zero mass thermal excitations of the CDV (1.7.82). One important question is to determine which of these two solutions is, from the thermodynamic point of view, globally favourite. Using the 2D Hamiltonian formalism [198], this can be done by computing the difference ΔF between the free energy, F, of the two solutions [84]. In the case under consideration this computation is not straightforward because ΔF is usually computed for solutions having the same asymptotical behavior.

The presence of the dilaton makes the asymptotics of the two classes of solutions of the AP model (linear and constant dilaton, respectively) different, thus preventing the standard computation of ΔF. This problem can be circumvented by defining the free energy of the solution with respect to its own vacuum [47]. This method has been applied, for example, in Ref. [47] to calculate ΔF for two classes of 4D solutions approaching asymptotically to AdS and to a solution with hyperscaling violation, respectively.

Using this prescription for the free energy F in the Euclidean action formalism, for the case under consideration we get:

$$\begin{aligned} F^{BH} &= -\frac{2\pi^2\mu_0}{\lambda}T^2 - 2\pi\alpha^2 T, \\ F^{T} &= -\kappa\mu_h^C = -2\pi\alpha^2 T, \\ \Delta F &= F^{BH} - F^{T} = -\frac{2\pi^2\mu_0}{\lambda}T^2, \end{aligned} \tag{2.4.26}$$

where F^{BH} is the free energy of the 2D black hole (1.7.78) obtained by subtracting the contribution of the ILDV, whereas F^{T} is the free energy of the thermal excitation of the CDV obtained by subtracting the contribution of its own vacuum. From Eq. (2.4.26) follows immediately that for any $T \neq 0$, $\Delta F < 0$ and the 2D dilatonic black hole is energetically preferred.

By construction, Eq. (2.4.26) does not give any information about the behavior at $T = 0$, being F defined with reference to the respective vacua at $T = 0$. Formally, at $T = 0$ the two vacua are degenerate, consistently with the degeneracy of the CDV and ILDV when the ADM mass is used to characterize the two solutions.

Moreover, the semi-classical approximation, on which the Euclidean action formalism is based, breaks down at $T \sim M_{gap}$, so that Eq. (2.4.26) cannot be trusted at $T = 0$.

At $T = 0$ there is no thermal contribution to the free energy and ΔF is given by the mass difference between the two vacua, $\Delta F_{T=0} = \Delta M = M^{ILDV} - M^{CDV}$.

We have already argued that we should use the covariant mass (1.7.88) as the physical mass instead of the ADM mass. Using this mass in the computation we find $\Delta F_{T=0} \to \infty > 0$. This means that the CDV is energetically preferred and that at $T = 0$ the 2D dilatonic black hole undergoes a quantum phase transition to the CDV. Let us note that, here, we are referring to the usual thermodynamical meaning

of phase transitions. In fact, we are considering a thermodynamical system, which can exist in two different configurations, the black hole given by Eq. (1.7.78) and the thermal excitations of the CDV given by (1.7.82). Comparing the free energy of the two configurations at the same temperature we discover that at $T = 0$ the free energy of the black hole is bigger than that of the CDV. This means that at zero temperature the black hole undergoes a phase transition to the CDV. We call this phase transition "quantum" because it happens at zero temperature and can be fully understood only at full quantum level. The free energy of the CDV diverges. In fact, in the limit $\mu \to 0$ the covariant mass (1.7.88) blows up and, classically, we can describe the phase transition as an instability of the ILDV in which the CDV expands to take over the spacetime. This description changes at quantum level, where the divergence of the covariant mass is cured by the presence of the mass gap. However, there is no reason to expect in this quantum description a change of sign of $\Delta F_{T=0}$.

From a four-dimensional perspective this quantum phase transition can be interpreted as a spontaneous dimensional reduction. In fact, the $(D+2)-$dimensional uplifting of the ILDV is a scale covariant geometry H^{D+2} with hyperscaling violation in $(D+2)-$dimensions, whereas the uplifting of the CDV is $AdS_2 \times R^D$, i.e. a geometry which is intrinsically two-dimensional, being the radius of R^D not dynamical. In terms of the uplifted geometries we have the $T = 0$ phase transition $H^{D+2} \to AdS_2 \times R^D$. However, we will study the uplifting procedure in the next Chapter to which the reader is recommended to refer for details.

This phase transition supports the suggestion of Ref. [168] about the existence of a spontaneous dimensional reduction of the spacetime to two dimensions near the Planck scale.

Let us conclude with some remarks about one loop corrections to the free energy (2.4.26). Our calculation is based on the semi-classical approximation. One loop corrections to F have been shown in Ref. [83, 202] to have the typical $\log T$ behavior, which gives a dangerous divergent term in the IR. However, this term does not contribute to the entropy of the CDV [202], we therefore expect our result to extend also beyond the semi-classical approximation.

2.5 Summary and conclusions

In this Chapter we have reviewed the AdS/CFT correspondence and discussed its applications in holographic relativistic hydrodynamics both in flat and curved spacetimes. Moreover we have also investigated holography, quantum phase transition and spontaneous dimensional reduction in two dimensions by means of dilaton gravity.

At first, we have shown how to define diffusion coefficients starting from a generic QFT parametrized by a stress-energy tensor expressed in terms of the fluid velocity and its derivatives. In particular, we focused on the shear viscosity. By means of the Kubo formula, we have defined the shear viscosity, η, for QFTs living in a Minkowski spacetime. Then we have proposed a definition of η for QFTs living in a sphere, called the analogous shear viscosity, $\tilde{\eta}$. This procedure is not as straightforward as in the case of flat spacetime, since the hydrodynamic limit of a quantum field theory in a curved spacetime is not well defined. In fact, in general, the definition of a transport coefficient such as the shear viscosity is associated to the translational invariance of the system, i.e. the conservation of the momentum. As a consequence,

from the associated conserved current one can derive the Fick's law of diffusion. For systems that break translational invariance, the hydrodynamic interpretation in terms of conserved quantities fails but hydrodynamics can be still defined as an expansion in the derivatives of the hydrodynamic fields. However, it is possible to define the shear viscosity through a Kubo formula also for QFTs on a spherical background, see Eq. (2.2.22), where the stress-energy tensor is only covariantly conserved. In addition, one can understand $\tilde{\eta}$ as the rate of entropy production due to a strain, which is the typical interpretation when the homogeneity is broken by external matter fields. From this point of view, QFTs dual to spherical BHs are very similar to QFTs dual to black branes where the translational symmetry is broken by non-homogeneous external fields, e.g. scalars [78, 249, 250].

The definition of the hydrodynamic limit of a QFT on the sphere is plagued by an issue related to the compactness of the space. In fact, in a compact space, the usual hydrodynamic limit as an effective theory describing the long-wavelength modes of the QFT has not a straightforward interpretation. Our proposal is that for QFTs dual to bulk spherical BHs, the hydrodynamical, long wavelength modes can be described by the $\ell \to \ell_0$ modes that probe large angles on the sphere. This is in analogy with the $k \to 0$ modes for QFTs dual to bulk black branes which probe large scales on the plane.

There is still a crucial difference between the two cases. When the breaking of translational symmetry is generated by external fields, the symmetry may be restored or not when the system flows to the IR [78]. In the BH case instead, because the breaking has a geometric and topological origin, translational symmetry cannot be restored in the IR.

Finally, we have discussed the features of holography and AdS/CFT in two dimensions. In particular, we focus on the case of dilaton gravity. By using the definition of the covariant mass as measure of the energy of the solutions as done in Chapter 1, we have compared energetically the two different vacua (CDV and LDV) of the theory. Then we have showed the existence of a zero temperature phase transition in which the vacuum with constant dilaton is energetically preferred. We have also speculated that this quantum phase transition could be related to the spontaneous dimensional reduction of the spacetime to two dimensions near the Planck scale described in Ref. [168].

Chapter 3

AdS/CFT applications

AdS/CFT applications in two different cases are discussed.

At first we compute the shear viscosity to entropy density ratio for the QFTs dual to planar and spherical AdS black holes both in Einstein and Gauss-Bonnet gravity in five spacetime dimensions. In particular we focus on the deep interplay between thermodynamics and phase transitions for black holes and the behaviour of transport coefficients in the hydrodinamical limit of the dual QFT when one goes from the IR to the UV regime of the theory.

Secondly, we recall the revisitation of the AP model already seen in the previous Chapter with the aim to explain some quantum features of the model. In particular we discuss the conformal symmetry breaking, its relation with the microscopic derivation of the 2D black hole entropy and the uplifting of the model to $(D+2)-$dimensional theories.

This Chapter is based on the following papers:

- M. Cadoni, A. M. Frassino and M. T., "*On the universality of thermodynamics and η/s ratio for the charged Lovelock black branes*", **JHEP 1605 (2016) 101**, arXiv:1602.05593.
- M. Cadoni, E. Franzin and M. T., "*Van der Waals-like Behaviour of Charged Black Holes and Hysteresis in the Dual QFTs*", **Phys.Lett. B768 (2017) 393-396**, arXiv:1702.08341.
- M. Cadoni, E. Franzin and M. T., "*Hysteresis in η/s for QFTs dual to spherical black holes*", **Eur.Phys.J. C77 (2017) no.12, 900**, arxiv:1703.05162.
- Mariano Cadoni, Matteo Ciulu and M. T., "*Symmetries, Holography and Quantum Phase Transition in Two-dimensional Dilaton AdS Gravity*", **Phys.Rev. D97 (2018) no.10, 103527**, arXiv:1711.02459.

Note: the units are $c = \hbar = k_b = 1$.

3.1 η/s for the charged GB black brane

As mentioned in the previous Chapter, a standard way to calculate the shear viscosity for a QFT is by using the Kubo formula (2.2.18) for the transverse momentum conductivity. In this section we will compute the retarded Green's function of the dual QFT using the gravity side of the correspondence.

At first, let us rewrite the GB BB solution (1.4.28),

$$f_- = \frac{r^2}{2\lambda L^2}\left[1-\sqrt{1-4\lambda\left(1-\frac{\omega_5 M L^2}{r^4}+\frac{4\pi}{3}\frac{G_N Q^2 L^2}{r^6}\right)}\right], \tag{3.1.1}$$

where $\alpha_0\alpha_2 = \alpha_2/L^2 = \lambda$. We know from the literature that the application of the usual AdS/CFT procedure for the computation of correlators gives, for the $U(1)$-charged Gauss-Bonnet black brane in five dimensions [182, 238],

$$\eta = \frac{s}{4\pi}\left[1-4\lambda\left(1-\frac{a}{2}\right)\right] \tag{3.1.2}$$

where $a = \frac{4\pi}{3}\frac{G_N Q^2 L^2}{r_+^6}$, and s is the entropy density S/V following from (1.5.46).

However, a drawback of the usual computation of the shear viscosity is that it does not work in the extremal $T = 0$ case because the metric function has a double zero at the horizon. For this reason, η in the case of extremal BB cannot be simply computed by taking the $T_H = 0$ limit in Eq. (3.1.2). Building on [264], a method of dealing with this problem has been developed in [67]. Recently, a very simple and elegant formula for computing correlators of the form (2.2.18) in QFTs dual to a gravitational bulk theory has been proposed in [265] (see also [78, 79]). This method also works in the extremal case; thus, in the following, we will use it to compute η for the charged GB BB [183].

Considering perturbations $g_{ab} = g^{(0)}_{ab} + h_{ab}$ of the background (3.1.1), at the linear level the field equations (1.4.44) give for the $h^y_x(t,r) = \psi(r)e^{-i\omega t}$ component of the perturbation

$$\partial_r\left[\sqrt{\gamma(r)}f_-(r)F(r)\partial_r\psi\right] + \omega^2\frac{\sqrt{\gamma(r)}F(r)}{N^2 f_-(r)}\psi = 0, \tag{3.1.3}$$

where $\gamma(r) = (r/L)^3$ is the determinant of the spatial metric, $f_-(r)$ is given by Eq. (3.1.1) and $F = N\left(1-\frac{\lambda L^2}{r}\partial_r f_-(r)\right)$. Notice that in the background (3.1.1), the component h^y_x decouples from the other perturbation modes.

Let us first consider the non extremal black brane. The extremal case will be discussed at the end of this Section. Following Ref. [265] we now denote with $\psi_0(r)$ the time independent solution of (3.1.3) which is regular on the horizon $r = r_+$ and such that $\psi_0 \to 1$ as $r \to \infty$. The other linearly independent solution $\psi_1(r)$ of Eq. (3.1.3) behaves as $1/r^4$ for $r = \infty$ and can be computed using the Wronskian method,

$$\psi_1 = \psi_0\int_r^\infty \frac{dr}{\psi_0^2\sqrt{\gamma}Ff_-}. \tag{3.1.4}$$

Expanding near the horizon $r = r_+$ we get at leading order

$$\psi(r) = -\frac{1}{\psi_0(r_+)}\frac{\ln(r-r_+)}{4\pi T_H\sqrt{\gamma(r_+)}\left[1-4\lambda(1-\frac{a}{2})\right]}, \tag{3.1.5}$$

where T_H is the Hawking temperature of the BB and a is defined as in Eq. (3.1.2). Solving now Eq. (3.1.3) near the horizon with infalling boundary conditions and for small ω, one gets at leading order in ω

$$\psi(r) = \psi_0(r_+)\left(1-\frac{i\omega}{4\pi T_H}\ln(r-r_+)\right). \tag{3.1.6}$$

Comparing Eq. (3.1.5) with Eq. (3.1.6) and expanding near the $r \to \infty$ boundary of AdS, one gets

$$\psi(r) = 1 + i\omega\psi_0^2(r_+)\sqrt{\gamma(r_+)}\left[1 - 4\lambda\left(1 - \frac{a}{2}\right)\right]\frac{1}{r^4}. \tag{3.1.7}$$

The usual AdS/CFT rules for computing boundary correlators tell us that the retarded Green function is $1/(16\pi G_N)$ the ratio between normalizable and non-normalizable modes so that, using (2.2.18), we have

$$\eta = \frac{s}{4\pi}\psi_0(r_+)^2\left[1 - 4\lambda\left(1 - \frac{a}{2}\right)\right]. \tag{3.1.8}$$

Because $\psi_0(r)$ goes to 1 as $r \to \infty$ and must be regular on the horizon, we have $\psi_0(r_+) = 1$ and Eq. (3.1.8) reproduces correctly the previous result (3.1.2).

Now, the second Eq. (1.5.46) can be used to define, implicitly, the horizon radius as a function of the BB Hawking temperature and the electric charge, thus allowing us to write also the shear viscosity (3.1.2) as a function of T_H and Q

$$\eta(T_H, Q) = \frac{1}{16\pi G_N}\left(\frac{r_+(T_H, Q)}{L}\right)^3\left[1 - 4\lambda\frac{\pi L^2 T_H}{N r_+(T_H, Q)}\right]. \tag{3.1.9}$$

In the same way, the entropy density in Eq. (1.5.46) can be written as a mere function of T_H and Q, so that we can write the shear viscosity to entropy ratio in the form

$$\frac{\eta}{s} = \frac{1}{4\pi}\left[1 - 4\lambda\frac{\pi L^2}{N r_+(T_H, Q)}T_H\right]. \tag{3.1.10}$$

It is also of interest to write explicitly the dependence of η/s from the normalization constant N:

$$\frac{\eta}{s} = \frac{1}{4\pi}\left[1 - 4N\pi L^2(1 - N^2)\frac{T_H}{r_+}\right]. \tag{3.1.11}$$

When the electric charge is set to zero, the ratio T_H/r_+ in Eq. (3.1.10) is $N/(\pi L^2)$ and η/s reaches the value in Eq. (2.3.25), as one expects. On the other hand, the dependence of η/s on T_H and N in the generic case is rather puzzling.

In view of the universality of the thermodynamic behavior of GB BB described in the previous sections one would naively expect also the shear viscosity to entropy ratio to be universal, i.e. that Eq. (3.1.11) becomes the same as in the RN case just by using the effective temperature $T = T_H/N$ instead of T_H. This is not the case. Only for $N = 1$, which corresponds to $\alpha_2 = 0$, i.e. exactly the RN case, η/s assumes the universal value $1/4\pi$, while for N generic we have a quite complicated dependence on N and T_H. This indicates strongly that the transport features of the dual QFT in the hydrodynamic regime contain more information about the underlying microscopic theory than that contained in the thermodynamic description. An investigation on the behavior of η/s at large and small T_H can shed light on this issue. In fact, as we have seen in Chapter 1, in these limits the BB allows for a simple thermodynamic description. We, therefore, expect this to be true also for the shear viscosity to entropy ratio.

η/s in the large and small T_H regime

The behavior of the shear viscosity (3.1.9) for large and small temperatures can be investigated in a way similar to that used for the BB thermodynamics.

Large T_H

For large T_H, the Hawking temperature is given by Eq. (1.5.49), thus leading to the following expression for the shear viscosity in Eq. (3.1.9),

$$\eta = \frac{1}{16\pi G_N}\left(\frac{\pi L T_H}{N}\right)^3 (1-4\lambda)\,. \tag{3.1.12}$$

The shear viscosity at large T_H scales as T_H^3. In this limit, the entropy density also depends on the temperature as T_H^3 (see Eq. (1.5.50)), the shear viscosity to entropy density ratio approaches Eq. (2.3.25) and reduces to the universal value $1/4\pi$ when $\lambda \to 0$. This is rather expected, because at large T_H the contribution of the electric charge can be neglected.

Small T_H

To investigate the small T_H behavior we invert Eq. (1.5.54) and we write the horizon radius as

$$r_+ - r_0 \simeq \frac{\pi L^2}{6N} T_H\,, \tag{3.1.13}$$

where r_0 is defined by Eq. (1.5.52). At small temperature the subleading term in the shear viscosity scales linearly in T_H

$$\eta \simeq \frac{1}{16\pi G_N}\left(\frac{r_0}{L}\right)^3 \left[1+\left(\frac{1}{2}-4\lambda\right)\frac{\pi L^2 T_H}{N r_0}\right]\,. \tag{3.1.14}$$

The behavior of the entropy density in the small T_H regime is given by the second equation in (1.5.55). Hence, in this limit, also the subleading term of the shear viscosity to entropy density ratio scales linearly

$$\frac{\eta}{s} \simeq \frac{1}{4\pi}\left[1-4\lambda\frac{\pi L^2 T_H}{N r_0}\right]\,. \tag{3.1.15}$$

The result $\eta/s = 1/4\pi$ for $T_H = 0$ has been already found and discussed in the literature in the case of the RN solution [67, 264]. It has been argued that at small temperatures, the dual QFT behaves as a "strange RN metal". The optical conductivity exhibits the generic perfect-metal behavior, but although we have a non-vanishing ground-state entropy, for the strange metal hydrodynamics continues to apply and energy and momentum can diffuse.

In the limit $T_H = 0$, the ratio becomes $\eta/s = 1/4\pi$ attaining the universal value one expects from the KSS bound. This result is what one naturally expects in view of the fact that at $T_H = 0$ the near-horizon solution of the GB brane gives exactly the same $AdS_2 \times R_3$ geometry of the RN solution. However, extra care is needed when one takes the $T_H \to 0$ limit in Eq. (3.1.10). Taking $T_H \to 0$ directly in Eq. (3.1.10) is not safe for several reasons. First, as discussed in Sect. 1.5 the semi-classical description for the BB breaks down at small temperature when the energy gap above extremality prevents excitations with finite energy. Second, as noted by Cai [238], although the $T_H \to 0$ limit is well defined, the usual computation of the shear viscosity to entropy ratio fails in the extremal case because the metric function as a double zero at the horizon. Third, also the computations shown at the beginning of this Section do not hold for $T_H = 0$ because the expressions (3.1.5) and (3.1.6) are ill defined for $T_H = 0$. However, the general method based on [265] for calculating η still works also for extremal BB.

η/s in the extremal case

Let us now extend the calculations of η described before to the case of the extremal brane. In the extremal case the function f_- given by Eq. (3.1.1) and its first derivative vanish when evaluated on the horizon. We have therefore at leading order near the horizon

$$f_-(r_+) = f'_-(r_+) = 0, \quad F(r_+) = N, \quad f_-(r) \simeq k(r - r_+)^2, \tag{3.1.16}$$

where k is some non zero constant. Using the previous expression in (3.1.4) one gets

$$\psi_1(r) = \frac{1}{kN\psi_0(r_+)\sqrt{\gamma(r_+)}} \frac{1}{(r - r_+)}. \tag{3.1.17}$$

On the other hand the near-horizon, small ω expansion gives now

$$\psi(r) = \psi_0(r_+) \left[1 + \frac{i\omega}{kN(r - r_+)}\right]. \tag{3.1.18}$$

Comparing Eqs. (3.1.17) and (3.1.18), near the $r \to \infty$ boundary of AdS_5 we find the expansion

$$\psi(r) = 1 + i\omega\psi_0^2(r_+)\sqrt{\gamma(r_+)} \left(\frac{1}{r^4}\right), \tag{3.1.19}$$

from which follows the shear viscosity

$$\eta = \frac{s}{4\pi}\psi_0(r_+)^2. \tag{3.1.20}$$

Using the same argument previously used to infer that $\psi_0(r_+) = 1$, we get for the shear viscosity to entropy ratio of the extremal GB black brane the universal value

$$\frac{\eta}{s} = \frac{1}{4\pi}. \tag{3.1.21}$$

It is interesting to notice that the universality of η/s for the extremal GB BB is a direct consequence of the universality of the $AdS_2 \times R_3$, extremal, near-horizon geometry. In fact the extremal, near-horizon metric background (1.4.43) does not depend on λ. The other source for a λ- or Q-dependence of η is the function F in Eq. (3.1.3). However, this contribution, hence the dependence of η from λ and Q, is removed by the condition $f'(r_+) = 0$, which implies that near the horizon the two-dimensional sections of the metric behave as AdS_2.

To conclude, let us now discuss the global behavior of η/s as a function of the temperature in order to gain some insight about the η/s bounds. Taking into account that $r_+(T_H)$ is a monotonically increasing function, one easily finds that also the function $P(T_H) = \pi L^2 T_H/(Nr_+) = 1 - 2\pi G_N Q^2 L^2/(3r_+^6)$ in Eq. (3.1.10) is a monotonically increasing function of T_H, with $P(0) = 0$ and $P(\infty) = 1$. The global behavior of η/s in Eq. (3.1.10) therefore is ruled by the sign of λ. For $\lambda < 0$, η/s is a monotonically *increasing* function of T_H, which raises from its minimum value $1/4\pi$ at $T_H = 0$ to its maximum value $(1 + 4|\lambda|)/4\pi$ for $T_H = \infty$, in full agreement with the KSS bound. On the other hand, for $0 < \lambda < 1/4$, η/s is a monotonically *decreasing* function of T_H, which drops from its maximum value $1/4\pi$ at $T_H = 0$ to its minimum value $(1 - 4\lambda)/4\pi$ for $T_H = \infty$, violating the KSS bound.

3.2 The shear viscosity to entropy density ratio for black holes

In the previous Section, we have computed the shear viscosity to entropy ratio for QFTs dual to charged black branes solutions in the GB theory. The main motivation for this calculation was to better understand the dependence of η on the temperature, the UV/IR flow and the universality of the KSS bound and its violations in QFT duals of higher curvature theories.

In this Section, following the method proposed in Refs. [78, 265], we extend our computation to the shear viscosity to entropy ratio for the QFTs dual to the BH solutions discussed in Sect. 1.6. By extending our calculation to QFTs dual to spherical black holes, we are not motivated by any issues of the dual QFT itself. Rather we want to gather information about the complicated thermodynamical phase portrait of charged spherical black holes in GR and GB gravity. In order to do so, we investigate transport coefficients in the dual QFT represents drawing our attention on the shear viscosity.

Linear perturbations in Einstein-Gauss-Bonnet gravity

We start by studying linearized Einstein's equations (1.6.57) which will be a fundamental issue in order to procede with the holographic computation of the shear viscosity.

Let us consider linear tensorial perturbations about the background (1.6.59) in Einstein-Gauss-Bonnet gravity, i.e. $g_{ab} \to g_{ab} + h_{ab}$. After suitable manipulations, the linearized equation of motion (1.6.57) are

$$\delta R^{j}_{i} + \lambda L^2\, \delta G_{(2)}{}^{j}_{i} + 8\pi\, G_5 \left(T_{(M)}{}^{k}_{i} h^{j}_{k} - \frac{\delta T_{(M)}{}^{ij}}{h_{ij}}\, h^{j}_{i} \right) = 0\,, \tag{3.2.22}$$

where $\delta T_{(M)}{}^{ij} = \left(\frac{\delta T_{(M)}{}^{ij}}{h_{ij}}\right) h_{ij}$ and the explicit form of the tensors δR^{j}_{i} and $\delta G_{(2)}{}^{j}_{i}$ can be found in Refs. [266, 267]. In the transverse and traceless gauge we can write

$$h_{ij}(r,t,\mathbf{x}) = r^2\, \phi(r,t)\, h_{ij}(\mathbf{x})\,, \tag{3.2.23}$$

where $\mathbf{x}$ is the direction of the sphere along which the perturbation propagates and h_{ij} is the eigentensor of the Lichnerowicz operator built on the background 3-sphere

$$(\triangle_L + \gamma)\, h_{ij} = 0\,, \quad \gamma = \ell(\ell+2) - 2\,. \tag{3.2.24}$$

The perturbations h_{ij} are both gauge-invariant and decouple [230–232, 266, 267]. This decoupling is a consequence of the spherical symmetry of the background and occurs for every value of ℓ and not only in the hydrodynamic limit $\ell = \ell_0$. Furthermore, assuming a harmonic time-dependence of the perturbation, $h^{j}_{i} = \phi(r,t)\, h^{j}_{i}(\mathbf{x}) = \psi(r)\, e^{-i\omega t}\, h^{j}_{i}(\mathbf{x})$, the perturbation $h^{j}_{i}(\mathbf{x})$ factorizes leading to a set of equations which depend only on t and r [266, 267]. Thus Eq. (3.2.22) reduces to a massive scalar equation

$$\frac{1}{r^3}\frac{d}{dr}\left[r^3 f(r) F(r) \frac{d\psi}{dr} \right] + \omega^2\, \frac{F(r)}{f(r)}\, \psi - m^2(r)\, \psi = 0\,, \tag{3.2.25}$$

where $F(r) \equiv 1 - \lambda L^2 f'(r)/r$ and the mass term is

$$m^2(r) = \frac{2-\gamma}{r^2}\left[1 - \lambda L^2 f''(r)\right] + T_{(M)}{}^{i}_{i} - \frac{\delta T_{(M)ij}}{\delta g_{ij}}\,. \tag{3.2.26}$$

Notice that the mass term depends on the angular part of the perturbation through the eigenvalue γ of the Lichnerowicz operator (3.2.24) and on higher-curvature corrections through the GB constant λ. In the black brane case, if translational invariance is preserved, the mass term is identically zero [75]. We stress that, although Eq. (3.2.25) holds for any ℓ, since we are interested in computing the shear viscosity (2.2.22), in the following we will take ℓ equal to its minimum value $\ell_0 = 1$ implying $\gamma = 1$.

There are no general exact analytical solutions of Eq. (3.2.25), but we can find approximate analytical solutions for $r \to \infty$ and in the near-horizon limit. In the generic case, one can compute the solutions only numerically.

The asymptotic solutions of Eq. (3.2.25) with $\omega = 0$ are given in terms of the modified Bessel functions of first and second kind. For $r \to \infty$, the non-normalizable mode ψ_0 and the normalizable mode ψ_1 behave as

$$\psi_0 = 1 - \frac{\lambda L^2}{2\left(1-\sqrt{1-4\lambda}\right) r^2} + \mathcal{O}\left(\log r/r^4\right), \tag{3.2.27}$$

$$\psi_1 = \frac{1}{r^4} + \mathcal{O}\left(1/r^6\right). \tag{3.2.28}$$

In Eq. (3.2.27) we have chosen the integration constant such that the non-normalizable mode ψ_0 goes to 1 as $r \to \infty$.

The near-horizon behavior of $\psi_0(r)$ is different for non-extremal and extremal BHs. In the case of non-extremal BHs at temperature T and extremal $T = 0$ BHs we write the metric function, respectively

$$f(r) = 4\pi T\,(r - r_+) + \frac{f''(r_+)}{2}\,(r-r_+)^2 + \mathcal{O}\left((r-r_+)^3\right), \tag{3.2.29}$$

$$f(r) = \frac{(r-r_0)^2}{l^2} + \mathcal{O}\left((r-r_+)^3\right), \tag{3.2.30}$$

where the extremal BH radius r_0 is defined in Eq. (1.6.65) and the AdS_2 length l is given by Eq. (1.6.66). In the non-extremal case, we write $\psi_0(r)$ using a power-series expansion, and we solve Eq. (3.2.25) order by order. At leading order we find:

$$\psi_0(r) = \psi_0(r_+)\left[1 + \frac{1 - \lambda L^2 f''(r_+)}{4\pi T r_+^2 - \lambda L^2 r_+ (4\pi T)^2}\,(r - r_+)\right] + \mathcal{O}\left((r-r_+)^2\right). \tag{3.2.31}$$

For the extremal case, the leading quadratic behavior of $f(r)$ implies $\psi_0(r_+) = 0$. The behavior of $\psi_0(r)$ in the near-horizon region is

$$\psi_0(r) = (r - r_0)^\nu, \quad \nu = \frac{1}{2}\left(-1 + \sqrt{1 + \frac{4l^2 - 8\lambda L^2}{r_0^2}}\right). \tag{3.2.32}$$

$\tilde{\eta}/s$ computation

For Einstein gravity coupled to matter, $\tilde{\eta}/s$ of the dual QFT is determined by means of the retarded Green function in Eq. (2.2.22) and it is given by the non-normalizable mode ψ_0 of the perturbation evaluated at the horizon,

$$\frac{\tilde{\eta}}{s} = \frac{1}{4\pi}\,\psi_0(r_+)^2\,. \tag{3.2.33}$$

This method can be generalized to include higher-curvature contributions [82, 183, 189]. As already shown in the case of GB BB, the computation uses a Wronskian method to determine the relation between the normalizable mode ψ_1 and the non-normalizable mode ψ_0. Since this relation does not depend on the mass term $m^2(r)$ in Eq. (3.2.25), the formula of Ref. [78] also holds for BHs in GB gravity:

$$\frac{\tilde{\eta}}{s} = \frac{1}{4\pi}\,\psi_0(r_+)^2\left[1-4\lambda\left(1-\frac{2\pi G_5 Q^2 L^2}{3r_+^6}\right)\right]\left(1+\frac{6\lambda L^2}{r_+^2}\right)^{-1}, \tag{3.2.34}$$

where $\psi_0(r)$ is the non-normalizable solution of Eq. (3.2.25) with $\omega = 0$.

For background solutions which do not break translational invariance, e.g. branes, the mass term $m^2(r)$ is identically zero and the zero-frequency solution is $\psi_0(r) = 1$ everywhere [78, 183]. On the contrary, in BH backgrounds, the translational invariance is broken, the mass term $m^2(r)$ is non-vanishing, the $\omega = 0$ solution for $\psi_0(r)$ is not constant and $\psi_0(r_+)$ must be calculated by integrating Eq. (3.2.25) with $\omega = 0$.

Large radius BHs $r_+ \gg L$, correspond to the large temperature regime $T \gg 1/L$. In this approximation we can invert $T(r_+)$ in Eq. (1.6.67) to get $r_+(T) = \pi L^2 T + \mathcal{O}(1/T)$. Then, using Eqs. (3.2.27) and (3.2.34) we get

$$\frac{\tilde{\eta}}{s} = \frac{1-4\lambda}{4\pi}\left[1-\frac{\lambda L^2\left(7-6\sqrt{1-4\lambda}\right)}{\pi^2\left(1-\sqrt{1-4\lambda}\right)L^4T^2}+\mathcal{O}\left(1/T^4\right)\right]. \tag{3.2.35}$$

As expected, in the large T regime, $\tilde{\eta}/s$ does not depend on the charge. For GR BHs, Eq. (3.2.35) is a decreasing function of the temperature, thus the KSS bound is violated and the universal value $1/4\pi$ is attained only for $T \to \infty$. For GB BHs, the behavior is qualitatively similar but as $T \to \infty$ the value of $\tilde{\eta}/s$ tends to $(1-4\lambda)/4\pi$.

In the extremal case, the metric function and its first derivative vanish when evaluated on the horizon and following Ref. [78] the shear viscosity to entropy ratio is given by

$$\frac{\tilde{\eta}}{s} = \frac{1}{4\pi}\,\psi_0(r_+)^2\left(1+\frac{6\lambda L^2}{r_0^2}\right)^{-1}. \tag{3.2.36}$$

Equation (3.2.32) tells us that $\psi_0(r_+) = 0$, which substituted in Eq. (3.2.36) means that $\tilde{\eta}/s$ goes to zero in the $T = 0$ extremal limit. The scaling at low temperatures of $\tilde{\eta}/s$ follows from simple matching argument [78] between scaling of the Green function and the near-horizon scaling (3.2.32)

$$\frac{\tilde{\eta}}{s} \sim T^{2\nu}\,, \tag{3.2.37}$$

where ν is given by (3.2.32). The scaling exponent satisfies $\nu \leqslant 1$ for

$$\lambda \geqslant \frac{l^4}{L^2 r_0^2} + \frac{l^2}{2L^2}\,. \tag{3.2.38}$$

The global behavior of $\tilde{\eta}/s$ as a function of T is obtained by numerically integrating Eq. (3.2.25) supplied with a power-series boundary condition for $\psi_0(r)$. In the following, we choose units $G_5 = L = 1$. For each value of the charge and the GB parameter, there exists a minimum mass (and hence a minimum radius) given by Eq. (1.6.63). We then integrate Eq. (3.2.25) outwards from the horizon to infinity. Next, we use a shooting method to determine $\psi_0(r_+)$ by requiring that $\psi_0(\infty) = 1$. Finally, the temperature and $\tilde{\eta}/s$ for each solution are computed with Eqs. (1.6.67) and (3.2.34).

AdS-Reissner-Nordström black holes

The plots of $\tilde{\eta}/s$ resulting from our numerical calculations for GR are shown in Fig. 3.1 for electrically neutral (left panel) and charged (right panel) BHs.

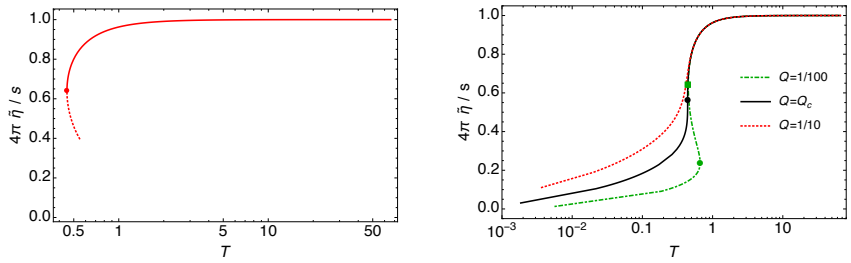

Figure 3.1: Global behavior of $\tilde{\eta}/s$ as a function of the temperature for GR BHs. *Left panel*: neutral AdS BHs. The solid line is the region above the critical radius, while the dotted line represents (part of) the region below the critical radius, where the BH is unstable and a thermal AdS solution is preferred; the dot marks the critical radius at $T = \sqrt{2}/\pi$. *Right panel*: AdS-RN BHs. We plot $\tilde{\eta}/s$ for three selected values of the BH charge: above, at and below the critical value $Q_c = 1/6\sqrt{5\pi}$, at which the system undergoes the second-order phase transition. The dots (square) mark the maximum (minimum) of the temperature as a function of the BH radius.

The KSS bound is always violated for small and intermediate values of temperature, whereas it is saturated from below for large temperatures. In this section we extend the discussion of Ref. [189]. For neutral AdS BHs, $\tilde{\eta}/s$ starts at the universal value $1/4\pi$ at large temperatures and decreases monotonically as T decreases, reaching a minimum non-zero value for the non-vanishing minimum temperature $T = \sqrt{2}/\pi$. Such a temperature corresponds to the minimum value of the BH radius, $r_0 = 1/\sqrt{2}$. At $r = r_0$ there is the Hawking-Page transition and for $r_+ \leqslant r_0$ there are no stable BH solutions [151] and thermal AdS is energetically preferred with respect to the BH. The dotted line in the left panel of Fig. 3.1 gives $\tilde{\eta}/s$ for BHs with radii less than r_0, whose behavior is a consequence of the growing of T for $r_+ \leqslant r_0$.

For AdS-RN BHs, $\tilde{\eta}/s$ decreases from $1/4\pi$ at large temperatures (independently from the charge), but the behavior for small and intermediate temperatures depends on the charge. As explained in Sect. 1.6, there exists a critical value of the charge $Q_c = 1/6\sqrt{5\pi}$ under which the system undergoes a phase transition. On the right panel of Fig. 3.1, we plot our numerical results for $\tilde{\eta}/s$ for the critical charge and for representative values of the charge above, at and below the critical value. The dots (squares) in the curves with $Q \leqslant Q_c$ mark the critical temperature T_{max} (T_{min}) corresponding, to the two local extrema of the function $T(r_+)$ of Eq. (1.6.67). At these

critical temperatures, the specific heat changes sign according to the discussion in Sect. 1.6. For $Q = Q_c$ we have $T_{min} = T_{max}$ and the function $T(r_+)$ has an inflection point. For $Q > Q_c$ the function $T(r_+)$ is monotonically increasing and BHs are always stable. The numerical values T_{min} and T_{max} are listed in Table 3.2 for a representative value of the charge below and at Q_c.

Interestingly, $\tilde{\eta}/s$ develops hysteresis for $0 < Q < Q_c$. This is evident for the $Q = 1/100$ solid black curve in the right panel of Fig. 3.1. We have also checked that curves with $Q < Q_c$ have a similar hysteretic behavior, whereas those with $Q > Q_c$ (as the $Q = 1/10$ orange dashed line) do not show this feature. Notice that the limit $Q \to 0$ in the plot of l.h.s of Fig. 3.1 is singular. As explained in Sect. 1.6, for $Q \to 0$ we have a discontinuity, i.e. we have no phase transition at $Q = 0$. Because the existence of the phase transition is a necessary condition for having hysteresis in $\tilde{\eta}/s$, this means that also $\tilde{\eta}/s$ as a function of the temperature is discontinuous at $Q = 0$: we have a more pronounced hysteretical behavior for $Q \to 0$, but hysteresis disappears completely at $Q = 0$. This hysteretic behavior is a direct consequence of the Van der Waals-like behavior of the AdS-RN BHs discussed in Sect. 1.6. It is related to the presence of two local extrema in the function $T(r_+)$ in Eq. (1.6.67) or equivalently, to the presence of two stable states (small and large BHs) connected by a meta-stable region (intermediate BHs). This phase portrait has been considered as a general explanation of hysteretic behavior for some variable of the system [268]. In particular, when the system evolves from high (low) to lower (higher) temperatures, a potential barrier prevents the evolution of the system from occurring as an equilibrium path between the two stable states [269]. Equilibrium will be reached passing through a meta-stable region and a path-dependence of $\tilde{\eta}/s$ is generated. In particular, starting from high temperatures, the system will reach low temperatures going directly from the minimum and vice-versa. The presence of these local extrema determines the patterns of signs of the BH specific heat and free energy, hence the local thermodynamical stability [163, 184]. Thus, hysteresis in $\tilde{\eta}/s$ and thermodynamical phase transition have the same origin and pattern. In fact, as already noted in Sect. 1.6, the phase diagram of AdS-RN BHs is very similar to that of a Van der Waals liquid/gas transition.

This is a very interesting result: $\tilde{\eta}/s$ for the dual QFT carries direct information about the thermodynamic phase transitions of the system. In the holographic context, a hysteretic behavior in the shear viscosity has been already observed in Ref. [247, 248] for AdS BHs with broken rotational symmetry and with a p-wave holographic superfluid dual. Moreover, it is known that nanofluids may exhibit hysteresis in the η-T plane [270].

Notice that, even though solutions with $Q > Q_c$ describe stable BHs in the overall range of T, our numerical computation does not hold in the small T regime as it uses a power-series near-horizon expansion. However, $\tilde{\eta}/s \to 0$ as $T \to 0$ with analytical scaling law (3.2.37) and scaling exponent ν given by Eq. (3.2.32) with $\lambda = 0$.

Neutral Gauss-Bonnet black holes

Our numerical results for $\tilde{\eta}/s$ as a function of T for neutral GB BHs are shown in Fig. 3.2 for selected values of the GB parameter λ in the range $0 < \lambda \leqslant 5/100$.

For large temperatures, the KSS bound is always violated due to the GB contribution and $4\pi\tilde{\eta}/s \to 1 - 4\lambda$. At intermediate temperatures, the behavior is qualitatively

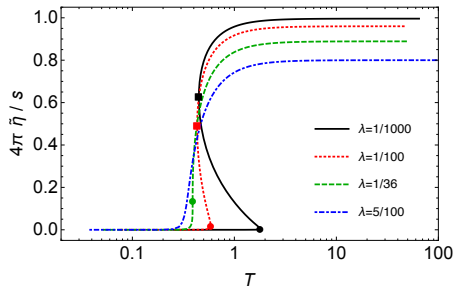

Figure 3.2: Global behavior of $\tilde{\eta}/s$ as a function of the temperature for GB BHs with $Q = 0$ for selected values of the GB coupling constant above, at and below the critical value. Dots (squares) mark the maximum (minimum) of the temperature as a function of the BH radius.

similar to that of RN BHs, with the GB parameter λ playing the role of the charge Q. As discussed in Sect. 1.6, there exists a critical value λ_c under which GB BHs can undergo a phase transition: by numerical investigation this value is $\lambda_c = 1/36$, in good agreement with Refs. [163, 194]. Curves with $0 < \lambda < \lambda_c$ (black solid and red dotted lines) show a hysteretic behavior of $\tilde{\eta}/s$ as a function of the temperature, whereas those with $\lambda > \lambda_c$ do not. For a given value $\lambda < \lambda_c$, we have two critical temperatures T_{max}, T_{min}, which are marked respectively by dots and squares in the curves of Fig. 3.2. Their numerical values for selected values of λ are listed in Table 3.1. Notice that similarly to the $Q \to 0$ case, the limit $\lambda = 0$ in the plots of Fig. 3.2 is singular. As explained in Sect. 1.6, for $\lambda = 0$ we have a discontinuity. This implies that also $\tilde{\eta}/s$ as a function of the temperature is discontinuous at $\lambda = 0$. We have a more pronounced hysteretical behavior for smaller and smaller values of λ, but hysteresis disappears completely at $\lambda = 0$.

The physical interpretation of the appearance of hysteresis in $\tilde{\eta}/s$ for the QFT dual to the neutral GB BH is completely analogue to that discussed for the AdS-RN BH. When λ reaches the critical value, the system undergoes a second-order Van der Waals-like phase transition and exhibits the hysteretic behavior in $\tilde{\eta}/s$.

Q	0			1/100		
λ	1/1000	1/100	λ_c	1/1000	5/1000	λ_c
T_{min}	0.448	0.431	0.390	0.448	0.440	0.397
T_{max}	1.787	0.587	0.390	0.638	0.559	0.397

Table 3.1: Critical temperatures for fixed values of Q and selected values of λ below and at the critical values. For the neutral GB BH the critical value of the coupling is $\lambda_c = 1/36$. For GB BHs with fixed charge $Q = 1/100$ the critical value of the coupling is $\lambda_c \approx 1/4$.

Charged Gauss-Bonnet black holes

The presence of both a non-vanishing charge and GB coupling constant makes the case of charged GB BHs more involved. However, as discussed in Sect. 1.6, the phase portrait becomes much simpler and has a Van der Waals-like form if we restrict our

considerations to the region where BHs are globally stable and holds either Q or λ fixed. In this situation we expect the qualitative behavior of $\tilde{\eta}/s$ as a function of T to be quite similar to that found for the AdS-RN and the neutral GB BHs. The

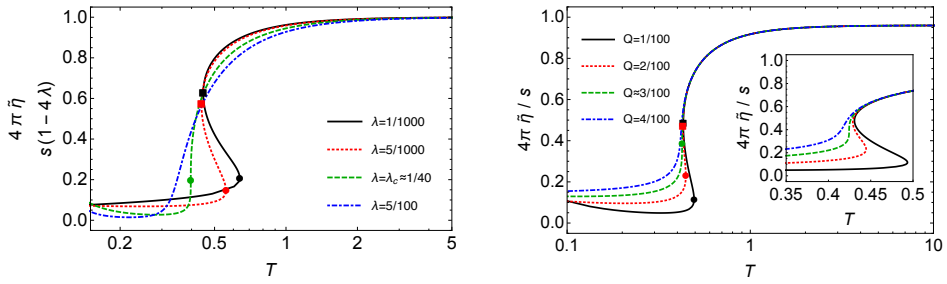

Figure 3.3: Global behavior of $\tilde{\eta}/s$ as a function of the temperature for charged GB BHs. *Left panel*: GB BHs with fixed charge $Q = 1/100$, and selected values of GB constant $\lambda = 1/1000,\ 5/1000,\ \sim 0.25,\ 5/100$. The value of $\tilde{\eta}/s$ is rescaled by a factor $1 - 4\lambda$; in this way the large T behavior of $4\pi\tilde{\eta}/s$, which for GB gravity is λ-dependent, has been normalized to 1. *Right panel*: GB BHs with fixed value of GB constant $\lambda = 1/100$, and selected values of charge $Q = 1/100,\ 2/100,\ \sim 3/100,\ 4/100$. Inset: zoom of the hysteresis region. Dots (squares) mark the local maximum T_{max} (local minimum T_{min}) of the temperature.

numerical results for $\tilde{\eta}/s$ as a function of T, confirm our expectation and are shown in Fig. 3.3 for Q fixed and selected values of the GB parameter λ (left panel) and for λ fixed and selected values of the charge Q (right panel). In both cases, the numerical results corroborate the analytical ones. For large temperatures, the KSS bound is always violated as $4\pi\tilde{\eta}/s \to 1 - 4\lambda$. At intermediate temperatures, the behavior of $\tilde{\eta}/s$ depends crucially on the values of the parameters Q and λ. For large values of Q (or for values of λ near to the unitarity bound $\lambda \lesssim 9/100$), large BHs are always stable, $\tilde{\eta}/s$ decreases monotonically with T and there is no hysteresis.

Notice that the limits $\lambda \to 0$, respectively $Q \to 0$, are singular in the plot on the left, respectively on the right, of Fig. 3.3. We have here a discontinuous behavior of $\tilde{\eta}/s$ similar to that found in the $Q \to 0$ limit for charged BHs in GR and to the $\lambda \to 0$ for the uncharged BHs of GB gravity.

The situation changes drastically for Q (or λ) of order 3/100 and smaller: the system may undergo a Van der Waals-like phase transition. The function $T(r_+)$ develops two local extrema T_{min} and T_{max}, signalizing the presence of two different stable thermodynamical phase (small and large BHs) connected by a meta-stable one, correspondingly, the $\tilde{\eta}/s$ curve as a function of T develops hysteresis. Two typical examples of this hysteretic behavior are shown in Fig. 3.3. On the left panel, for fixed $Q = 1/100$, we see the onset of hysteresis, corresponding to the thermodynamical phase transition, when $\lambda \lesssim 0.025$. On the right panel, for fixed $\lambda = 1/100$, we see the onset of hysteresis and the thermodynamical phase transition when $Q \lesssim 3/100$. The corresponding values of the critical temperatures are marked by the dots (T_{max}) and squares (T_{min}) in Fig. 3.3 and their numerical values are listed in Table 3.1 and Table 3.2 for selected values of the parameters Q and λ.

Analogous results can be found by choosing different Q and λ. Notice that, for stable BH solutions with values of λ and Q above the critical values, our numerical computation cannot reach $T \sim 0$, because it uses a power-series near-horizon expansion

λ	0		1/100		
Q	1/100	Q_c	1/100	2/100	Q_c
T_{min}	0.449	0.441	0.431	0.429	0.425
T_{max}	0.664	0.441	0.494	0.445	0.425

Table 3.2: Critical temperatures for fixed values of λ and selected values Q below and at the critical values. For the AdS-RN BH the critical charge is $Q_c = 1/6\sqrt{5\pi}$. For GB BHs with fixed coupling constant $\lambda = 1/100$ the critical charge is $Q_c \approx 3/100$.

which does not hold in the extremal case. However, from Eqs. (3.2.32) and (3.2.37), which describe analytically the near-extremal behavior we conclude that $\tilde{\eta}/s \to 0$ smoothly as $T \to 0$.

3.3 AdS/CFT applications in 2D gravity

In this Section we recall the revisitation of the AP model already seen in Chapter 1 from a quantum perspective [84]. The goal of our reconsideration is twofolds. On the one hand, we want to describe the symmetries of the model and the pattern of conformal symmetry breaking. We will explain its dynamical consequences (generation of an IR scale and the appearance of Goldstone modes) focusing mainly on bulk gravitational features of the solutions. On the other hand, we would like to connect and translate the formulation of the boundary theory in terms of the Schwarzian action of Ref. [202] in the language of Refs. [169, 170, 201], i.e. in the language of canonical realization of the asymptotic symmetry group of AdS_2.

We will show that the pattern of conformal symmetry breaking and its dynamical consequences can be simply described using bulk Killing vectors, the covariant (bulk) mass definition of Refs. [206–208] and the flow between a "symmetry-respecting" vacuum and a "symmetry-violating" vacuum. In this way we can easily understand, from a purely 2D bulk gravitational perspective, the generation of an IR scale (the mass gap/scale of conformal symmetry breaking in the conformal correlators) and the appearance of local Goldstone modes. We will also relate the microscopic counting of the degrees of freedom responsible for the thermodynamical entropy of the black hole to the breaking of the conformal symmetry and to the associated (quasi) Goldstone modes

Finally, we will show how the solution (1.7.78) can be uplifted to a $(D+2)-$dimensional geometry describing the flow from a $AdS_2 \times R^D$ geometry in the IR to a $(D+2)-$dimensional geometry with hyperscaling violation in the UV.

Symmetries and symmetry breaking

Let us discuss the symmetries of the different vacua of the AP model. The isometry group of AdS_2 is the $SL(2,R) \sim SO(1,2)$ group generated by three Killing vectors. In Schwarzschild coordinates (1.7.78) they represent time translations $\mathcal{T}$, dilatations and special conformal transformations. However, the $SL(2,R)$ symmetry is only a symmetry of the metric. The whole solution contains also the dilaton which, under isometric transformations generated by the Killing vector χ, transforms as $\delta\mu = \mathcal{L}_\chi \mu =$

$\chi^\mu \partial_\mu \mu$ [201]. Notice that a constant dilaton will preserve the $SL(2,R)$ symmetries of the metric, whereas a non constant dilaton will necessarily break explicitly the $SL(2,R)$ symmetry. On the other hand, the 2D metric allows for the killing vector (1.7.86), which is also always a symmetry of the dilaton ($\delta\mu = 0$). Thus, a non constant dilaton breaks explicitly the full $SL(2,R)$ symmetry group of AdS_2 down to its subgroup H generated by the Killing vector (1.7.86).

In the case of the static solutions (1.7.78) the residual symmetry is the time translations $\mathcal{T}$ and the symmetry breaking pattern is $SL(2,R) \to \mathcal{T}$ [201]. As a consequence, the CDV of the AP model preserves the full $SL(2,R)$ symmetries of AdS_2, whereas the LDV breaks $SL(2,R) \to \mathcal{T}$. In this way we can describe the IR/UV flow CDV$\to$LDV as a symmetry breaking of the full $SL(2,R)$ group down to time translations.

The parameter controlling the symmetry breaking is $\partial_x \mu = \mu_0 \lambda$. Any $\mu_0 \neq 0$ value breaks the $SL(2,R)$ symmetry to $\mathcal{T}$ and generates a mass-scale in the IR, set by λ, which is of the same order of magnitude of the mass gap (1.7.85).

Thus, the presence of a non constant dilaton breaks the conformal symmetry of the AdS_2 background and generates in the quantum regime a mass gap through $\mu_0 \neq 0$. Further, it also affects the asymptotic symmetries of AdS_2 [201] and the dynamics of the boundary theory. In particular, the latter can be constructed using boundary curves $t(u)$, where u is the time coordinate in the one-dimensional regularized boundary of AdS_2 [202].

Actually, the two descriptions, that of Refs. [169, 201], which uses canonical realization of the asymptotic symmetry group (ASG) of AdS_2 and that of Ref. [202] give similar results but using different languages and a different coordinate system.

The ASG of AdS_2 [170, 201] is given by reparametrizations of the type $\xi^t = \epsilon(t), \quad \xi^x = x\epsilon'(t)$ and is generated by a single copy of the Virasoro algebra. This transformations map the boundary curves $t(u)$ into curves $t(u) = u + \epsilon(u)$. On the other hand, they act on the asymptotic expansion of the metric [27, 169, 201]

$$g_{tt} = -\lambda^2 x^2 + \gamma_{tt}(t) + o(x^{-2}), \tag{3.3.39}$$

$$g_{tx} = \frac{\gamma_{tx}(t)}{\lambda^3 x^3} + o(x^{-5}), \tag{3.3.40}$$

$$g_{xx} = \frac{1}{\lambda^2 x^2} + \frac{\gamma_{xx}(t)}{\lambda^4 x^4} + o(x^{-6}), \tag{3.3.41}$$

by transforming the values of the boundary fields γ.

In the case of the CDV (which is called "pure AdS_2" in Ref. [202]), the dilaton is constant, $\mu_0 = 0$, and we do not have the explicit breaking of the $SL(2,R)$ conformal symmetry. The full Virasoro ASG is spontaneously broken by the AdS_2 bulk geometry down to the $SL(2,R)$ group of isometries. The zero modes can be characterized either by the boundary curves $t(u)$ (in the language of Ref. [202]) or by the boundary deformations γ (in the language of Ref. [170, 201]). These zero modes can be viewed as the Goldstone modes associated to the spontaneous breaking of the ASG [202]. However, these modes are not local, there is no local action one can write for them and this is related to the fact that the central charge c in the Virasoro algebra is zero.

In the case of the LDV (which is called "nearly AdS_2" in Ref. [202]), as discussed above, the non constant value of the dilaton breaks explicitly $SL(2R) \to \mathcal{T}$. This gives, in the language of Ref. [202] a new dimensional coupling constant, the renormalized boundary value of the dilaton $\phi_r(u)$, which can be used to constrain the shape of $t(u)$ and to produce a local, Schwarzian action for the pseudo-Goldstone bosons $t(u)$.

Conversely, in the language of Refs. [170, 201], the explicit breaking of the conformal symmetry is described by the asymptotic expansion for the dilaton $\mu = \mu_0\rho(t)x + +o(x^2)$ with the boundary field $\rho(t)$ transforming as $\delta\rho = \epsilon\dot{\rho} + \dot{\epsilon}\rho$ under the action of the ASG [170, 201].

The two boundary fields can be identified: $\phi_r(u) = \mu_0\rho(t(u))$. In both descriptions the physical effect of the explicit symmetry breaking is to make the Goldstone modes local and to generate a non vanishing central charge in the Virasoro algebra,

$$c = 12\mu_0, \tag{3.3.42}$$

through the anomalous transformation of the boundary stress energy tensor T_{tt} under the action of the ASG. In fact, we have $T^{(1)}_{tt} = \phi_r\{t(u), u\}$ for the boundary theory of Ref. [202], whereas $T^{(2)}_{tt} = -2\mu_0/\lambda\ddot{\rho}$ for the boundary theory of Refs. [170, 201]. The central charge c takes the form given by Eq. (3.3.42) if we choose $\rho = 1$. We can always make this choice by fixing the u-reparametrization in the boundary which corresponds, in the language of Refs. [170, 201], to consider deformations of the dilaton near the on-shell solution (see [170, 201] for details).

The stress energy tensor $T^{(2)}_{tt}$ can be brought in the form $T^{(1)}_{tt}$. In fact, by considering finite transformations associated with the infinitesimal ones characterized by $\epsilon = u$, by using the transformation of the boundary field ρ and by setting $\rho = 1$ one finds $T^{(2)}_{tt} = (c/12)\{t(u), u\}$. The link between the origin of Schwarzian action and the presence of a non constant dilaton was emphasized also in Ref. [271], where it was shown that in a holographic framework the effective action of the AP model can be put in a Schwarzian form using the anomalous trace Ward identity. In particular, the anomaly turns out to be proportional to the source of the scalar operator dual to the dilaton, which is the analogue of our function $\rho(t)$.

Summarizing, the explicit breaking of the conformal symmetry, $SL(2, R) \to \mathcal{T}$ generated by a non-constant dilaton has two effects. First, it generates at the quantum level an IR scale in the form of mass gap, $M_{gap} \sim \lambda$, separating the CDV from the LDV.

Second, it transforms the global Goldstone modes of the CDV associated with the spontaneous breaking of the ASG into local pseudo-Goldstone modes, producing a central charge $c = 12\mu_0$ in the Virasoro algebra associated to the ASG. This central charge therefore counts the number of pseudo-Goldstone modes. From this perspective we can identify the degrees of freedom responsible for the entropy of the 2D dilatonic black hole as these pseudo-Goldstone modes. The microscopic derivation of the entropy of the 2D dilatonic black hole given in Ref. [169] can be seen as counting the states of these modes. In fact, following Ref. [169] we can write the thermodynamical black hole entropy $\Delta S = S - S_ext$ in terms of the cental charge c and the eigevalue of the L_0 Virasoro operator, $\Delta S = 2\pi\sqrt{cL_0/6}$. Using Eq. (3.3.42) and the expression of L_0 in terms of the black hole mass we can easily recover Eq. (1.7.80). It is also interesting to notice that the mass gap in the chiral 2D CFT can be also understood as finite size effect generated by a plane/cylinder transformation of the vacuum of a CFT with non vanishing central charge $c = 12\mu_0$ [272, 273].

Up-lifting to (D+2)-dimensions

In this Section we show as the up-lifting to $D + 2)$-dimensions of our 2D solution generates an hyperscalin violating geometry.

In $(D+2)$−dimensions the model is described by the action

$$S = \int d^{D+2}x\sqrt{-g_{(D+2)}}R_{(D+2)} + \mathcal{L}_M, \tag{3.3.43}$$

where L_M is the Lagrangian for matter fields, which may also contains explicit coupling of matter fields to the dilaton.

For simplicity we assume that after dimensional reduction to two spacetime dimensions, the term $\mathcal{L}_M$ either reproduce exactly the potential (1.7.77) or a potential, which can be approximated by (1.7.77). We look for brane solutions of the model, i.e. solutions for which the D-dimensional spatial sections have planar topology R^D and the dilaton, μ, plays the role of the radius: $ds^2_{(D+2)} = ds^2_{(2)} + \mu^{2/D}dx_i dx^i$. In general, the dimensional reduction of the action (3.3.43) on this background produces kinetic terms for the dilaton μ in the 2D dilaton gravity action. This terms can be put to zero by a Weyl rescaling of the 2D metric [207]. This corresponds to use, instead, the dimensional reduction

$$ds^2_{(D+2)} = \mu^{\frac{1-D}{D}}ds^2_{(2)} + \mu^{\frac{2}{D}}dx_i dx^i. \tag{3.3.44}$$

One can check that the dimensional reduction now produces the AP action (1.7.75). Using Eq. (3.3.44) and the form of the 2D solution given by Eq. (1.7.78), one can easily realize that the $(D+2)$−dimensional solution interpolates between an hyperscaling violating geometry at large x and an $AdS_2 \times R^D$ geometry at small x. In fact, for $x \to \infty$ the term proportional to x in the dilaton dominates, and the change of radial coordinate, $x \propto r^{-2D/(D+1)}$, brings the metric in the scale covariant form given in Ref. [48]

$$ds^2_{(D+2)} = r^{-2\frac{D-\theta}{D}}\left(-r^{-2(z-1)}dt^2 + dr^2 + dx_i dx^i\right). \tag{3.3.45}$$

The hyperscaling violating parameter θ and the dynamical exponent z are:

$$\theta = \frac{D(D-1)}{D+1}, \quad z = \frac{2D}{D+1}. \tag{3.3.46}$$

Conversely, in the near horizon limit the term proportional to x in the dilaton, can be neglected with respect to the constant term and the metric (3.3.44) gives an $AdS_2 \times R^D$ geometry. This can be also considered as the limiting case $\theta = 0, z = \infty$ of the hyperscaling violating geometry (3.3.45).

3.4 Summary and conclusions

In this Chapter we have computed the shear viscosity to density entropy ratio for 5D charged black branes and black holes both in general relativity and GB theories. Moreover, we have discussed some important applications of AdS/CFT from a bulk point of view and the consequences of the conformal symmetry breaking we have in the case of two dimensions dilaton gravity. In the case of black branes, we have computed the shear viscosity to entropy density ratio both for the non-extremal and the extremal case. We have found that consistently with the geometrical and thermodynamic picture presented in Chapter 1, universality of η/s is lost in the UV but is restored in the IR. The ratio η/s has a non-universal temperature-dependent behavior for non-extremal black branes but attains the universal $1/4\pi$ value at extremality. This result implies that η/s is completely determined by the IR behavior and is completely

insensitive to the UV regime of the dual QFT. This is largely expected because transport features in the hydrodynamic regime should be determined by IR physics. On the other hand, it is not entirely clear if this result has a general meaning or it is a just a consequence of the peculiarities of the charged GB black brane (higher curvature corrections vanish on the $AdS_2 \times R_3$ background).

We have found that η/s is a smooth monotonic function of the temperature. Going to small temperatures, it always flows to the universal value $1/4\pi$ but this value is a *minimum* for $\lambda < 0$ and *maximum* for $\lambda > 0$. Thus, the QFT dual to GB-Maxwell gravity with $\lambda < 0$ gives a nice example of temperature-flow of η/s always bounded from below by $1/4\pi$. On the other hand, the KSS-bound-violating flow we obtain in the theory for $0 < \lambda < 1/4$ remains open to further investigations.

For what concerns 5D charged black holes, the computation of the shear viscosity to density entropy ratio has given interesting results. As expected, the large T behavior of $\tilde{\eta}/s$, corresponding to the flow to the UV fixed point, reproduces the universal value $1/4\pi$ or $(1-4\lambda)/4\pi$ in the GB case. When the bulk BH solution has a regular and stable extremal limit (like e.g. charged BHs) and remains stable at small T, $\tilde{\eta}/s \to 0$ as $T \to 0$ with a $T^{2\nu}$ scaling law. In this latter case, the system flows in the IR to the $AdS_2 \times S^3$ geometry.

Our most important result is the behavior of $\tilde{\eta}/s$ at intermediate temperatures. A second-order, Van der Waals-like, phase transition occurs when the control parameters go below their critical values [184, 185]. In this situation BHs may also undergo a first order phase transition controlled by the temperature. This corresponds to the transition from small to large BHs connected through a meta-stable intermediate region. As a consequence, $\tilde{\eta}/s$ as a function of T always develops hysteresis and it becomes multi-valued as expected for a first order phase transition [247]. Notice that in our case the first and second-order phase transitions are both necessary in order to have the hysteretic behavior in η/s. Even though, similarly to the case discussed in Ref. [247] the multi-valuedness of η/s is directly related only to the first order one. The role of the second-order phase transition is to allow for the existence of the first order one.

The mechanism that generates hysteresis in $\tilde{\eta}/s$ is the same that is responsible for the phase transition and can be traced back to non-equilibrium thermodynamics. When a control parameter, i.e. the charge Q or the GB coupling constant ℓ, is below its critical value, the function $T(r_+)$ develops both a local maximum and minimum. The regions below the maximum and above the minimum correspond to two stable solutions, i.e. small and large BHs, respectively. The region between these two is represented by an unstable (meta-stable) region of intermediate BHs. When the system evolves from large (small) BHs to small (large) BHs, a potential barrier prevents the evolution of the system from occurring as an equilibrium path between the two stable states [269]. Equilibrium will be reached passing through a meta-stable region [268], and a path-dependence of $\tilde{\eta}/s$ is generated. The presence of these local extrema determines the patterns of signs of the BH specific heat and free energy, hence the local thermodynamical stability [163, 184]. This interesting result represents the first attempt to infer about BH thermodynamics through a detailed analysis of a transport coefficient as the shear viscosity.

Let us stress the fact that the definition of $\tilde{\eta}$ for spherical backgrounds is channel-dependent. In general we have three different determinations of $\tilde{\eta}$ for shear, sound

and transverse (scalar) perturbations. In this thesis we have focused on transverse perturbations. It would be of interest to check whether the behavior of the viscosity found for the transverse channel also extends to the sound and shear channels. The computation of our analogue $\tilde{\eta}$ in these other two channels is rather involved and we have left it for future investigations.

Finally, in the case of 2D dilaton gravity, starting from the revisitation of the AP model presented in Chapter 1, we focused mainly on bulk features of the model. We have given a description of the pattern of conformal symmetry breaking, which is complementary to that emerging in the dual CFT [202].

This pattern is quite similar to that pertinent to hyperscaling-violating geometries in higher dimensions, to which we show the AP model can be uplifted. In fact, as a result of the flow between a "symmetry-violating" vacuum and a "symmetry-respecting" vacuum at the quantum level an IR scale is generated in the form of a mass gap. The other effect of the conformal symmetry breaking is to make local the Goldstone modes associated with the asymptotic symmetries of the 2D spacetime. This generates a non-vanishing central charge in the dual conformal theory, which explains at microscopic level the entropy of the 2D black hole [169].

We have also shown that several features of the boundary theory described in Ref. [202] can be easily translated in our language, which is based on bulk quantities and on the asymptotic symmetries of the spacetime.

Part II

The Dark Universe

Chapter 4

Gravity as an emergent phenomenon

Despite its great success in describing various phenomena in nature, for example black holes and gravitational waves, the debate about the validity of general relativity (GR) at every energy scale still goes on in the gravitational physics community. The predictions of GR are in good agreement with observations at Solar system scales, but at cosmological and galactic ones we need to add new exotic components of matter in order to fit the data. In particular, from cosmological observations we know that the baryonic content of matter in the universe is about 5%, whereas the remaining 95% is made of some dark and unknown components which interact only gravitationally and extremely weak coupled with baryonic matter. These are called dark matter (25% of the universe) and dark energy (70% of the universe) and their true nature is still mysterious. For this reason, a new theoretical framework is necessary to explain all these phenomena.

The most conservative approach (the ΛCDM model) assumes the existence of the two dark components. However, to date there is still no direct evidence of the existence of dark matter and dark energy. It is therefore natural to consider large scales (IR) modifications of GR as a viable alternative to the existence of dark matter. In the last thirty years, the number of theories developed to extend general relativity both in the IR and in the UV is rather wide. Among the others, the attempt to find a quantum theory of gravity has triggered the idea that gravity can emerge from some underlying microscopic quantum theory [85, 86, 88–94]. In particular, the works of Verlinde [87] and Dvali *et al* [90, 91, 97, 133–137] have gained a lot of interest in the community.

The main motivations behind these formulations are the understanding of (quantum) spacetime structure at short distances and the puzzles of black hole physics. On the other hand, it has become increasingly evident that a crucial requirement for these theories is the explanation of the dark side of our universe. In the second part of this thesis, we will address these kind of problems by focusing on the galactic regime of gravity both from a classical and quantum perspective. This will be done in the framework of Verlinde's emergent gravity together with the microscopic description of spacetime of Dvali *et al*. In particular, we will focus on the phenomenology usually attributed to explain it can emerge from the quantum nature of spacetime [274, 275]. The interesting fact is that, in this approach, no particles out of the standard model are needed. In the last Chapter of the thesis, we will adopt a conservative approach

to the problem and we will propose a new (classical) solution of general relativity, a sine-Gordon solitonic scalar star, that can account for a possible dark matter candidate [276] in our universe.

In this Chapter, we will first review both the emergent gravity paradigm of Verlinde and the corpuscolar description of gravity of Dvali *et al.*

Note: we set the speed of light as $c = 1$.

4.1 Emergent gravity

The idea that the classical spacetime structure and gravity could emerge together from some underlying microscopic quantum theory is an old one [85]. The power of this emergent paradigm is that it must depend loosely on the details of the underlying microscopic theory and it is essentially determined by its fundamental quantum nature. In particular, even if we do not properly know the nature of the quantum constituents of spacetime, recent theoretical progresses in the field suggest that the fundamental features of the quantum theory such as entanglement can play an important role in formation of geometric structure as spacetime [95]. In this theoretical framework the spacetime geometry is viewed as representing the entanglement structure of the microscopic quantum state. Gravity emerges from this quantum information theoretic viewpoint as describing the change in entanglement caused by matter [87]. These ideas are well understood in the case of AdS/CFT correspondence, whereas when one tries to extend these concepts to a more realistic representation of our universe, i.e. de Sitter universe, some problems arise due to the presence of a cosmological horizon. However, a better investigations of quantum entanglement in this kind of background has led Verlinde to formulate his proposal about emergent gravity [87].

In this Section we will review his approach to this topic with the aim to put the basis for the next Chapters of the thesis.

Entanglement properties of de Sitter spacetime

The role of entanglement is fundamental in the definition of the emerging properties of spacetime. In general, one can think that the presence of an horizon in de Sitter (dS) spacetime (no timelike boundaries at infinity such as in the case of Anti-de Sitter spacetime) can prevent the existence of a quantum description in terms of a holographic correspondence, namely (A)dS/CFT. Instead, this peculiar feature of dS suggests that the properties of the (presently unknown) quantum degrees of freedom at very large scales are completely different from the ones at small scales.

As an horizon, also the dS horizon carries a certain amount of entropy and, correspondingly, it has a temperature, accordingly to Bekenstein-Hawking formulas. The horizon entropy scales as an area, as expected. The existence of a horizon entropy and temperature signalize that, microscopically, de Sitter space can be considered as a thermal state filled of some internal degrees of freedom in which part of them are being "thermalized". Differently from a static black hole, in the dS case we have slow thermalization with time scale of order Hubble time, resulting from the accelerated expansion of the universe. Interactions and connections between the microscopic constituents of spacetime are provided by quantum entanglement. In de Sitter spacetime, one should consider two different regimes of quantum entanglement: on the

one hand, we have the *long range* entanglement connecting bulk excitations with the horizon ones. On the other one, we have the *short range* entanglement characterizing the interactions between horizon internal degrees of freedom and satisfying an area law. The latter is true for cosmological or black holes horizons.

The novel idea is that these quantum states associated with the horizon entropy are considered as maximally entangled with bulk excitations carrying a typical energy set by the temperature. In this picture, the thermal excitations responsible for the de Sitter entropy constitute the positive dark energy, which, together with the accelerated expansion of the universe, are caused by the slow thermalization of the emergent spacetime. From a quantum perspective, de Sitter space corresponds to an ensemble of metastable quantum states that together carry the Bekenstein-Hawking entropy associated with the cosmological horizon. The metastability has purely an entropic origin: the high degeneracy together with the ultra-slow dynamics prevent the microscopic system to relax to the true ground state. At long timescales the microscopic de Sitter states contain a thermal volume law contribution to the entanglement entropy. This behavior is typical of glassy systems, where two different dynamics lead to different physical configurations, even if the microscopic constituents are always the same [277–279].

In this perspective, one can derive the effective macroscopic dynamics charaterizing the "short" scale dynamics of gravity given by Einstein's equations from a minimization of an area law for the entanglement entropy. For example, a similar procedure has been done in condensed matter physics, where a strict area law arises almost exclusively in ground states of gapped systems with strong short range correlations. In the case of de Sitter space, due to the long range interactions and to thermalization a non-zero volume law entropy arises. Its contribution is subleading with respect to the area contribution at short distances but it cannot be neglected at large distances where it will be the dominant part of the entropy of the system. This phenomenon can be considered as responsible for the presence of a cosmological horizon in de Sitter universe.

Hints from quantum gravity: the dark matter problem

The emergent gravity scenario described above must have also important consequences for the behaviour of gravity at galactic scales. This is a crucial point because galactic scales are those pertinent to the dark matter phenomenology. One is therefore lead to look to this emergent scenario for solving the dark matter puzzle.

As already mentioned, the cosmological observations indicates that the 95% of the universe is represented by a mysterious form of matter and energy, the dark matter (25%) and the dark energy (70%). In the emergent gravity paradigm, where everything is emerging from some underlying microscopic quantum theory, no exotic matter should be needed to fit the data. Rather, one should think to dark matter and dark energy as well, as emerging from quantum properties of spacetime.

One way to tackle the problem is to consider galactic dynamics and, in particular, galaxies rotational curves. At galactic scales, we know that the flattening of rotational curves is controlled by the Hubble acceleration, $a_0 = H_0 = 1/L$, where L is the de Sitter radius [1] [120, 121]. In particular, the dark matter effects in galactic dynam-

[1] The cosmological constant is related to the de Sitter radius by $\Lambda = 6/L$.

ics arise when the Newtonian acceleration becomes comparable to the cosmological acceleration. This leads to the definition of a critical radius, r_0, at which the dark matter effects take places. In a detailed mathematical and physical picture, this can be translated in a competition between the two kind of entanglement described above: on the one hand, the short range entanglement is responsible for the emerging of Einstein gravity and, in the weak field regime, for the Newtonian dynamics. This dictates how matter should behave at Solar system scales and at galactic ones in the core of the galaxy, i.e. for $r \leqslant r_0$. As a consequence, this baryonic matter carries a certain amount of entropy which is proportional to the area of the region in which it is stored. On the other one, the long range entanglement is responsible for the accelerated expansion of the universe, thus leading to the cosmic acceleration $a_0 = 1/L$. This pure quantum effect contributes with a (thermal) volume contribution to the total entropy of spacetime in a galactic region and it is important for $r \geqslant r_0$.

In the emergent gravity perspective we are dealing with, the dark matter effects can be understood as a reaction of spacetime (which in the efective description can be thought as a the dark energy fluid) to the presence of baryonic matter. The quantum properties of spacetime turns the effective description of the universe into an effective fluid description or, depending of the specific realization, an elastic theory of quantum degrees of freedom. When one takes into account the presence of baryonic matter in the weak field regime of the interaction, spacetime reacts as an elastic medium, thus generating an elastic force from which it is possible to derive the acceleration of stars in galaxies, i.e.

$$a_{\mathrm{MOND}}(r) = \sqrt{\tilde{a}_0\, a_B(r)}\ , \tag{4.1.1}$$

where $\tilde{a}_0 = a_0/6$ and $a_B(r) = Gm_B(r)/r^2$. This formula exactly matches the MOND acceleration [120, 121]. This relation can be also written as

$$v^2 \approx \sqrt{a_0\, G_N\, m_B}, \tag{4.1.2}$$

which exactly matches the Tully-Fisher relation at these scales [115]. Both the formulas perfectly fit the data about the rotational curves of stars in galaxies and describe galactic dynamics. We skip the derivation of these results and we refer the reader to the lecture of Verlinde's paper [87] for the details. Eqs. (4.1.1) and (4.1.2) show that we do not need particles out of the standard model to understand the physics at galactic scales, rather, we should better investigate the quantum properties of spacetime. We conclude noticing that the Verlinde's results are valid only for static spacetime and, in their derivation, de Sitter spacetime is taken as a pre-existing background. A more involved formulation of the theory is necessary to include the real nature of this quantum degrees of freedom and dynamical spacetime too.

In the next Chapter we will show how it is possible to formulate the emergent gravity paradigm presented here in the quantum perspective of corpuscolar gravity of Dvali *et al*, e.g. [91, 275], with the aim to better understand the quantum origin of Eqs. (4.1.1) and (4.1.2).

4.2 Corpuscolar gravity

In the previous Section we have seen how entanglement plays a fundamental role in the emerging of dS universe and of a dark force at galactic scales. From Verlinde's

point of view, the nature of the elementary microscopic quantum degrees of freedom is not specified and their dynamics defines the macroscopic properties of spacetime. Among the various attempts to give a detailed description of the nature of these degrees of freedom, a series of papers of Dvali and collaborators have suggested the possibility to understand gravity as emerging from a Bose-Einstein condensate of gravitons [90, 91, 97, 133–137]. In this Section we will summarize the content of these papers and report the basic ingredients of this approach with the aim to put the basis for the next Chapters, where the notion of corpuscolar gravity will be fundamental.

Gravity as a Bose-Einstein condensate

Einstein's theory is a classical theory of gravity. Viewed as a quantum theory, GR is a theory that propagates a unique weakly-coupled quantum particle with zero mass and spin-2. At low energies a consistent definition of the quantum self-coupling constant of the theory can be a dimensionless parameter given by

$$\alpha_{GR} = \frac{L_P^2}{\lambda^2}, \tag{4.2.3}$$

where L_P is the Planck length, $L_P = \sqrt{\hbar G_N}$ and λ is the typical Compton wavelength of the particle. When $\lambda \ll L_P$ the theory becomes strongly coupled. This fact indicates that GR can be seen as a quantum theory only in the weak coupling regime. In order to not violate unitarity in the trans-Planckian regime some mechanism able to prevent such a problem should exist. This shall enable us to compute gravitational amplitudes at arbitrarily short distances.

A possibility to avoid this hypothesis is to consider Einstein gravity as a *self-complete* quantum field theory (in a non-Wilsonian way). This concept can be explained as follows: when gravitons are in a regime such that their energy is approaching values greater than the Planck energy, the system is induced to produce particles with a very large wavelength $\lambda \gg L_P$ and a large occupation number N_G. In this way, unitarity is restored being the probability to produce particles with momentum greater than $\hbar/L_P$ very low and exponentially suppressed. When the number of produced particles N_G sufficiently grows, the system undergoes the so-called *classicalization* process. From a quantum perspective classicalization or classicality means that any classical object is understood as a quantum bound-state of high occupation number $N_G \gg 1$. Conversely, given a quantum system, when the number of particles increases such that $N_G \gg 1$, the system become classical. For this reason we can talk about *corpuscolar gravity*. Among the variety of macroscopic and classical objects one can take into account, black holes (and solitons as well) seems to be the simplest ones. They can be described by a single quantum characteristic, N_G. For this purpose this number serves as the main measure of classicality.

The occupation number of gravitons is a universal quantity irrespective of the particular nature of the source. In particular black holes maximizes the number N_G, i.e. N_G reaches its maximum value for wavelength of the order of the Schwarzschild radius of the object. From this perspective, black holes are the most classical object among all possible objects of a given characteristic wavelength. Universality of N_G leads us to a quantum-mechanical picture of a black hole which does not introduce any classical geometric feature of the system. Instead it is fully characterized by the single parameter N_G.

Black holes in corpuscolar gravity

The starting point of the corpuscolar picture of gravity is that black holes can be seen as a self-sustained Bose-Einstein condensate (BEC) made of N_G gravitons at the point of *maximal packing*. The maximal packing condition means that the size of the system, λ, depends on the occupation number N_G in such a way that it is impossible to further increase N_G without increasing λ. This ensure that once the maximal packing condition is reached, the system can be always described as a Bose-Einstein condensate of gravitons and the number of particles, N_G, become the only characteristic of the system. By using this picture it is possible to explain all the fascinating and puzzling properties of black holes such as the Hawking radiation, the black holes negative specific heat and entropy and, finally, holography.

The interesting fact is that, in this picture, black holes represent Bose-Einstein condensates of gravitons at the critical point of a quantum phase transitions. This can be explained as a consequence of the gravitational collapse of matter. Indeed, the condition for a formation of a black hole, i.e. that matter reaches the Schwarzschild radius $r = 2Gm$, allows the system to reach the critical point at which it becomes self-sustained (or maximally packed from a quantum point of view) condensate of N_G particles. This is due to the self-similarity of the quantum depletion: every times the system changes its size, the occupation number N_G changes correspondingly in such a way the system always stays at the critical point of the quantum phase transition. In this way, for example, it is possible to explain the Hawking radiation: if the wavelength of the gravitons at the fundamental state decreases, the system shrinks. Then in order to satisfy the maximal packing condition, the system is forced to emit a certain number of particles. This shows how the occupation number N_G plays an important role also in defining the size of the system.

A way to calculate the number N_G and evaluate the graviton wavelength in the BEC, i.e. the energy of the gravitons is as follows. As mentioned before, the graviton-graviton coupling constant can be defined by using the dimensionless constant α given in Eq. (4.2.3). The graviton-graviton coupling constant can be understood as the relativistic generalization of the Newtonian interaction between gravitons. In terms of α, the latter can be written as

$$V(r)_{\text{Newton}} = -\hbar\frac{\alpha}{r}. \tag{4.2.4}$$

In case of massive particles, r represents the De Broglie wavelength of the particle. Since gravitons are massless particles, we have to use the Compton wavelength.

It is easy to see from Eq. (4.2.3) that the interaction among gravitons is extremely weak. However, since gravitons are bosons they can self-condensate and their occupation number can become extremely large. In this condition, the effects of the mutual interaction become important and each graviton can feel a stronger and stronger binding potential, thus leading to a critical occupation number,

$$N_G = N_c = \frac{1}{\alpha}. \tag{4.2.5}$$

At the critical point the condensate become *self-sustained* and this exactly represents a black hole state. The condition of self-sustainability can be also obtained by equating the kinetic energies of individual quanta, E_k, with the collective binding potential, V,

$$E_k + V = (1 - \alpha N_G)\,\frac{\hbar}{\lambda} = 0, \tag{4.2.6}$$

which is satisfied for the critical occupation number in Eq. (4.2.5). As mentioned before, the critical point also corresponds to the point of maximal packing of the condensate. This means that the system is so densely packed that the occupation number N_G becomes its only defining characteristic. In particular, by using Eqs. (4.2.3) and (4.2.5) we obtain

$$\lambda = \sqrt{N_G} L_P, \qquad \alpha = \frac{1}{N_G}. \tag{4.2.7}$$

In case of black holes, we can also relate the gravitons' occupation number to their mass. In fact, for a black hole λ is given by $\lambda = 2Gm$, which in turn determines the condition to obtain a black hole from the gravitational collapse of matter, the equation above con be also written as

$$m = \sqrt{N_G} m_P, \tag{4.2.8}$$

where m_P is the Planck mass. Formulae (4.2.7) and (4.2.8) will play a key role in the development we present in the next Chapters.

Let us note that the critical point in Eq. (4.2.7) can be achieved for arbitrary N_G but, in general, λ cannot arbitrarily decrease beyond $\sqrt{N_G} L_P$. In fact, the decrease of gravitons' wavelength is always balanced by a decrease of N_G due to quantum depletion and leakage of the condensate. In this way the condensate can collapse but it looses particles at the same rate and the system always stay at the critical point. For example, this mechanism can explain the Hawking radiation.

For what concerns this thesis, we will not report the explanation of other fascinating and puzzling topics in black hole physics due to the corpuscolar picture of gravity. We refer the reader to the papers [90, 91, 97, 133–137]. Let us conclude by noticing that the corpuscolar gravity picture is able to describe not only black hole physics but also the de Sitter and inflationary universe [91, 99, 280, 281]. As we will see in the next Chapter, the de Sitter universe can be described as a Bose-Einstein condensate of gravitons with typical wavelength of the order of the Hubble radius, L. In this case the occupation number of gravitons is

$$N_{dS} = \frac{L^2}{L_P^2}. \tag{4.2.9}$$

In this picture, the de Sitter universe behaves as a black hole, with the Hubble radius replacing the Schwarzschild radius. The typical energy of gravitons in this regime is of the order of $E_{dS} = \hbar/L$. Indeed, following [91, 280] it is also possible to calculate the Hubble temperature. We argue that in the case of de Sitter universe, the equivalent of Hawking radiation, i.e. the depletion of the condensate and the leakage of particles, can be understood at macroscopic level as the enhancing of a dark energy fluid. This is a consequence of the condition of maximal packing (or maximally entangled quantum degrees of freedom in the language of Verlinde's emergent gravity, see Sect. 4.1) in the case of a cosmological condensate. Indeed when the energy of gravitons increase, $E_g > E_{dS}$, for example due to quantum fluctuations, the cosmological gravitons' wavelength decrease correspondingly, $\lambda_g < L$, and gravitons can feel a stronger and stronger binding potential, $V \propto \hbar/\lambda_g > V_{dS} \propto \hbar/L$. In order to the system to not collapse and stay always in the condensate phase, it must increase the number of particles in the condensate (DE particles in the effective fluid description). As a consequence, the BEC increase its size, i.e. it expands, according to Eq. (4.2.9). This, in turns,

satisfies also the third principle of thermodynamics which implies entropy of a system cannot decrease, i.e. the occupation number of a system can never decrease. In this sense, this idea can be seen as a translation, in the corpuscolar gravity dictionary, of a recent proposal about the origin of de Sitter spacetime from the maximization of entanglement entropy in a Freedman-Robertson-Walker-Lamaître universe [282]. However, the detailed study of cosmological BECs and the origin of dark energy will not be addressed in this thesis but and is left for future investigations.

Chapter 5

Emergent gravity in a corpuscular picture

The possibility that the gravitational interaction could emerge together with the spacetime structure from some underlying microscopic quantum theory is not only a fascinating topic in theoretical physics. It represents also a concrete route to follow to find the signature of quantum gravitational effects at macroscopic scales. Indeed, following [87], in the next two Chapters, we will show how some aspects of the gravitational physics at galactic scales, which are generally attributed to the phenomenology of dark matter, can be explained in a corpuscolar picture of emergent gravity.

In particular, in this Chapter, we study and investigate the emergent laws of gravity when dark energy and the de Sitter spacetime are modelled as a critical Bose-Einstein condensate of a large number of soft gravitons N_G. We argue that this scenario requires the presence of various regimes of gravity in which N_G scales in different ways. This is similar to the different entanglement entropies scenarios we have introduced in the previous Chapter describing Verlinde's emergent gravity [87]. Moreover, the local gravitational interaction affecting baryonic matter can be naturally described in terms of gravitons pulled out from this Dark Energy condensate (DEC). For what concerns the galactic dynamics, we then explain the additional component of the acceleration at galactic scales, commonly attributed to dark matter, as the reaction of the DEC to the presence of baryonic matter. This additional dark force is also associated to gravitons pulled out from the DEC and correctly reproduces the MOND acceleration. We finally calculate the mass ratio between the contribution of the apparent dark matter and the baryonic matter in a region of size r at galactic scales and show that it is consistent with the ΛCDM predictions. The Chapter is based on:

- M. Cadoni, R. Casadio, A. Giusti and M. T., "*Emergence of a Dark Force in Corpuscular Gravity*", **Phys.Rev. D97 (2018) no.4, 044047**, arXiv:1801.10374.

- M. Cadoni, R. Casadio, A. Giusti, W. Mück and M. T. "*Effective Fluid Description of the Dark Universe*", **Phys.Lett. B776 (2018) 242-248**, arXiv:1707.09945.

Note: we use units with $c = 1$, while the Newton and Planck constants are expressed in terms of the Planck length and mass as $G_N = \ell_p/m_p$ and $\hbar = \ell_p m_p$, respectively.

5.1 Quantum compositeness and the scaling of graviton number

In a pure emergent gravity approach, the true quantum nature of gravity cannot be fully neglected in our present universe, even at astrophysical and cosmological scales. As a consequence, the geometric description given by Einstein gravity (or modifications thereof) should only emerge in suitable regimes and for specific observables. In particular, as mentioned in Chapter 4, it has been conjectured that the quantum state of our universe could be thought of as a BEC [91] containing a certain number N_G of (very soft and virtual) gravitons with typical energy ε_G, very much like the gravitational field of a black hole [90]. The presence of baryonic matter must affect the quantum state of this BEC of gravitons and, at least in some crude approximation, one can then expect an energy balance, akin to the Hamiltonian constraint of GR, holds in the form

$$H_B + H_G = 0, \tag{5.1.1}$$

where H_B is the matter energy and H_G the analogue quantity for the graviton state.

It is now crucial that our present universe appears to be mostly driven by dark energy, and as such it is characterised by the Hubble radius,

$$L = H^{-1}, \tag{5.1.2}$$

of the visible portion. Furthermore, the presence of baryonic matter (stars and planets) defines a typical size R_B, around which gravity is well approximated by Newtonian physics. These two length scales satisfy the hierarchy

$$R_H \ll R_B \ll L, \tag{5.1.3}$$

where $R_H = 2\,G_N\,m_B$ is the Schwarzschild radius of a source of baryonic mass m_B. The quantum state of gravity should entail such scales. In particular, we expect to identify different regimes of gravity for each scale from the way both the number of gravitons N_G and their typical energy ε_G scale with the mass $m = m(r)$ and the size r of the region we are considering.

In the corpuscular description, one is mainly concerned with *self-gravitating* systems, i.e. compact sources of typical size R_B. To this class belong both marginally bound systems, which are described by BEC at the critical point (black holes) and non-marginally bound systems (compact stars, horizonless objects) which are described by BEC away from the critical point. In terms of the graviton coupling $\alpha \simeq \ell_p^2/r^2$ the two regimes respectively correspond to $\alpha = 1/N_G$ and $\alpha < 1/N_G$ [90].

In terms of the Hamiltonian constraint (5.1.1) the marginally bound condition corresponds to systems for which the mass is equal to the graviton interaction energy [283]. This is the case, for istance, of very compact (collapsing) stars or black holes. Indeed, if we consider these objects as made of N interacting identical components and, for simplicity, we also neglect any emission of radiation, the total energy is conserved and always equals the ADM mass M of the system. Moreover, we know that in general relativity the energy conservation is given by the Hamiltonian constraint associated to the freedom of time reparametrization. Thus (5.1.1) becomes $H_G + H_B = M$, where H_G and H_B are the gravitational and matter Hamiltonian obtained by varying the

action with respect to the lapse function and M emerges from boundary terms. At small scales, i.e. for r of the order of the size of compact sources, the number of gravitons N_G affected by the presence of matter sources can be obtained by describing the Newtonian (and first post-Newtonian [283, 284]) potential by means of a quantum coherent state, for which one generically finds a quadratic scaling of N_G with the mass [90],

$$N_G \sim \frac{m_B^2}{m_p^2}, \tag{5.1.4}$$

where m_B is the mass of the localised baryonic source. Since the (negative) Newtonian energy is given by

$$U_N \simeq N_G\, \varepsilon_G \simeq -\frac{G_N\, m_B^2}{r}, \tag{5.1.5}$$

the typical energy of the individual (virtual) quanta is again given by the Compton relation

$$\varepsilon_G \simeq -\frac{\ell_p\, m_p}{r}, \tag{5.1.6}$$

and, using the mass/radius relation for black holes, $m_B \simeq r = R_H$, Eq. (5.1.5) implies an holographic scaling with r, namely

$$N_G \sim \frac{r^2}{\ell_p^2} \sim -\frac{1}{\rho_H}, \tag{5.1.7}$$

where ρ_H is the (negative) graviton energy density around a black hole.

Notice that, for non-marginally bound gravitational systems, the scaling relation (5.1.4) still holds [283, 284], but the holographic (5.1.7) does in general not. The corpuscular description can be generalized to cosmological spacetimes [91] in absence of baryonic matter. In this framework, the dS universe of size L, sourced by a constant dark energy density ρ_Λ, can be described, similarly to a black hole, as a critical BEC [280]. In fact, the main feature of the dark energy sourcing the dS space-time, namely that it satisfies the vacuum equation of state $p = -\rho_\Lambda$, is naturally realised in a BEC, as was shown in Refs. [285–288].

An ideal universe of size L solely containing self-coupled gravitons as a description of vacuum (dark) energy should behave like the de Sitter spacetime. In GR, one then needs a cosmological constant term, or constant vacuum energy density ρ_Λ, so that the Friedman equation reads

$$H^2 \equiv \left(\frac{\dot{a}}{a}\right)^2 \simeq G_N\, \rho_\Lambda. \tag{5.1.8}$$

Upon integrating on the volume inside the Hubble radius (5.1.2), we obtain

$$L \simeq G_N\, L^3\, \rho_\Lambda \simeq G_N\, m_\Lambda. \tag{5.1.9}$$

This relation looks like the expression of the horizon radius for a black hole of ADM mass m_Λ, which has led to conjecture that the dS spacetime could likewise be described as a condensate of gravitons [91, 280]. One can in fact introduce a corpuscular

description on assuming that the (soft virtual) graviton self-interaction gives rise to a condensate of N_Λ gravitons of typical Compton length equal to L [91], so that the total (positive dark) energy

$$m_\Lambda \simeq N_\Lambda \, \varepsilon_\Lambda \simeq N_\Lambda \, \frac{\ell_p \, m_p}{L}, \tag{5.1.10}$$

and, from Eq. (5.1.9), it follows immediately that

$$N_\Lambda \sim \frac{m_\Lambda^2}{m_p^2} = \frac{L^2}{\ell_p^2}, \tag{5.1.11}$$

which shows that one needs a huge $N_\Lambda \gg 1$ for a macroscopic universe. Note also that we have

$$\rho_\Lambda \sim \frac{m_\Lambda}{L^3} \sim \frac{1}{N_\Lambda}, \tag{5.1.12}$$

so that the number of gravitons in the vacuum increases for smaller vacuum energy, and

$$L \sim m_\Lambda \sim \frac{1}{\sqrt{\rho_\Lambda}}. \tag{5.1.13}$$

It seems sufficiently clear that in the corpuscolar gravity picture, geometric quantities as black hole area or radius are encoded in the notion of gravitons occupation number, N_G. For instance, this can help us to encode a physical concept as black hole entropy in a simple and intuitive way. Indeed, in what follows we will explain how translate the key point of Verlinde's emergent gravity, i.e. the different entanglement scaling in dS spacetime (see Chapter 4) in the corpuscolar gravity picture we are dealing with.

Holographic regimes of gravity

We have shown that black holes and the dS universe can be described by a critical BEC of gravitons we dubbed DEC. We have also seen that criticality for the BEC implies the holographic scalings (5.1.7) and (5.1.11) for N_G. Being all the gravitons packed in the ground state, the entropy of the DEC is given by N_G, implying that Eqs. (5.1.7) and (5.1.11) are equivalent to the BH area law [1].

Eqs. (5.1.4) and (5.1.11) define the *holographic regimes of gravity*: for volumes of both cosmological (in absence of baryonic matter) and Newtonian size, one can argue that the relevant number of gravitons scales holographically, that is

$$N_G^A(r) \sim \frac{m^2(r)}{m_p^2} \sim \frac{r^2}{\ell_p^2}, \quad \text{for } r \simeq L \text{ and } r \simeq R_B, \tag{5.1.14}$$

where $m = m(r)$ is an appropriate mass function inside the volume. More precisely, $N_G(L)$ can be viewed as the total number of gravitons inside the visible universe, whereas $N_G(R_B)$ is the number of gravitons that respond locally to the presence of the baryonic sources of mass m_B, by changing their energy from $\varepsilon_G(L)$ to some $\varepsilon_G(R_B) < \varepsilon_G(L)$ in order to enforce the Newtonian dynamics. The holographic scaling (5.1.14) therefore applies to two very different, albeit equally non-extensive, regimes of gravity.

[1] Factors of order one will be usually neglected unless necessary.

The holographic scaling relations (5.1.7) and (5.1.4) were first found for black holes [91], and only Eq. (5.1.4) was then shown to hold for general compact sources in Refs. [283, 284]. From Eqs. (5.1.4), it follows that we get the BH area law (5.1.14) in the regime where the relevant mass $m = m(r)$ of the condensate scales linearly with the size r of the source.

The holographic regime of gravity holds for sure in the case of black holes and the de Sitter space, and we assume that Eq. (5.1.14) also remains a very good approximation at all typical scales r for which gravity is well described by GR. This assumption is based on the fact that the holographic nature of gravity is a generic consequence of the Einstein-Hilbert action. Note, however, the change in sign of the graviton energy from the positive cosmological mass (5.1.10) to the negative Newtonian energy (5.1.5): this is a clear signal that the two holographic regimes, at small and very large scales, respectively, are indeed different, which suggests that at intermediate scales the behaviour of gravity deviates from the holographic description, as we will see in the next section.

Before we proceed, a word of caution is in order: since the gravitons in the condensate are considered as virtual (non-propagating) modes, their number N_G is not directly observable, nor is their individual energy ε_G. In fact, one can think of these quantities as convenient intermediate variables which will not appear in our final expression for the matter dynamics. These gravitons could however become observable if they are scattered off the coherent state, for instance by their self-interaction, which leads to the depletion of the DEC. This effect produces the Hawking radiation around black holes [90] and primordial perturbations during inflation [91, 289], but will be totally neglected in this thesis.

Extensive regime of gravity

There are several reasons, coming both from the microscopic and from the emergent space-time description, for arguing that the holographic regime (5.1.14) of gravity can not hold throughout the whole range of scales (5.1.3). In particular, this implies the existence of a new infrared scale $R_H < r_0 < L$, where the behaviour of gravity deviates from the holographic description.

The first indication comes from the fact that the two holographic regimes at small and very large scales, although satisfying the same scaling relation (5.1.14), are indeed different. We recalled above that the graviton energy changes in sign going from the positive cosmological mass (5.1.10) to the negative Newtonian energy (5.1.5). This implies the two holographic regimes must be connected by a *mesoscopic* phase, in which gravity may deviate from the holographic behaviour (5.1.14).

The second indication comes from Verlinde's argument about the pattern of entanglement entropy in dS space [87]. As pointed out in Chapter 4, unlike black holes, the dS spacetime must contain a thermal volume contribution to the entanglement entropy, coming from very low energy modes. In our description of the dS spacetime, this implies an extensive term for the graviton number associated with the DEC.

The third and strongest indication comes from the fact that, locally, without baryonic matter, the DEC of the dS space-time has a constant energy density characterized by an extensive behaviour. In fact, at galactic scales, we cannot consider the cosmic condensate as a whole, but just as a medium with (positive) constant energy density

ρ_G equal to the cosmological value (5.1.12), that is

$$\rho_G \simeq \rho_\Lambda \sim \frac{m_p}{L^2\,\ell_p}. \tag{5.1.15}$$

The total graviton energy inside a region of size r is therefore given by

$$m_G(r) \simeq \frac{4\pi}{3}\,\rho_\Lambda\, r^3 \sim \frac{m_p\, r^3}{L^2\,\ell_p} = N_G(r)\,\varepsilon_\Lambda. \tag{5.1.16}$$

The number of gravitons contained in this spherical region is therefore an *extensive* quantity, scaling as the volume,

$$N_G \simeq \frac{r^3}{L\,\ell_p^2} \sim \frac{m_G(r)}{m_p} \tag{5.1.17}$$

where we again assumed the Compton relation $\varepsilon_\Lambda \sim \ell_p\, m_p/L$ from Eq. (5.1.10). A crucial check for the validity of the scaling relation (5.1.17) is that it correctly reproduces the cosmological relation (5.1.11) precisely for $r = L$.

We are therefore lead to assume that, if baryonic matter is totally neglected, at the intermediate scales $R_B \ll r \ll L$, the graviton state is approximately described by the extensive regime (5.1.17), i.e. it is ruled by the *extensive regime of gravity*:

$$N_G^V(r) \sim \frac{m}{m_p} \sim \frac{r^3}{L\,\ell_p^2}, \quad \text{for } R_B \ll r \ll L. \tag{5.1.18}$$

This behaviour will be argued to interpolate somehow between the two (different) holographic regimes (5.1.14) at $r \simeq L$ and $r \simeq R_B$. One of the main results we will present here is that it is the tension between the two scalings (5.1.14) and (5.1.18) that leads to deviations from the local Newtonian dynamics [87]: the response of the graviton condensate to the presence of baryonic matter makes both the holographic and the extensive regimes important at galactic scales.

The physical picture behind this corpuscular description is again similar to Verlinde's [87]. For compact sources of size $R_B \simeq R_H$ and at cosmological scales L, gravity allows for a corpuscular description in which it is described by a critical BEC of gravitons. The effective theory in these two regimes is GR [2], whose peculiar non-extensive, holographic character is encoded by the relations (5.1.7) and (5.1.11). Notice that these two regimes corresponds to length scales differing by several orders of magnitude (about 60 if we take $r = \ell_p$ and $r = L$), and the same holds for the graviton wavelengths in the two regimes.

A specific merit of the corpuscular picture we started to build is however that these two holographic regimes are truly different, as the relation (5.1.14) refers to the total number of gravitons in the cosmological condensate for $r \simeq L$, whereas it only counts the number of gravitons affected by the local matter sources for $r \simeq R_B \gtrsim R_H$. We recall once more the difference is clearly signalled by the opposite signs of $\varepsilon_\Lambda > 0$ and $\varepsilon_B < 0$.

At intermediate scales the condensate has the intrinsic extensive behaviour (5.1.17), which is a peculiar feature of thermalization processes (corresponding to the slow

[2] Since the universe is expanding, one might argue that the cosmological description is in fact closer to a modified $f(R) \simeq R^2$ theory of gravity [284].

dynamics of glassy systems in Verlinde's description). Strictly speaking the graviton number N_G^V inside a spherical region is not physically measurable. In fact N_G^V is not conserved and, for a small region, it is expected to have large relative fluctuations. For regions of galactic or cosmological size, the relative fluctuations are small but we can hardly conceive a physical process apt to measure N_G^V. On the other hand, our final results are independent from N_G^V and we do not need to be concerned about its measurability.

In principle, there could be concerns about the impact that an extensive, volume-scaling, term for N_G can have on the cosmological evolution, in particular for late-time cosmology. At late times, the cosmological dynamics is described by the holographic regime characteristic of the dS space-time as discussed above. Actually, it has been recently shown by Carroll *et al* [282] that this is a quite general result. Assuming the validity of a generalized second law of thermodynamics and that the entropy increases up to a finite maximum value, any Robertson-Walker space-time must approach a dS space-time in the future, independently of the gravitational dynamics and matter content of the universe. In their argument, Carroll *et al* assume the presence of a constant density term in the generalized entropy, which has the same form of our extensive term (5.1.17). However, they show that at late times, i.e. for large values of the scale factor, this term is subleading with respect to the holographic one, the latter approaching a constant value and scaling like the area of the dS horizon. Translated in our corpuscular description, this means that our extensive term (5.1.17) plays a role at intermediate galactic scales, but becomes completely irrelevant for the late-time cosmological evolution.

Baryonic matter and the emergence of a dark force

So far we have considered the cosmological condensate without baryonic matter. One could just consider baryonic matter always existed inside the DEC, initially in a very diluted form, so that its effect on the gravitons of the cosmological BEC was initially negligible. In time, the baryonic matter clumped and started affecting the DEC locally, which is the situation we find in the universe today. In particular, the presence of local baryonic sources pulls out gravitons from the DEC, which give rise to the local gravitational forces. Alternatively, the simplest way to introduce baryonic matter in our scenario is to assume that it arises as bound states in the DEC, i.e. to consider it as produced by gravitons pulled out from the cosmological condensate at the typical matter scales R_μ, where μ denotes the mass of single point-like matter sources. This may occur owing to density perturbations in the BEC. An uniform, spherically symmetric over-density region of the BEC is isotropically compressed, because pressure gradients act only on the surface of the sphere, generating a compact source of baryonic matter, which can itself be described by a non-critical BEC or by critical BEC if the critical density is reached and a black hole is formed.

In the next Sections, we will first discuss the behaviour of the condensate with baryonic matter in the diluted approximation, when we can neglect the local reaction of the condensate. When we go beyond this approximation, we have to take into account the reaction of the cosmic condensate to the presence of the baryonic matter. We will see that this can be described as a dark force, mediated by gravitons pulled out from the cosmic BEC at galactic scales, which can explain the phenomenology at galactic scales commonly attributed to dark matter.

An important point to be stressed is that the dark force is a local effect. The cosmological BEC at horizon scales L remains largely unaffected. This means that deviations from Eq. (5.1.11) for the cosmological BEC remain negligible at present, albeit they are crucial in order to describe the local dynamics properly, as we are going to start showing next. Our description is consistent as long as we are only concerned with the gravitational dynamics at galactic scales and we do not use our model to describe the whole cosmological history of our universe. In order to do this, it is likely that more input is needed.

5.2 Baryonic Matter in the diluted approximation

We now want to see in more details what happens when very diluted baryonic matter is formed on top of the condensate of gravitons. In this approximation, matter can be considered as being made of, say N_μ almost point-like sources of mass μ, at rest and equally distanced very far apart. We can therefore neglect the local reaction of the condensate to their presence, which also means that the gravitational interactions among matter sources are negligible. Since sources are homogeneously distributed, our results should also be a good approximation for baryonic matter with homogeneous density. We will see that the leading-order effect of baryonic matter is to subtract gravitons from the condensate.

Diluted matter in the de Sitter universe

Let us first see what happens when we introduce baryonic matter into the de Sitter universe, whose metric takes the form

$$ds^2 = -f(r)\,dt^2 + f^{-1}(r)\,dr^2 + r^2\,d\Omega^2. \tag{5.2.1}$$

Since in the diluted approximation the cumulative effect of many sources is just the sum of the single contributions, we start by considering the case of a single point-like source of mass μ. In the weak field regime, the metric function in Eq. (5.2.1) is given by the Schwarzschild-dS form

$$f(r) = 1 - \frac{r^2}{L^2} + 2\,\phi(r), \tag{5.2.2}$$

where

$$\phi(r) = -\frac{G_N\,\mu}{r} \tag{5.2.3}$$

is the Newtonian potential generated by the source of mass μ. The size L_H of the cosmological horizon can be found by solving the condition $f(r) = 0$ for small departures from L (i.e. for $|\phi| \ll 1$), which yields

$$L_H = L\,[1 + \phi(L)] + o(\phi^2) \sim L - \ell_p\,\mu/m_p. \tag{5.2.4}$$

Adding N_μ similar matter sources would reduce the Hubble radius to

$$L_H \sim L - \frac{1}{2}\,N_\mu\,R_H, \tag{5.2.5}$$

where here $R_H = 2\,G_N\,\mu$ is the typical gravitational radius of each source. The effect of the presence of diluted matter is thus to reduce the size of the cosmological horizon, which in turn implies a number of gravitons in the cosmological condensate $N_G < N_\Lambda$ according to Eq. (5.1.11). Let us note, however, that such a change is relatively minuscule because of the hierarchy (5.1.3), and the fact that baryonic matter accounts for at most 5% of the total energy in the universe. We can therefore safely neglect the difference between L_H and L in the following.

Diluted matter in the corpuscular model

Before we introduce the diluted baryonic matter in the DEC, let us refine the corpuscular description of the dS universe. In Refs. [283, 284], it was shown that the maximal packing condition which yields the scaling relations (5.1.14) for a black hole actually follow from the energy balance (5.1.1) when matter becomes totally negligible. In the present case, matter is absent *a priori* and $H_B = 0$, so that one is left with

$$H_G^{(0)} = U_N^{(0)} + U_{PN}^{(0)} = 0, \tag{5.2.6}$$

with the negative Newtonian energy

$$U_N^{(0)} \simeq N_\Lambda\,\varepsilon_\Lambda = -N_\Lambda\,\frac{\ell_p\,m_p}{L}, \tag{5.2.7}$$

and the positive "post-Newtonian" contribution

$$U_{PN}^{(0)} = N_\Lambda\,\frac{\sqrt{N_\Lambda}\,\ell_p^2\,m_p}{L^2}. \tag{5.2.8}$$

One therefore recovers the scaling relation (5.1.11) from Eq. (5.2.6) with no extra "vacuum energy" [284].

The same result (5.2.5) can now be obtained using the Hamiltonian constraint (5.1.1) in which we include the contribution of N_μ diluted baryonic sources of mass μ,

$$H_B^{(1)} = N_\mu\,\mu. \tag{5.2.9}$$

Since matter is very diluted and cold, μ again just equals the proper mass, and local gravitational energy is negligible. We can therefore write

$$H_G^{(1)} = U_N^{(1)} + U_{PN}^{(1)}, \tag{5.2.10}$$

where the Newtonian and post-Newtonian terms have the forms given in Eqs. (5.2.7) and (5.2.8). The energy balance (5.1.1) then tells us that the condensate must respond to the presence of this homogeneous matter by changing the graviton number N_Λ, that is

$$N_\Lambda\,\frac{\ell_p\,m_p}{L} \simeq N_\mu\,\mu + N_\Lambda^{3/2}\,\frac{\ell_p^2\,m_p}{L^2}, \tag{5.2.11}$$

which yields

$$\begin{aligned} L =& \frac{\ell_p\,m_p\,N_\Lambda}{2\,N_\mu\,\mu}\left(1-\sqrt{1-\frac{4\,N_\mu\,\mu}{\sqrt{N_\Lambda}\,m_p}}\right) \\ \simeq& \sqrt{N_\Lambda}\,\ell_p + N_\mu\,\ell_p\,\mu/m_p + \mathcal{O}(N_\Lambda^{-1}), \end{aligned} \tag{5.2.12}$$

where we used $N_\mu\,\mu \ll N_\Lambda\,m_p$ for our dark energy dominated universe. Using now the scaling (5.1.11), i.e. $N_\Lambda \sim L_H^2/\ell_p^2$, one easily recovers Eq. (5.2.5).

The fact that the two estimates (respectively based on the form of the Schwarzschild-dS metric and on the corpuscular model) give the same result for the change of the Hubble horizon due to presence of baryonic matter is a highly non trivial check of the validity of our BEC description of the dS universe, and in particular of the validity of the energy balance (5.2.10) and of the form of the post-Newtonian term U_{PN}.

Diluted matter and scalings of the graviton number

The change in the dS horizon size (5.2.5) induced by the baryonic matter will result in a reduction of the number of gravitons N_Λ with energy ε_Λ according to Eq. (5.1.11), that is

$$\delta N_\Lambda \simeq -\frac{2\,\mu\,L}{m_p\,\ell_p}, \tag{5.2.13}$$

where N_Λ is given in (5.1.11)). The same result holds also for a black hole of mass μ, with L replaced with the black hole radius R_H [87]. Actually, this result is a quite generic consequence of the holographic scaling (5.1.14) for the graviton number. In fact, let us take a sphere of radius $r \ll L$, for which the number of gravitons in the condensate inside this sphere is given by Eq. (5.1.14), and compare the change of the graviton number as a function of the radial distance from the centre of the sphere with and without matter. Without the mass, the radial distance s is equal to r, whereas a baryonic point-like mass μ at the center of the sphere changes the radial distance of a quantity equal to $ds \simeq [1-\phi(r)]\,dr$, according to the weak field limit of the Schwarzschild metric. Thus, the number of gravitons in Eq. (5.1.14) changes due to the presence of matter according to

$$\frac{d(\delta N_\Lambda)}{ds} = \frac{d}{ds}\left(N_\Lambda|_{\mu\neq 0} - N_\Lambda|_{\mu=0}\right) \simeq \phi(r)\,\frac{dN_\Lambda}{dr} \simeq -\frac{2\,\mu}{m_p\,\ell_p}. \tag{5.2.14}$$

On the other hand, in the diluted approximation $|\phi(r)| \ll 1$ and $dr \simeq ds$. We can thus write the previous equation as

$$\frac{d(\delta N_\Lambda)}{dr} \simeq -\frac{2\,\mu}{m_p\,\ell_p}. \tag{5.2.15}$$

For future convenience, we will define $N_B = -\delta N_\Lambda$ as the number of gravitons subtracted from the cosmological condensate (the DEC) inside a sphere of radius r by the presence of the baryonic source of mass μ. By integrating the above equation, one finds

$$N_B \simeq -\frac{2\,\mu\,r}{m_p\,\ell_p}. \tag{5.2.16}$$

Extending the validity of Eq. (5.2.5) from the cosmological horizon to a region of radius r as given in Eq. (5.2.14) is a quite strong and highly non trivial assumption. In the corpuscular description of gravity, this implies that we are assuming not only the whole dS space filled with dark energy can be considered as a graviton condensate with Compton length L, but that this description also holds for regions of any size r, and for those gravitons with Compton length of order r. The rational behind

this assumption is the fact that at solar system scales we know that gravity is well described by GR, whose action is directly related with the holographic scaling (5.1.14). It should be stressed that this holds only in the holographic regime of gravity (5.1.14) but not in the extensive regime (5.1.18). This means that our universe looks like a critical graviton condensate at small (solar system) scales and very large (Hubble radius) scales, whereas at intermediate (galactic) scales we see an extensive behaviour. In order to give a precise meaning for the transition from cosmological to intermediate scales, we can use arguments similar to those used by Verlinde in Ref. [87].

We suppose that, as shown in [87], the "dark matter" effects arise from the competition between the "area-law" (5.1.14) and volume behaviour (5.1.18) for the graviton number. This implies the existence of two regimes: the baryonic matter dominated regime in which $N_B(r) > N_G^V(r)$ and a dark energy dominated regime $N_B(r) < N_G^V(r)$. In particular, we expect the dark force effects to be negligible for $N_B(r) \gg N_G^V(r)$. Let us now look for the transition between these two regimes, when the corresponding graviton numbers become comparable, that is $|N_B(r)| \simeq N_G^V(r)$, or

$$\frac{2\,\mu\,r}{m_p\,\ell_p} \simeq \frac{r^3}{\ell_p^2\,L}. \tag{5.2.17}$$

When this equality holds, most of the dark energy gravitons in the cosmological condensate contained inside the volume of size r are affected by the presence of the source of mass μ, and we obtain

$$r \equiv r_0 \simeq \sqrt{\frac{2\,\mu}{m_p}\,L\,\ell_p} = \sqrt{R_H\,L}, \tag{5.2.18}$$

where r_0 is the mesoscopic scale introduced in Section 5.1. For a given (spherical) region with a certain amount of mass μ localised about its center, r_0 sets the scale at which dark matter phenomena are not negligible. Using for μ the value for the mass of a galaxy in Eq. (5.2.17), one finds the observationally correct order of magnitude for deviations from the Newtonian dynamics. For instance, for a typical spiral galaxy with $m_B = 10^{11}$ solar masses, we have $r_0 = 6\,\mathrm{kpc}$, whereas for a typical dwarf galaxy with $m_B = 10^7$ solar masses, we have $r_0 = 80\,\mathrm{pc}$.

To describe the transition between the holographic and the extensive regimes, it is convenient to introduce the local (size-dependent) parameter

$$\gamma = \frac{N_B}{N_G^V}. \tag{5.2.19}$$

For $\gamma > 1$, we are in the area-scaling regime (5.1.14), where baryonic matter dominates, gravity is well described by GR, and most of the gravitons in the fluid belong to the condensate. Conversely, for $\gamma < 1$, we are in volume-scaling regime (5.1.14) and dark energy dominates. In this regime, the effects of the dark energy gravitons on baryonic matter are not negligible and give rise to the dark matter phenomena.

Let us conclude with some comments about the physical meaning of the diluted approximation and on the meaning of Eq. (5.2.19). Within this approximation, baryonic matter has no local gravitational interactions with the condensate. On the other hand, it also has no effects at cosmological scales. Rephrased in terms of the graviton number, the diluted regime applies in the region where $\gamma > 1$, i.e. when most gravitons inside a sphere of radius r belong to the *local* condensate (i.e. we are considering the sphere of radius r as a condensate of gravitons of Compton length r).

5.3 Clumped matter and emergence of the dark force

Let us now describe what happens when we go beyond the diluted approximation and baryonic matter begins to clump. The N_μ point-like sources of mass μ form clusters of baryonic matter with typical mass $m_B(r) = N_\mu \mu$. For simplicity, we consider a mass distribution with spherical symmetry. Now the DEC will react to the presence of matter, and we will interpret this reaction as a dark force responsible for the phenomenology commonly attributed to dark matter which reproduces correctly the MOND acceleration.

We first assume that only a fraction of the gravitons in the DEC are affected by the local matter, so that the condensate reacts not at the full cosmological scale L, but at a local scale of size r. In particular, since we are considering spherically symmetric sources, the baryonic matter of mass m_B will pull the gravitons out of the DEC from inside the sphere of radius r with a dark energy mass given by $M = M(r)$. Therefore we now have three scales in our problem: the typical size of the matter lumps R_B, the range of the condensate reaction r and L, which satisfy the hierarchy

$$R_H \ll R_B \lesssim r \ll L. \tag{5.3.1}$$

In the following we will consider the dynamics of test particles at distances $r \gg R_B$, so that the baryonic source of mass $m_B(r)$ can be well approximated by a point-like source. Physically, this means that we are considering the dynamics of galaxies at distances far away from the galactic core. We will first briefly review the results of Ref. [274] based on a balance between the number of gravitons, we will then give the description based on the Hamiltonian constraint, finally we will proceed by using the competition between the area and volume regimes to derive the "dark acceleration".

Matter clumping and graviton number balance

The starting point of our analysis is that in a corpuscular description of gravity, the gravitational acceleration felt by a test particle is the macroscopic manifestation of the self-interaction of gravitons in the condensate.

Moreover, as already mentioned, the basis of the corpuscular picture of gravity [90, 91] is that the classical gravitational field of an (isolated) object of mass m is in fact a quantum coherent state of gravitons with occupation number [283, 284, 290]

$$N \sim \frac{m^2}{m_p^2} \,. \tag{5.3.2}$$

These gravitons are closely bound to the source and interact with other objects nearby, e.g. a test particle. If r is the distance between the test particle and the massive object, the effective interaction energy for each graviton is $\varepsilon(r) = \hbar/r$. Therefore, we can express the Newtonian gravitational acceleration felt by the test particle as in terms of ε and N as

$$a(r) = \frac{G_N\, m}{r^2} \sim \frac{\varepsilon^2(r)}{m_p^2\, \ell_p} \sqrt{N}. \tag{5.3.3}$$

The argument generalises straightforwardly to a spherically symmetric distribution of mass. In this case, however, not all gravitons can contribute to the acceleration of the test particle, but only those that are bound to the mass inside the radius r.

Henceforth, let us denote by $N_{\rm eff}(r)$ the effective number of gravitons which contribute to the acceleration of a test particle at radius r.[3] Thus, in the case at hand, it is $N_{\rm eff}(r) = m^2(r)/m_{\rm p}^2$, and (5.3.3) can be expressed in terms of the Compton energy ε and specific number $N_{\rm eff}$ of gravitons involved in the process as

$$a(r) = \frac{G_N\, m(r)}{r^2} \sim \frac{\varepsilon^2(r)}{m_{\rm p}^2\, \ell_{\rm p}} \sqrt{N_{\rm eff}(r)}. \tag{5.3.4}$$

In the above argument it is important that the gravitons are in the normal (non-condensed) phase, for which we can use the effective law $\varepsilon(r) = \hbar/r$.

We shall call *corpuscular acceleration* the quantity

$$a(r) \sim \frac{\varepsilon^2(r)}{m_{\rm p}^2\, \ell_{\rm p}} \sqrt{N_{\rm eff}(r)}. \tag{5.3.5}$$

Although we have derived this formula for the non-condensed gravitons, which generate the Newtonian acceleration, it turns out to hold also for the acceleration caused by the condensed gravitons, as we will verify in the following. Therefore, every population of gravitons, with an effective number of contributing gravitons $N_{\rm eff}(r)$ and a mean interaction energy $\omega(r)$, will contribute an acceleration $a(r)$ given by (5.3.3) to the total acceleration of a test particle. As an example, it is easy to show that Eq. (5.3.5) correctly reproduces the de Sitter acceleration for an accelerating expanding universe [274]. Consider now the reaction of the cosmological BEC of total mass m_Λ to the presence of the baryonic matter source of mass $m_{\rm B}(r)$. Since $m_{\rm B} \ll m_\Lambda$, most of the gravitons will remain in the condensed phase and their number is given, according to Eq. (5.1.14), by

$$N_{\rm DE} \sim \frac{(m_\Lambda - m_{\rm B})^2}{m_{\rm p}^2}. \tag{5.3.6}$$

On the other hand, the total number of gravitons in the system is given by $N_\Lambda \sim m_\Lambda^2/m_{\rm p}^2$. This implies that there are $N_\Lambda - N_{\rm DE}$ gravitons which are not in the condensed phase and, therefore, behave differently from the condensate. Since the number of gravitons which give rise to the local gravitational potential generated by the baryonic mass is $N_{\rm B} = m_{\rm B}^2/m_{\rm p}^2$ and, from Eqs. (5.3.6), we have

$$N_\Lambda - N_{\rm DE} \sim \frac{L\, m_{\rm B}}{\ell_{\rm p}\, m_{\rm p}} - \frac{m_{\rm B}^2}{m_{\rm p}^2}, \tag{5.3.7}$$

it follows that there are $N_{\rm DF} \sim L\, m_{\rm B}/\ell_{\rm p}\, m_{\rm p}$ gravitons which mediate the interaction between the baryonic matter and the DEC. What we have just shown is that the quantum field of gravitons that arises when baryonic matter is placed within a DE fluid comprises three types of gravitons: first, those in the condensed phase forming the cosmological DE fluid, second, the non-condensed gravitons closely bound to the baryonic matter responsible for the Newtonian acceleration and, third, the non-condensed gravitons permeating space-time, which have been "pulled out" of the condensate by the baryonic mass. Each of these graviton populations contributes an acceleration (5.3.5)

[3] The number $N_{\rm eff}(r)$ is not a good classical observable and must not be confused with the number of gravitons inside the radius r. Such a number does not exist, because, relativistically, there is no notion of a local number density.

to the total acceleration of the test particle, which correspond precisely to the three contributions to the acceleration in Eq. (6.1.13).

The effective number of non-condensed gravitons $N_{DF}(r)$ that contribute to the acceleration of a test particle at the radius r can be guessed by requiring that its overall scaling is again holographic and must depend on the baryonic mass m_B. This yields

$$N_{DF}(r) \sim \frac{r^2\, m_B(r)}{\ell_p\, m_p\, L}. \tag{5.3.8}$$

From Eqs. (5.3.5) and (5.3.8) with $N_{eff} = N_{DF}(r)$, we obtain

$$|a_{DF}(r)| \sim \sqrt{\frac{G_N\, m_B(r)}{L\, r^2}} \sim \sqrt{\frac{a_B(r)}{L}}, \tag{5.3.9}$$

which is the MOND acceleration (4.1.1) up to a numerical factor. Therefore, the corpuscular picture naturally explains the presence of a dark force and the approximate coincidence of the MOND acceleration a_0 with the Hubble constant $H \approx 1/L$.

Let us conclude with a few remarks. First, the previous arguments give order-of-magnitude estimates only, without precise numerical factors and without information on the directions of the various contributions to the acceleration. Second, all expressions must receive higher order corrections in $G_N\, m_B/L$, as can be seen, e.g., from the different signs of the two terms in Eq. (5.3.7). Presumably, these corrections will be responsible for the cross-over between the Newtonian and the MOND regimes as well as between the MOND and the de Sitter regimes.

Matter clumping and energy balance

In the previous discussion we have shown that it is possible to define the MOND acceleration by counting the gravitons' number in a BEC. Alternatively the MOND acceleration (4.1.1) can be obtained the Hamiltonian constraint (5.1.1). In the following we will focus only on this second approach.

Once the regular matter starts clumping, the matter energy changes to

$$H_B = m_B + E_B, \tag{5.3.10}$$

where $m_B \simeq N_\mu\, \mu$ and E_B accounts for the total kinetic energy of matter and non-gravitational interactions. Some gravitons will acquire a new Compton length in response to the local lumps of matter, and the gravitational Hamiltonian in the constraint Eq. (5.1.1) takes the form

$$H_G = H_\Lambda + H_{BG} + H_{DF}, \tag{5.3.11}$$

where H_Λ is the energy of the DEC, whose specific form is not essential for the present derivation; H_{BG} is the Newtonian gravitational energy of the localised matter sources,

$$H_{BG} = -\frac{G_N\, m_B^2}{R_B} = -N_B\, \frac{\ell_p\, m_p}{R_B}, \tag{5.3.12}$$

with N_B the number of soft gravitons whose Compton length equals the typical size R_B of matter lumps [4]; finally, the "dark force" term is given by the gravitational interaction

[4] There would also be a (positive) post-Newtonian energy but we shall neglect that as it is much smaller than H_{BG} for compact sources far from becoming black holes.

energy between baryonic matter and dark energy of mass $M(r)$ inside the sphere of radius r, that is

$$H_{DF} = -\frac{G_N\, m_B\, M(r)}{r}. \tag{5.3.13}$$

We can rewrite H_{DF} in terms of an effective dark force mass m_{DF} as

$$\frac{G_N\, m_B\, M(r)}{r} \simeq \frac{G_N\, m_{DF}^2}{r}, \tag{5.3.14}$$

which implies the simple relation between masses

$$m_{DF}^2 = m_B\, M(r). \tag{5.3.15}$$

Because the dark matter term arises from the interaction of the baryonic source with the gravitons in the DEC inside the volume of size r, the energy of the gravitons will change to $\varepsilon \simeq m_p\, \ell_p/r$. From the extensive scaling (5.1.18), it follows that

$$M(r) \simeq \frac{m_p\, r^2}{\ell_p\, L}. \tag{5.3.16}$$

We can now evaluate the gravitational acceleration associated to the dark force component (5.3.14) of the condensate. Using the estimate (5.3.16) in Eq. (5.3.15), we obtain the dark acceleration

$$a_{DF} \sim \frac{G_N\, m_{DM}}{r^2} \simeq \sqrt{\frac{1}{L}\,\frac{G_N\, m_B}{r^2}} = \sqrt{\frac{a_B(r)}{L}}, \tag{5.3.17}$$

where $a_B(r)$ is the Newtonian baryonic acceleration, $a_B = -G_N m_B(r)/r^2$ a distances r. Again, this result indeed matches the MOND formula (4.1.1) up to a factor of $1/6$.

We can further show that the above derivation, based on the energy balance (5.3.11), is perfectly compatible and consistent with the derivation in Section 5.3, which is instead based on the graviton numbers. In fact, we can associate to the dark energy mass $M(r)$ interacting with the baryonic mass a number of gravitons equal to the number of gravitons $N_{DF}(r)$ pulled out from the DEC. This number scales holographically as

$$N_{DF}(r) = \frac{m_{DF}^2}{m_p^2}. \tag{5.3.18}$$

By combining Eqs. (5.3.15) and (5.3.18), we find

$$M(r) = N_{DF}(r)\,\frac{m_p^2}{m_B}, \tag{5.3.19}$$

and Eq. (5.3.16) finally yields the total number of gravitons associated to the dark force

$$N_{DF}(r) = \frac{m_B\, r^2}{\ell_p\, m_p\, L}, \tag{5.3.20}$$

which exactly matches Eq. (5.3.8) obtained in Section 5.3.

We further note the dark acceleration can also be written as a function of the number of dark gravitons, thus obtaining the same expression (5.3.5) found in in Section 5.3. In fact, by combining Eqs. (5.3.19) and (5.3.15), we find

$$a_{DF} = \frac{G_N\, m_{DF}}{r^2} = \frac{\ell_p}{r^2}\,\sqrt{N_{DF}(r)}, \tag{5.3.21}$$

or, equivalently, using the Compton energy of the dark gravitons $\varepsilon = m_p\,\ell_p/r$,

$$a_{DF} = \frac{\varepsilon^2(r)}{m_p^2\,\ell_p}\,\sqrt{N_{DF}(r)}, \tag{5.3.22}$$

which is exactly the corpuscular acceleration (5.3.5) introduced before and in Ref. [274] for $N_{eff} = N_{DF}(r)$.

Area/volume competition and heuristic derivation of MOND

Here we present a heuristic derivation of the MOND acceleration (4.1.1), which uses the Hamiltonian constraint (5.3.11) and the competition between the holographic and extensive regimes described in Section 5.1. The novelty is that we will be able to reproduce correctly also the numerical factors of Eq. (4.1.1) in this scenario. The key observation is that, owing to the fact that the DEC responds only locally to the presence of baryonic matter, we can simply write the contribution H_{DF} in Eq. (5.3.11) in terms of the energy subtracted from dark energy gravitons to generate the local Newtonian gravity.

For simplicity, we consider baryonic matter in the form of a single point-like source of mass m_B, but the results can be easily generalised to the case of an extended but localised source inside a volume of size R_B. By analogy with the electromagnetic force, the energy density ρ_G associated with a gravitational (acceleration) field, that is

$$a_B = -\frac{G_N\, m_B}{r^2}, \tag{5.3.23}$$

inside a sphere of radius r, and volume $V(r) = 4\,\pi\, r^3/3$, is given by

$$\rho_G = \frac{a_B^2}{8\,\pi\, G_N}, \tag{5.3.24}$$

where m_B is the source of the gravitational field. It is easy to find that the energy subtracted from dark energy gravitons in order to clump the amount of matter m_B inside the spherical region is, therefore,

$$E_G = -\rho_G\, V = -\frac{G_N\, m_B^2}{6\, r}, \tag{5.3.25}$$

where m_B now denotes the baryonic mass contained inside $V(r)$.

Consistently with Eq. (5.3.15), we can view this energy as due to the existence of a "dark force", whose effective source is a "dark mass" m_{DF}, which does work on the system. In analogy to what happens at cosmological scales, we can think that the effect of the mass m_B centered inside a spherical region of volume $V(r)$, is to deform the sphere by an amount given by Eq. (5.2.5) with L replaced by r. The deformation is therefore,

$$u(r) = \phi_B(r)\, L, \tag{5.3.26}$$

where ϕ_B is the gravitational potential generated by the mass m_B and L is still the dS radius. The work done by the "dark force" on the system will be given by

$$W = F_{DF}\, u(r) = \frac{G_N^2\, m_{DF}^2\, m_B}{r^3}\, L. \tag{5.3.27}$$

It should be stressed that this contribution is of holographic nature: it is the work done by the dark force to deforme the *surface* of the sphere. For energy conservation, it must equal the energy E_G contained in the volume $V(r)$. By equating Eqs. (5.3.25) and (5.3.27), we easily obtain

$$\frac{G_N\, m_{DF}^2}{r^2} = -\frac{m_B}{6\, L}. \tag{5.3.28}$$

If we now use the form for the "dark gravitational acceleration" used in (5.3.17),

$$a_{DF} = -\frac{G_N\, m_{DF}}{r^2} \tag{5.3.29}$$

and the Newtonian acceleration (5.3.23), Eq. (5.3.28) can be written as

$$a_{DF}(r) = \sqrt{\frac{a_B}{6\, L}}, \tag{5.3.30}$$

which exactly matches the MOND acceleration (4.1.1). Let us stress that Eq. (4.1.1) is precisely obtained by identifying the *volume* (extensive) subtraction (5.3.25) from the condensate with the dark *area* (holographic) contribution (5.3.27).

Cosmic balance

If one puts together the argument based on the graviton number of Section 5.3 and the energy balance of Section 5.3, the ratio between an *apparent dark matter* mass distribution and baryonic matter can be estimated and shown to be consistent with the predictions of the ΛCDM model.

Let us denote with U_{DF} the energy associated with the dark gravitons. This energy can be written in terms of the number N_{DF} of "dark force" gravitons inside a sphere of radius r and their Compton energy $\varepsilon = -m_p\, \ell_p/r$ as

$$U_{DF} = N_{DF}\, \varepsilon = -N_{DF}\, \frac{m_p\, \ell_p}{r}. \tag{5.3.31}$$

In the ΛCDM description, U_{DF} must be seen as originating from the interaction of an *apparent dark matter* mass M_{DM} with the baryonic matter of mass m_B and its self-interaction, that is

$$U_{DF} = -\frac{G_N\, m_{DM}\, m_B}{r} - \frac{G_N\, m_{DM}^2}{r}. \tag{5.3.32}$$

Equating the above two expressions for U_{DF}, we get

$$N_{DF} = \frac{m_{DM}^2}{m_p^2} + \frac{m_{DM}\, m_B}{m_p^2}. \tag{5.3.33}$$

Let us stress that the apparent dark matter mass m_{DM} must not be confused with the *effective dark force mass* m_{DF} of Eq. (5.3.15). In fact, consistency of Eq. (5.3.33) with Eq. (5.3.18) requires $m_{DF}^2 = m_{DM}^2 + m_{DM}\, m_B$.

On using Eq. (5.3.6), $N_{DF} \sim N_\Lambda - N_{DE}$, and recalling that $N_\Lambda \sim L^2/\ell_p^2$ and $m_\Lambda = m_p\, L/\ell_p$, we obtain

$$m_{DM}\, m_B + m_{DM}^2 = 2\, m_\Lambda\, m_B - m_B^2, \tag{5.3.34}$$

which can be written as

$$x^2 + x + 1 = \frac{2\, m_\Lambda}{m_B}, \tag{5.3.35}$$

where we defined the ratio $x = m_{DM}/m_B$. In particular, the latter equation is solved by

$$\frac{m_{DM}}{m_B} = \frac{\sqrt{8\,(m_\Lambda/m_B) - 3} - 1}{2}. \tag{5.3.36}$$

If we now recall that observations yield $m_B \simeq 0.05\, m_\Lambda$, we finally obtain

$$\frac{m_{DM}}{m_B} \simeq 5.77, \tag{5.3.37}$$

which is in the right ballpark of the ΛCDM prediction for the present relative abundance of dark and baryonic matter.

5.4 Summary and conclusions

Starting from the corpuscolar description of gravity given in [90, 91], in this Chapter we have investigated the emergent laws of gravity distinguishing different scaling regimes and deriving the implications of our emergent gravity scenario at galactic scales. First, we have shown how to model our dark energy dominated universe as a critical BEC with a large number N_G of soft gravitons. Then we have shown that the local behaviour of this DEC requires, besides the usual holographic regime, an extensive regime of gravity in which the graviton number scales with the volume of space. Baryonic matter and local (Newtonian) gravitational forces fits naturally in this description as gravitons pulled out from the DEC. For what concerns the galactic regime of gravity, in this framework, the galaxy rotation curves far away from the galactic center [i.e. the MOND formula (4.1.1)] can likewise be derived from the reaction of the DEC to the presence of baryonic matter, without assuming the existence of any sort of dark matter. We have also evaluated the mass ratio of the apparent dark matter and baryonic component and found it in agreement with the prediction of the ΛCDM model.

We would like to conclude by remarking that two important points have not yet been addressed, but deserve further investigation. The first one concerns the microscopic origin of the cosmological evolution. Our model applies solely to the present dark energy dominated universe. We did not tackle the problem of giving a description of the history of the universe using a critical BEC of soft gravitons. Although this is a quite involved problem, there are several indications that it may indeed be possible. The results of Refs. [91, 99, 289] about the description of inflation and general cosmological space-times [280] represent promising steps along this direction. Moreover, the results of Ref. [282] not only assert that the dS space-time necessarily appears at late times in any cosmological evolution consistent with the generalized second law

of thermodynamics, but also imply that the presence of an extensive, volume-scaling, term for the graviton number is perfectly consistent with this late time cosmological evolution. Last but not least, the fact that our model predicts the correct present relative abundance of the various forms of matter gives us a further hint that we are going in the right direction.

The second point concerns the microscopic origin of horizons. Most of the scenarios for emergent gravity assume in an explicit or implicit way the presence of event, cosmological or acceleration, horizons (see, *e.g.* Ref. [291]). Horizons are a key ingredient for explaining the holographic regimes of gravity and play, therefore, a crucial role also in our BEC description of black holes an the dS space-time. At the level of the BEC, one may easily generate acoustic horizons [292]. However, it is not clear if acoustic horizons in a BEC can be directly linked to space-time horizons in the emergent gravity scenario. In fact, acoustic horizons in BEC are mainly of kinematic origin, whereas in an emergent gravity theory containing black holes and the dS space-time, their origin should be dynamical.

Chapter 6

Effective description of gravity at galactic scales

A key issue for every model of emergent gravity is the existence of an effective description reproducing Einstein's general relativity or at least a metric theory of gravity. One must envisage the way in which the metric space-time structure of gravity encoded in GR emerges out of the microscopic description. This is a quite stringent requirement and it is not enough to predict an infrared modification of the laws of gravity, such as the MOND relation (4.1.1). This relation must be embedded in the framework of GR or, at least, in a metric theory of gravity describing a modification thereof. This is for instance a drawback of Verlinde's original proposal [87]. The proposed modification of the laws of gravity at galactic scales reproduces the MOND relation (4.1.1), but a metric covariant description of the model has not been proposed yet (see, however, Refs. [126, 293, 294]).

This Chapter is devoted to the derivation of an effective metric theory of gravity at cosmological and galactic scales. We start by considering the emergent gravity description based on a BEC of gravitons discussed in the previous Chapter. Because we know that GR holds true at least at Solar system scales, we generically expect our effective theory to represent an IR modification of the Einstein's theory. As a guideline for constructing this effective, IR modified gravity theory, we will use a simple well-known fact: in the cosmological regime, at late times, our universe is a dark energy dominated universe and it can be described in a metric framework as GR sourced by a perfect fluid with constant energy density ρ and equation of state $p = -\rho$ [130]. If one takes into account the corpuscolar gravity picture described in the previous Chapter, the dark energy dominated universe can be seen as a Bose-Einstein condensate of gravitons (DEC). In this picture, we will show that using quite general assumptions, as the generation of baryonic matter and the consequently reaction of the condensate, the DEC allows for an effective covariant metric description in which the fluid becomes anisotropic [130, 274]. In this description, the additional component of the galaxy acceleration, commonly attributed to dark matter, is explained as a radial pressure generated by the reaction of the dark energy fluid to the presence of baryonic matter. In particular, we will find the static, spherically symmetric solution for the metric in terms of the Misner-Sharp mass function and the fluid pressure. At galactic scales, we correctly reproduce the leading MOND-like $\log(r)$ and subleading $(1/r)\log(r)$ terms in the weak-field expansion of the potential. Our description also

predicts a tiny (of order 10^{-6} for a typical spiral galaxy) Machian modification of the Newtonian potential at galactic scales, which is controlled by the cosmological acceleration.

The Chapter is entirely based on:

- M. Cadoni, R. Casadio, A. Giusti, W. Mück and M. T. "*Effective Fluid Description of the Dark Universe*", **Phys.Lett. B776 (2018) 242-248**, arXiv:1707.09945.

Note: we use units with $c = 1$, while the Newton and Planck constants are expressed in terms of the Planck length and mass as $G_N = \ell_p/m_p$ and $\hbar = \ell_p m_p$, respectively.

6.1 Anisotropic fluid space-time

We start by considering a static, spherically symmetric system, for which one can employ the Schwarzschild-like metric

$$ds^2 = -f(r)\, e^{\gamma(r)}\, dt^2 + \frac{dr^2}{f(r)} + r^2 d\Omega^2. \tag{6.1.1}$$

It is known that this metric is, in all generality, a solution to Einstein's equations with the energy-momentum tensor of an anisotropic fluid [295, 296],

$$T^{\mu\nu} = (\varepsilon + p_\perp)\, u^\mu u^\nu + p_\perp g^{\mu\nu} - (p_\perp - p_\parallel)\, v^\mu v^\nu, \tag{6.1.2}$$

where the vectors u^μ and v^μ satisfy $u^\mu u_\mu = -1$, $v^\mu v_\mu = 1$, and $u^\mu v_\mu = 0$. Explicitly, the fluid velocity is $u^\mu = \left(f^{-1/2}\, e^{-\gamma/2}, 0, 0, 0\right)$ and $v^\mu = \left(0, f^{1/2}, 0, 0\right)$ points radially outwards. The energy density is given by ε, and $p_\perp$ and $p_\parallel$ denote the pressures perpendicular and parallel to the space-like vector v^μ, respectively. Energy-momentum conservation is equivalent to the hydrostatic equilibrium condition, and imposes constraints on these quantities.

The Einstein equations with the energy-momentum tensor (6.1.2) are solved by

$$f(r) = 1 - \frac{2\, G_N\, m(r)}{r}, \tag{6.1.3a}$$

$$\gamma'(r) = \frac{8\pi\, G_N\, r}{f(r)} \left(\varepsilon + p_\parallel\right), \tag{6.1.3b}$$

where primes denote differentiation with respect to r, and

$$m(r) = 4\pi \int_0^r d\tilde{r}\, \tilde{r}^2\, \varepsilon(\tilde{r}) \tag{6.1.3c}$$

is the Misner-Sharp mass function representing the total energy inside a sphere of radius r. Finally, the tangential pressure follows from energy-momentum conservation,

$$p_\perp = p_\parallel + \frac{r}{2}\left[{p_\parallel}' + \frac{1}{2}\left(\varepsilon + p_\parallel\right)\left(\frac{f'}{f} + \gamma'\right)\right]. \tag{6.1.4}$$

Let us then consider a test particle comoving with the fluid, so that its four-velocity is u^μ. The four-acceleration necessary to keep it at a fixed coordinate radius

r is given by $a^\mu = u^\nu \nabla_\nu u^\mu$. In the frame of Eq. (6.1.1), only the radial component of this acceleration does not vanish and is given by

$$a^r \equiv a = \frac{1}{2}\left(f\gamma' + f'\right) = \frac{G_N\, m(r)}{r^2} + 4\pi\, G_N\, r\, p_\parallel(r). \tag{6.1.5}$$

In Newtonian language, the first term has the obvious interpretation as the acceleration that counters the gravitational pull of the central mass. The second term may be interpreted as the acceleration caused by the radial pressure. The same result can be obtained by considering the geodesic motion along a circular orbit of radius r, with $\theta = \pi/2$ and constant angular velocity $\Omega = d\phi/dt$. Of course, this is the physically relevant situation for the motion of stars within a galaxy. Starting with the four-velocity $u^\mu = C(r)\,(1, 0, 0, \Omega)$, with $C(r)$ such that $u_\mu u^\mu = -1$, and solving the geodesic equation at fixed r and $\theta = \pi/2$, one obtains $\Omega^2 = e^\gamma\, a/r$, with a again given by Eq. (6.1.5).

The above equations can describe a variety of physical situations. De Sitter space is equivalent to an isotropic DE fluid with the constant energy density ε_{DE} and pressure $p_{\parallel DE} = p_{\perp DE} = p_{DE}$ satisfying

$$\varepsilon_{DE} = -p_{DE} = \frac{3}{8\pi\, G_N\, L^2}. \tag{6.1.6}$$

This yields

$$f(r) = 1 - \frac{r^2}{L^2}, \tag{6.1.7}$$

with $\gamma = 0$, and

$$a_{DE}(r) = -\frac{r}{L^2}. \tag{6.1.8}$$

Being maximally symmetric, de Sitter space does not allow for circular geodesics, which is confirmed by the fact that a_{DE} is negative. This acceleration describes the accelerating cosmological expansion of the universe. Notice that, because of its vacuum equation of state (6.1.6), the DE fluid component does not contribute to γ but enters only in f via the de Sitter term.

Pressureless baryonic matter can be easily added to de Sitter space,

$$\varepsilon = \varepsilon_B + \varepsilon_{DE}, \tag{6.1.9}$$

where ε_{DE} is again given in Eq. (6.1.6). The Misner-Sharp mass function will split correspondingly,

$$m(r) = m_B(r) + m_{DE}(r) = m_B(r) + \frac{r^3}{2\, G_N\, L^2} \tag{6.1.10}$$

and the metric function f turns out to be

$$f(r) = 1 - \frac{2\, G_N\, m_B(r)}{r} - \frac{r^2}{L^2}. \tag{6.1.11}$$

This leads to a Newtonian acceleration term

$$a_B(r) = \frac{G_N\, m_B(r)}{r^2}, \tag{6.1.12}$$

in addition to (6.1.8). If the baryonic matter is localized within a radius R_B then, for $r > R_B$, the space-time is identical to the Schwarzschild-de Sitter solution.

The observed galaxy rotation curves imply that, in addition to a_{DE} (which, in this context, is actually negligible) and a_B, there is an acceleration caused by a dark force,

$$a = a_B + a_{DE} + a_{DF}. \tag{6.1.13}$$

Let us stress the fact that we are thinking to dark matter not as an independent form of matter (we are not supposing the existence of any form of matter a part from the baryonic one), but rather that the phenomena usually attributed to it are a consequence of the interaction between the baryonic matter and the DE fluid. We therefore assume the energy density and the Misner-Sharp in the cosmos are given respectively by Eqs. (6.1.9) and (6.1.10). Taking the baryonic matter as approximately pressureless, we write

$$p_{\parallel} = p_{\parallel_{DE}} + p_{\parallel_{DF}}, \tag{6.1.14}$$

where $p_{\parallel_{DF}}$ is the pressure that generates the dark force. In the next Section, we will derive $p_{\parallel_{DF}}$ from the point of view of a corpuscular interpretation of gravity in general, and of the de Sitter space in particular.

At galactic scales, we can neglect the DE terms p_{DE} and ε_{DE}. Splitting the total radial gravitational acceleration into the baryonic acceleration a_B and the dark acceleration a_{DF}, Eq. (6.1.5) now gives

$$a_B + a_{DF} \simeq \frac{G_N\, m_B(r)}{r^2} + 4\pi\, G_N\, r\, p_{\parallel_{DF}}(r). \tag{6.1.15}$$

The first term on the right hand side is exactly a_B, thus the dark acceleration is completely due to the pressure of the anisotropic fluid. Eq. (6.1.15) is valid as long as Eq. (6.1.2) holds, i.e. if we choose an effective descriprion of gravity sourced by an anisotropic fluid. This is an important point, because it implies that the modifications to GR at galactic scales commonly attributed to dark matter can be generated by the pressure $p_{\parallel}$ in our effective fluid description. Since this pressure term can be thought of as a reaction of the DE fluid to the presence of baryonic matter, it is conceptually very similar to Verlinde's description of dark forces as the elastic response of the DE medium to the presence of baryonic sources [87]. Note also that $p_{\parallel_{DF}}$ will necessarily give rise to an anisotropic component $p_{\perp DF}$ according to the conservation Eq. (6.1.4).

6.2 Metric at galactic scales

In the previous Chapter we have seen that the corpuscolar description of gravity allows us to define the number of non-condensed gravitons N_{DF} that contribute to the acceleration of a test particle at galactic scales. Consequently, we can define the dark acceleration a_{DF} which, up to numerical factors, matches the MOND formula. However, from Eq. (6.1.15) we can see that it is possible to relate the dark acceleration to the dark pressure that generates the dark force experienced by baryonic matter in galaxies. Putting together Eq. (6.1.15) and Eq. (5.3.9) the pressure necessary to sustain the dark force takes the following form

$$p_{\parallel_{DF}} \sim \frac{1}{4\pi r^2}\sqrt{\frac{m_B(r)}{G_N\, L}}. \tag{6.2.16}$$

Thus starting from Eqs. (6.1.9), (6.1.14) and (6.2.16), we will now evaluate the metric of the anisotropic fluid space-time. For any given distribution of baryonic matter $\varepsilon_B = \varepsilon_B(r)$, Eqs. (6.1.3a)-(6.1.3c) determine the metric function $f = f(r)$ and

$$\gamma' = \frac{2}{r\,f(r)}\left[G_N\, m_B'(r) + \sqrt{\frac{G_N\, m_B(r)}{L}}\right] . \tag{6.2.17}$$

We examine for simplicity the case of baryonic matter localised inside a sphere of radius $R_B \ll r_0$, so that the baryonic mass has a constant profile $m_B(r) = m_B$, for $r > R_B$. This approximation is good when we consider a galaxy at distances much bigger than its bulk. Since we are now interested in scales $r \sim r_0 \ll L$, we again neglect the DE terms, and the metric functions can be easily obtained from Eqs. (6.2.17) and (6.1.3a)–(6.1.3c),

$$\begin{aligned} f(r) &= 1 - \frac{2\,G_N\, m_B}{r} \\ \gamma_{DF} &= 2\,K\left[\ln\left(\frac{r}{r_0}\right) + \ln\left(1 - \frac{2\,G_N\, m_B}{r}\right)\right] , \end{aligned} \tag{6.2.18}$$

where $K = \sqrt{G_N\, m_B/L}$ and the integration constant was set in terms of the infrared scale r_0, which now represents the typical radius at which the "dark force" effects take place.

The non-vanishing function γ_{DF} represents the metric effects in our fluid description of the dark force. Since our effective fluid description holds only for $r_0 \lesssim r \ll L$, we neglect γ_{DF} for $r \lesssim r_0$ and $r \sim L$. Most of the physical information about the rotation curves of the galaxies is contained in the weak-field approximation of the metric component $g_{00} = -f\,e^{\gamma}$. At galactic scales, this corresponds to the regime $G_N\, m_B \ll r \sim r_0 \ll L$, which also implies $\gamma_{DF} \sim 0$. Keeping only terms up to $\log^2(r/r_0)$ and $1/r^2$, we have

$$-g_{00} \simeq \;\; 1 - (1+2\,K)\,\frac{2\,G_N\, m_B}{r} + 2\,K\,\ln\left(\frac{r}{r_0}\right) - K\,(1+2\,K)\,\frac{4\,G_N\, m_B}{r}\ln\left(\frac{r}{r_0}\right) , \tag{6.2.19}$$

where we exactly find the logarithmic corrections to the gravitational potential one expects at galactic scales, as MOND (or the Tully-Fisher relation) suggests [116, 120, 297]. Moreover, it contains the subleading $(1/r)\log(r/r_0)$ corrections, which have also been observed in galactic rotation curves [298, 299]. A third feature of the above metric element is the presence of a small correction to the Newtonian potential, which can be seen as a modification of $G_N\, m_B$, and depends on L in K. This correction is therefore of Machian character, but is tiny because K is of order 10^{-6} for a spiral galaxy with $m_B \sim 10^{11}\, m_\odot$, and of order 10^{-9} for a dwarf galaxy with $m_B \sim 10^{7}\, m_\odot$. This effect is hence not detectable presently, owing to the uncertainties in the determination of the baryonic mass of the galaxies.

Because of the competition between $\log(r/r_0)$ and $1/r$ terms (and also the dS term r^2/L^2 if one goes to distances comparable with the cosmological horizon) in the weak-field expansion, it is useful to introduce, beside r_0, the scales r_1 and r_2 representing the distances at which the MOND acceleration term equals respectively the Newtonian and the dS term. Hence, our effective fluid description holds for $r_0 < r < r_2$. The IR scale r_0 is the typical distance at which the rotation curves of galaxies deviate from the

Newtonian prediction, $r_0 \sim \sqrt{G_N\, m_B\, L}$. In Verlinde's model of Ref. [87], the IR scale r_0 is determined by the competition between area and volume terms in the entropy, and is given by $r_0 = \sqrt{2\, G_N\, m_B\, L}$. In our case, we have $r_1 = \sqrt{3}\, r_0$ and $r_2 = \sqrt{r_0\, L/(2\sqrt{3})}$. Notice that, as expected, $r_1 \sim r_0$. The window in which the Newtonian contribution to the potential is not obscured by the logarithmic term is therefore very narrow. As specific examples, let us take the typical spiral and dwarf galaxies discussed above. For the spiral galaxy, we have $r_0 \simeq 6\,\mathrm{kpc}$, $r_1 \simeq 10\,\mathrm{kpc}$, $r_2 \simeq 10^3\,\mathrm{kpc}$. For the dwarf galaxy we have instead $r_0 \simeq 80\,\mathrm{pc}$, $r_1 \simeq 130\,\mathrm{pc}$, $r_2 \simeq 300\,\mathrm{pc}$.

We have considered here only the case of a constant profile for the baryonic mass function outside a sphere of radius $R \ll r_0$. However, Eqs. (6.2.17) and (6.1.3a)-(6.1.3c) in principle allow for the determination of the metric for every given distribution of baryonic matter $m_B = m_B(r)$. For instance, one can consider Jaffe's profile [300] for the baryonic energy density $\varepsilon_B = \tilde{A}/r^4$, which corresponds to $m_B(r) = m_0 - A/r$. We have checked that this profile reproduces the results for the case of a constant baryonic mass at large distances, as expected.

6.3 Summary and conclusions

We have constructed an infrared-modified theory of gravity which gives the effective fluid description of our emergent gravity theory based on BEC of gravitons. Using quite general assumptions and a microscopic description of the fluid in terms of a Bose-Einstein condensate of gravitons discussed in the previous Chapter, we have found the static, spherically symmetric solution for the metric in terms of the Misner-Sharp mass function of baryonic matter and the fluid pressure. In particular, we have shown that the additional component of the acceleration at galactic scales can be completely attributed to the radial pressure of the fluid, whose interpretation in the corpuscular model is that this is part of the reaction of the condensate of gravitons to the presence of baryonic matter. Moreover, we have shown that it is possible to correctly reproduce the leading MOND $\log(r)$ and subleading $(1/r)\log(r)$ terms at galactic scales in the weak-field expansion of the potential. Our model also predicts a tiny modification of the Newtonian potential at galactic scales which is controlled by the cosmological acceleration.

Chapter 7

Solitonic stars as dark matter candidates

In the previous Chapters we have seen how it is possible to describe dark matter phenomenology in galaxies without assuming the existence of any (extra) exotic form of matter. In this Chapter we will start from a more conservative point of view and assume that dark matter can exist as particular gravitational configurations [301–304] or as particles which are not part of the standard model [305–309].

In the literature several candidates for dark matter, like WIMPS or axions, have been proposed. Here we focus on scalar fields as possible dark matter candidates. Scalar fields plays an important role in different contexts of gravitational physics like e.g. cosmology, holography and many others. For instance, in the first part of this thesis we have discussed their relevance in 2D gravity models. For this reason, in this Chapter we present an exact, analytic, static, spherically symmetric, four-dimensional solution of minimally coupled Einstein-scalar gravity, sourced by a scalar field which can be considered as a possible dark matter candidate. Its profile has the form of the sine-Gordon soliton and it is a horizonless, everywhere regular and positive-mass solution — it can be therefore considered as a solitonic star. The scalar potential behaves as a constant near the origin and vanishes at infinity. In particular, the solitonic scalar star interpolates between an anti-de Sitter and an asympototically flat spacetime. Unfortunately, due to numerical issue, we were not able to determine with confidence whether or not the star-like background solution is stable.

This chapter is based on:

- E. Franzin, M. Cadoni and M. T. "*Sine-Gordon solitonic scalar stars and black holes*", **Phys.Rev. D97 (2018) no.12, 124018**, arXiv:1805.08976.

Throughout the Chapter we adopt $c = 16\pi G = 1$ units.

7.1 Scalar fields and their role in astrophysics

To date, it is well-known that visible baryonic matter accounts for only a small part of the total mass of the universe. The most reliable and conservative approach to dark matter is the ΛCDM model [10], but several alternatives have been introduced to take into account some problems present in the model — from modifications of general relativity [120], to particle dark matter [12] and emergent gravity approaches [87, 274,

275]. However, as dark matter is most likely non-baryonic, it is interesting to consider asymptotically flat self-gravitating objects made up of massive fundamental (pseudo) scalar fields.

In the first part of the thesis we have investigated the role of scalar fields in 2D dilaton gravity and holography. Here we want to study the properties of (real) scalar fields and their astrophysical consequences [14].

Boson stars [310, 311] are the most famous example: they are non-topological solitonic configurations of massive *complex* scalar fields non-linearly coupled to themselves through a self-interacting scalar potential and to gravity. Stable and compact configurations have also been proposed as alternatives to astrophysical and primordial black holes [312, 313]. In fact, gravitational collapse could stop before the object reaches its Schwarzschild radius to produce a horizonless object that mimics some observational features of black holes [314–316], but that may still be distinguished from signatures in the gravitational-wave waveform [317–321].

In boson stars, the constituent complex scalar fields are globally invariant under U(1) symmetry and, as a consequence, there exists a conserved Noether current. For *real* massive scalar fields there is no such a current and the situation is very different: there are no static solutions. However there exist oscillatons [322], for which both the metric and the scalar field are periodically oscillating in time. For completeness, there are other examples of (non minimally coupled) real scalar field configurations that give rise to compact objects, i.e. [323, 324].

The key observation is that boson stars and oscillatons are found by fixing the scalar potential. Then, the metric functions and the scalar profile are determined by solving the Einstein-Klein-Gordon equations. In the case we will study in the following, on the contrary, we fix the scalar profile, we determine the scalar potential dynamically and we show that static regular self-gravitating solutions made up of real scalar fields are allowed.

We study exact, analytic, static, spherically symmetric, four-dimensional solutions of minimally coupled Einstein-scalar gravity. We derive a horizonless, everywhere regular, positive-mass solution. The solutions is sourced by a scalar field whose profile is identical to that of the sine-Gordon soliton [325]. These solitons have a wide range of applications in several areas of non-linear physics, e.g. non-linear molecular and DNA dynamics, the Josephson effect, ferromagnetic waves, non-linear optics, superconductivity and many others [326–328]. In two-dimensional gravity, there exists a relationship between the sine-Gordon dynamics and the black-hole metric degrees of freedom [329, 330], while a sine-Gordon star is known in Brans-Dicke gravity [331]. Thus, it is remarkable that a sine-Gordon soliton may also act as a gravitational scalar source in general relativity.

The energy density of the horizonless solution is negative close to the origin but it is balanced by a positive energy density in the asymptotic region to produce a positive total gravitational mass. Plus, this self-gravitating configuration sourced by a sine-Gordon scalar profile has compactness of $\mathcal{O}(0.1)$. For these reasons, we call it a sine-Gordon solitonic scalar star. To derive the solution we utilize a slightly different version of the solution-generating method proposed in Ref. [332] which has been successfully used to obtain a large number of exact, static, asymptotically flat or anti-de Sitter (AdS) black-hole and black-brane solutions [46, 47, 333–335].

Let us note that, even if black-hole solutions sourced by scalar fields in asymptot-

ically flat spacetimes are generically forbidden by no-hair theorems[1], yet black holes solutions sourced by sine-Gordon soliton are allowed [276]. However, we will not discuss this type of solutions in this thesis.

7.2 Solitonic solutions

We consider four-dimensional Einstein gravity minimally coupled to a self-interacting real scalar field ϕ,

$$S = \int d^4x \sqrt{-g} \left(\mathcal{R} - \frac{1}{2} \partial_\mu \phi \, \partial^\mu \phi - V(\phi) \right), \tag{7.2.1}$$

and we look for asymptotically flat, static, spherically symmetric solutions $ds^2 = -U(r)\, dt^2 + U(r)^{-1} dr^2 + R^2(r)\, d\Omega_2^2$ sourced by a scalar which inherits the spacetime symmetries [343, 344] and whose stress-energy tensor is

$$T_{\mu\nu} = \partial_\mu \phi \, \partial_\nu \phi - g_{\mu\nu} \left(\frac{1}{2} \partial_\mu \phi \, \partial^\mu \phi + V(\phi) \right). \tag{7.2.2}$$

Introducing an auxiliary dimensionless coordinate $x \equiv r_0/r$, with r_0 arbitrary length scale — which we will see proportional to the gravitational mass of the solution and inverse proportional to the square root of the amplitude of the scalar potential — the solution of the field equations can be entirely parametrized by a single function $P(x)$ and can be recast in the form,

$$R(x) = \frac{r_0 P}{x}, \quad \phi(x) = 2 \int dx \sqrt{-\frac{1}{P} \frac{d^2 P}{dx^2}}, \tag{7.2.3}$$

$$U(x) = \frac{r_0^2 P^2}{x^2} \left(c_2 + \frac{2}{r_0^2} \int \frac{x \, dx}{P^4} + \frac{c_1}{r_0^3} \int \frac{x^2 \, dx}{P^4} \right), \tag{7.2.4}$$

$$V[\phi(x)] = \frac{x^2}{2 r_0^2 P^2} \left[2 - x^2 \frac{d}{dx} \left(x^2 \frac{d}{dx} \frac{U P^2}{x^2} \right) \right], \tag{7.2.5}$$

where c_1 and c_2 are integration constants, whose value can be determined by the boundary conditions of the spacetime.

The r-asymptotic region corresponds to $x = 0$, while the r-origin corresponds either to $x = \infty$ when $P(x)$ has no zeros at finite values, or to $x = x_0$ when $P(x_0) = 0$. Because of its relation with the radius R of the 2-sphere, $P(x)$ must be a positive, analytic and monotonically decreasing function. Moreover, the condition of asymptotic flatness requires $P(0) = 1$ and reality of the scalar field implies $d^2P/dx^2 \leqslant 0$. When $P(x)$ has a zero at a finite value x_0, $U(x_0)$ becomes singular and in view of its integral form (7.2.4), quite generically the spacetime will develop a curvature singularity. The only way to avoid such a curvature singularity, but still have non-trivial solutions, is to impose an asymptotically constant scalar field profile and an exponential decreasing of d^2P/dx^2. In fact, from the field equations it turns out that the scalar curvature is given by

$$\mathcal{R} = 2V - \frac{x^4 U}{r_0^2 P} \frac{d^2 P}{dx^2},$$

[1] No-hair theorems relate the existence of hairy black holes to the non-convexity of the potential [336–338] and to the violation of the positive energy theorem [339, 340] with some notable exceptions [341, 342].

hence, the exponential behaviour of d^2P/dx^2 is needed to kill the power-law divergences in $\mathcal{R}$. The simplest choice for a function P satisfying all the conditions above is

$$P(x) = 2 - e^{-x}\,. \tag{7.2.6}$$

For the rest of the Chapter we switch back to the radial coordinate r. From Eq. (7.2.3), the metric function R is

$$R(r) = r\left(2 - e^{-r_0/r}\right), \tag{7.2.7}$$

and surprisingly enough, the scalar field profile turns out to be identical to that of the solitons (kinks) of the sine-Gordon theory [325],

$$\phi(r) = \pi - 4\arcsin\frac{e^{-r_0/2r}}{\sqrt{2}}\,. \tag{7.2.8}$$

The scalar field stays always finite, goes to zero asymptotically as $\phi \sim r_0/r$, whereas it behaves exponentially near the origin, i.e. $(\phi - \pi) \sim e^{-r_0/2r}$ as $r \to 0$.

For non-zero values of the integration constant c_1, the metric function U in Eq. (7.2.4) has a curvature singularity in $r = 0$, it describes either a black hole ($c_1/r_0 < 0$) or a naked singularity ($c_1/r_0 > 0$). However, for $c_1 = 0$ it describes a horizonless and perfectly regular solution with no curvature singularities. In this case, fixing c_2 in order to have an asymptotically flat solution, i.e. $U(r) \to 1$ as $r \to \infty$, we get,

$$\begin{aligned} U(r) = \frac{r^2}{96r_0^2}\Bigg[&-4P\left(\frac{6r_0}{r} + 5\right) - \frac{32r_0}{rP} - 8\left(\frac{3r_0}{r} + 1\right) \\ &+ P^2\Bigg(a^2 - 12\,\mathrm{Li}_2\left(1 - \frac{P}{2}\right) + 2\left(\frac{6r_0}{r} + 11\right)\log\frac{P}{2} \\ &+ 2\left(\frac{r_0}{r} + 3\right)\left(\frac{3r_0}{r} + 2\right)\Bigg)\Bigg], \end{aligned} \tag{7.2.9}$$

where $a^2 = 96r_0^2c_2 = 16 + 22\log 2 + \pi^2 - 6\log^2 2$. Near the origin the metric functions behave as $R(r) = r$ and $U(r) = r^2/L^2 + 1$, i.e. it describes an AdS spacetime with AdS length $L^2 = 6r_0^2/a^2$. Let us note that the star-like branch cannot be considered as the $c_1 \to 0$ limit of the black-hole branch as such a limit is singular.

The gravitational mass M of the solution can be easily inferred from the $1/r$ term in the asymptotic expansion of the metric function $U(r)$; it is positive and given by $M = 16\pi r_0/3$. As the scalar field is spread all over the radial direction, this solution does not have a hard surface. Yet we could define an effective radius r_{eff} within which 99% of the mass is contained. It turns out to be, roughly, $r_{\text{eff}}/r_0 \approx 98$, almost three times larger than its Schwarzschild radius. This also means that the compactness of this solution is about 0.17, a value compatible with other boson and fluid stars but not black holes — see e.g. Fig. 4 of Ref. [345].

Our solution represents an extremely non-trivial gravitational configuration, which we call a sine-Gordon solitonic scalar star. The solution itself has a solitonic nature because it has a positive mass, it is completely free of spacetime singularities and it interpolates between two maximally symmetric spacetimes — an asymptotically flat spacetime at $r = \infty$ and an AdS spacetime at $r = 0$.

The expression for the potential (7.2.5) can be computed analytically but is cumbersome. We give in Fig. 7.1 its plot both as a function of r and ϕ. As expected the potential goes to zero asymptotically ($r \to \infty$, i.e. $\phi \to 0$) as a quintic power ϕ^5 and has a minimum there. Near the origin ($r \to 0$ i.e. $\phi \to \pi$), it approaches a negative constant $V = -3/2L^2 = -a^2/4r_0^2$ consistently with its AdS behaviour. It is interesting to notice that the potential is positive for large values of r (see the inset in Fig. 7.1), reaches a maximum at around $r/r_0 \approx 5.01$ then crosses the axis for $r/r_0 \approx 4.08$ and goes down to negative values to approach exponentially the constant negative AdS value.

Equation of state

Despite the fact that in general a scalar field does not obey an equation of state [346], the stress-energy tensor of the scalar field (7.2.2) can also be interpreted as produced by a non-perfect, anisotropic fluid with both radial and perpendicular pressure,

$$-T_0^0 = \rho = \frac{1}{2}U\phi'^2 + V = \mathcal{T} + V\,, \tag{7.2.10}$$

$$T_1^1 = p_{\rm rad} = \frac{1}{2}U\phi'^2 - V\,, \quad T_2^2 = p_{\rm tan} = -\rho\,. \tag{7.2.11}$$

In Fig. 7.2 on the left we plot the energy density ρ, its kinetic contribution $\mathcal{T}$, and the radial pressure $p_{\rm rad}$ as functions of r, while on the right we plot the position-dependent equation of state $p_{\rm rad} = p_{\rm rad}(\rho)$.

Although the energy density is negative for small values of r, the gravitational mass is positive. The existence of this positive mass solution results from the peculiar highly non-linear interaction of the scalar field producing a negative energy density in the inner region balanced by the positive energy density in the asymptotic region. In order to see if this balance may produce a stable configuration, we have to investigate the stability of our solution.

7.3 Stability analysis

To discuss the stability of our solution we consider s-wave radial perturbations (they are generically expected to be the least stable) about the background, i.e. $U(r)+\delta U(t,r)$,

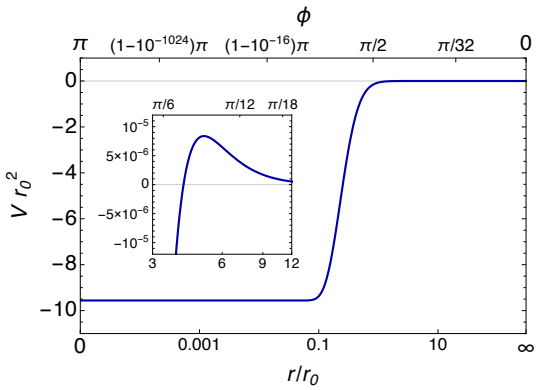

Figure 7.1: Plot of the scalar potential as a function of r and ϕ. Inset: Zoom on the maximum.

$R(r) + \delta R(t, r)$ and $\phi(r) + \delta\phi(t, r)$.

By expanding the field equations up to linear order in the perturbation fields and by making use of the background equations, the perturbation equations reduce to two constraints and a dynamic equation for $\delta\phi$ [347].

Furthermore, assuming harmonic time dependence for the scalar perturbation

$$\delta\phi(t, r) \equiv e^{-i\omega t} R(r)\psi(r)\,,$$

the master equation for radial perturbations reads

$$\frac{d^2\psi}{dr_*^2} + \left(\omega^2 - V_{\rm eff}\right)\psi = 0\,, \tag{7.3.12}$$

where r_* is a "tortoise" coordinate $dr_*/dr = 1/U(r)$ and

$$\frac{V_{\rm eff}}{U} = \frac{1 - UR'^2}{R^2} + \frac{\left(VR^2 - 2\right)\phi'^2}{4R'^2} + \frac{V_\phi R\phi'}{R'} - \frac{V}{2} + V_{\phi\phi}\,, \tag{7.3.13}$$

where $V_\phi = dV/d\phi$ and $V_{\phi\phi} = d^2V/d\phi^2$. $V_{\rm eff}$ can be given in a complicated yet analytical form that we do not report here.

The asymptotic behaviour of the effective potential is $V_{\rm eff} \sim 2r_0/r^3$ as $r \to \infty$ while near the origin it diverges as $V_{\rm eff} \sim r_0^2/64r^4$ as $r \to 0$. For $0.14 \lesssim r/r_0 \gtrsim 5.87$ it is negative while for $r \gtrsim 5.87$ it is positive and has a local maximum for $r/r_0 \approx 8.11$. Its plot is shown in Fig. 7.3.

To show that the background solution is linearly stable, we need to show that there are no solutions to Eq. (7.3.12) with $\omega^2 < 0$ satisfying appropriate boundary conditions.

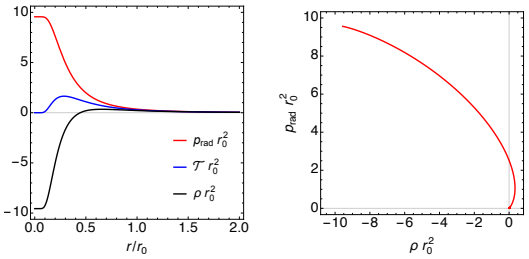

Figure 7.2: Left: The energy density ρ, its kinetic contribution $\mathcal{T}$ and the radial pressure $p_{\rm rad}$ as functions of the radial coordinate r. Right: Equation of state.

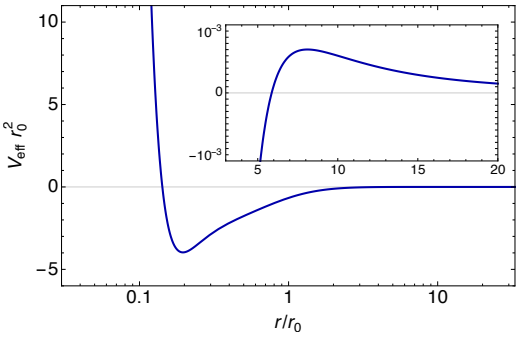

Figure 7.3: Plot of the effective potential (7.3.13) as a function of r. Zeros for $r/r_0 \approx 0.14$ and $r/r_0 \approx 5.87$. Extrema for $r_{\rm min}/r_0 \approx 0.20$ and $r_{\rm max}/r_0 \approx 8.11$. Inset: Zoom on the local maximum.

At spatial infinity we can use purely outgoing, free-wave, boundary conditions, i.e. $\psi_\infty \sim e^{i\omega r_*}$. Boundary conditions near the origin are more complicated, due to the behaviour of $V_{\rm eff}$ near $r = 0$. More technically, $r = 0$ is a non-Fuchsian point and as a consequence, the solution ψ_0 near the origin is not a polynomial. Equation (7.3.12) cannot be solved in terms of simple functions in this limit for any ω^2, nevertheless, for marginally stable solutions ($\omega^2 = 0$) the solution behaves as $\psi_0(\omega^2 = 0) \sim e^{-r_0/r}/r$. For this reason we expect that ψ_0 must also be exponentially suppressed for $\omega^2 \neq 0$.

Because of the very steep barrier at the origin, neither the Simon's criterion [348] based on the area of $V_{\rm eff}$, nor an S-deformation method [349] are applicable.

In addition, both the barrier at the origin and the lack of more precise boundary conditions near the origin make the numerical integration of Eq. (7.3.12) very challenging. For some values of the parameters it is possible to find solutions to Eq. (7.3.12) for negative and positive values of ω^2, but such results are highly dependent on the initial parameters. More importantly, we had difficulty in keeping control on the numerical error which (generically) grows of several orders of magnitude at $r \approx r_{\rm min}$. For these reasons, we cannot state whether or not the background solution is stable against linear perturbations.

To conclude, it is possible to show that also the black hole branch (we are not discussing here) is unstable against linear perturbations [276]. Although the limit $c_1/r_0 \to 0$ of the black-hole branch is singular, the instability of the black-hole background solution suggests instability also for the star-like branch. Yet, the instability time scale could be extremely large (even larger than the Hubble time) and the sine-Gordon solitonic scalar star may still have astrophysical interest as a possible dark matter candidate.

7.4 Summary and conclusions

In this Chapter we have derived and studied an exact, analytic, static, spherically symmetric, four-dimensional solution of minimally coupled Einstein-scalar gravity sourced by configuration of the scalar field which has the form of a sine-Gordon soliton. Our solution can be considered as a possible candidate of dark matter. Depending on the value of the parameter c_1/r_0, it describes either a black hole or a star-like solution that we called sine-Gordon solitonic scalar star. The scalar potential is not given *a priori* but it is determined by the field equations.

The sine-Gordon solitonic scalar star is a horizonless, everywhere regular, asymptotically flat spacetime with positive mass and compactness of $\mathcal{O}(0.1)$. The scalar potential behaves as a negative constant near the origin and goes to zero as ϕ^5 at spatial infinity. Likewise, the energy density of the solution is negative and finite near the origin, becomes positive at a certain radius and vanishes in the asymptotic region. In that sense, this solution interpolates from the AdS spacetime near the origin and the Schwarzschild spacetime at spatial infinity. The negative energy density near the origin is overcompensated by the positive energy density in the asymptotic region, so that the total mass of the star is positive.

This peculiar behaviour resembles that of gravastars [350]. These exotic compact objects have been proposed as alternatives to black holes [351] and they are objects whose interior is described by a patch of de Sitter space (characterized by negative pressure) smoothly connected to the Schwarzschild exterior through an intermediate

region filled with some (exotic) matter. In analogy with the gravastar picture, our solution can be regarded as an *anti*-gravastar or the string-inspired AdS bubbles [352]. The advantage with respect to these models is that our solution does not require junction conditions with the drawback of a very complicated scalar potential. Notice, however, that our solution is not as compact as a typical gravastar.

The solution-generating method introduced and the result discussed bode well for a possible analytical interpolating solution between de Sitter and Schwarzschild spacetimes, but its search is left for future work.

Unfortunately, we were not able to determine with confidence whether or not the background solution is stable against linear perturbations. Because of the form of the effective potential, the study of linear perturbations is indeed very complicated both analytically and numerically. This kind of solutions are often plagued by instabilities [353, 354] and probably a full numerical simulation is required. Results on the black-hole branch may suggest linear instability also in the star-like branch. However, the number of unstable modes in the black-hole branch is finite and the instability time scale could be sufficiently large to let the sine-Gordon solitonic scalar star still have some astrophysical interest as a possible dark matter candidate.

Another interesting point that we have not investigated here is the formation mechanism of such a solution. While the solitonic nature of the scalar profile is comprehensible, the origin of the scalar potential is more mysterious. Again, a full numerical study of gravitational collapse of scalar matter should be necessary to completely answer this question.

Conclusions

In this thesis we have investigated various aspects of gravitational physics with the aim to shed light on the deep relation between the infrared and ultraviolet regimes of gravity. In doing so, we have focused on very challenging topics, black holes, holography, the emergent properties of spacetime and gravity itself and their consequences for the gravitational dynamics at galactictic scales.

Throughout this thesis, holography and the holographic principle have been used as a guiding principle in the understanding of quantum properties of the gravitational interaction. Due to their peculiar features, black holes represent the ideal laboratory to test gravity from the quantum to the classical regime. This become very clear in the AdS/CFT correspondence, where classical properties of black holes can be translated in quantum properties of dual quantum fields and viceversa. Black hole hydrodynamics and the computation of the shear viscosity to density entropy ratio are an explicit realization of these ideas.

Another important issue we have focused on in this thesis is about the true quantum nature of spacetime and its implications at large scales. Recent investigations have shown that classical spacetime and Einstein's gravity can be understood as emerging from some underlying microscopic quantum theory. We have seen that a natural manifestation of the emergent gravity paradigm appears in the corpuscolar picture of gravity, where black holes and de Sitter spacetime can be considered as a Bose-Einstein condensates of N_G gravitons. From this quantum perspective, classical gravity emerges in the limit $N_G \gg 1$. An interesting fact is that when one tries to describe the gravitational interaction at all scales (from the Solar system to the cosmological ones, passing through the galactic scales) into a corpuscolar picture of gravity, one realizes that at galactic ones, no exotic matter is needed to describe the phenomenology commonly attributed to dark matter. Indeed, the latter can be considered as a result of the interaction between cosmological gravitons and baryonic matter. However, in a more conservative approach, real scalar fields can account for a possible dark matter candidate. Scalar fields cover a wide range of applications in physics (e.g. the Higgs boson in particle physics). In gravity, for example, they are very useful to study quantum gravity in a simplified context.

Here we present a summary of the most important results obtained in this thesis and prospects for future investigations.

In the first part of the thesis we have investigated geometrical, thermodynamical and holographic properties of two dimensional and higher dimensional black holes in AdS spacetime in the context of the AdS/CFT correspondence. The deep interplay between the infrared and ultraviolet regimes of gravity manifests in black holes (branes) hydrodynamics. The computation of the shear viscosity to density entropy ratio clearly

shows how the system flows between the two regimes ot the theory. Moreover we have showed that, contrarily to what is generally done in AdS/CFT, e.g. to use the holographic dualities to learn about transport coefficients in the hydrodynamic limit of strongly coupled QFTs by investigating bulk gravity configurations, the computation of η/s has been also usefull to gain information about the non trivial thermodynamical behaviour of black holes, like e.g. phase transitions. This is true also in the case of dilaton gravity, where a detailed analysis of the gravitational solutions, their dual CFT description and their symmetries can be used to gain information about quantum phase transition from the IR (classical) to the UV (quantum) regimes of gravity in 2D.

In Chapter 1 we have solved Einstein's equations in higher dimensions to find black branes and black holes solutions in Lovelock, Einstein and Gauss-Bonnet (GB) gravity in presence of an electromagnetic field. We have investigated their geometrical and thermodynamical properties in five dimensional Reissner-Nordström (RN) and GB gravity. In the case of black branes we have focused mainly on GB gravity, even if we think the results can be extended to Lovelock gravity, too. We have showed that, when expressed in terms of effective physical parameters, the thermodynamic behaviour of charged GB black branes is completely indistinguishable from that of charged Einstein black branes. Moreover, the extremal, near-horizon limit of the two classes of branes is exactly the same as they allow for the same $AdS_2 \times R3$, near-horizon, exact solution. This implies that, although in the UV the associated dual QFTs are different, they flow in the IR to the same fixed point. In the case of two dimensional dilaton gravity we have firstly revised the Almeiri-Polchinksi model and its properties. In particular, we have found that the model admits two kind of different vacua, we have called constant dilaton vacuum (CDV) and linear dilaton vacuum (LDV). Then we have proposed a covariant definition of the black holes mass that it can be useful to define the energy of the solution, since it appears to be invariant under Weyl transformation of the metric. Finally, we have shown that when up-lifted to $(D+2)-$dimensions, the vacuum solutions produce different spacetimes, an intrinsically 2D spacetime for the CDV and hyperscaling violating geometry for the LDV, whose forms are $AdS_2 \times R_D$ and H_{D+2}, respectively.

In Chapter 2 we have reviewed the AdS/CFT correspondence and discussed its applications in holographic relativistic hydrodynamics both in flat and curved spacetimes. For what concerns holographic hydrodynamics, we have focused on the shear viscosity. Following the standard rules of AdS/CFT correspondence, we have first defined the shear viscosity for quantum field theories (QFTs) dual to AdS black branes in flat spacetime by means of the Kubo formula. Then we have focused on curved spacetime and defined hydrodynamics and the shear viscosity for the QFTs dual to AdS spherical black holes by means of an anlogous Kubo formula. Even if the spherical background intrinsically breaks the translational symmetry, thus preventing the standard definition of the shear viscosity in terms of conserved quantities, it can be interpreted as the rate of entropy production due to a particular perturbation of the background. Finally, in the case of 2D dilaton gravity, we have compared energetically the two different vacua (CDV and LDV) of the theory. Then we have showed the existence of a zero temperature phase transition in which the vacuum with constant dilaton is energetically preferred. We have also speculated that this quantum phase transition could be related to the spontaneous dimensional reduction of the spacetime to two dimensions near the Planck scale.

In Chapter 3 we have computed the shear viscosity to density entropy ratio, η/s, for five dimensional charged black branes and black holes both in general relativity and GB theories. For what concerns branes, we have found that η/s is a monotonic function of the temperature and the universality of η/s is lost in the UV but is restored in the IR. We expected this result because transport features in the hydrodynamic regime should be determined by IR physics. On the other hand, it is not entirely clear if this result has a general meaning or it is a just a consequence of the peculiarities of the charged GB black brane. Indeed, the dual QFT to GB gravity shows an interesting temperature-dependent flow of η/s depending on the value of the GB coupling constant. This problem remains open to future investigations. In the case of spherical black holes, the computation of the analogous shear viscosity to density entropy ratio, $\tilde{\eta}/s$, has shown interesting results, especially for what concerns the IR and UV regimes of gravity. At large and small temperatures, we have found that $\tilde{\eta}/s$ is a monotonic increasing function of the temperature. In particular, at large temperatures it approaches a constant value, whereas, at small temperatures, when the black hole has a regular, stable extremal limit, $\tilde{\eta}/s$ goes to zero with scaling law behaviour. Whenever the phase diagram of the black hole has a Van der Waals-like behaviour, i.e. it is characterised by the presence of two stable states (small and large black holes) connected by a meta-stable region (intermediate black holes), the system evolution must occur through the meta-stable region and temperature-dependent hysteresis of $\tilde{\eta}/s$ is generated by non-equilibrium thermodynamics. In the case of two dimensional dilaton gravity, we have showed that the effect of the symmetry breaking is both the generation of an infrared scale (a mass gap) and to make local the Goldstone modes associated with the asymptotic symmetries of the 2D spacetime. In this way a non vanishing central charge is generated in the dual conformal field theory, which accounts for the microscopic entropy of the 2D black hole.

In the second part of the thesis we have investigated the emergent gravity scenario in the context of corpuscolar gravity and its applications at galactic scales. What is clear from the results we have obtained in this part of the thesis is that, in order to describe gravity at galactic scales, an infrared modification of the theory is needed. This kind of modifications are driven by the microscopic (UV) nature of gravity which can be described in terms of a Bose-Einstein condensate of gravitons.

In Chapter 4 we have reviewed both the Verlinde's emergent gravity paradigm [87] and the corpuscolar gravity picture of Dvali *et al* [91].

In Chapter 5 we have investigated the emergent laws of gravity distinguishing different scaling regimes and deriving the implications of our emergent gravity scenario at galactic scales. We have firstly described the de Sitter universe in a corpuscolar picture of gravity as a Bose-Einstein condensate of N_G cosmological gravitons (the DEC). Moreover we have demonstrated that the local behaviour of this condensate requires, besides the usual holographic regime at the scales of clumped (baryonic) matter where number of gravitons and entropy scale as an area, an extensive regime of gravity in which the graviton number scales with the volume of the space. In this picture, we have shown that baryonic matter and local (Newtonian) gravitational forces fits naturally in this description as gravitons pulled out from the DEC. For what concerns the galactic scales, we have demonstrated that the galaxy rotational curves can be described without assuming the existence of exotic matter. Indeed,

the phenomenology commonly attributed to dark matter (the flattening of rotational curves) can be described as a reaction of the DEC to the presence of localized baryonic matter. In this way we have been able to correctly reproduce the famous MOND formula for the velocity of stars in galaxies. Finally, we have calculated the mass ratio between the contribution of the apparent dark matter and the baryonic matter in a region of size r at galactic scales and showed that it is consistent with the ΛCDM predictions. In particular, we have noticed how the application of the corpuscolar picture of gravity to de Sitter universe lead to the possibility to give a quantum description of the origin of dark energy. However, we have left the investigation of this interesting point for the future. Another argument we leave for future investigations is about the origin of horizons. They play a key role in the corpuscolar picture of emergent gravity. Indeed the holographic properties of spacetime refer to the existence of cosmological (or black holes) horizon whose origin is still mysterious.

In Chapter 6 we have shown how the corpuscolar picture of gravity shown in Chapter 5 allows for an effective description in terms of general relativity (GR) sourced by an anisotropic fluid. We have constructed an infrared-modified theory of gravity which gives the effective fluid description of our emergent gravity theory based on BEC of gravitons. In this picture, the additional component of the acceleration of stars at galactic scales can be completely attributed to the radial pressure of the fluid, whose interpretation in the corpuscular model is that this is part of the reaction of the condensate of gravitons to the presence of baryonic matter. We have also shown that it is possible to correctly reproduce the leading MOND $\log(r)$ and subleading $(1/r)\log(r)$ terms at galactic scales in the weak-field expansion of the potential. Our model also predicts a tiny modification of the Newtonian potential at galactic scales which is controlled by the cosmological acceleration.

Finally, in Chapter 7 we have adopted a more conservative approach to the dark matter problem. We have derived an exact, analytic, static, spherically symmetric, four-dimensional solution of minimally coupled Einstein-scalar gravity, sourced by a scalar field which, for instance, can account for a possible dark matter candidate. We have studied its geometrical and thermodynamical properties. The importance of this results is represented by the solution-generating method: contrarily to the standard procedure, we have formulated a general one to solve Einstein's equations starting from the profile of the real scalar field and not from the explicit expression of the potential. As a result, the scalar field profile takes the form of a sine-Gordon soliton. The solution is horizonless, everywhere regular, asymptotically flat spacetime with positive mass and compactness of $\mathcal{O}(0.1)$. We have called it a sine-Gordon solitonic scalar star. We have also studied the stability of the solution: unfortunately, due to numerical issues, we have not been able to infer with great confidence if the star is stable or not against linear perturbations. Results on the black-hole branch of solutions may suggest linear instability also in the star-like branch. However, the instability time scale could be sufficiently large to let the sine-Gordon solitonic scalar star still have some astrophysical interest as a possible dark matter candidate.

Bibliography

[1] A. Einstein, "Grundgedanken der allgemeinen Relativitätstheorie und Anwendung dieser Theorie in der Astronomie," *Sitzungsber. Preuss. Akad. Wiss. Berlin* (1915) 315.

[2] A. Einstein, "Zur allgemeinen Relativitätstheorie," *Sitzungsber. Preuss. Akad. Wiss. Berlin* (1915) 778.

[3] A. Einstein, "Erklärung der Perihelbewegung des Merkur aus der allgemeinen Relativitätstheorie," *Sitzungsber. Preuss. Akad. Wiss. Berlin* (1916) 831.

[4] A. Einstein, "Feldgleichungen der Gravitation," *Sitzungsber. Preuss. Akad. Wiss. Berlin* (1916) 844.

[5] C. M. Will, "The Confrontation between General Relativity and Experiment," *Living Rev. Rel.* **17** (2014) 4, arXiv:1403.7377 [gr-qc].

[6] **Virgo, LIGO Scientific** Collaboration, B. P. Abbott *et al.*, "Observation of Gravitational Waves from a Binary Black Hole Merger," *Phys. Rev. Lett.* **116** no. 6, (2016) 061102, arXiv:1602.03837 [gr-qc].

[7] **Virgo, LIGO Scientific** Collaboration, B. P. Abbott *et al.*, "GW151226: Observation of Gravitational Waves from a 22-Solar-Mass Binary Black Hole Coalescence," *Phys. Rev. Lett.* **116** no. 24, (2016) 241103, arXiv:1606.04855 [gr-qc].

[8] **Virgo, LIGO Scientific** Collaboration, B. Abbott *et al.*, "GW170817: Observation of Gravitational Waves from a Binary Neutron Star Inspiral," *Phys. Rev. Lett.* **119** no. 16, (2017) 161101, arXiv:1710.05832 [gr-qc].

[9] **GROND, SALT Group, OzGrav, DFN, INTEGRAL, Virgo, Insight-Hxmt, MAXI Team, Fermi-LAT, J-GEM, RATIR, IceCube, CAASTRO, LWA, ePESSTO, GRAWITA, RIMAS, SKA South Africa/MeerKAT, H.E.S.S., 1M2H Team, IKI-GW Follow-up, Fermi GBM, Pi of Sky, DWF (Deeper Wider Faster Program), Dark Energy Survey, MASTER, AstroSat Cadmium Zinc Telluride Imager Team, Swift, Pierre Auger, ASKAP, VINROUGE, JAGWAR, Chandra Team at McGill University, TTU-NRAO, GROWTH, AGILE Team, MWA, ATCA, AST3, TOROS, Pan-STARRS, NuSTAR, ATLAS Telescopes, BOOTES, CaltechNRAO, LIGO Scientific, High Time Resolution Universe Survey, Nordic Optical Telescope, Las Cumbres Observatory Group, TZAC Consortium, LOFAR, IPN, DLT40, Texas Tech University, HAWC, ANTARES, KU, Dark Energy Camera**

GW-EM, CALET, Euro VLBI Team, ALMA Collaboration, B. P. Abbott *et al.*, "Multi-messenger Observations of a Binary Neutron Star Merger," *Astrophys. J.* **848** no. 2, (2017) L12, arXiv:1710.05833 [astro-ph.HE].

[10] **Planck** Collaboration, P. A. R. Ade *et al.*, "Planck 2015 results. XIII. Cosmological parameters," *Astron. Astrophys.* **594** (2016) A13, arXiv:1502.01589 [astro-ph.CO].

[11] G. Bertone, D. Hooper, and J. Silk, "Particle dark matter: Evidence, candidates and constraints," *Phys. Rept.* **405** (2005) 279–390, arXiv:hep-ph/0404175 [hep-ph].

[12] G. Bertone, ed., *Particle Dark Matter: Observations, Models and Searches*. Cambridge University Press, Cambridge, UK, 2010.

[13] S. Capozziello and M. De Laurentis, "Extended Theories of Gravity," *Phys. Rept.* **509** (2011) 167–321, arXiv:1108.6266 [gr-qc].

[14] D. J. E. Marsh and A.-R. Pop, "Axion dark matter, solitons, and the cusp-core problem," *Mon. Not. Roy. Astron. Soc.* **451** (2015) 2479, arXiv:1502.03456 [astro-ph.CO].

[15] J. Magaña and T. Matos, "A brief Review of the Scalar Field Dark Matter model," in *Journal of Physics Conference Series*, vol. 378 of *Journal of Physics Conference Series*, p. 012012. Aug., 2012. arXiv:1201.6107.

[16] J. D. Bekenstein, "Black holes and the second law," *Lett. Nuovo Cim.* **4** (1972) 737–740.

[17] J. D. Bekenstein, "Black holes and entropy," *Phys. Rev.* **D7** (1973) 2333–2346.

[18] S. W. Hawking, "Black hole explosions," *Nature* **248** (1974) 30–31.

[19] S. W. Hawking, "Particle Creation by Black Holes," *Commun. Math. Phys.* **43** (1975) 199–220. [,167(1975)].

[20] B. S. DeWitt, "Quantum Theory of Gravity. 1. The Canonical Theory," *Phys. Rev.* **160** (1967) 1113–1148.

[21] O. Aharony, S. S. Gubser, J. M. Maldacena, H. Ooguri, and Y. Oz, "Large N field theories, string theory and gravity," *Phys. Rept.* **323** (2000) 183–386, arXiv:hep-th/9905111 [hep-th].

[22] C. Rovelli, "Loop quantum gravity: the first twenty five years," *Class. Quant. Grav.* **28** (2011) 153002, arXiv:1012.4707 [gr-qc].

[23] L. Freidel, "Group field theory: An Overview," *Int. J. Theor. Phys.* **44** (2005) 1769–1783, arXiv:hep-th/0505016 [hep-th].

[24] S. W. Hawking, "The Information Paradox for Black Holes," 2015. arXiv:1509.01147 [hep-th]. https://inspirehep.net/record/1391640/files/arXiv:1509.01147.pdf.

[25] S. D. Mathur, "The Information paradox: A Pedagogical introduction," *Class. Quant. Grav.* **26** (2009) 224001, arXiv:0909.1038 [hep-th].

[26] A. Strominger and C. Vafa, "Microscopic origin of the Bekenstein-Hawking entropy," *Phys. Lett.* **B379** (1996) 99, arXiv:hep-th/9601029 [hep-th].

[27] M. Cadoni and S. Mignemi, "Entropy of 2-D black holes from counting microstates," *Phys. Rev.* **D59** (1999) 081501, arXiv:hep-th/9810251 [hep-th].

[28] S. Hossenfelder, "Experimental Search for Quantum Gravity," in *Classical and quantum gravity: Theory, Analysis and Applications*. 2010. arXiv:1010.3420 [gr-qc].

[29] G. 't Hooft, "Dimensional reduction in quantum gravity," *Conf. Proc.* **C930308** (1993) 284–296, arXiv:gr-qc/9310026 [gr-qc].

[30] L. Susskind, "The World as a hologram," *J. Math. Phys.* **36** (1995) 6377–6396, arXiv:hep-th/9409089 [hep-th].

[31] J. M. Maldacena, "The Large N limit of superconformal field theories and supergravity," *Int. J. Theor. Phys.* **38** (1999) 1113–1133, arXiv:hep-th/9711200 [hep-th]. [Adv. Theor. Math. Phys.2,231(1998)].

[32] S. Ryu and T. Takayanagi, "Holographic derivation of entanglement entropy from AdS/CFT," *Phys. Rev. Lett.* **96** (2006) 181602, arXiv:hep-th/0603001 [hep-th].

[33] N. Ogawa, T. Takayanagi, and T. Ugajin, "Holographic Fermi Surfaces and Entanglement Entropy," *JHEP* **01** (2012) 125, arXiv:1111.1023 [hep-th].

[34] K. Narayan, T. Takayanagi, and S. P. Trivedi, "AdS plane waves and entanglement entropy," *JHEP* **04** (2013) 051, arXiv:1212.4328 [hep-th].

[35] S. Cremonini and X. Dong, "Constraints on renormalization group flows from holographic entanglement entropy," *Phys. Rev.* **D89** no. 6, (2014) 065041, arXiv:1311.3307 [hep-th].

[36] S. A. Hartnoll, "Lectures on holographic methods for condensed matter physics," *Class. Quant. Grav.* **26** (2009) 224002, arXiv:0903.3246 [hep-th].

[37] S. A. Hartnoll, C. P. Herzog, and G. T. Horowitz, "Building a Holographic Superconductor," *Phys. Rev. Lett.* **101** (2008) 031601, arXiv:0803.3295 [hep-th].

[38] G. T. Horowitz and M. M. Roberts, "Holographic Superconductors with Various Condensates," *Phys. Rev.* **D78** (2008) 126008, arXiv:0810.1077 [hep-th].

[39] C. P. Herzog, "Lectures on Holographic Superfluidity and Superconductivity," *J. Phys.* **A42** (2009) 343001, arXiv:0904.1975 [hep-th].

[40] G. T. Horowitz, "Introduction to Holographic Superconductors," *Lect. Notes Phys.* **828** (2011) 313–347, arXiv:1002.1722 [hep-th].

[41] M. Cadoni, G. D'Appollonio, and P. Pani, "Phase transitions between Reissner-Nordstrom and dilatonic black holes in 4D AdS spacetime," *JHEP* **03** (2010) 100, arXiv:0912.3520 [hep-th].

[42] M. Cadoni and P. Pani, "Holography of charged dilatonic black branes at finite temperature," *JHEP* **04** (2011) 049, arXiv:1102.3820 [hep-th].

[43] S. S. Gubser and F. D. Rocha, "The gravity dual to a quantum critical point with spontaneous symmetry breaking," *Phys. Rev. Lett.* **102** (2009) 061601, arXiv:0807.1737 [hep-th].

[44] B. Gouteraux and E. Kiritsis, "Generalized Holographic Quantum Criticality at Finite Density," *JHEP* **12** (2011) 036, arXiv:1107.2116 [hep-th].

[45] B. Gouteraux and E. Kiritsis, "Quantum critical lines in holographic phases with (un)broken symmetry," *JHEP* **04** (2013) 053, arXiv:1212.2625 [hep-th].

[46] M. Cadoni and M. Serra, "Hyperscaling violation for scalar black branes in arbitrary dimensions," *JHEP* **11** (2012) 136, arXiv:1209.4484 [hep-th].

[47] M. Cadoni and S. Mignemi, "Phase transition and hyperscaling violation for scalar Black Branes," *JHEP* **06** (2012) 056, arXiv:1205.0412 [hep-th].

[48] X. Dong, S. Harrison, S. Kachru, G. Torroba, and H. Wang, "Aspects of holography for theories with hyperscaling violation," *JHEP* **06** (2012) 041, arXiv:1201.1905 [hep-th].

[49] K. Narayan, "On Lifshitz scaling and hyperscaling violation in string theory," *Phys. Rev.* **D85** (2012) 106006, arXiv:1202.5935 [hep-th].

[50] E. Perlmutter, "Hyperscaling violation from supergravity," *JHEP* **06** (2012) 165, arXiv:1205.0242 [hep-th].

[51] M. Ammon, M. Kaminski, and A. Karch, "Hyperscaling-Violation on Probe D-Branes," *JHEP* **11** (2012) 028, arXiv:1207.1726 [hep-th].

[52] J. Bhattacharya, S. Cremonini, and A. Sinkovics, "On the IR completion of geometries with hyperscaling violation," *JHEP* **02** (2013) 147, arXiv:1208.1752 [hep-th].

[53] M. Alishahiha and H. Yavartanoo, "On Holography with Hyperscaling Violation," *JHEP* **11** (2012) 034, arXiv:1208.6197 [hep-th].

[54] P. Dey and S. Roy, "Lifshitz metric with hyperscaling violation from NS5-Dp states in string theory," *Phys. Lett.* **B720** (2013) 419–423, arXiv:1209.1049 [hep-th].

[55] J. Sadeghi, B. Pourhasan, and F. Pourasadollah, "Thermodynamics of Schrödinger black holes with hyperscaling violation," *Phys. Lett.* **B720** (2013) 244–249, arXiv:1209.1874 [hep-th].

[56] M. Alishahiha, E. O Colgain, and H. Yavartanoo, "Charged Black Branes with Hyperscaling Violating Factor," *JHEP* **11** (2012) 137, arXiv:1209.3946 [hep-th].

[57] B. S. Kim, "Hyperscaling violation : a unified frame for effective holographic theories," *JHEP* **11** (2012) 061, arXiv:1210.0540 [hep-th].

[58] M. Edalati, J. F. Pedraza, and W. Tangarife Garcia, "Quantum Fluctuations in Holographic Theories with Hyperscaling Violation," *Phys. Rev.* **D87** no. 4, (2013) 046001, arXiv:1210.6993 [hep-th].

[59] J. Gath, J. Hartong, R. Monteiro, and N. A. Obers, "Holographic Models for Theories with Hyperscaling Violation," *JHEP* **04** (2013) 159, arXiv:1212.3263 [hep-th].

[60] S. Cremonini and A. Sinkovics, "Spatially Modulated Instabilities of Geometries with Hyperscaling Violation," *JHEP* **01** (2014) 099, arXiv:1212.4172 [hep-th].

[61] M. Hassaïne, "New black holes of vacuum Einstein equations with hyperscaling violation and Nil geometry horizons," *Phys. Rev.* **D91** no. 8, (2015) 084054, arXiv:1503.01716 [hep-th].

[62] M. Bravo-Gaete, S. Gomez, and M. Hassaine, "Towards the Cardy formula for hyperscaling violation black holes," *Phys. Rev.* **D91** no. 12, (2015) 124038, arXiv:1505.00702 [hep-th].

[63] G. Kofinas, "Hyperscaling violating black holes in scalar-torsion theories," *Phys. Rev.* **D92** no. 8, (2015) 084022, arXiv:1507.07434 [hep-th].

[64] A. Salvio, "Holographic Superfluids and Superconductors in Dilaton-Gravity," *JHEP* **09** (2012) 134, arXiv:1207.3800 [hep-th].

[65] D. Roychowdhury, "Hydrodynamics from scalar black branes," *JHEP* **04** (2015) 162, arXiv:1502.04345 [hep-th].

[66] G. Policastro, D. T. Son, and A. O. Starinets, "The Shear viscosity of strongly coupled N=4 supersymmetric Yang-Mills plasma," *Phys. Rev. Lett.* **87** (2001) 081601, arXiv:hep-th/0104066 [hep-th].

[67] M. Edalati, J. I. Jottar, and R. G. Leigh, "Transport Coefficients at Zero Temperature from Extremal Black Holes," *JHEP* **01** (2010) 018, arXiv:0910.0645 [hep-th].

[68] A. Buchel, "On universality of stress-energy tensor correlation functions in supergravity," *Phys. Lett.* **B609** (2005) 392–401, arXiv:hep-th/0408095 [hep-th].

[69] P. Benincasa, A. Buchel, and R. Naryshkin, "The Shear viscosity of gauge theory plasma with chemical potentials," *Phys. Lett.* **B645** (2007) 309–313, arXiv:hep-th/0610145 [hep-th].

[70] Y. Kats and P. Petrov, "Effect of curvature squared corrections in AdS on the viscosity of the dual gauge theory," *JHEP* **01** (2009) 044, arXiv:0712.0743 [hep-th].

[71] K. Landsteiner and J. Mas, "The Shear viscosity of the non-commutative plasma," *JHEP* **07** (2007) 088, arXiv:0706.0411 [hep-th].

[72] N. Iqbal and H. Liu, "Universality of the hydrodynamic limit in AdS/CFT and the membrane paradigm," *Phys. Rev.* **D79** (2009) 025023, arXiv:0809.3808 [hep-th].

[73] E. I. Buchbinder and A. Buchel, "The Fate of the Sound and Diffusion in Holographic Magnetic Field," *Phys. Rev.* **D79** (2009) 046006, arXiv:0811.4325 [hep-th].

[74] P. Kovtun, D. T. Son, and A. O. Starinets, "Holography and hydrodynamics: Diffusion on stretched horizons," *JHEP* **10** (2003) 064, arXiv:hep-th/0309213 [hep-th].

[75] P. Kovtun, D. T. Son, and A. O. Starinets, "Viscosity in strongly interacting quantum field theories from black hole physics," *Phys. Rev. Lett.* **94** (2005) 111601, arXiv:hep-th/0405231 [hep-th].

[76] H. Song, S. A. Bass, U. Heinz, T. Hirano, and C. Shen, "200 A GeV Au+Au collisions serve a nearly perfect quark-gluon liquid," *Phys. Rev. Lett.* **106** (2011) 192301, arXiv:1011.2783 [nucl-th]. [Erratum: Phys. Rev. Lett.109,139904(2012)].

[77] M. Brigante, H. Liu, R. C. Myers, S. Shenker, and S. Yaida, "Viscosity Bound Violation in Higher Derivative Gravity," *Phys. Rev.* **D77** (2008) 126006, arXiv:0712.0805 [hep-th].

[78] S. A. Hartnoll, D. M. Ramirez, and J. E. Santos, "Entropy production, viscosity bounds and bumpy black holes," *JHEP* **03** (2016) 170, arXiv:1601.02757 [hep-th].

[79] R. A. Davison, B. Goutéraux, and S. A. Hartnoll, "Incoherent transport in clean quantum critical metals," *JHEP* **10** (2015) 112, arXiv:1507.07137 [hep-th].

[80] A. Rebhan and D. Steineder, "Violation of the Holographic Viscosity Bound in a Strongly Coupled Anisotropic Plasma," *Phys. Rev. Lett.* **108** (2012) 021601, arXiv:1110.6825 [hep-th].

[81] K. A. Mamo, "Holographic RG flow of the shear viscosity to entropy density ratio in strongly coupled anisotropic plasma," *JHEP* **10** (2012) 070, arXiv:1205.1797 [hep-th].

[82] M. Cadoni, E. Franzin, and M. Tuveri, "Hysteresis in η/s for QFTs dual to spherical black holes," *Eur. Phys. J.* **C77** no. 12, (2017) 900, arXiv:1703.05162 [hep-th].

[83] A. Almheiri and J. Polchinski, "Models of AdS_2 backreaction and holography," *JHEP* **11** (2015) 014, arXiv:1402.6334 [hep-th].

[84] M. Cadoni, M. Ciulu, and M. Tuveri, "Symmetries, Holography and Quantum Phase Transition in Two-dimensional Dilaton AdS Gravity," arXiv:1711.02459 [hep-th].

[85] A. D. Sakharov, "Vacuum quantum fluctuations in curved space and the theory of gravitation," *Sov. Phys. Dokl.* **12** (1968) 1040–1041. [Gen. Rel. Grav.32,365(2000)].

[86] T. Padmanabhan, "Emergent Gravity Paradigm: Recent Progress," *Mod. Phys. Lett.* **A30** no. 03n04, (2015) 1540007, arXiv:1410.6285 [gr-qc].

[87] E. P. Verlinde, "Emergent Gravity and the Dark Universe," arXiv:1611.02269 [hep-th].

[88] T. Padmanabhan, "Thermodynamical Aspects of Gravity: New insights," *Rept. Prog. Phys.* **73** (2010) 046901, arXiv:0911.5004 [gr-qc].

[89] T. Padmanabhan, "The Atoms Of Space, Gravity and the Cosmological Constant," *Int. J. Mod. Phys.* **D25** no. 07, (2016) 1630020, arXiv:1603.08658 [gr-qc].

[90] G. Dvali and C. Gomez, "Black Hole's Quantum N-Portrait," *Fortsch. Phys.* **61** (2013) 742–767, arXiv:1112.3359 [hep-th].

[91] G. Dvali and C. Gomez, "Quantum Compositeness of Gravity: Black Holes, AdS and Inflation," *JCAP* **1401** (2014) 023, arXiv:1312.4795 [hep-th].

[92] T. Jacobson, "Thermodynamics of space-time: The Einstein equation of state," *Phys. Rev. Lett.* **75** (1995) 1260–1263, arXiv:gr-qc/9504004 [gr-qc].

[93] S. Bhattacharyya, V. E. Hubeny, S. Minwalla, and M. Rangamani, "Nonlinear Fluid Dynamics from Gravity," *JHEP* **02** (2008) 045, arXiv:0712.2456 [hep-th].

[94] G. E. Volovik, "Superfluid analogies of cosmological phenomena," *Phys. Rept.* **351** (2001) 195–348, arXiv:gr-qc/0005091 [gr-qc].

[95] M. Van Raamsdonk, "Building up spacetime with quantum entanglement," *Gen. Rel. Grav.* **42** (2010) 2323–2329, arXiv:1005.3035 [hep-th]. [Int. J. Mod. Phys.D19,2429(2010)].

[96] T. Jacobson, "Entanglement Equilibrium and the Einstein Equation," *Phys. Rev. Lett.* **116** no. 20, (2016) 201101, arXiv:1505.04753 [gr-qc].

[97] G. Dvali and C. Gomez, "Black Hole's 1/N Hair," *Phys. Lett.* **B719** (2013) 419–423, arXiv:1203.6575 [hep-th].

[98] R. Casadio, A. Giugno, O. Micu, and A. Orlandi, "Thermal BEC black holes," *Entropy* **17** (2015) 6893–6924, arXiv:1511.01279 [gr-qc].

[99] R. Casadio, A. Giugno, and A. Giusti, "Corpuscular slow-roll inflation," arXiv:1708.09736 [gr-qc].

[100] L. Berezhiani, "On Corpuscular Theory of Inflation," *Eur. Phys. J.* **C77** no. 2, (2017) 106, arXiv:1610.08433 [hep-th].

[101] A. Almheiri, D. Marolf, J. Polchinski, and J. Sully, "Black Holes: Complementarity or Firewalls?," *JHEP* **02** (2013) 062, arXiv:1207.3123 [hep-th].

[102] J. Maldacena and L. Susskind, "Cool horizons for entangled black holes," *Fortsch. Phys.* **61** (2013) 781–811, arXiv:1306.0533 [hep-th].

[103] F. Zwicky, "Die Rotverschiebung von extragalaktischen Nebeln," *Helv. Phys. Acta* **6** (1933) 110–127. [Gen. Rel. Grav.41,207(2009)].

[104] S. M. Faber and J. S. Gallagher, "Masses and mass-to-light ratios of galaxies," *Ann. Rev. Astron. Astrophys.* **17** (1979) 135–183.

[105] J. de Swart, G. Bertone, and J. van Dongen, "How Dark Matter Came to Matter," arXiv:1703.00013 [astro-ph.CO]. [Nature Astron.1,0059(2017)].

[106] P. J. E. Peebles and B. Ratra, "The Cosmological constant and dark energy," *Rev. Mod. Phys.* **75** (2003) 559–606, arXiv:astro-ph/0207347 [astro-ph].

[107] **Supernova Search Team** Collaboration, A. G. Riess *et al.*, "Observational evidence from supernovae for an accelerating universe and a cosmological constant," *Astron. J.* **116** (1998) 1009–1038, arXiv:astro-ph/9805201 [astro-ph].

[108] A. A. Penzias and R. W. Wilson, "A Measurement of excess antenna temperature at 4080-Mc/s," *Astrophys. J.* **142** (1965) 419–421.

[109] **Planck** Collaboration, P. A. R. Ade *et al.*, "Planck 2013 results. XVI. Cosmological parameters," *Astron. Astrophys.* **571** (2014) A16, arXiv:1303.5076 [astro-ph.CO].

[110] A. A. Klypin, A. V. Kravtsov, O. Valenzuela, and F. Prada, "Where are the missing Galactic satellites?," *Astrophys. J.* **522** (1999) 82–92, arXiv:astro-ph/9901240 [astro-ph].

[111] B. Moore, S. Ghigna, F. Governato, G. Lake, T. R. Quinn, J. Stadel, and P. Tozzi, "Dark matter substructure within galactic halos," *Astrophys. J.* **524** (1999) L19–L22, arXiv:astro-ph/9907411 [astro-ph].

[112] W. J. G. de Blok, "The Core-Cusp Problem," *Adv. Astron.* **2010** (2010) 789293, arXiv:0910.3538 [astro-ph.CO].

[113] M. Boylan-Kolchin, J. S. Bullock, and M. Kaplinghat, "Too big to fail? The puzzling darkness of massive Milky Way subhaloes," *Mon. Not. Roy. Astron. Soc.* **415** (2011) L40, arXiv:1103.0007 [astro-ph.CO].

[114] M. Boylan-Kolchin, J. S. Bullock, and M. Kaplinghat, "The Milky Way's bright satellites as an apparent failure of LCDM," *Mon. Not. Roy. Astron. Soc.* **422** (2012) 1203–1218, arXiv:1111.2048 [astro-ph.CO].

[115] R. B. Tully and J. R. Fisher, "A New method of determining distances to galaxies," *Astron. Astrophys.* **54** (1977) 661–673.

[116] S. S. McGaugh, J. M. Schombert, G. D. Bothun, and W. J. G. de Blok, "The Baryonic Tully-Fisher relation," *Astrophys. J.* **533** (2000) L99–L102, arXiv:astro-ph/0003001 [astro-ph].

[117] S. McGaugh, "The Baryonic Tully-Fisher Relation of Gas Rich Galaxies as a Test of LCDM and MOND," *Astron. J.* **143** (2012) 40, arXiv:1107.2934 [astro-ph.CO].

[118] S. Nojiri, S. D. Odintsov, and V. K. Oikonomou, "Modified Gravity Theories on a Nutshell: Inflation, Bounce and Late-time Evolution," *Phys. Rept.* **692** (2017) 1–104, arXiv:1705.11098 [gr-qc].

[119] G. R. Dvali, G. Gabadadze, and M. Porrati, "4-D gravity on a brane in 5-D Minkowski space," *Phys. Lett.* **B485** (2000) 208–214, arXiv:hep-th/0005016 [hep-th].

[120] M. Milgrom, "A Modification of the Newtonian dynamics as a possible alternative to the hidden mass hypothesis," *Astrophys. J.* **270** (1983) 365–370.

[121] M. Milgrom, "MOND theory," *Can. J. Phys.* **93** no. 2, (2015) 107–118, arXiv:1404.7661 [astro-ph.CO].

[122] S. McGaugh, "Milky Way Mass Models and MOND," *Astrophys. J.* **683** (2008) 137–148, arXiv:0804.1314 [astro-ph].

[123] R. H. Sanders, "Resolving the virial discrepancy in clusters of galaxies with modified newtonian dynamics," *Astrophys. J.* **512** (1999) L23, arXiv:astro-ph/9807023 [astro-ph].

[124] M. Milgrom and R. H. Sanders, "Perspective on MOND emergence from Verlinde's "emergent gravity" and its recent test by weak lensing," arXiv:1612.09582 [astro-ph.GA].

[125] D.-C. Dai and D. Stojkovic, "Inconsistencies in Verlinde's emergent gravity," *JHEP* **11** (2017) 007, arXiv:1710.00946 [gr-qc].

[126] S. Hossenfelder, "Covariant version of Verlinde's emergent gravity," *Phys. Rev.* **D95** no. 12, (2017) 124018, arXiv:1703.01415 [gr-qc].

[127] T. Harko and F. S. N. Lobo, "Could pressureless dark matter have pressure?," *Astropart. Phys.* **35** (2012) 547–551, arXiv:1104.2674 [gr-qc].

[128] T. Harko and F. S. N. Lobo, "Two-fluid dark matter models," *Phys. Rev.* **D83** (2011) 124051, arXiv:1106.2642 [gr-qc].

[129] S. Bharadwaj and S. Kar, "Modeling galaxy halos using dark matter with pressure," *Phys. Rev.* **D68** (2003) 023516, arXiv:astro-ph/0304504 [astro-ph].

[130] T. Faber and M. Visser, "Combining rotation curves and gravitational lensing: How to measure the equation of state of dark matter in the galactic halo," *Mon. Not. Roy. Astron. Soc.* **372** (2006) 136–142, arXiv:astro-ph/0512213 [astro-ph].

[131] K.-Y. Su and P. Chen, "Comments on 'Modeling Galaxy Halos Using Dark Matter with Pressure'," *Phys. Rev.* **D79** (2009) 128301, arXiv:0905.2084 [astro-ph.CO].

[132] H. Zhao, "An Uneven Vacuum Energy Fluid as Λ, Dark Matter, MOND and Lens," *Mod. Phys. Lett.* **A23** (2008) 555–568, arXiv:0802.1775 [astro-ph].

[133] G. Dvali and C. Gomez, "Self-Completeness of Einstein Gravity," arXiv:1005.3497 [hep-th].

[134] G. Dvali, S. Folkerts, and C. Germani, "Physics of Trans-Planckian Gravity," *Phys. Rev.* **D84** (2011) 024039, arXiv:1006.0984 [hep-th].

[135] G. Dvali, G. F. Giudice, C. Gomez, and A. Kehagias, "UV-Completion by Classicalization," *JHEP* **08** (2011) 108, arXiv:1010.1415 [hep-ph].

[136] G. Dvali, C. Gomez, and A. Kehagias, "Classicalization of Gravitons and Goldstones," *JHEP* **11** (2011) 070, arXiv:1103.5963 [hep-th].

[137] G. Dvali and C. Gomez, "Black Holes as Critical Point of Quantum Phase Transition," *Eur. Phys. J.* **C74** (2014) 2752, arXiv:1207.4059 [hep-th].

[138] M. J. Rees, "Astrophysical evidence for black holes," in *Symposium on Black Holes and Relativistic Stars (dedicated to memory of S. Chandrasekhar) Chicago, Illinois, December 14-15, 1996*. 1997. arXiv:astro-ph/9701161 [astro-ph].

[139] S. W. Hawking, "Information loss in black holes," *Phys. Rev.* **D72** (2005) 084013, arXiv:hep-th/0507171 [hep-th].

[140] C. Bambi, "Astrophysical Black Holes: A Compact Pedagogical Review," *Annalen Phys.* **530** (2018) 1700430, arXiv:1711.10256 [gr-qc].

[141] J. D. Bekenstein, "Quantum black holes as atoms," in *Recent developments in theoretical and experimental general relativity, gravitation, and relativistic field theories. Proceedings, 8th Marcel Grossmann meeting, MG8, Jerusalem, Israel, June 22-27, 1997. Pts. A, B*, pp. 92–111. 1997. arXiv:gr-qc/9710076 [gr-qc].

[142] K. Schwarzschild, "Über das Gravitationsfeld eines Massenpunktes nach der Einsteinschen Theorie," *Sitzungsberichte der Königlich Preußischen Akademie der Wissenschaften (Berlin)* (1916) 189–196.

[143] R. P. Kerr, "Gravitational field of a spinning mass as an example of algebraically special metrics," *Phys. Rev. Lett.* **11** (1963) 237–238.

[144] H. Reissner, "Über die Eigengravitation des elektrischen Feldes nach der Einsteinschen Theorie," *Ann. Phys.* **355** (1916) 106.

[145] G. Nordström, "On the Energy of the Gravitational Field in Einstein's Theory," *Verhandl. Koninkl. Ned. Akad. Wetenschap., Afdel. Natuurk., Amsterdam* **26** (1918) 1201.

[146] E. T. Newman, R. Couch, K. Chinnapared, A. Exton, A. Prakash, and R. Torrence, "Metric of a Rotating, Charged Mass," *J. Math. Phys* **6** (1965) 918.

[147] J. D. Bekenstein, "Black hole hair: 25 - years after," in *Physics. Proceedings, 2nd International A.D. Sakharov Conference, Moscow, Russia, May 20-24, 1996*, pp. 216–219. 1996. arXiv:gr-qc/9605059 [gr-qc].

[148] T. Johannsen, "Testing the No-Hair Theorem with Observations of Black Holes in the Electromagnetic Spectrum," *Class. Quant. Grav.* **33** no. 12, (2016) 124001, arXiv:1602.07694 [astro-ph.HE].

[149] S. Carlip, "Black Hole Thermodynamics," *Int. J. Mod. Phys.* **D23** (2014) 1430023, arXiv:1410.1486 [gr-qc].

[150] R. Emparan and H. S. Reall, "Black Holes in Higher Dimensions," *Living Rev. Rel.* **11** (2008) 6, arXiv:0801.3471 [hep-th].

[151] D. Birmingham, "Topological black holes in Anti-de Sitter space," *Class. Quantum Grav.* **16** (1999) 1197, arXiv:hep-th/9808032 [hep-th].

[152] D. Lovelock, "The Einstein tensor and its generalizations," *J. Math. Phys.* **12** (1971) 498–501.

[153] R.-G. Cai, "A Note on thermodynamics of black holes in Lovelock gravity," *Phys. Lett.* **B582** (2004) 237–242, arXiv:hep-th/0311240 [hep-th].

[154] A. Castro, N. Dehmami, G. Giribet, and D. Kastor, "On the Universality of Inner Black Hole Mechanics and Higher Curvature Gravity," *JHEP* **07** (2013) 164, arXiv:1304.1696 [hep-th].

[155] X. O. Camanho and J. D. Edelstein, "A Lovelock black hole bestiary," *Class. Quant. Grav.* **30** (2013) 035009, arXiv:1103.3669 [hep-th].

[156] T. Takahashi and J. Soda, "Pathologies in Lovelock AdS Black Branes and AdS/CFT," *Class. Quant. Grav.* **29** (2012) 035008, arXiv:1108.5041 [hep-th].

[157] R. C. Myers and J. Z. Simon, "Black Hole Thermodynamics in Lovelock Gravity," *Phys. Rev.* **D38** (1988) 2434–2444.

[158] V. Iyer and R. M. Wald, "Some properties of Noether charge and a proposal for dynamical black hole entropy," *Phys. Rev.* **D50** (1994) 846–864, arXiv:gr-qc/9403028 [gr-qc].

[159] E. Caceres, M. Sanchez, and J. Virrueta, "Holographic Entanglement Entropy in Time Dependent Gauss-Bonnet Gravity," *JHEP* **09** (2017) 127, arXiv:1512.05666 [hep-th].

[160] X. O. Camanho, J. D. Edelstein, G. Giribet, and A. Gomberoff, "Generalized phase transitions in Lovelock gravity," *Phys. Rev.* **D90** no. 6, (2014) 064028, arXiv:1311.6768 [hep-th].

[161] A. M. Frassino, D. Kubiznak, R. B. Mann, and F. Simovic, "Multiple Reentrant Phase Transitions and Triple Points in Lovelock Thermodynamics," *JHEP* **09** (2014) 080, arXiv:1406.7015 [hep-th].

[162] B. P. Dolan, A. Kostouki, D. Kubiznak, and R. B. Mann, "Isolated critical point from Lovelock gravity," *Class. Quant. Grav.* **31** no. 24, (2014) 242001, arXiv:1407.4783 [hep-th].

[163] R.-G. Cai, "Gauss-Bonnet black holes in AdS spaces," *Phys. Rev.* **D65** (2002) 084014, arXiv:hep-th/0109133 [hep-th].

[164] R. Jackiw, "Two lectures on two-dimensional gravity," in *2nd Latin American School on Theoretical Physics: Strings and Fundamentals (LASSF II) Caracas, Venezuela, October 23-27, 1995*. 1995. arXiv:gr-qc/9511048 [gr-qc].

[165] E. Witten, "Two-dimensional gravity and intersection theory on moduli space," *Surveys Diff. Geom.* **1** (1991) 243–310.

[166] D. Grumiller, W. Kummer, and D. V. Vassilevich, "Dilaton gravity in two-dimensions," *Phys. Rept.* **369** (2002) 327–430, arXiv:hep-th/0204253 [hep-th].

[167] R. Jackiw, "Lower Dimensional Gravity," *Nucl. Phys.* **B252** (1985) 343–356.

[168] S. Carlip, "Spontaneous Dimensional Reduction?," *AIP Conf. Proc.* **1483** (2012) 63–72, arXiv:1207.4503 [gr-qc].

[169] M. Cadoni and S. Mignemi, "Asymptotic symmetries of AdS(2) and conformal group in d = 1," *Nucl. Phys.* **B557** (1999) 165–180, arXiv:hep-th/9902040 [hep-th].

[170] M. Cadoni, P. Carta, D. Klemm, and S. Mignemi, "AdS(2) gravity as conformally invariant mechanical system," *Phys. Rev.* **D63** (2001) 125021, arXiv:hep-th/0009185 [hep-th].

[171] D. G. Boulware and S. Deser, "String Generated Gravity Models," *Phys. Rev. Lett.* **55** (1985) 2656.

[172] J. T. Wheeler, "Symmetric Solutions to the Maximally Gauss-Bonnet Extended Einstein Equations," *Nucl. Phys.* **B273** (1986) 732–748.

[173] J. T. Wheeler, "Symmetric Solutions to the Gauss-Bonnet Extended Einstein Equations," *Nucl. Phys.* **B268** (1986) 737–746.

[174] T. Jacobson and R. C. Myers, "Black hole entropy and higher curvature interactions," *Phys. Rev. Lett.* **70** (1993) 3684–3687, arXiv:hep-th/9305016 [hep-th].

[175] X.-H. Ge and S.-J. Sin, "Shear viscosity, instability and the upper bound of the Gauss-Bonnet coupling constant," *JHEP* **05** (2009) 051, arXiv:0903.2527 [hep-th].

[176] D. Kastor, S. Ray, and J. Traschen, "Mass and Free Energy of Lovelock Black Holes," *Class. Quant. Grav.* **28** (2011) 195022, arXiv:1106.2764 [hep-th].

[177] E. B. Bogomolny, "Stability of Classical Solutions," *Sov. J. Nucl. Phys.* **24** (1976) 449. [Yad. Fiz.24,861(1976)].

[178] M. K. Prasad and C. M. Sommerfield, "An Exact Classical Solution for the 't Hooft Monopole and the Julia-Zee Dyon," *Phys. Rev. Lett.* **35** (1975) 760–762.

[179] J. M. Maldacena, J. Michelson, and A. Strominger, "Anti-de Sitter fragmentation," *JHEP* **02** (1999) 011, arXiv:hep-th/9812073 [hep-th].

[180] M. Cadoni and C. N. Colacino, "Thermodynamical behavior of composite stringy black holes," *Nucl. Phys.* **B590** (2000) 252–260, arXiv:hep-th/0004037 [hep-th].

[181] S. M. Carroll, M. C. Johnson, and L. Randall, "Extremal limits and black hole entropy," *JHEP* **11** (2009) 109, arXiv:0901.0931 [hep-th].

[182] X.-H. Ge, Y. Matsuo, F.-W. Shu, S.-J. Sin, and T. Tsukioka, "Viscosity Bound, Causality Violation and Instability with Stringy Correction and Charge," *JHEP* **10** (2008) 009, arXiv:0808.2354 [hep-th].

[183] M. Cadoni, A. M. Frassino, and M. Tuveri, "On the universality of thermodynamics and η/s ratio for the charged Lovelock black branes," *J. High Energy Phys.* **05** (2016) 101, arXiv:1602.05593 [hep-th].

[184] A. Chamblin, R. Emparan, C. V. Johnson, and R. C. Myers, "Charged AdS black holes and catastrophic holography," *Phys. Rev.* **D60** (1999) 064018, arXiv:hep-th/9902170 [hep-th].

[185] A. Chamblin, R. Emparan, C. V. Johnson, and R. C. Myers, "Holography, thermodynamics and fluctuations of charged AdS black holes," *Phys. Rev.* **D60** (1999) 104026, arXiv:hep-th/9904197 [hep-th].

[186] D. Kubizňák and R. B. Mann, "P-V criticality of charged AdS black holes," *J. High Energy Phys.* **07** (2012) 033, arXiv:1205.0559 [hep-th].

[187] D. Kubizňák, R. B. Mann, and M. Teo, "Black hole chemistry: thermodynamics with Lambda," *Class. Quantum Grav.* **34** (2017) 063001, arXiv:1608.06147 [hep-th].

[188] S. H. Hendi, R. B. Mann, S. Panahiyan, and B. Eslam Panah, "van der Waals like behavior of topological AdS black holes in massive gravity," *Phys. Rev.* **D95** (2017) 021501, arXiv:1702.00432 [gr-qc].

[189] M. Cadoni, E. Franzin, and M. Tuveri, "Van der Waals-like Behaviour of Charged Black Holes and Hysteresis in the Dual QFTs," *Phys. Lett.* **B768** (2017) 393, arXiv:1702.08341 [hep-th].

[190] S. W. Hawking and D. N. Page, "Thermodynamics of Black Holes in anti-De Sitter Space," *Commun. Math. Phys.* **87** (1983) 577.

[191] R. A. Konoplya and A. Zhidenko, "Eikonal instability of Gauss-Bonnet–(anti-)–de Sitter black holes," *Phys. Rev.* **D95** no. 10, (2017) 104005, arXiv:1701.01652 [hep-th].

[192] Y. M. Cho and I. P. Neupane, "Anti-de Sitter black holes, thermal phase transition and holography in higher curvature gravity," *Phys. Rev.* **D66** (2002) 024044, arXiv:hep-th/0202140 [hep-th].

[193] C. Hu, X. Zeng, and X. Liu, "Phase transition and critical phenomenon of AdS black holes in Einstein-Gauss-Bonnet gravity," *Sci. China Phys. Mech. Astron.* **56** (2013) 1652.

[194] S. He, L.-F. Li, and X.-X. Zeng, "Holographic Van der Waals-like phase transition in the Gauss-Bonnet gravity," *Nucl. Phys.* **B915** (2017) 243, arXiv:1608.04208 [hep-th].

[195] M. Cvetič, S. Nojiri, and S. D. Odintsov, "Black hole thermodynamics and negative entropy in de Sitter and anti-de Sitter Einstein-Gauss-Bonnet gravity," *Nucl. Phys.* **B628** (2002) 295, arXiv:hep-th/0112045 [hep-th].

[196] A. Strominger, "Les Houches lectures on black holes," in *NATO Advanced Study Institute: Les Houches Summer School, Session 62: Fluctuating Geometries in Statistical Mechanics and Field Theory Les Houches, France, August 2-September 9, 1994*. 1994. arXiv:hep-th/9501071 [hep-th].

[197] C. G. Callan, Jr., S. B. Giddings, J. A. Harvey, and A. Strominger, "Evanescent black holes," *Phys. Rev.* **D45** no. 4, (1992) R1005, arXiv:hep-th/9111056 [hep-th].

[198] M. Caldarelli, G. Catelani, and L. Vanzo, "Action, Hamiltonian and CFT for 2-D black holes," *JHEP* **10** (2000) 005, arXiv:hep-th/0008058 [hep-th].

[199] A. Almheiri and B. Kang, "Conformal Symmetry Breaking and Thermodynamics of Near-Extremal Black Holes," *JHEP* **10** (2016) 052, arXiv:1606.04108 [hep-th].

[200] J. Preskill, P. Schwarz, A. D. Shapere, S. Trivedi, and F. Wilczek, "Limitations on the statistical description of black holes," *Mod. Phys. Lett.* **A6** (1991) 2353–2362.

[201] M. Cadoni and S. Mignemi, "Symmetry breaking, central charges and the AdS(2) / CFT(1) correspondence," *Phys. Lett.* **B490** (2000) 131–135, arXiv:hep-th/0002256 [hep-th].

[202] J. Maldacena, D. Stanford, and Z. Yang, "Conformal symmetry and its breaking in two dimensional Nearly Anti-de-Sitter space," *PTEP* **2016** no. 12, (2016) 12C104, arXiv:1606.01857 [hep-th].

[203] L. F. Abbott and S. Deser, "Stability of Gravity with a Cosmological Constant," *Nucl. Phys.* **B195** (1982) 76–96.

[204] A. Achucarro and M. E. Ortiz, "Relating black holes in two-dimensions and three-dimensions," *Phys. Rev.* **D48** (1993) 3600–3605, arXiv:hep-th/9304068 [hep-th].

[205] M. Cadoni and S. Mignemi, "Nonsingular four-dimensional black holes and the Jackiw-Teitelboim theory," *Phys. Rev.* **D51** (1995) 4319, arXiv:hep-th/9410041 [hep-th].

[206] R. B. Mann, "Conservation laws and 2-D black holes in dilaton gravity," *Phys. Rev.* **D47** (1993) 4438–4442, arXiv:hep-th/9206044 [hep-th].

[207] M. Cadoni, "Conformal equivalence of 2-D dilaton gravity models," *Phys. Lett.* **B395** (1997) 10–15, arXiv:hep-th/9610201 [hep-th].

[208] J. Gegenberg, G. Kunstatter, and D. Louis-Martinez, "Classical and quantum mechanics of black holes in generic 2-d dilaton gravity," in *Heat Kernels and Quantum Gravity Winnipeg, Canada, August 2-6, 1994*. 1995. arXiv:gr-qc/9501017 [gr-qc].

[209] S. Ferrara and R. Kallosh, "Supersymmetry and attractors," *Phys. Rev.* **D54** (1996) 1514–1524, arXiv:hep-th/9602136 [hep-th].

[210] S. Ferrara, R. Kallosh, and A. Strominger, "N=2 extremal black holes," *Phys. Rev.* **D52** (1995) R5412–R5416, arXiv:hep-th/9508072 [hep-th].

[211] S. Ferrara and R. Kallosh, "Universality of supersymmetric attractors," *Phys. Rev.* **D54** (1996) 1525–1534, arXiv:hep-th/9603090 [hep-th].

[212] D. Astefanesei, N. Banerjee, and S. Dutta, "(Un)attractor black holes in higher derivative AdS gravity," *JHEP* **11** (2008) 070, arXiv:0806.1334 [hep-th].

[213] S. S. Gubser, I. R. Klebanov, and A. M. Polyakov, "Gauge theory correlators from noncritical string theory," *Phys. Lett.* **B428** (1998) 105, arXiv:hep-th/9802109 [hep-th].

[214] E. Witten, "Anti-de Sitter space and holography," *Adv. Theor. Math. Phys.* **2** (1998) 253, arXiv:hep-th/9802150 [hep-th].

[215] D. T. Son and A. O. Starinets, "Viscosity, Black Holes, and Quantum Field Theory," *Ann. Rev. Nucl. Part. Sci.* **57** (2007) 95, arXiv:0704.0240 [hep-th].

[216] V. E. Hubeny, "The AdS/CFT Correspondence," *Class. Quant. Grav.* **32** no. 12, (2015) 124010, arXiv:1501.00007 [gr-qc].

[217] L. Susskind and E. Witten, "The Holographic bound in anti-de Sitter space," arXiv:hep-th/9805114 [hep-th].

[218] J. McGreevy, "Holographic duality with a view toward many-body physics," *Adv. High Energy Phys.* **2010** (2010) 723105, arXiv:0909.0518 [hep-th].

[219] P. Kovtun and A. Ritz, "Black holes and universality classes of critical points," *Phys. Rev. Lett.* **100** (2008) 171606, arXiv:0801.2785 [hep-th].

[220] S. A. Hartnoll, "Quantum Critical Dynamics from Black Holes," arXiv:0909.3553 [cond-mat.str-el].

[221] N. Banerjee and S. Dutta, "Holographic Hydrodynamics: Models and Methods," arXiv:1112.5345 [hep-th].

[222] M. Tuveri, L. Fatibene, and M. Ferraris, "The emergent gravity's entropy Ansatz from an augmented variational principle," *J. Phys. Conf. Ser.* **841** no. 1, (2017) 012038.

[223] R. Baier, P. Romatschke, D. T. Son, A. O. Starinets, and M. A. Stephanov, "Relativistic viscous hydrodynamics, conformal invariance, and holography," *J. High Energy Phys.* **04** (2008) 100, arXiv:0712.2451 [hep-th].

[224] P. Kovtun, "Lectures on hydrodynamic fluctuations in relativistic theories," *J. Phys.* **A45** (2012) 473001, arXiv:1205.5040 [hep-th].

[225] P. Romatschke, "Relativistic Viscous Fluid Dynamics and Non-Equilibrium Entropy," *Class. Quantum Grav.* **27** (2010) 025006, arXiv:0906.4787 [hep-th].

[226] M. Crossley, P. Glorioso, and H. Liu, "Effective field theory of dissipative fluids," *JHEP* **09** (2017) 095, arXiv:1511.03646 [hep-th].

[227] O. M. Pimentel, G. A. González, and F. D. Lora-Clavijo, "The Energy-Momentum Tensor for a Dissipative Fluid in General Relativity," *Gen. Rel. Grav.* **48** no. 10, (2016) 124, arXiv:1604.01318 [gr-qc].

[228] G. Policastro, D. T. Son, and A. O. Starinets, "From AdS/CFT correspondence to hydrodynamics," *J. High Energy Phys.* **09** (2002) 043, arXiv:hep-th/0205052 [hep-th].

[229] I. P. Neupane and N. Dadhich, "Entropy Bound and Causality Violation in Higher Curvature Gravity," *Class. Quantum Grav.* **26** (2009) 015013, arXiv:0808.1919 [hep-th].

[230] H. Kodama and A. Ishibashi, "A master equation for gravitational perturbations of maximally symmetric black holes in higher dimensions," *Prog. Theor. Phys.* **110** (2003) 701, arXiv:hep-th/0305147 [hep-th].

[231] A. Ishibashi and H. Kodama, "Stability of higher dimensional Schwarzschild black holes," *Prog. Theor. Phys.* **110** (2003) 901, arXiv:hep-th/0305185 [hep-th].

[232] G. Gibbons and S. A. Hartnoll, "A gravitational instability in higher dimensions," *Phys. Rev.* **D66** (2002) 064024, arXiv:hep-th/0206202 [hep-th].

[233] M. A. Rubin and C. R. Ordóñez, "Eigenvalues and Degeneracies for n-dimensional tensor spherical harmonics," *J. Math. Phys.* **25** (1984) 2888.

[234] M. A. Rubin and C. R. Ordóñez, "Symmetric Tensor Eigen Spectrum of the Laplacian on n Spheres," *J. Math. Phys.* **26** (1985) 65.

[235] A. Higuchi, "Symmetric Tensor Spherical Harmonics on the N Sphere and Their Application to the de Sitter Group SO(N,1)," *J. Math. Phys.* **28** (1987) 1553. (Erratum: ibid. **43**, 6385 (2002)).

[236] S. Cremonini, "The Shear Viscosity to Entropy Ratio: A Status Report," *Mod. Phys. Lett.* **B25** (2011) 1867–1888, arXiv:1108.0677 [hep-th].

[237] M. Brigante, H. Liu, R. C. Myers, S. Shenker, and S. Yaida, "The Viscosity Bound and Causality Violation," *Phys. Rev. Lett.* **100** (2008) 191601, arXiv:0802.3318 [hep-th].

[238] R.-G. Cai, Z.-Y. Nie, and Y.-W. Sun, "Shear Viscosity from Effective Couplings of Gravitons," *Phys. Rev.* **D78** (2008) 126007, arXiv:0811.1665 [hep-th].

[239] R.-G. Cai, Z.-Y. Nie, N. Ohta, and Y.-W. Sun, "Shear Viscosity from Gauss-Bonnet Gravity with a Dilaton Coupling," *Phys. Rev.* **D79** (2009) 066004, arXiv:0901.1421 [hep-th].

[240] D. Astefanesei, N. Banerjee, and S. Dutta, "Moduli and electromagnetic black brane holography," *JHEP* **02** (2011) 021, arXiv:1008.3852 [hep-th].

[241] X.-H. Ge, S.-J. Sin, S.-F. Wu, and G.-H. Yang, "Shear viscosity and instability from third order Lovelock gravity," *Phys. Rev.* **D80** (2009) 104019, arXiv:0905.2675 [hep-th].

[242] X. O. Camanho, J. D. Edelstein, and M. F. Paulos, "Lovelock theories, holography and the fate of the viscosity bound," *J. High Energy Phys.* **05** (2011) 127, arXiv:1010.1682 [hep-th].

[243] T. Jacobson, A. Mohd, and S. Sarkar, "Membrane paradigm for Einstein-Gauss-Bonnet gravity," *Phys. Rev.* **D95** (2011) 064036, arXiv:1107.1260 [gr-qc].

[244] A. Bhattacharyya and D. Roychowdhury, "Viscosity bound for anisotropic superfluids in higher derivative gravity," *J. High Energy Phys.* **03** (2015) 063, arXiv:1410.3222 [hep-th].

[245] M. Sadeghi and S. Parvizi, "Hydrodynamics of a black brane in Gauss-Bonnet massive gravity," *Class. Quantum Grav.* **33** (2016) 035005, arXiv:1507.07183 [hep-th].

[246] Y.-L. Wang and X.-H. Ge, "Shear Viscosity to Entropy Density Ratio in Higher Derivative Gravity with Momentum Dissipation," *Phys. Rev.* **D94** no. 6, (2016) 066007, arXiv:1605.07248 [hep-th].

[247] J. Erdmenger, P. Kerner, and H. Zeller, "Non-universal shear viscosity from Einstein gravity," *Phys. Lett.* **B699** (2011) 301, arXiv:1011.5912 [hep-th].

[248] J. Erdmenger, P. Kerner, and H. Zeller, "Transport in Anisotropic Superfluids: A Holographic Description," *J. High Energy Phys.* **01** (2012) 059, arXiv:1110.0007 [hep-th].

[249] P. Burikham and N. Poovuttikul, "Shear viscosity in holography and effective theory of transport without translational symmetry," *Phys. Rev.* **D94** (2016) 106001, arXiv:1601.04624 [hep-th].

[250] L. Alberte, M. Baggioli, and O. Pujolas, "Viscosity bound violation in holographic solids and the viscoelastic response," *J. High Energy Phys.* **07** (2016) 074, arXiv:1601.03384 [hep-th].

[251] H.-S. Liu, H. Lu, and C. N. Pope, "Magnetically-Charged Black Branes and Viscosity/Entropy Ratios," *J. High Energy Phys.* **12** (2016) 097, arXiv:1602.07712 [hep-th].

[252] A. Buchel and R. C. Myers, "Causality of Holographic Hydrodynamics," *JHEP* **08** (2009) 016, arXiv:0906.2922 [hep-th].

[253] D. M. Hofman, "Higher Derivative Gravity, Causality and Positivity of Energy in a UV complete QFT," *Nucl. Phys.* **B823** (2009) 174–194, arXiv:0907.1625 [hep-th].

[254] S. Cremonini, U. Gürsoy, and P. Szepietowski, "On the Temperature Dependence of the Shear Viscosity and Holography," *J. High Energy Phys.* **08** (2012) 167, arXiv:1206.3581 [hep-th].

[255] S. Cremonini and P. Szepietowski, "Generating Temperature Flow for eta/s with Higher Derivatives: From Lifshitz to AdS," *J. High Energy Phys.* **02** (2012) 038, arXiv:1111.5623 [hep-th].

[256] S. Jain, N. Kundu, K. Sen, A. Sinha, and S. P. Trivedi, "A Strongly Coupled Anisotropic Fluid From Dilaton Driven Holography," *JHEP* **01** (2015) 005, arXiv:1406.4874 [hep-th].

[257] S. Jain, R. Samanta, and S. P. Trivedi, "The Shear Viscosity in Anisotropic Phases," *JHEP* **10** (2015) 028, arXiv:1506.01899 [hep-th].

[258] M. Cadoni and P. Carta, "The AdS / CFT correspondence in two-dimensions," *Mod. Phys. Lett.* **A16** (2001) 171–178, arXiv:hep-th/0102064 [hep-th].

[259] P. H. Ginsparg and G. W. Moore, "Lectures on 2-D gravity and 2-D string theory," in *Proceedings, Theoretical Advanced Study Institute (TASI 92): From Black Holes and Strings to Particles: Boulder, USA, June 1-26, 1992*, pp. 277–469. 1993. arXiv:hep-th/9304011 [hep-th]. https://inspirehep.net/record/36050/files/arXiv:hep-th_9304011.pdf. [,277(1993)].

[260] S. Cacciatori, D. Klemm, and D. Zanon, "W(infinity) algebras, conformal mechanics, and black holes," *Class. Quant. Grav.* **17** (2000) 1731–1748, arXiv:hep-th/9910065 [hep-th].

[261] A. Strominger, "AdS(2) quantum gravity and string theory," *JHEP* **01** (1999) 007, arXiv:hep-th/9809027 [hep-th].

[262] G. W. Gibbons and P. K. Townsend, "Black holes and Calogero models," *Phys. Lett.* **B454** (1999) 187–192, arXiv:hep-th/9812034 [hep-th].

[263] S. Carlip, "Challenges for Emergent Gravity," *Stud. Hist. Phil. Sci.* **B46** (2014) 200–208, arXiv:1207.2504 [gr-qc].

[264] T. Faulkner, H. Liu, J. McGreevy, and D. Vegh, "Emergent quantum criticality, Fermi surfaces, and AdS(2)," *Phys. Rev.* **D83** (2011) 125002, arXiv:0907.2694 [hep-th].

[265] A. Lucas, "Conductivity of a strange metal: from holography to memory functions," *JHEP* **03** (2015) 071, arXiv:1501.05656 [hep-th].

[266] G. Dotti and R. J. Gleiser, "Gravitational instability of Einstein-Gauss-Bonnet black holes under tensor mode perturbations," *Class. Quantum Grav.* **22** (2005) L1, arXiv:gr-qc/0409005 [gr-qc].

[267] G. Dotti and R. J. Gleiser, "Linear stability of Einstein-Gauss-Bonnet static spacetimes. Part I. Tensor perturbations," *Phys. Rev.* **D72** (2005) 044018, arXiv:gr-qc/0503117 [gr-qc].

[268] D. R. Knittel, S. P. Pack, S. H. Lin, and L. Eyring, "A thermodynamic model of hysteresis in phase transitions and its application to rare earth oxide systems," *J. Chem. Phys.* **67** (1977) 134.

[269] G. Bertotti, *Hysteresis in Magnetism: For Physicists, Materials Scientists, and Engineers*. Academic Press, San Diego, CA, USA, 1998.

[270] C. T. Nguyen, F. Desgranges, N. Galanis, G. Roy, T. Maré, S. Boucher, and H. Angue Mintsa, "Viscosity data for Al_2O_3-water nanofluid-hysteresis: is heat transfer enhancement using nanofluids reliable?," *Int. J. Therm. Sci.* **47** (2008) 103.

[271] M. Cvetič and I. Papadimitriou, "AdS_2 holographic dictionary," *JHEP* **12** (2016) 008, arXiv:1608.07018 [hep-th]. [Erratum: JHEP01,120(2017)].

[272] M. Cadoni and M. Cavaglia, "Open strings, 2-D gravity and AdS / CFT correspondence," *Phys. Rev.* **D63** (2001) 084024, arXiv:hep-th/0008084 [hep-th].

[273] M. Cadoni and P. Carta, "2-D black holes, conformal vacua and CFTs on the cylinder," *Phys. Lett.* **B522** (2001) 126–132, arXiv:hep-th/0107234 [hep-th].

[274] M. Cadoni, R. Casadio, A. Giusti, W. Mueck, and M. Tuveri, "Effective Fluid Description of the Dark Universe," *Phys. Lett.* **B776** (2018) 242–248, arXiv:1707.09945 [gr-qc].

[275] M. Cadoni, R. Casadio, A. Giusti, and M. Tuveri, "Emergence of a Dark Force in Corpuscular Gravity," *Phys. Rev.* **D97** (2018) 044047, arXiv:1801.10374 [gr-qc].

[276] E. Franzin, M. Cadoni, and M. Tuveri, "Sine-Gordon solitonic scalar stars and black holes," *Phys. Rev.* **D97** no. 12, (2018) 124018, arXiv:1805.08976 [gr-qc].

[277] R. Nandkishore and D. A. Huse, "Many-Body Localization and Thermalization in Quantum Statistical Mechanics," *Annu. Rev. Condens. Matter Phys.* **6** (2015) 15–38.

[278] D. A. Huse, R. Nandkishore, V. Oganesyan, A. Pal, and S. L. Sondhi, "Localization-protected quantum order," *Phys. Rev. B* **88** (2013) 014206.

[279] T. Grover, "Certain General Constraints on the Many-Body Localization Transition," arXiv:1405.1471 [cond-mat.dis-nn].

[280] P. Binetruy, "Vacuum energy, holography and a quantum portrait of the visible Universe," arXiv:1208.4645 [gr-qc].

[281] A. Giugno and A. Giusti, "Domestic Corpuscular Inflaton," arXiv:1806.11168 [gr-qc].

[282] S. M. Carroll and A. Chatwin-Davies, "Cosmic Equilibration: A Holographic No-Hair Theorem from the Generalized Second Law," arXiv:1703.09241 [hep-th].

[283] R. Casadio, A. Giugno, and A. Giusti, "Matter and gravitons in the gravitational collapse," *Phys. Lett.* **B763** (2016) 337–340, arXiv:1606.04744 [hep-th].

[284] R. Casadio, A. Giugno, A. Giusti, and M. Lenzi, "Quantum corpuscular corrections to the Newtonian potential," *Phys. Rev.* **D96** no. 4, (2017) 044010, arXiv:1702.05918 [gr-qc].

[285] G. E. Volovik, "Vacuum energy and cosmological constant: View from condensed matter," 2001. arXiv:gr-qc/0101111 [gr-qc].

[286] G. E. Volovik, "The Universe in a helium droplet," *Int. Ser. Monogr. Phys.* **117** (2006) 1–526.

[287] G. E. Volovik, "Cosmological constant and vacuum energy," *Annalen Phys.* **14** (2005) 165–176, arXiv:gr-qc/0405012 [gr-qc].

[288] M. Nishiyama, M.-a. Morita, and M. Morikawa, "Bose Einstein condensation as dark energy and dark matter," arXiv:astro-ph/0403571 [astro-ph].

[289] R. Casadio, F. Kuehnel, and A. Orlandi, "Consistent Cosmic Microwave Background Spectra from Quantum Depletion," *JCAP* **1509** (2015) 002, arXiv:1502.04703 [gr-qc].

[290] W. Mück, "On the number of soft quanta in classical field configurations," *Can. J. Phys.* **92** no. 9, (2014) 973–975, arXiv:1306.6245 [hep-th].

[291] M. Cadoni and P. jain, "How is the Presence of Horizons and Localized Matter Encoded in the Entanglement Entropy?," *Int. J. Mod. Phys.* **A32** no. 15, (2017) 1750083, arXiv:1703.02505 [hep-th].

[292] C. Barcelo, S. Liberati, and M. Visser, "Analog gravity from Bose-Einstein condensates," *Class. Quant. Grav.* **18** (2001) 1137, arXiv:gr-qc/0011026 [gr-qc].

[293] D.-C. Dai and D. Stojkovic, "Comment on 'Covariant version of Verlinde's emergent gravity'," *Phys. Rev.* **D96** no. 10, (2017) 108501, arXiv:1706.07854 [gr-qc].

[294] R.-G. Cai, S. Sun, and Y.-L. Zhang, "Emergent Dark Matter in Late Universe on Holographic Screen," arXiv:1712.09326 [hep-th].

[295] M. Cosenza, L. Herrera, M. Esculpi, and L. Witten, "Some models of anisotropic spheres in general relativity," *J. Math. Phys.* **22** (1981) 118.

[296] L. Herrera and N. O. Santos, "Local anisotropy in self-gravitating systems," *Phys. Rept.* **286** (1997) 53.

[297] E. Battaner and E. Florido, "The Rotation curve of spiral galaxies and its cosmological implications," *Fund. Cosmic Phys.* **21** (2000) 1–154, arXiv:astro-ph/0010475 [astro-ph].

[298] J. F. Navarro, C. S. Frenk, and S. D. M. White, "The Structure of cold dark matter halos," *Astrophys. J.* **462** (1996) 563–575, arXiv:astro-ph/9508025 [astro-ph].

[299] G. Bertone and J. Silk, "Particle dark matter," in *In *Bertone, G. (ed.): Particle dark matter* 3-13*. 2010.

[300] W. Jaffe, "A Simple model for the distribution of light in spherical galaxies," *Mon. Not. Roy. Astron. Soc.* **202** (1983) 995–999.

[301] R. Sharma, S. Karmakar, and S. Mukherjee, "Boson star and dark matter," *Submitted to: Gen. Rel. Grav.* (2008) , arXiv:0812.3470 [gr-qc].

[302] B. Carr, F. Kuhnel, and M. Sandstad, "Primordial Black Holes as Dark Matter," *Phys. Rev.* **D94** no. 8, (2016) 083504, arXiv:1607.06077 [astro-ph.CO].

[303] C. Rovelli and F. Vidotto, "Planck stars," *Int. J. Mod. Phys.* **D23** no. 12, (2014) 1442026, arXiv:1401.6562 [gr-qc].

[304] M. Visser, C. Barcelo, S. Liberati, and S. Sonego, "Small, dark, and heavy: But is it a black hole?," arXiv:0902.0346 [gr-qc]. [PoSBHGRS,010(2008)].

[305] G. Jungman, M. Kamionkowski, and K. Griest, "Supersymmetric dark matter," *Phys. Rept.* **267** (1996) 195–373, arXiv:hep-ph/9506380 [hep-ph].

[306] B. Shakya, "The Status of Neutralino Dark Matter," *AIP Conf. Proc.* **1604** (2014) 98–104, arXiv:1312.7505 [hep-ph].

[307] F. D. Steffen, "Gravitino dark matter and cosmological constraints," *JCAP* **0609** (2006) 001, arXiv:hep-ph/0605306 [hep-ph].

[308] J. L. Feng, "Dark Matter Candidates from Particle Physics and Methods of Detection," *Ann. Rev. Astron. Astrophys.* **48** (2010) 495–545, arXiv:1003.0904 [astro-ph.CO].

[309] M. Yu. Khlopov, "Particle Dark Matter Candidates," *Mod. Phys. Lett.* **A32** (2017) 1702001, arXiv:1704.06511 [hep-ph].

[310] F. E. Schunck and E. W. Mielke, "General relativistic boson stars," *Class. Quantum Grav.* **20** (2003) R301, arXiv:0801.0307 [astro-ph].

[311] S. L. Liebling and C. Palenzuela, "Dynamical Boson Stars," *Living Rev. Relativ.* **20** (2017) 5, arXiv:1202.5809 [gr-qc].

[312] E. W. Mielke and F. E. Schunck, "Boson stars: Alternatives to primordial black holes?," *Nucl. Phys.* **B564** (2000) 185–203, arXiv:gr-qc/0001061 [gr-qc].

[313] F. S. Guzmán and J. M. Rueda-Becerril, "Spherical boson stars as black hole mimickers," *Phys. Rev.* **D80** (2009) 084023, arXiv:1009.1250 [astro-ph.HE].

[314] C. F. B. Macedo, P. Pani, V. Cardoso, and L. C. B. Crispino, "Astrophysical signatures of boson stars: quasinormal modes and inspiral resonances," *Phys. Rev.* **D88** no. 6, (2013) 064046, arXiv:1307.4812 [gr-qc].

[315] E. Barausse, V. Cardoso, and P. Pani, "Can environmental effects spoil precision gravitational-wave astrophysics?," *Phys. Rev.* **D89** no. 10, (2014) 104059, arXiv:1404.7149 [gr-qc].

[316] F. H. Vincent, Z. Meliani, P. Grandclément, E. Gourgoulhon, and O. Straub, "Imaging a boson star at the Galactic center," *Class. Quantum Grav.* **33** no. 10, (2016) 105015, arXiv:1510.04170 [gr-qc].

[317] C. F. B. Macedo, P. Pani, V. Cardoso, and L. C. B. Crispino, "Into the lair: gravitational-wave signatures of dark matter," *Astrophys. J.* **774** (2013) 48, arXiv:1302.2646 [gr-qc].

[318] V. Cardoso, E. Franzin, and P. Pani, "Is the gravitational-wave ringdown a probe of the event horizon?," *Phys. Rev. Lett.* **116** no. 17, (2016) 171101, arXiv:1602.07309 [gr-qc]. Erratum: Phys. Rev. Lett. **117**, 089902(E) (2016).

[319] V. Cardoso, S. Hopper, C. F. B. Macedo, C. Palenzuela, and P. Pani, "Gravitational-wave signatures of exotic compact objects and of quantum corrections at the horizon scale," *Phys. Rev.* **D94** no. 8, (2016) 084031, arXiv:1608.08637 [gr-qc].

[320] V. Cardoso, E. Franzin, A. Maselli, P. Pani, and G. Raposo, "Testing strong-field gravity with tidal Love numbers," *Phys. Rev.* **D95** no. 8, (2017) 084014, arXiv:1701.01116 [gr-qc].

[321] N. Sennett, T. Hinderer, J. Steinhoff, A. Buonanno, and S. Ossokine, "Distinguishing Boson Stars from Black Holes and Neutron Stars from Tidal Interactions in Inspiraling Binary Systems," *Phys. Rev.* **D96** no. 2, (2017) 024002, arXiv:1704.08651 [gr-qc].

[322] E. Seidel and W. M. Suen, "Oscillating soliton stars," *Phys. Rev. Lett.* **66** (1991) 1659.

[323] A. Füzfa, M. Rinaldi, and S. Schlögel, "Particlelike distributions of the Higgs field nonminimally coupled to gravity," *Phys. Rev. Lett.* **111** no. 12, (2013) 121103, arXiv:1305.2640 [gr-qc].

[324] S. Schlogel, M. Rinaldi, F. Staelens, and A. Fuzfa, "Particlelike solutions in modified gravity: the Higgs monopole," *Phys. Rev.* **D90** no. 4, (2014) 044056, arXiv:1405.5476 [gr-qc].

[325] J. Rubinstein, "Sine-Gordon Equation," *J. Math. Phys.* **11** (1970) 258–266.

[326] G. Gaeta, C. Reiss, M. Peyrard, and T. Dauxois, "Simple models of non-linear DNA dynamics," *Riv. Nuovo Cim.* **17** no. 4, (1994) 1–48.

[327] A. Barone and G. Paternò, *Physics and applications of the Josephson effect*. Wiley, New York, USA, 1982.

[328] J. Cuevas-Maraver, P. Kevrekidis, and F. Williams, eds., *The sine-Gordon Model and its Applications*. Springer, Heidelberg, Germany, 2014.

[329] J. Gegenberg and G. Kunstatter, "Solitons and black holes," *Phys. Lett.* **B413** (1997) 274–280, arXiv:hep-th/9707181 [hep-th].

[330] M. Cadoni, "2-D extremal black holes as solitons," *Phys. Rev.* **D58** (1998) 104001, arXiv:hep-th/9803257 [hep-th].

[331] W.-J. Su and J. Yan, "A sine-Gordon soliton star model with a mix of dark energy and Fermi matter," *Can. J. Phys.* **90** no. 12, (2012) 1279–1285.

[332] M. Cadoni, S. Mignemi, and M. Serra, "Exact solutions with AdS asymptotics of Einstein and Einstein-Maxwell gravity minimally coupled to a scalar field," *Phys. Rev.* **D84** (2011) 084046, arXiv:1107.5979 [gr-qc].

[333] M. Cadoni, M. Serra, and S. Mignemi, "Black brane solutions and their solitonic extremal limit in Einstein-scalar gravity," *Phys. Rev.* **D85** (2012) 086001, arXiv:1111.6581 [hep-th].

[334] M. Cadoni and E. Franzin, "Asymptotically flat black holes sourced by a massless scalar field," *Phys. Rev.* **D91** no. 10, (2015) 104011, arXiv:1503.04734 [gr-qc].

[335] M. Cadoni, E. Franzin, and M. Serra, "Brane solutions sourced by a scalar with vanishing potential and classification of scalar branes," *J. High Energy Phys.* **01** (2016) 125, arXiv:1511.03986 [gr-qc].

[336] J. D. Bekenstein, "Nonexistence of baryon number for static black holes," *Phys. Rev.* **D5** (1972) 1239.

[337] J. D. Bekenstein, "Novel 'no scalar hair' theorem for black holes," *Phys. Rev.* **D51** (1995) 6608.

[338] D. Sudarsky, "A Simple proof of a no-hair theorem in Einstein-Higgs theory," *Class. Quantum Grav.* **12** (1995) 579.

[339] T. Torii, K. Maeda, and M. Narita, "Scalar hair on the black hole in asymptotically anti-de Sitter space-time," *Phys. Rev.* **D64** (2001) 044007.

[340] T. Hertog, "Towards a Novel no-hair Theorem for Black Holes," *Phys. Rev.* **D74** (2006) 084008, arXiv:gr-qc/0608075.

[341] C. A. R. Herdeiro and E. Radu, "Kerr black holes with scalar hair," *Phys. Rev. Lett.* **112** (2014) 221101, arXiv:1403.2757 [gr-qc].

[342] C. A. R. Herdeiro and E. Radu, "Asymptotically flat black holes with scalar hair: a review," in *Proceedings of the 7th Black Holes Workshop*, C. A. R. Herdeiro, V. Cardoso, J. P. S. Lemos, and F. C. Mena, eds., no. Int. J. Mod. Phys. D24, p. 1542014. Aveiro, Portugal, Dec. 18–19, 2014. arXiv:1504.08209 [gr-qc].

[343] I. Smolić, "Symmetry inheritance of scalar fields," *Class. Quantum Grav.* **32** no. 14, (2015) 145010, arXiv:1501.04967 [gr-qc].

[344] I. Smolić, "Constraints on the symmetry noninheriting scalar black hole hair," *Phys. Rev.* **D95** no. 2, (2017) 024016, arXiv:1609.04013 [gr-qc].

[345] P. Amaro-Seoane, J. Barranco, A. Bernal, and L. Rezzolla, "Constraining scalar fields with stellar kinematics and collisional dark matter," *J. Cosmol. Astropart. Phys.* **1011** (2010) 002, arXiv:1009.0019 [astro-ph.CO].

[346] M. S. Madsen, "A Note on the Equation of State of a Scalar Field," *Astrophys. Space Sci.* **113** (1985) 205.

[347] K. A. Bronnikov, J. C. Fabris, and A. Zhidenko, "On the stability of scalar-vacuum space-times," *Eur. Phys. J.* **C71** (2011) 1791, arXiv:1109.6576 [gr-qc].

[348] B. Simon, "The Bound State of Weakly Coupled Schrodinger Operators in One and Two-Dimensions," *Annals Phys.* **97** (1976) 279.

[349] M. Kimura, "A simple test for stability of black hole by S-deformation," *Class. Quantum Grav.* **34** (2017) 235007, arXiv:1706.01447 [gr-qc].

[350] P. O. Mazur and E. Mottola, "Gravitational condensate stars: An alternative to black holes," arXiv:gr-qc/0109035 [gr-qc].

[351] M. Visser and D. L. Wiltshire, "Stable gravastars: An alternative to black holes?," *Class. Quantum Grav.* **21** (2004) 1135, arXiv:gr-qc/0310107 [gr-qc].

[352] U. H. Danielsson, G. Dibitetto, and S. Giri, "Black holes as bubbles of AdS," *J. High Energy Phys.* **10** (2017) 171, arXiv:1705.10172 [hep-th].

[353] V. Cardoso, P. Pani, M. Cadoni, and M. Cavaglià, "Ergoregion instability of ultracompact astrophysical objects," *Phys. Rev.* **D77** (2008) 124044, arXiv:0709.0532 [gr-qc].

[354] V. Cardoso, L. C. B. Crispino, C. F. B. Macedo, H. Okawa, and P. Pani, "Light rings as observational evidence for event horizons: long-lived modes, ergoregions and nonlinear instabilities of ultracompact objects," *Phys. Rev.* **D90** no. 4, (2014) 044069, arXiv:1406.5510 [gr-qc].

[355] A. Buchel, J. T. Liu, and A. O. Starinets, "Coupling constant dependence of the shear viscosity in N=4 supersymmetric Yang-Mills theory," *Nucl. Phys.* **B707** (2005) 56–68, arXiv:hep-th/0406264 [hep-th].

[356] A. Buchel, R. C. Myers, and A. Sinha, "Beyond eta/s = 1/4 pi," *JHEP* **03** (2009) 084, arXiv:0812.2521 [hep-th].

[357] T. Ciobanu and D. M. Ramirez, "Shear hydrodynamics, momentum relaxation, and the KSS bound," *arXiv:1708.04997* (2017) , arXiv:1708.04997 [hep-th].

[358] G. T. Horowitz and J. Polchinski, "Gauge/gravity duality," arXiv:gr-qc/0602037 [gr-qc].

[359] V. C. Rubin, N. Thonnard, and W. K. Ford, Jr., "Rotational properties of 21 SC galaxies with a large range of luminosities and radii, from NGC 4605 /R = 4kpc/ to UGC 2885 /R = 122 kpc/," *Astrophys. J.* **238** (1980) 471.

[360] M. Persic, P. Salucci, and F. Stel, "The Universal rotation curve of spiral galaxies: 1. The Dark matter connection," *Mon. Not. Roy. Astron. Soc.* **281** (1996) 27, arXiv:astro-ph/9506004 [astro-ph].

[361] H. Kodama, "Conserved Energy Flux for the Spherically Symmetric System and the Back Reaction Problem in the Black Hole Evaporation," *Prog. Theor. Phys.* **63** (1980) 1217.

[362] R. Massey, T. Kitching, and J. Richard, "The dark matter of gravitational lensing," *Rept. Prog. Phys.* **73** (2010) 086901, arXiv:1001.1739 [astro-ph.CO].

[363] M. Milgrom, "MOND laws of galactic dynamics," *Mon. Not. Roy. Astron. Soc.* **437** no. 3, (2014) 2531–2541, arXiv:1212.2568 [astro-ph.CO].

[364] S. S. McGaugh, "Mond Prediction for the Velocity Dispersion of the "feeble Giant" Crater ii," *Astrophys. J.* **832** no. 1, (2016) L8, arXiv:1610.06189 [astro-ph.GA].

[365] S. D. Mathur, "The Fuzzball proposal for black holes: An Elementary review," *Fortsch. Phys.* **53** (2005) 793–827, arXiv:hep-th/0502050 [hep-th].

[366] K. A. Bronnikov, R. A. Konoplya, and A. Zhidenko, "Instabilities of wormholes and regular black holes supported by a phantom scalar field," *Phys. Rev.* **D86** (2012) 024028, arXiv:1205.2224 [gr-qc].

[367] A. Anabal'on and N. Deruelle, "On the mechanical stability of asymptotically flat black holes with minimally coupled scalar hair," *Phys. Rev.* **D88** (2013) 064011, arXiv:1307.2194 [gr-qc].

[368] K. A. Bronnikov, M. S. Chernakova, J. C. Fabris, N. Pinto-Neto, and M. E. Rodrigues, "Cold black holes and conformal continuations," *Int. J. Mod. Phys.* **D17** (2008) 25, arXiv:gr-qc/0609084 [gr-qc].

[369] K. A. Bronnikov and A. V. Khodunov, "Scalar field and gravitational instability," *Gen. Rel. Gravit.* **11** (1979) 13.

[370] R. Blankenbecler, M. L. Goldberger, and B. Simon, "The Bound States of Weakly Coupled Long Range One-Dimensional Quantum Hamiltonians," *Annals Phys.* **108** (1977) 69.

[371] B. Kleihaus, J. Kunz, E. Radu, and B. Subagyo, "Axially symmetric static scalar solitons and black holes with scalar hair," *Phys. Lett.* **B725** (2013) 489–494, arXiv:1306.4616 [gr-qc].

[372] O. Bechmann and O. Lechtenfeld, "Exact black hole solution with selfinteracting scalar field," *Class. Quantum Grav.* **12** (1995) 1473–1482, arXiv:gr-qc/9502011 [gr-qc].

[373] Azreg-Aïnou, Mustapha, "Selection criteria for two-parameter solutions to scalar-tensor gravity," *Gen. Rel. Gravit.* **42** (2010) 1427–1456, arXiv:0912.1722 [gr-qc].

[374] D. A. Solovyev and A. N. Tsirulev, "General properties and exact models of static self-gravitating scalar field configurations," *Class. Quantum Grav.* **29** (2012) 055013.